Optimising Therapeutic Outcomes in CNS Disorders: Pharmaceutical and Pharmacokinetic Approaches.

Aminah KH E S E Almurjan
Doctor of Philosophy

Aston University
December 2021

Aston University

Optimising Therapeutic Outcomes in CNS disorders: A Pharmaceutical and Pharmacokinetic Approach

Aminah KH E S E Almurjan

Doctor of philosophy

December 2021

Thesis summary

Central nervous system (CNS) disorders have been highlighted by the World Health Organisation (WHO) as one of the biggest threats to public health. This study aimed to improve the clinical outcomes in CNS disorders, with focus on major depression, through pharmaceutical and pharmacokinetic approaches by the use of transdermal base creams and patches for the delivery of a phytochemical and the use of in-silico modelling to optimise antidepressant dosing in challenging populations such as pregnant women.

The flavonoid hesperetin, as a potential candidate for CNS disorders, was incorporated into commercial base creams (Vanish-Pen™, Doublebase™ gel, Versatile™, and Pentravan®). *In-vitro* drug release studies were conducted at week 0 showing that Pentravan® formulation released the highest percentage of hesperetin (12.69 % (0.68 %)), while Versatile™ released the lowest (4.53 % (0.65 %)). Storage studies on Vanish-pen™ and Doublebase™ were consistent for 10 weeks when stored at 4°C and 25°C, respectively, while Versatile™ showed consistent profiles when stored at both 4°C and 25°C. Significant changes were detected in the release profiles of Pentravan® during storage at both temperatures.

Transdermal hesperetin patch systems were developed using either Dow Corning® BIO-PSA 7-4501 silicone adhesive or Eudragit® E100 acrylic adhesive. The silicone-based patch that contains 5.5 % glycerol provided the highest release, 39.9 % (0.37 %), but during storage for 3 weeks at 4°C and 25°C, the release significantly decreased. The Eudragit®-based patch that produced the highest release (8 % (0.06 %)) was composed of 5% glycerol and 45% of triacetin. However, during storage the acrylic-based patches degraded. Silicone-based transdermal patches showed higher drug release than creams which could potentially be useful for systemic hesperetin delivery for the treatment of CNS disorders, while hesperetin creams could be more suitable for the localised delivery to the skin for the treatment of skin cancers.

In order to highlight non-pharmaceutical approaches to optimise CNS therapeutic outcomes, we applied pharmacokinetic modelling to examine potential dose adjustments that would be required in challenging population groups, namely pregnancy, for two antidepressants, paroxetine and sertraline.

Paroxetine has been demonstrated to undergo gestation related reductions in plasma concentrations, to an extent which is dictated by the polymorphic state of CYP 2D6. However, knowledge of appropriate dose titrations is lacking. A pharmacokinetic modelling approach was applied to examine gestational changes in trough plasma concentrations for CYP 2D6 phenotypes, followed by necessary dose adjustment strategies to maintain paroxetine levels within a therapeutic range of 20-60 ng/mL. A decrease in trough plasma concentrations was simulated throughout gestation for all phenotypes. A significant number of ultra-rapid (UM) phenotype subjects possessed trough levels below 20 ng/mL (73-76 %) compared to extensive metabolisers (EM) (51-53 %). For all phenotypes studied there was a requirement for daily doses in-excess of the standard 20 mg dose throughout gestation. The following doses are suggested to be optimal: for EM, 30 mg daily in trimester 1 followed by 40 mg daily in trimesters 2 and 3, for poor-metabolisers (PM), 20 mg daily dose in trimester 1 followed by 30 mg daily in trimesters 2 and 3, and for UM, a 40 mg daily dose throughout gestation. Sertraline is also known to undergo changes in pharmacokinetics during pregnancy. CYP 2C19 has been implicated in the inter-individual variation in clinical effect associated with sertraline activity. However, knowledge of suitable dose titrations during pregnancy and within CYP 2C19 phenotypes is lacking. A pharmacokinetic modelling virtual clinical trials approach was implemented to assess gestational changes in trough plasma concentrations for CYP 2C19 phenotypes and to identify appropriate dose titration strategies to stabilise sertraline levels within a defined therapeutic range throughout gestation. Sertraline trough plasma concentrations decreased throughout gestation, with maternal volume expansion and reduction in plasma albumin being identified as possible causative reasons. All CYP 2C19 phenotypes required dose increase throughout gestation. For EM and UM phenotypes, doses of 100-150 mg daily are required throughout gestation. For PM, 50 mg daily during trimester 1 followed by a dose of 100 mg daily in trimesters 2 and 3 are required.

Transdermal system is a promising approach to obtain the CNS benefits of phytochemicals and to overcome the limitations associated with their oral delivery, while more studies are needed to be used clinically. Using PBPK modelling for adjusting the doses of CNS medications in challenging populations could improve quality of life and prevent empirical interventions.

Keywords: CNS disorders; Mental disorders; Depression; Hesperetin; Formulation; PBPK; Pregnancy; SSRI.

Acknowledgements

First, I would like to praise and thank God for granting me strengths and blessings to accomplish this work.

I would like to express my deepest gratitude and appreciation to my supervisor Dr. Raj Badhan for his continuous invaluable support. Completing this work would not be possible without his guidance, invaluable advice, encouragement, kindness, and patience. I see myself extremely lucky to have him as a supervisor who is truly humble, cared deeply about the progression of my work, and always respond to my queries so promptly. I'm forever grateful and I aspire to be like him one day.

I would like to express my sincerest gratitude to Kuwait University for giving me this scholarship, sponsoring my postgraduate studies, and supporting me financially.

Deepest thanks to all the lab technicians especially Rachel and Hayley, for their patience, technical help, and support.

Thank you to all my colleagues in Aston University for all the support throughout my PhD at all points. Shital, Basma, Abdulkhaliq, Dania, Annsar, Carlo, Abdul Ershad, Ola, Alfredo, He, Ruba, Shoag, Dilawar, Rhys, Zakia, Thu, Tu, Anwar. It has been an honour and pleasure to work alongside you all.

My greatest gratitude and love go to my husband, Abdulrahman Alhassan, I find it difficult to express my appreciation because it is immeasurable. Thank you for being an amazing husband and father. Thank you for your continuous cheerful optimism even during uncertainties. Thank you for sharing this entire journey with me with providing limitless love, support, and patience. I dedicate this work to you.

I am deeply grateful for my family; my father: Khaled AlMurjan, my mother: Amal AlJawdar, and my lovely sisters: Haya, Heba, Hanouf, Dalia, Worood, for their continuous prayers and encouragement.

Thank you, my son, Abdulaziz, for your inspirational smiles that kept me moving forward.

List of Publications

List of published peer reviewed articles

Almurjan, A., Macfarlane, H. and Badhan, R.K.S., *Precision dosing-based optimisation of paroxetine during pregnancy for poor and ultrarapid CYP2D6 metabolisers: a virtual clinical trial pharmacokinetics study.* Journal of Pharmacy and Pharmacology, 2020. **72**(8): p. 1049-1060.

Almurjan, A., Macfarlane, H. and Badhan, R.K.S., *The application of precision dosing in the use of sertraline throughout pregnancy for poor and ultrarapid metabolizer CYP 2C19 subjects: A virtual clinical trial pharmacokinetics study.* Biopharmaceutics & Drug Disposition, 2021. **42**(6): p. 252-262.

List of Abstracts

Aminah Almurjan and Raj Badhan., 2018. Novel formulation approaches for the treatment of epilepsy in children – transdermal drug delivery. LHS PG research day, Aston University, Birmingham, UK

Aminah Almurjan and Raj Badhan., 2019. Novel formulation approaches for delivering the flavonoid (*hesperetin*) through the skin. The Academy of Pharmaceutical Sciences (APS), University of Greenwich, London.

List of Contents

List of abbreviations

AAG	Alpha-1 acidic glycoprotein
AD	Alzheimer disease
ADAM	Advanced dissolution, absorption, and metabolism
ADME	Absorption, distribution, metabolism, and elimination
AIC	Akaike information criterion
ALS	Amyotrophic lateral sclerosis
AUC	Area under the concentration time profile curve
AUMC	The area under the first instant of the systemic drug concentration curve
BDNF	Brain-derived neurotrophic factor
C	Concentration
C°	Celsius
CA	Compartmental analysis
CL	Clearance
CL_b	Blood clearance
CL_h	Hepatic clearance
CL_{int}	Intrinsic clearance
CL_p	Plasma clearance
CL_{po}	Systemic clearance following oral drug administration
CL_T	Total clearance
C_{max}	Maximum concentration
CNS	Central nervous system
Cs	Solubility concentration
C_{ss}	Steady state concentration
CYP	Cytochrome P450
D	Diffusion coefficient
DDI	Drug-drug interaction
DSC	Differential scanning calorimetry
EM	Extensive metaboliser
F	Bioavailability
fa	Fraction of dose absorbed
FDA	Food and Drug Administration
fu	Unbound fraction of drug in plasma
g	Gram
GFR	Glomerular filtration rate

GST	Glutathione S-transferase
GW	Gestational week
h	Hour
HD	Huntington disease
HPLC	High-performance liquid chromatography
HPMC	Hydroxypropyl methylcellulose
HSA	Human serum albumin
IM	intermediate metaboliser
IR	immediate release
J	Flux
K	Elimination rate constant
Ka	Absorption rate constant
Km	Michaelis constant
KP	Korsmeyer-Peppas
Kp	Tissue-partition coefficient
LOD	Limit of detection
LOQ	Limit of quantification
MAT	Mean absorption time
MDD	Major depressive disorder
mg	Milligram
min	Minute
mL	Millilitre
mol	Mole
MRT	Mean residence time
MS	Multiple sclerosis
MW	Molecular weight
NATS	N-Acetyl transferases
NCA	Non compartmental analysis
ng	nanogram
nm	Nanometer
O/w	Oil in water
OAT	Organic anionic transporters
OCT	Organic cationic transporters
P	Partition coefficient
Papp	Apparent permeability
PBPK	Physiologically based pharmacokinetics
PBS	Phosphate buffered saline

PD	Parkinson disease
PEG	Polyethylene glycol
P-gp	P-glycoprotein
PIB	Polyisobutylene
PK	Pharmacokinetics
pKa	Dissociation rate constant
PLO	Pluronic lecithin organogel
PM	Poor metaboliser
PSA	Pressure sensitive adhesive
PVP	Polyvinylpyrrolidone 30
R	Dose rate
RSD	Relative Standard Deviation
SC	Stratum corneum
SD	Standard Deviation
SERT	Serotonin transporter
SSRI	Selective serotonin reuptake inhibitor
SULTS	Sulphotransferases
t	Time
$t_{1/2}$	Half-life
TCA	Tricyclic antidepressant
TDM	Therapeutic drug monitoring
Tg	Glass transition temperature
UGT	Uridine 5’-diphospho-glucuronosyltransferase
UM	Ultrarapid metaboliser
Vd	Volume of distribution
Vmax	maximum velocity of the metabolic reaction
W/o	Water in oil
WHO	World Health Organisation
XR	Extended release
µg	Microgram
µL	Microliter
µM	Micromole

List of Figures

List of Tables

Chapter 1

General Introduction

1.1 Disorders of the central nervous system

It has been highlighted by the World Health Organisation (WHO) that one of the biggest threats to public health is central nervous system (CNS) disorders [1]. The leading cause of global disability-adjusted life-years (DALYs) in 2019/2020 remained neurological disorders, contributing to 16.5 % of deaths [2]. A major challenge for successful CNS drug delivery is the passage across the blood brain barrier (BBB), which restricts the entry of small molecular weight drugs based upon attainment of prerequisite physiochemical properties for cell membrane permeability, such as low molecular weight (< 500), high lipophilicity, low hydrogen-bonding potential, and molecular flexibility [3, 4].

The BBB is an impermeable barrier formed from brain microvascular endothelial cells, pericytes, astrocyte end feet, extracellular matrix, and neurons (Figure 1.1) [5]. Endothelial cells are highly selective when controlling the passage of exogenous and endogenous compounds into the brain [6]. Poor clinical efficacy of some CNS medications is due to the impermeable nature of the BBB hindering molecular flux [7-11]. In addition to the physicochemical drug properties, the passage of drug molecules into the brain is restricted by three key features of the BBB physiology: (i) an extensive tight junction (TJ) protein network limited paracellular drug transport; (ii) limited transcytosis and the lack of fenestrations resulting in limited transcellular transport of drug molecules; (iii) an extensive network of active drug transporter proteins [12, 13].

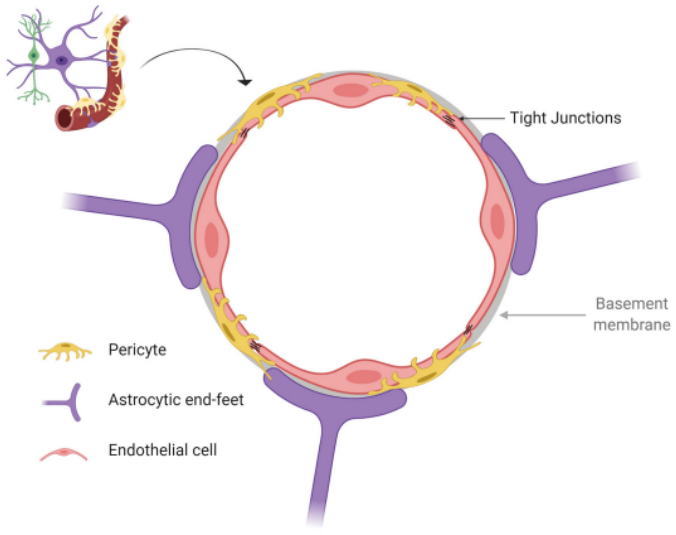

Figure 1.1 The components of the blood brain barrier.

Obtained from [6]

Key CNS disorders include Parkinson's disease, multiple sclerosis, epilepsy, Alzheimer and other dementias, neuroinfections, neurological disorders associated with malnutrition, pain associated with neurological disorders, stroke, traumatic brain injuries, schizophrenia, and depression [1].

1.2 Depression and its prevalence

Major depressive disorder is ranked by the World Health Organisation as the 4th global leading cause of disability [14]. The lifetime prevalence of depression is 20 % in the worldwide general population with a higher prevalence in females, 5:2 is the female to male ratio [15]. Approximately 280 million people in the world are suffering from depression [16]. Depression is the second cause of disability in the ranking of Disability Adjusted Life Years (DALY) for the age category 15-44 years old [17].

1.2.1 Diagnosis and risk factors of depression

The criteria of the Diagnostic and Statistical Manual of Mental Health, Fourth Edition (DSMIV) is used to diagnose depression appropriately. Five of the nine DSMIV symptoms should be present in a patient continuously for a period of minimally 2 weeks to be diagnosed with depression. DSMIV symptoms are the loss of pleasure or interest, weight or appetite alteration significantly, depressed mood, energy loss or fatigue, suicidal tendencies, worthlessness feelings, low concentration or thinking ability, psychomotor retardation, and sleep disturbances such as insomnia or hyposomnia [15].

It is indeed challenging to link depression to one specific factor as a complex interaction of psychological, social, and biological factors can result in depression. People who experience specific stressful life events have increased potential to develop depression. Several other risk factors could contribute to depression such as genetics, chronic pain, substance abuse, poor nutrition, and certain chronic medical conditions such as sleep disorders, thyroid condition, cancer, diabetes, multiple sclerosis [18]. In addition, several medications could potentially provoke depression including antihypertensives, anti-obesity agents, antivirals, contraceptives, and corticosteroids [19].

1.2.2 Pharmacological treatment

The major hypothesis of depression is the monoamine hypothesis which explains that depression is caused by deficiency of the monoaminergic transmitters in the brain including serotonin (5-HT), dopamine (DA), and norepinephrine. The symptoms of depression may arise from altered neurotransmitters' storage, synthesis, or release, in addition to the disruption of receptors sensitivity or the functions of subcellular messengers. Anti-depressant therapeutics

targeting the monoaminergic system are the mainstay treatment options (Table 1.1) [15, 20], with the choice of treatment approaches being tailored to personal preferences and to the particular medical condition of the patient.

Table 1.1 Treatment approaches for depression

Treatment	Examples
Selective Serotonin Reuptake Inhibitors (SSRIs)	Fluoxetine, paroxetine, sertraline, citalopram, mirtazapine
Tricyclic Antidepressants (TCAs)	Amitriptyline, imipramine
Monoamine-Oxidase Inhibitors (MAOIs)	Iproniazide
Serotonin-Norepinephrine Reuptake Inhibitors (SNRIs)	Venlafaxine, duloxetine
Herbal drugs	St. John's wort
Other therapeutics	Mood stabilisers, lithium salts, antiepileptics
Non-chemical therapies	Light therapy, magnetic stimulation, psychotherapy, cognitive therapy

The goal of treatment is achieving full remission which is described by DSMIV as possessing no significant symptoms of depression for the past two months. Both emotional and physical symptoms should be resolved during remission. Remission focuses on restoring the patient's full functional capacity, which includes returning to work, resuming hobbies and personal interests, and restoring personal relationships. Relapse refers to the return of a depressive symptoms while in remission [21]. Other diagnostic scales to indicate remission and improvement are Clinical Global Impressions-Severity Scale (CGI-S), The Hamilton Depression Rating Scale (HAM-D), and Montgomery and Asberg Depression Rating Scale (MADRS) [22].

1.2.3 Poor treatment outcomes in depression

Although most patients are able to recover with treatment from the most severe symptoms of depression, the rate of recurrence is high with 75 % of the patients who recover experiencing one or more episodes of major depression within 10 years [15]. Moreover, in 70 % of depressed patients whom are taking an adequate course of one antidepressant, remission is not achieved [23, 24]. The risks related to recurrence are familial factors, individual’s mentality, number of previous episodes, comorbid conditions, demographic characteristics, treatment failures, and partial symptomatic response [25-28].

Taking into consideration that depression is more prevalent in women, depression during pregnancy is a serious and prevalent condition with incidence rates as high as 20 % [29]. Recent reports in the UK have suggested that 1 in 25 women (aged 20–35 years) who die by

suicide, do so during the perinatal periods (conception, pregnancy and postnatal) [30]. The use of mental health services by pregnant women is low, approximately 14 %, when compared to non-pregnant women, approximately 25 % [30]. Barriers to seeking help by distressed pregnant women include cultural barriers, the inability to disclose or acknowledge their feelings, lack of awareness of depression symptoms and how to seek help, and the negative attitudes of healthcare professionals, family and friends [31].

There is a serious need to better manage depression or discover new antidepressants to treat the unresolved conditions or to follow approaches that could improve clinical response. The level of unmet needs in mental disorders is significant with high recurrence rates and high rates of unachieved remission as discussed above. Moreover, patient non-adherence to antidepressants is a significant issue with about 50% of patients discontinue the treatment of depression prematurely [32]. The reasons for non-adherence and discontinuation of antidepressants were side effects, high cost, delayed onset of action, complicated dosing or titration of the drug, poor instruction by the clinician, lack of follow up, and misperceptions about antidepressants [32].

Key barriers to optimisation of care include social stigma, lack of trained providers, lack of resources, in addition to the prevalence of unwanted therapeutic side effects, and inconvenient formulations choices (e.g. immediate release versus modified release drug formulation systems). Increasing the efficiency of health systems, intensive monitoring, developing new therapeutic intervention strategies could significantly improve the outcome of depression treatment [33].

1.3 Chemical approaches to optimising outcomes in CNS disorders: phytochemicals as novel CNS drug candidates

Phytochemicals, which are chemicals derived from natural extracts of plants and vegetables, have been highlighted as possible novel potential therapeutic agents for CNS disorders. Flavonoids are a major category of phytochemicals and consists of over 6500 compounds [34, 35]. The structure of flavonoids consists of two aromatic rings A and C and a heterocyclic benzene ring (B ring) (Figure 1.2) [36]. The position of the attached substitution (R_x) categorises the flavonoids into seven major subgroups, namely flavonols, flavones, flavanols, flavanones, anthocyanins, catechins, and isoflavones (Table 1.2) [36, 37].

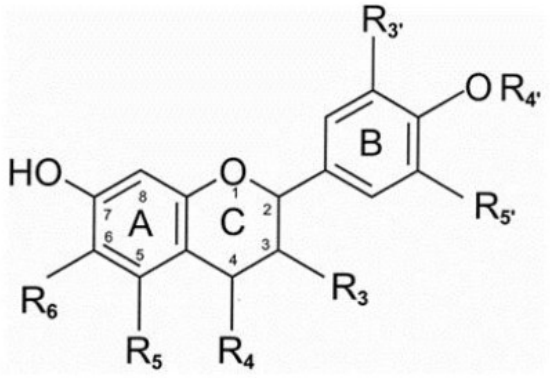

Figure 1.2 The chemical structure of flavonoid

Flavonoids consist of two aromatic rings (A and B) linked through ring (C). Based on the pattern of hydroxylation and substitution (Rx), there are 7 subclasses of flavonoids [38].

Table 1.2 Main groups of flavonoids with compounds and food sources examples.

	Example	**Source**
Flavonols	Quercertin, kaempferol, myicetin	Blueberry, black tea, leek, yellow onion, cherry, apple, tomato, curly kale.
Flavanones	Hesperetin, naringenin, eridodicytol	Orange juice, lemon juice, grapefruit juice.
Flavones	Chrysin, lubeolin, tangeretin, tricetin, sinensetin, apigenin, nobiletin	Celery, parsley, capsicum.
Isoflavones	Daidzein, genisten, glycitein	Soybean, tofu, soy flour
Catechins	(-) Epicatechin, (+) catechin gallocatechin, epigallocatechin, epigallocatechin 3-gallate	Beans, cherry, chocolate apricot, peach, red wine, grapes, green tea
Flavanols	Taxifolin, silibinin, silymarin, pinobaskin	Cocoa, chocolates, cocoa beverages.
Anthocyanins	Petunidin, malvidin, peonidin, cyanidin, delphinindin.	Red berries, black grapes, blackcurrant, blackberries, rhubarb, plum, red cabbage, strawberries, cherries

Flavonoids possess several pharmacological actions including antineoplastic, anti-inflammatory, antidiabetic, antidepressant, antiviral, antiallergic, gastro-protective and hepato-protective activities [39-41]. In addition, they have been reported to induce CNS related effects

such as the protection of neurons from neuro-inflammation and neurotoxins in degenerative disease status [42-48]. A reduced risk of neurodegenerative diseases, including Alzheimer disease (AD), multiple sclerosis (MS), Parkinson disease (PD), Huntington disease (HD), and amyotrophic lateral sclerosis (ALS) has been linked to regular consumption of flavonoids, this is due to their antioxidant and neuroprotection capabilities [43].

Supporting the proposal of flavonoids as potential candidates for neurological diseases, it has been shown that several flavonoids are able to cross the BBB and access the central nervous system, including hesperetin, naringenin, and epigallocatechin gallate (EGCG) [43]. Clinical evidence has shown that flavonoids possess a protective function to dopamine neurons by the prevention of apoptosis and oxidative damage [49, 50]. Flavonoids target sites are thought to be widespread, but many studies have focused on the interaction with the $GABA_A$ receptor, where several flavonoids demonstrated inhibitory actions on $GABA_{A,}$ showing anticonvulsant activity [38, 51-54].

Studies have shown the potential anti-depressive effects of flavonoids and strongly suggesting that these natural products are novel candidate compounds for mental health disorders [55-62]. There are several possible mechanisms underlying the antidepressant effects of flavonoids. Flavonoids can restore the levels of monoamines in the brain, increase the levels of serotonin and dopamine in the CNS, and up-regulate monoaminergic neurotransmitters [63-65]. Furthermore, they reduce hyperglycaemia and neuroinflammation, and supress oxidative stress by their antioxidant effects. Flavonoids can interact with the presynaptic $5\text{-}HT_{1A}$, dopaminergic D_1, D_2, D_3, noradrenergic α2, and k-opioid receptors [66-69].

Flavonoids have demonstrated several effects on the brain-derived neurotrophic factor (BDNF). The atrophy of hippocampus induced by depression is linked to the increased secretion of cortisol or the abnormal low levels of BDNF [70]. It has been demonstrated that flavonoids can increase the levels and the expression of BDNF in the hippocampus, restore the downregulation of BDNF induced by stress, and activate BDNF signalling pathway [71-75].

The flavonoid hesperetin was able to markedly reduce the oxidative stress, amyloidogenesis, cognitive dysfunction and neuroinflammation in mice brains, which were induced by amyloid-beta (Aβ) and LPS injections to represent the pathological changes Alzheimer's disease [76]. Lipopolysaccharide (LPS) is a biomolecule that induces inflammatory genes and mediators, and the abnormal Aβ production in the brain elevates oxidative stress, neuroinflammation, and neurodegeneration [77, 78].

The effects of hesperetin against Parkinson's Disease (PD) have been studied in rats by inducing PD-like symptoms using 6-hydroxydopamine (6-OHDA). In this study, the administration of hesperetin was able to reduce the motor dysfunction and reduce oxidative stress by regulating neuroinflammation, apoptotic cell loss, and regulating the transcription factor Nrf2 [76, 79]. In addition, hesperetin delayed the onset of seizure in epileptic mice (induced by kainic acid) when administered orally in a dose-dependent way by inhibiting the proinflammatory kinases in the hippocampus [52].

In cadmium-induced neurodegeneration study, hesperetin was administered for five weeks and was able to protect the brain against oxidative stress and activate endogenous antioxidant defence mechanisms [80]. Several studies have analysed the positive impacts of hesperetin against different neurodegeneration models in neuronal cell lines [81-86].

More research into flavonoids is desperately needed to help reduce the knowledge gap between pre-clinical research and clinical implementation. Although there is promising evidence, phytochemicals lack the necessary concrete scientific solidity to be safely carried forward into clinical levels of research, simply because they have not been studied sufficiently.

1.4 Formulation approaches to optimising clinical outcomes in CNS disorders: topical/Transdermal drug delivery

The most frequently used route for administering medications remains the oral route with most of the newly approved drugs being licenced in orally dosed formulation [87]. However, the exposure to first-pass metabolism, the requirement for multiple dosing regimens, and the side effects could lead to poor compliance and reduced clinical outcomes. As an alternative, transdermal drug delivery is considered historically safe and innovative way of administering medications. This route is with comparable efficacy to oral administration but provides better compliance, prolonged release, and improved bioavailability by avoiding first-pass metabolism [88, 89].

The skin is considered to be the largest organ in the human body, with a total weight of between 3.5-10 kg and a surface area of at least 2 m^2 [90]. The skin provides a barrier that protects the body from the external environmental hazards such as ultraviolet (UV) radiation, microorganisms, chemicals, and allergens [90]. The skin is comprised of the epidermis, dermis, subcutaneous tissues, and appendages (Figure 1.3). The epidermis layer is 50–100 μm thick and composed of 10-20 layers of cells. The primary skin layers comprise the epidermis are the *stratum basale, stratum spinosum, stratum granulosum, stratum lucidum,* and the *stratum corneum*. The *stratum basale*, which is also referred to as the basal layer, contains

keratinocytes, melanocytes, langerhans cells and merkel cells. Langerhans cells are formed in the bone marrow and then localise in the *stratum basale* and are one of the classical antigen

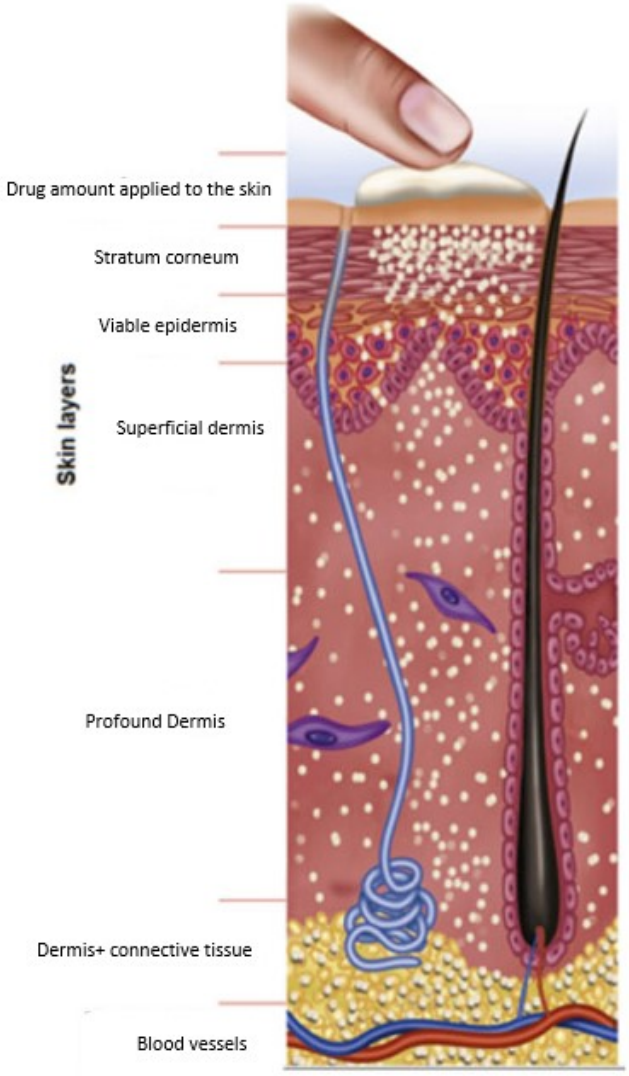

presenting cells responsible for the immune response of skin. Melanocytes form melanin that provides the pigmentation of hair, skin, and eyes, and absorbs harmful UV radiation to protect the skin from releasing free radicals in the basal layer. The primary function of merkel cells is for cutaneous sensation and are localised mainly in touch sensitive sites such as the lips and finger tips [90, 91].

Figure 1.3 Skin composition.

Obtained from [92]

The uppermost layer of the epidermis is the *stratum corneum (SC)*, which is the penetration controlling layer and the major barrier to environmental toxins. This layer regulates water loss from the body. It consists of high density and low hydration cells. The thickness of the *stratum*

corneum is 10–20 μm and composed of corneocytes [93]. Corneocytes are non-nucleated, flat, and dead cells comprised of insoluble bundled keratin in a lipid bilayer. Corneocytes are interconnected by membrane junctions called corneodesmosomes, these contribute to the stratum corneum cohesion. Lipids compose the intercellular space between the corneocytes providing a competent barrier function. Lipid domains consist of ceramides, free fatty acids, cholesterol, cholesterol sulfate, and cholesterol esters [90].

The dermis thickness is approximately 2-5 mm and consists of elastic connective tissue and collagen fibrils providing elasticity, flexibility, and support. The dermis slightly affects the permeation of most drugs but may reduce the ability of highly lipophilic drugs to permeate to deeper tissues. An extensive vascular network is present within the dermis. This network provides oxygen and nutrients to tissues, regulates body temperature, removes waste products and toxins from the tissues, and supports wound repair and immune response. Because of this extensive blood supply, a concentration gradient occurs between the topically applied chemicals and the dermis ensuring that the permeating chemicals are reaching the systemic blood supply through the dermo-epidermal junction [90, 94, 95].

1.4.1 Transdermal passage of drugs

Following the application of a drug formulation onto the skin, penetration through the *stratum corneum* occurs by intercellular (between the cells), transcellular (through the cells), or transappendageal pathways. The majority of compounds utilise intercellular routes [96], with the intercellular lipid bilayers in the *stratum corneum* providing the only continuous pathway through the *stratum corneum* (Figure 1.4). The transport of a compound within the intercellular lipids can occur by the diffusion through the polar head groups (polar pathway) or through the lipid core (lipid pathway) [97, 98]. The transcellular route is the crossing of a drug through the corneocytes and it is considered as the polar pathway through the *stratum corneum* (Figure 1.4). The keratin matrix in the corneocytes is polar in nature, therefore the compounds need to partition between the lipid domains that surround the corneocytes and the polar environment inside the corneocytes. The transappendageal route is a minor pathway for drugs which represent the passage of drugs through hair follicles, sweat glands, and sebaceous glands [99]. The amount of these appendages in skin surface represents only 0.1-1 % and this route is considered not significant [90].

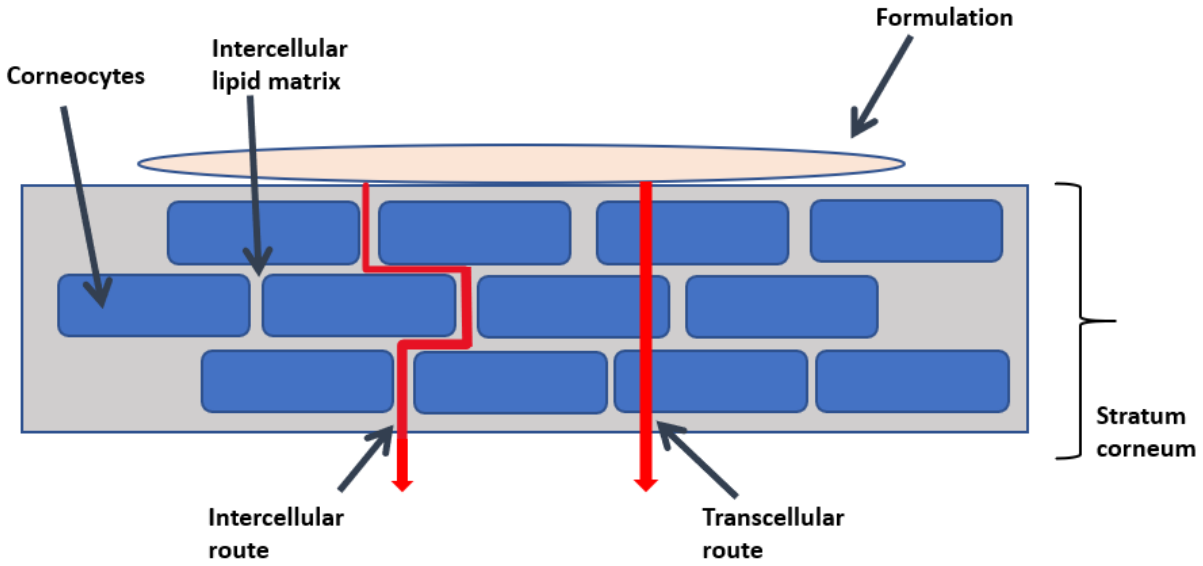

Figure 1.4 Representation of Intercellular and transcellular pathways for the penetration of drug molecules through the *stratum corneum*.

For successful transdermal delivery, a drug must be able to diffuse through a complex mixture of lipids with hydrophobic and hydrophilic domains in order to pass through intercellular channels [100] in addition to possessing specific physicochemical properties (Table 1.3) [101-103].

Table 1.3 Summary of drug characteristics required for transdermal drug delivery.

Molecular weight	< 500 Da
Log P	< 5
Melting point	< 200 °C
Aqueous solubility	≥ 1 mg/ml

The transfer of a drug through the skin can be quantified by the application of Fick's law of diffusion (Equation 1):

$$J = \frac{\mathrm{P} \cdot \mathrm{D} \cdot \Delta \mathrm{C}}{\mathrm{T}} \qquad (1)$$

whereby *J* is the flux or steady state permeation, *P* is the partition coefficient of the drug between the *stratum corneum* and the formulation, *D* is the diffusion coefficient of the permeant across the *stratum corneum*, ΔC is the difference in the permeant concentration across the *stratum corneum*, and *T* represents the thickness of the *stratum corneum* which can be referred as the diffusional path length [99].

In this law, diffusion is assumed to be the mass transfer of individual solutes, driven by random molecular movement and the rate of transport. The concentration of the drug and the surface area of which the drug is applied proportionally affect the rate of drug transport in which the amount of drug transported into the SC is increased by increasing the surface area of applications. The thickness of SC (T), which is variable depending on the anatomical site, is inversely proportional to the rate of drug transport. Introducing polar molecules to a lipophilic drug decreases lipophilicity and thus reduces the partition coefficient, resulting in a decreased rate of transport of drug across the skin [99].

1.4.2 Topical and transdermal formulation systems

The delivery of drugs to/through the skin can be accomplished using topical and transdermal dosage forms applied on the skin. Topical drug delivery is intended to treat local skin disorders with the retainment of the drug within the skin, while transdermal drug delivery is the delivery of a drug to the systemic circulation through the skin.

The general classification of these dosage forms incorporates solids, semisolids, and liquids systems. Gels, creams, and ointments are the most developed and utilised topical semisolid dosage forms, primarily because they allow easy application for the delivery of drug into the skin targeting localised dermatological disorders such as psoriasis, dermatitis, and eczema. Drugs have been applied to the skin to treat superficial diseases for many thousands of years. For instance, the use of potions, salves ointments, and patches, comprising of animal, mineral, plant extracts were already popular in Babylonian medicine and in ancient Egypt (~ 3000 BC) [104, 105]. However, the routine use of these dosage forms as transdermal systems for drug delivery only became common practice towards the end of the 20th century.

Transdermal drug delivery is the delivery of a compound through the skin and into the blood stream to treat systemic disorders. Delivering therapeutic agents through the skin enables drugs to bypass oral first pass enzymatic or chemical degradation in the liver or gastrointestinal tract. Therefore, transdermal delivery is of interest for drugs with limited oral bioavailability and short half-lives.

1.4.2.1 Semisolid emulsions (creams)

An emulsion is a mixture of two immiscible or partially miscible liquids, in which one is distributed in the form of fine droplets in the other. The most commonly used class of emulsions is the semisolid emulsions including creams and lotions for dermatological use [106].

Creams are semisolid emulsion preparations containing one or more drug molecules dispersed or dissolved in a suitable base. Creams are semisolids possessing a relatively fluid consistency and formulated as water-in-oil (w/o) or oil-in-water (o/w) emulsions depending on the base used. Two general classes of bases are utilised in creams, these are water-in-oil emulsion bases and oil-in-water emulsion bases. The base used in the semisolid formulation is a vehicle that can impact the effectiveness of the formulation. Creams spread more easily over the skin than the ointments and they are more cosmetically acceptable.

Water-in-oil (w/o) creams provide some degree of occlusion, possess good emollient properties, insoluble in water but contain water, and can absorb small quantities of water. Examples of w/o bases are petrolatum rose water ointment USP ('cold cream'), hydrous lanolin, Eucerin®, and Hydrocream®. Whereas o/w creams are easily removed by water, but they are insoluble in water, nonocclusive, and non-greasy. Examples include hydrophilic ointment USP, Unibase®, Dermabase®, Pentravan®, and Versatile™. The base is selected according to several factors including the requirement of occlusion or water washability, the condition of skin, and the desired extent and rate of absorption [99, 107, 108].

The process of developing new transdermal formulations is time-consuming due to the effort in choosing the matrix type, the drug loading, and the enhancers with their content, which will influence the permeation of the drug from the formulation through the skin [109]. Companies such as Fagron© and Medisca® have developed 'ready-to-use' compounding bases that are designed to suit different skin requirements and compatible with broad range of drugs. These vehicles are easy to use with simple compounding steps and are designed according to the latest knowledge of topical vehicle tolerance and safety.

1.4.2.2 Transdermal patches

The first transdermal patch was developed in 1979 and approved by US FDA was Transderm Scop® (scopolamine) for the treatment of motion sickness. Patches that were developed after scopolamine were nitroglycerin for angina pectoris, clonidine for hypertension, oestradiol for hormone replacement therapy for females, fentanyl for pain, nicotine for smoking cessation, and testosterone for hypogonadism [95, 110].

Transdermal patches can be formulated in two common systems: liquid/gel reservoir and solid matrix patches (Figure 1.5). In liquid/gel reservoir, a fluid or a semisolid that contain the drug is sequestered in a cavity formed between a permeable film and an impermeable backing film. The permeable membrane separates the reservoir from the adhesive layer. The steps of manufacturing the reservoir patches (also called form-fill-seal patches) and process of coating-drying are illustrated in Figure 1.6. The membrane in liquid/gel reservoir systems controls the release rate of the drug from the patch providing a constant rate of drug release from the system supporting zero-order kinetics (Figure 1.7). The primary limitation of this system is the possibility of reservoir rupture and leakage leading to drug toxicity. Another disadvantage of drug in reservoir system is the requirement of larger patch to achieve the delivery goal. The potential problems that might arise during the manufacturing process of reservoir patch include: machine misalignment defect, fold defect, cut into the patch, air bubble defect, and gel splash defect [95, 111].

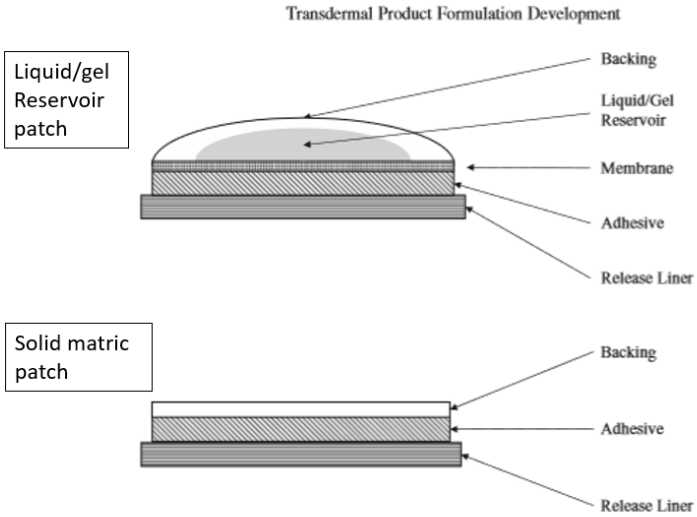

Figure 1.5 Two types of Transdermal patches: liquid/gel reservoir and solid matrix patches. Obtained from [90].

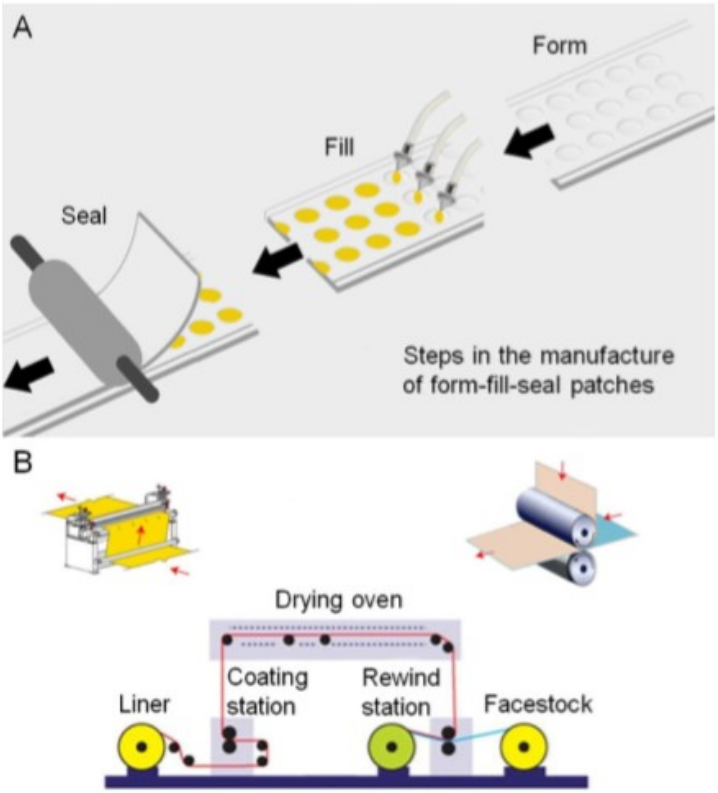

Figure 1.6 Process of manufacture for reservoir patches.

(A) Form-filling-sealing process; (B) Coating and drying process. Obtained from [111]

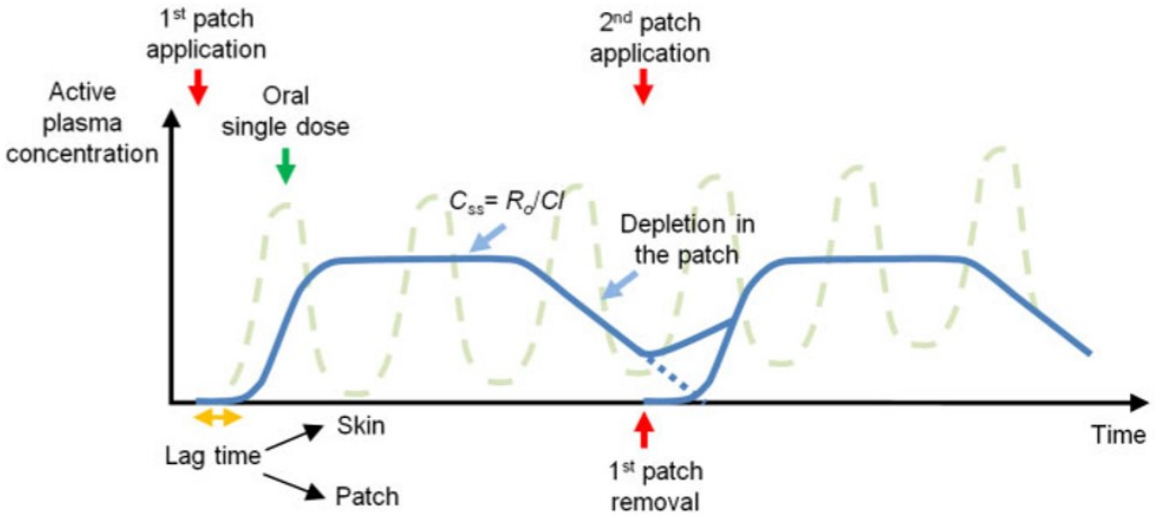

Figure 1.7 Drug plasma concentration profile after liquid/gel reservoir patch application

The lag-time represent the time taken for a drug to appear in systemic circulation following patch application. The figure depicts the depletion and removal of the patch as well as the corresponding profile for repeated oral dosing of the same drug. *Css* representing steady-state concentration, *R* is the dose rate, *Cl* is the clearance. Figure obtained from [111].

Because of the leakage problems associated with reservoir patch system, matrix patch systems were introduced and became the dominant products in the transdermal formulations market [111]. Matrix patches are more flexible, thinner, more comfortable and adhering, and the manufacturing is less expensive. A patch that does not contain liquid reservoir is regarded as matrix patch. In matrix patches, the drug is mixed with a polymeric or viscous adhesive in the same layer to deliver the drug and to adhere to the skin. Incorporating the drug into a pressure sensitive adhesive (PSA) provides not only adhesion but also a control on drug delivery rate [90, 95, 111].

The adhesive in transdermal patches (Figure 1.5) is a primary material that is responsible of attaching the formulation to the skin. Silicone polymers, acrylic copolymers, and rubber are three main types of pressure sensitive adhesive (PSA) polymers used often in transdermal patches. Acrylic PSAs are of low cost and excellent affinity for pharmaceutical compounds [90, 112]. However, a disadvantage is the presence of monomers that are unreacted and can be toxic. Whereas silicone PSAs offer high drug delivery, low irritation, and low reactivity. On the other hand, they have low solubility with drugs and their cost is high [90, 112]. Rubber adhesives demonstrate low cost and are typically chemically inert. The poor affinity of rubber adhesive for drugs and excipients and their low solvents solubility are key disadvantages [90, 112].

Backing films and release liners serve to protect and contain the transdermal drug formulation (Figure 1.5). The backing film contains and protects the formulation during the wear period and throughout the shelf life. The choice of backing material is critical due to its influence on the adhesion, delivery profile, appearance of the patch, and wearability. Some backings are laminates of several materials (e.g., ethylene vinyl acetate, polyethylene, positron emission tomography) which provide the desired properties [113, 114]. These materials must hinder unwanted absorption of the drug or other excipients. The backing film controls moisture evaporation and skin occlusion. The release liner protects the adhesive during storage. It must provide consistent and steady release from the adhesive throughout the shelf life of the product without interacting with the other components of the patch [113, 114].

1.4.2.3 Transdermal formulations in CNS disorders

Transdermal drug delivery for CNS indicated therapeutics offers the benefit of sustained drug release, reduce dosage frequency, improve patient's compliance and the possibility of reduced CNS side effects. Currently, a few CNS indicated transdermal formulations are available. A selegiline patch is available commercially (Emsam®) for the treatment of depression [115]. The bioavailability obtained from the selegiline transdermal system was compared to single

oral dose [116], with a significantly higher bioavailability with transdermal delivery, 73 %, compared to oral delivery, 4 %, suggesting that the transdermal system was able to reduce first-pass metabolism and provide sustained release pharmacokinetics [116].

Transdermal patch systems using matrix patches for CNS disorders are also commercially available with rotigotine (for restless legs syndrome and Parkinson's disease), rivastigmine (for Alzheimer's disease and Parkinson's disease dementia), capsaicin (for neuropathic pain associated with postherpetic neuralgia in nondiabetic adults), and lidocaine (for chronic pain from postherpetic neuralgia) [117].

1.5 Pharmacokinetic approaches to optimising clinical outcomes in CNS disorders: pharmacokinetic modelling and therapeutic drug monitoring

Clinical pharmacokinetics and therapeutic drug monitoring (TDM) are necessary tools to understand approaches to optimise clinical outcomes through rational therapeutic interventions. Clinical pharmacokinetics and TDM are of particular importance in neurologic and psychiatric disorders. Antipsychotics have variabilities in first-pass effect, absorption, and volume of distribution between different individuals and some antipsychotics have long elimination half-lives. TDM provides a treatment guidance framework to support medicines optimisation, through highlighting the necessity for personalised and individualised treatment regimens for patients, particularly special populations including pregnant women and paediatrics. Psychoactive agents such as SSRIs, antiepileptics, benzodiazepines, tricyclic antidepressants, antimigraine drugs, antipsychotic drugs, psychostimulants, and opioid analgesics are heterogeneous groups of drugs that are subject to interindividual variability which emphasis the requirement of individualised TDM. To this end, TDM could improve the management of DDIs, overdose, adherence, tolerability, genetic variabilities, and subsequently improve clinical response [118-121].

Key to current TDM approaches is the application of pharmacokinetic analysis to both assess the drug plasma concentrations in the context of a therapeutic range, and to support dose titrations with prior knowledge of the pharmacokinetic properties of drugs.

1.5.1 Basic principles of pharmacokinetics

Pharmacokinetics is the field of pharmacology which studies movement of drug molecules in the body. This involves the processes of drug absorption, distribution, metabolism and elimination [122, 123].

1.5.1.1 Absorption

Absorption is the process of transferring drug molecules from the administration site to the systemic circulation. For a drug to be absorbed after administering it as a solid formulation by oral route, disintegration and dissolution processes in the gastrointestinal fluid are required [124]. The dissolution rate is impacted by its water solubility, manufacturing processes, particle size, and the formulation excipients. Arthur Noyes and Willis Rodney Whitney [125] described the influence of the formulation and drug-specific properties on the rate of *in-vitro* drug dissolution in equation 2.

$$\frac{dC}{dt} = k \,.\, (C_s - C) \qquad (2)$$

where *Cs* is solubility concentration, *C* is the drug concentration in bulk media and *k* is the drug dissolution rate constant.

For a drug to be absorbed after dissolution, there is a requirement to permeate into the gastrointestinal epithelial enterocytes lining. The absorption through this barrier occurs by passive diffusion or active transport (carrier-mediated transport) as illustrated in Figure 1.8 [126, 127].

Passive transport involves drug molecules diffusing across the epithelial lining from an area of high concentration to an area of lower concentration until equilibrium is attained. Passive diffusion in the gastrointestinal tract could be by transcellular route (for lipophilic molecules) or paracellular route (for hydrophilic molecules). The transcellular routes involve the permeation of drug molecules through the enterocytes, while the paracellular route is the passage of drug molecules through aqueous pores in the membrane (between the enterocytes) (Figure 1.8). Passive diffusion of drug molecules is affected by gastric pH and the degree of drug ionisation in which unionised molecules, that possess higher lipid solubility, diffuse more easier than ionised molecules. For active transport, drug molecules require energy (liberated from the hydrolysis of ATP) to travel across the membrane barrier against the concentration gradient with the help of drug transporter proteins located in the membrane.

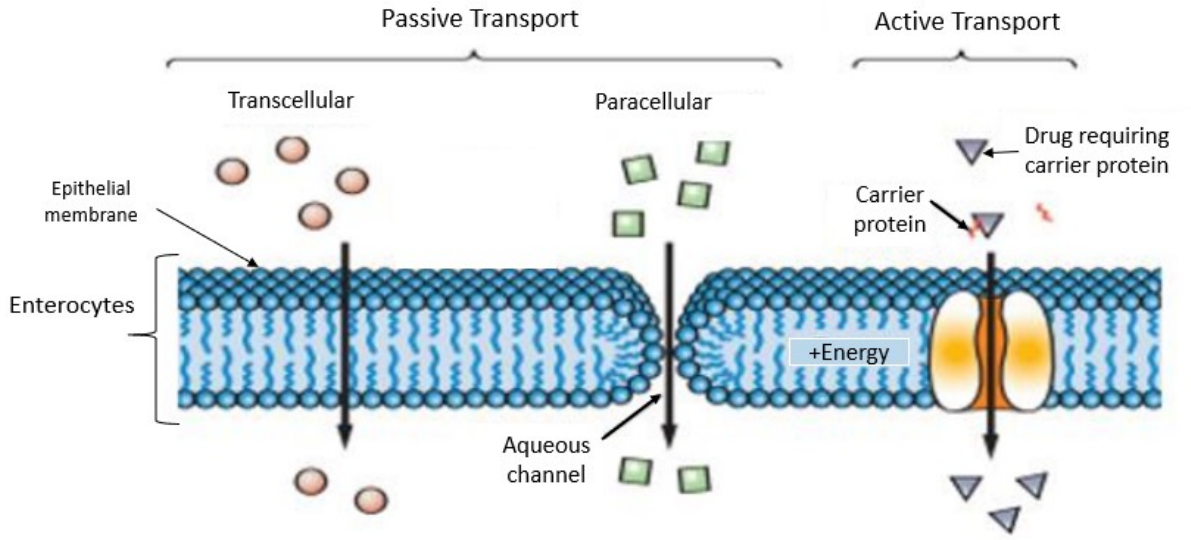

Figure 1.8 Modes of drug transport across the epithelial lining including the passive transport and active transport.

Circles represent transcellular diffusion of molecules through the enterocytes, squares represent paracellular diffusion through aqueous channel (between enterocytes), and triangles represent the active transport of a drug through membrane carrier proteins.

1.5.1.2 Distribution

Following absorption, drug molecules distribute across tissues through diffusion out of the systemic circulation. However, hindrances to this process can occur with binding to plasma proteins, such as human serum albumin (HSA) and alpha-1 acidic glycoprotein (AAG) [128, 129]. The capability of a drug to distribute into a specific tissue or organ depends on the extent of perfusion to the tissue. The liver, brain, and kidneys are rapidly perfused organs that receive a high supply of drugs that are carried in plasma, while adipose tissues and skeleto-muscular system are slowly perfused tissues that receive limited amounts of drugs and could result in delayed clinical response [128, 129].

The partitioning of drugs into tissues depends on the composition of tissue. Hydrophilic drugs are partitioned into high water organs and tissues, such as the muscles, while lipophilic drugs partition into the fat rich organs including liver, adipose, kidney, and brain [128, 129]. The distribution of a drug into its target site is also dependant on the binding capability of drug into plasma proteins. The drug must be in its unbound state to distribute in the circulation and elicit a clinical response, while protein bound drugs will not produce clinical effects [128, 129].

1.5.1.3 Metabolism

The metabolism of the drug is the alteration of drug's chemical structure to produce easily eliminated molecules following enzymatic processes occurring primarily in the liver. Hepatic drug metabolism is usually mediated by Cytochrome P450 (CYP) enzymes or by non-CYP enzyme pathways, and it usually occurs in two phases, Phase-I and Phase-II metabolism [130-133].

Phase-I metabolism occurs through CYP enzymes to obtain intermediate metabolites which will further be conjugated by Phase-II metabolism. CYP enzymes are located in the endoplasmic reticulum or the mitochondria and at least 57 functional CYPs genes have been identified and classified [134]. CYP1, CYP2, and CYP3 subfamilies are responsible for the metabolism of approximately 75 % of drugs and xenobiotics [134]. Of all the characterised human CYPs, the CYP3A4 is most abundant and has the greatest number of drug substrates, inhibitors and inducers when compared to the other CYP enzymes [134].

Phase-II is the process of conjugating the products of Phase-I metabolism through glucuronidation, acetylation, sulphation, methylation, and glutathione and Acyl Co-enzyme A conjugation. Phase-II enzymes include Uridine 5'-diphospho-glucuronosyltransferase (UGT), Sulphotransferases (SULTS), N-Acetyl transferases (NATs), glutathione S-transferase (GST), and methyl transferase [131, 133, 135, 136].

1.5.1.4 Excretion

Excretion is the process of removing the products of metabolism irreversibly from the body by the kidneys, as the primary route, or by biliary excretion. The process of drug excretion through the kidneys includes glomerular filtration, tubular secretion, and tubular reabsorption.

Tubular secretion, mainly at the proximal tubules, is the active transfer of materials to the renal tubular lumen from the peritubular capillaries through protein transporters. These protein transporters include the organic anionic transporters (OAT), the organic cationic transporters (OCT), and the multi-drug resistance-associated proteins (MRPs). Tubular secretion of drug compounds can be influenced by renal blood flow, plasma binding, and intrinsic clearance [137, 138].

Tubular reabsorption is the passive process of transporting drugs from the kidney back into the systemic circulation and it mainly occurs at the proximal tubules. Large, ionised, or hydrophilic molecules are not expected to undergo tubular reabsorption. Urine flow rate can affect the reabsorption of molecules in which the higher the urine flow rate the lower is the reabsorption due to the reduced concentration gradient and contact time [138].

1.5.2 Pharmacokinetic parameters used in TDM

Applying TDM to optimise clinical outcomes requires consideration of key pharmacokinetic parameters obtained from plasma drug concentration versus time profiles. These include the clearance (*CL*), volume of distribution (*Vd*), half-life ($t_{1/2}$), area under the curve (AUC), and bioavailability (*F*) [139].

Clearance is the process of drug elimination from the body, and it reflects the volume of body fluid from which the drug is excreted per unit time [139, 140]. The liver and kidneys are the main drug clearance sites, but other sites could also contribute such as sweat and saliva. The total clearance (CL_T) of a drug is the sum of the clearances from all organs where the elimination of a drug occurs, including blood clearance (CL_b) and plasma clearance (CL_p) (Equation 3).

$$CL_T = CL_b + CL_p + CL_{other} \qquad (3)$$

The volume of distribution (*Vd*) is referred to the apparent volume in which the drug is present to provide a particular concentration (*C*). Drugs distribute differently according to their properties, i.e, lipophilic drugs distribute to adipose tissues, while hydrophilic drugs distribute into the water fractions of organs and tissue. A factor that can affect the *Vd* of a drug is its binding capacity to blood (erythrocytes), plasma proteins, and tissues, resulting in low volumes of distribution. The volume of distribution may be expressed with respect to the administered dose and the expected blood/plasma concentration (*C*) [139, 140] (Equation 4)

$$Vd = \frac{Dose}{C} \qquad (4)$$

The half-life ($t_{1/2}$) represents the duration of time for the plasma concentration of a drug to be reduced by 50 %. The half-life depends on the clearance and the volume of distribution of a drug, therefore, any alterations in protein binding may impact both the *CL* and *Vd*, and consequently will influence the half-life of a drug (Equation 5).

$$t_{1/2} = (0.693)\ .\ \frac{Vd}{CL} \qquad (5)$$

The AUC measures the systemic drug exposure following administration through any route. AUC can be determined using the trapezoidal rule in the calculation of the area under the curve of drug concentration-time profile. For an oral dose, the AUC can be estimated with respect to the dose and the total clearance (Equation 6):

$$AUC_{oral} = \frac{Dose_{oral}}{CL_T} \qquad (6)$$

Bioavailability (*F*) represents the fraction of the administered dose that reach the systemic circulation. For intravenous administration, *F*=1 since the drug reaches the systemic circulation immediately. For oral administration routes, the bioavailability is usually less than 1, due to the potential first pass effect, chemical degradation by pH changes along the gastrointestinal tract, the potential secretion by of efflux proteins, or metabolism due to the influence of drug metabolism enzymes [139, 140] (Equation 7)

$$F = \frac{AUC_{oral}}{AUC_{iv}} \quad (7)$$

To determine such pharmacokinetic parameters, approaches such as empirical or compartmental modelling are used, through the application of pharmacokinetic models.

1.5.3 Empirical pharmacokinetics modelling

Empirical pharmacokinetics requires the presence of existing clinical data (plasma concentrations) to determine pharmacokinetic metrics. Empirical pharmacokinetic modelling utilises two approaches termed compartmental and non-compartmental modelling [141, 142].

1.5.3.1 Compartmental modelling

Compartmental modelling incorporates pharmacokinetics concepts including absorption, distribution, metabolism, and elimination into logical mathematical terms. This enables the modelling of complex physiological activities by considering the body as one or more compartments which will allow the prediction of drugs' pharmacokinetics and illustrate the parameter of that system. Parameters including volume of distribution, area under the curve (AUC), half-life, and elimination rates could be determined with compartmental modelling [143]. A compartment is considered as a unit or a box that represent multiple tissues having the same rate of drug distribution [144]. The assumption is that the compartments does not represent any specific tissue and the drug concentration is homogenous in the compartment.

1.5.3.2 Non-compartmental analysis (NCA)

Non-compartmental analysis (NCA) is model-independent approach and an empirical method relying on a collection of individuals clinical data [145]. Because there is no compartment that needs to be assumed to fit the drug pharmacokinetics profile, NCA requires less restrictive assumptions to conduct the modelling method when compared to compartmental analysis [146]. Model development process in NCA is more manageable and straightforward for modellers with less experience. When opposed to compartmental modelling, NCA requires fewer plasma samples and sampling time may not be as crucial. NCA is used to calculate

important parameters including mean residence time (MRT), mean absorption time (MAT), and the area under the first instant of the systemic drug concentration curve (AUMC). NCA results are usually a generalisation of a compartmental analysis, but they are nevertheless valuable for providing a broad picture extrapolation of a drug's pharmacokinetics profile, especially when it is still in early stage of development [143].

1.5.4 Physiologically based pharmacokinetic (PBPK) modelling

Physiologically based pharmacokinetic (PBPK) modelling is a mechanistic approach that, unlike the empirical approaches, does not depend on clinical and preclinical data to extrapolate the drug to predict its pharmacokinetic parameters [147-149]. Physiologically based pharmacokinetic (PBPK) modelling has proceeded as a promising approach to overcome drug development challenges [150, 151]. PBPK is a system biology approach that uses a mechanistic method to predict and estimate drug's pharmacokinetics using physiological and biological mechanisms of species [152]. To describe the best estimates of drug's pharmacokinetics in the body, PBPK use both mathematical models and drug specific properties including the metabolic, physicochemical, and pharmacogenomic data achieved by preclinical or *in-vitro* pharmaceutical experiments and species-specific physiological, anatomical and pathophysiological parameters [152].

In PBPK modelling, compartments reflect different body organs (Figure 1.9), and the body processes that affects drug concentrations are modelled in mathematical expressions that aid in quantifying drug disposition in a particular organ or tissue [150-152]. With PBPK, the physiology of the organs involved in drug's pharmacokinetics is also modelled. For example, with the administration of an oral drug, several factors that affects the release of drug from its delivery system into the systemic circulation should be considered such as gastric emptying, regional variations of drug, intestinal pH and geometry, metabolising enzymes, and transporter proteins across the small intestine [152]. Other pharmacokinetics processes are also modelled including tissue partitioning, drug permeability, absorption, metabolism, and clearance, due to the potential impact on drug disposition [150-152].

Several factors could influence the variability of drug's pharmacokinetics, these include demographics (sex, gender, body surface area, ethnicity, and body weight), genetic phenotypes (polymorphism), drug-drug interactions (DDI), environmental factors (diet and smoking), and physiologic factors (pregnancy, hepatic and renal impairment or other disease states) [153, 154]. Clinical trials often recruit individuals with normal biochemical and physiological body composition, while recruiting special populations such as pregnant women, paediatrics, patients with renal and liver diseases, and geriatrics, is still challenging. This

resulted in poorly made clinical decisions regarding drug doses due to the lack of enough clinical pharmacokinetics studies on these special populations.

PBPK modelling is a unique and powerful tool due to the incorporation of biochemical and physiological differences between populations, thus, describe drug's pharmacokinetic parameters that are population specific where there is limited clinical data available [155]. PBPK allows better understanding of differences in pharmacokinetics parameters during the gestation period with understanding the physiological changes in each trimester that could influence drug exposure suggesting dose adjustments. Also, PBPK could be used for paediatrics and geriatrics to understand physiological and anatomical changes which could influence drug pharmacokinetic parameters at different scenarios.

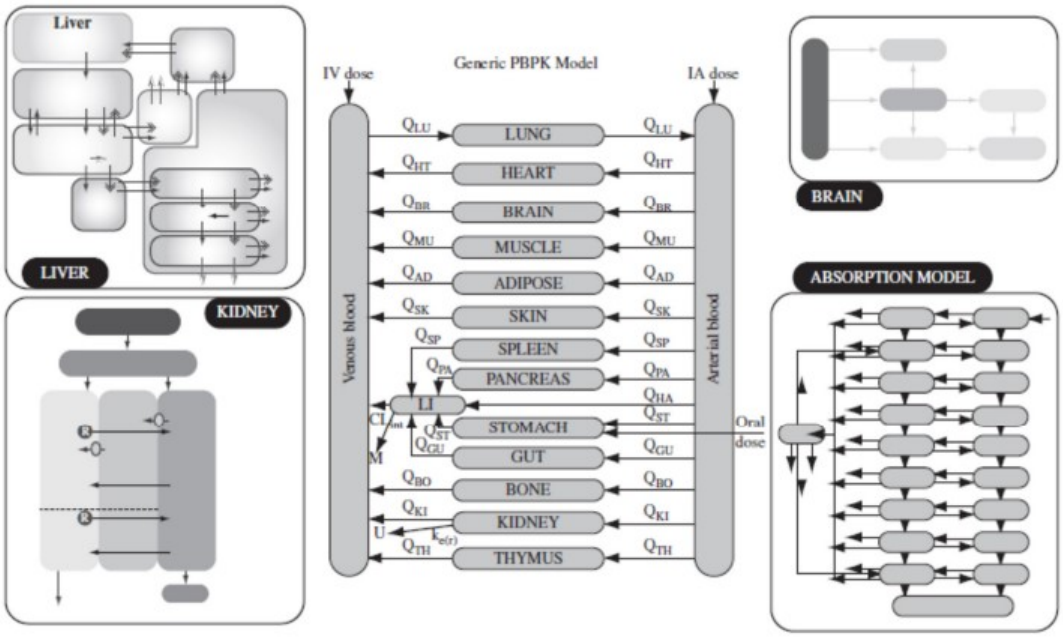

Figure 1.9 Schematic diagram of PBPK models.

Obtained from [156]

1.5.4.1 Software based PBPK modelling approaches

Because of the advancement of technology in pharmacokinetic modelling, PBPK models are currently constructed into computer software programs to enhance the capacity of predictability of the models. This approach in predicting pharmacokinetics parameters using a software is called in silico PBPK modelling. In silico PBPK modelling is beneficial in addressing drug development challenges such as cost at preclinical stages when clinical data are not available by predicting the potentially unsafe drugs and exclude them at early drug development stages.

A primary example of such tools is the Simcyp® Simulator (https://www.certara.com/), which is a population-based simulator that provides virtual trial simulation systems and includes genomic, physiologic, and demographic genomic databases with algorithms accounting for the variability of patients. The behaviour of drug in virtual patient populations can be predicted allowing the identification of individuals with extreme risk. Simcyp® allows linking *in-vitro* data of drug to *in-vivo* pharmacokinetic/pharmacodynamic profiles and *in-vivo* drug absorption, distribution, metabolism, excretion. This is beneficial when conducted prior to human studies to explore the potential complexities and to support drug development decision making. With Simcyp®, researchers can save time and money, drug labels could be optimised, and patients' risk decrease. Additional features are proposed by this software program including the simulation for virtual specific populations (paediatrics, obese, pregnant women, renal and liver impairments, and others), complex pharmacokinetic simulations involving metabolite profile, simulating drug-drug interactions, and clearance prediction models [157].

1.5.4.2 Application of PBPK modelling in medicines optimisation

Conner et al. 2018, addressed and evaluated the drug-drug interactions of the common antiepileptic drug valproic acid (VPA) by developing PBPK models for adults and children. This study adds UGT enzyme kinetics and an advanced ADAM model for extended release (XR) formulation of valproic acid to existing physiologically based pharmacokinetic (PBPK) models for VPA. The model was successfully validated with observed data with and without DDIs [158]. Also, the same group developed a lamotrigine PBPK model for IR and ER formulations which accurately predicted DDIs and lamotrigine IR/XR disposition in adults and children [159]. The authors suggested that their developed models can be used to improve the efficacy and safety of valproic acid and lamotrigine at different unexplored case scenarios [158, 159].

Furthermore, examples of PBPK modelling for CNS therapeutics was examined in a study by Huang et al., 2017, in the development of a model for atomoxetine, which is used for attention deficit hyperactivity disorder (ADHD). Their developed models demonstrated successful validation and predictions which suggested that their models can be extrapolated to different DDIs, ethnicities, and paediatrics at different scenarios for atomoxetine [160].

Badhan et al. 2019 [161] used software-based PBPK modelling to explore DDI and the need of dose optimisation of methadone when used concurrently with rifampicin. The model predicted the need of methadone dose increase to maintain the plasma concentrations within the therapeutic window when administered with rifampicin, also, their prediction demonstrated that during rifampicin cessation, a dose reduction of 10 mg every 2 days prior to rifampicin cessation was required to maintain methadone therapeutic levels [161]. PBPK in this study

aims to reduce the risk of illicit drug use and suboptimal therapy in patients taking methadone for the management of opioid use disorder concurrently with rifampicin.

Kneller et al. 2019 explored the pharmacokinetics of aripiprazole with investigating CYP2D6 phenotypes using PBPK, their predictions suggested that only poor metabolisers require dose adjustments [162].

In addition, several studies conducted over the last decade have shown the importance of PBPK in improving clinical outcomes in special population groups such as pregnancy, paediatrics, renal patients, and the elderly. Polasek et al. (2013) conducted PBPK modelling on elderly and predicted a reduced metabolic clearance with four drugs that showed good model predictability [163]. PBPK modelling was successful in predicting altered plasma concentrations of 7 drugs in diabetic patients and another study demonstrated the usefulness of PBPK in predicting the observed plasma profiles of 151 drugs in chronic kidney disease patients [164, 165].

Mendes et al (2015) [166] predicted the systemic exposure of antiretroviral (ARV) drugs using PBPK modelling, and their model was successful in the optimisation of ARV drugs in pregnant women. Further, Alqahtani et al (2015) [167] developed a PBPK model that predicted the pharmacokinetics of indomethacin in pregnant women (second trimester) adequately. Walsh et al (2016) [168] demonstrated the importance of PBPK simulations in managing actinomycin D dosing in young patients as their model gave good actinomycin D predictions.

Jogiraju et al. (2017) utilised PBPK modelling by Simcyp® simulator to explore the influence of pregnancy on the pharmacokinetics of 3 drugs (metformin, tacrolimus, oseltamivir). The model successfully predicted the changes observed in C_{max} and AUC in each trimester when compared to post-partum. Simcyp® model outputs were useful in corelating the results with pregnancy-induced alteration in hepatic CYP3A4 activity (tacrolimus), renal blood flow (metformin, oseltamivir), and reduced plasma protein levels (tacrolimus) [169].

Zhou et al. (2019) illustrated the importance of PBPK modelling in exploring ceftazidime exposure in renal impairment patients. They demonstrated the alterations noticed in pharmacokinetics parameters of ceftazidime when comparing renal patients and healthy volunteers which include the increase in mean plasma AUC values with increasing the severity of renal impairment [170].

Zakaria et al. (2018) explored the pharmacokinetics of clopidogrel in Malaysian population groups and illustrated the impact of inter-ethnic variability on the attainment of the target plasma concentration of clopi-H4, which is the active metabolite of clopidogrel. This was explored under the effect of different CYP2C19 polymorphisms through PBPK modelling. A significant difference was illustrated in the C_{max} of clopi-H4 when comparing extensive metabolisers (EM) and poor metabolisers (PM) phenotypes with the tested population groups. A partial recovery of the C_{max} of PMs was attained by suggesting a high-dose strategy using a high loading dose and followed by a maintenance dose, this resulted in higher PM subjects reaching the therapeutic minimum target concentration of clopi-H4 [171].

Olafuyi et al. (2017a) developed a paediatric physiologically based pharmacokinetic model to explore the influence of rifampicin (CYP3A4-inducer) when concomitantly used with artemether and lumefantrine (AL) for tuberculosis co-infected malaria subjects. The predictions for 2-5 years old children illustrated that no subjects reached the target day 7 concentration which necessitates dose adjustments. Olafuyi et al. (2017a), adapted a treatment regimen which resulted in more than 60 % of subjects reaching the required target concentration [172]. Olafuyi et al. (2017b) applied PBPK modelling to evaluate the impact of antiretroviral-mediated DDIs on piperaquine antimalarial therapy during gestation. They demonstrated the safe use of piperaquine during pregnancy as the day 7 concentrations were optimal and consistent. Their model predictions also highlighted that the pharmacokinetics of piperaquine was significantly altered with antiretroviral-mediated DDIs during pregnancy [173].

1.5.4.3 Translational pharmacokinetics

As highlighted in the previous section, PBPK modelling has had a considerable impact on academic, regulatory, and clinical decisions throughout the last decade. The US FDA have utilised modelling and simulation strategies to address questions regarding drug development, regulatory and therapeutic issues [174].

Drug-drug interactions of guanfacine with moderate CYP3A4 inhibitors or inducers were predicted by employing PBPK modelling using Simcyp® to optimise dosing strategies in adolescents and children. The dosing recommendations for guanfacine based on these predictions were FDA approved without the requirement of conducting further clinical studies [175].

Another example of regulatory and clinical impact of PBPK modelling is the evaluation of quetiapine systemic exposure in adults, children, and adolescents after administration of immediate release (IR) and extended release (XR) formulations. Simcyp® was used to

compare the two formulations and the model prediction indicated that children and adolescents would receive equivalent exposures if the XR formulation was given once daily, or the IR formulation was given twice daily at similar total doses per day. This was a high-impact application of paediatric PBPK modelling in that the requirement of clinical study was avoided and Quetiapine XR® was approved for paediatric labelling [176].

The exposure of deflazacort in children and adolescents was evaluated using PBPK modelling with the simulation of DDIs. Dosage recommendations were provided in the presence of moderate to severe CYP3A4 inducers and inhibitors and have been accepted as supporting evidence for the deflazacort label's proposed dosing recommendations [177].

In 'high-impact' scenarios, model-informed biosimulation through the application of PBPK modelling in virtual clinical trials predicts the dose that is most likely to optimise efficacy and/or minimise toxicity for a given patient based on their unique covariates known to impact medication response. This is limited to trained healthcare providers and academic hospitals with strong expertise in clinical pharmacology. Examples include the use of these models for antibiotics precision dosing in critically ill patients [178], metformin dose suggestion for renal impairment patients [179], chemotherapy and immunosuppressants in critical paediatric disorders [180-182].

1.6 Thesis aims and objectives

The overall aim of this study is to improve the clinical outcomes in CNS (primarily mental health) disorders through pharmaceutical and pharmacokinetic approaches. The pharmaceutical approach focuses upon the use of hesperetin, as a potential novel phytochemical candidate for CNS disorders, utilising transdermal formulations including creams and patches. Hesperetin was chosen due to its novelty, potential candidate for CNS disorders, few transdermal studies, and its suitable physiochemical properties for transdermal delivery. While the pharmacokinetic approach includes the use of PBPK modelling to demonstrate the application of this technology to support optimising possible clinical outcomes in the treatment of mental health in pregnant women, using virtual clinical trials to improve pharmacokinetics profiles of the antidepressants paroxetine and sertraline. Paroxetine and sertraline are widely prescribed for depression, and they were chosen due to their complex pharmacokinetic profiles during pregnancy that needs to be addressed

The format and work contained within this thesis is translational in nature, aiming to demonstrate the importance and potential of considering both pharmaceutical and pharmacokinetic approaches in optimising clinical outcomes.

To realise those aims, the overall objectives were:

- **Chapter 2:** To develop hesperetin cream formulation systems using commercially available compounding pharmaceutical base creams including Vanish-pen™, Doublebase™, Versatile™, and Pentravan® and to identify the most appropriate vehicle in terms of drug release with understanding the release kinetics. Furthermore, to assess the formulations during storage for 10 weeks at temperatures 4 ºC and 25 ºC using morphological characterisation, organoleptic properties assessment, pH assessment, *in-vitro* drug release studies, and kinetics assessment.

- **Chapter 3:** To develop hesperetin transdermal patch systems using Dow Corning® BIO-PSA 7-4501 silicone adhesive and Eudragit® E100 with different plasticisers (polyvinylpyrrolidone 30 (PVP 30), Tween® 20, glycerol, triacetin), and to identify the most appropriate transdermal patch in terms of visual mechanical properties and efficient drug release. Moreover, to evaluate the patches during storage for 3 weeks at temperatures 4 ºC and 25 ºC using morphological characterisation, visual mechanical properties assessment, pH assessment, *in-vitro* drug release studies, and kinetics assessment.

- **Chapter 4:** To apply the principles of mechanistic pharmacokinetic modelling and virtual clinical trials to elucidate the causative effects of the decrease in plasma paroxetine levels during gestation and to provide a clinically relevant dosing adjustment strategy that could be implemented to maintain plasma paroxetine levels during gestation, when taking into consideration the CYP 2D6 phenotype status patients.

- **Chapter 5:** To apply the principles of PBPK modelling and virtual clinical trials for the evaluation of the influence of gestation on plasma sertraline levels and to provide a clinically relevant dosing titration strategy for CYP 2C19 phenotype status during gestation by maintaining the required sertraline plasma concentration levels.

Chapter 2

Topical and transdermal delivery of hesperetin for CNS disorders using commercial compounding cream bases

2.1 Introduction

Flavonoids found in citrus fruits (oranges and grapefruit) are termed citrus flavonoids, and include hesperetin, naringin, diosmin, rutin, naringenin, and quercetin [183]. Hesperetin has been studied widely and demonstrated several pharmacological effects including neuroprotection, anticancer, anti-inflammatory, antioxidant, antidepressant, hypolipidemic, and anticonvulsant properties [52, 76, 81, 184-187].

It has been suggested that hesperetin can cross the BBB and reach the CNS where it exerts its neuroprotective properties [76, 185, 187]. The safety, efficacy, and cheap availability of hesperetin make it a candidate drug for pre-clinical and clinical studies for the management of neurodegenerative disorders.

In major depressive disorder, the effects of hesperetin in improving depression has been explored with a range of possible mechanisms [67, 74, 188, 189]. Hesperidin and its aglycone hesperetin have shown an antidepressant and anxiolytic effects when administered to diabetic rats which was achieved by activating the nuclear factor erythroid-2-related factor 2 (Nrf2)/antioxidant response element (ARE) pathway in the brain [188, 189]. Nrf2/ARE pathway is the most important antioxidant pathway to date and is found to be inactivated in prolonged high glucose condition causing diabetic complications including depression and anxiety [189].

Another study showed that hesperidin and hesperetin exerted antidepressant-like effects in both chronic and acute treatment in mice [74]. This study suggested that the antidepressant effects are mediated by increasing BDNF levels in hippocampus and inhibiting l-arginine-NO-cGMP pathway [74]. In a further study, the antidepressant effect of hesperidin in mice was studied and highlighted that the pharmacological effects are related to interactions with the serotonergic 5-HT(1A) receptor [67].

In addition to its CNS-related effects, it was demonstrated that hesperetin can prevent angiogenesis, induce cancer cells apoptosis, reduce cancer cell proliferation, and suppress cell migration [190]. Studies have revealed the efficiency of hesperetin against human skin carcinoma cells [191, 192], carcinoid cancer [193], breast cancer [194, 195], lung cancer [196, 197], prostate cancer [198], and gastric cancer [199].

2.1.1 Physicochemical properties of hesperetin

Hesperetin has a molecular weight of 302.28 g/mol, logP value of 2.4, and a melting point of 227.5 °C, with 3 hydrogen bond donors and 6 hydrogen bond acceptors [200-202]. It is a trihydroxyflavanone with three hydroxy groups at the 3'-, 5- and 7-positions with an additional methoxy substituent at 4'-position (Figure 2.1) [185]. Hesperetin is the aglycone form of hesperidin and it is absorbed in the small intestine. The majority of hesperetin metabolites are obtained by the first-pass metabolism of hesperetin in intestinal cells into hesperetin 7-*O*-glucuronide and 3′-*O*-glucuronid, while the remaining metabolites consisted of sulfoglucuronides [203].

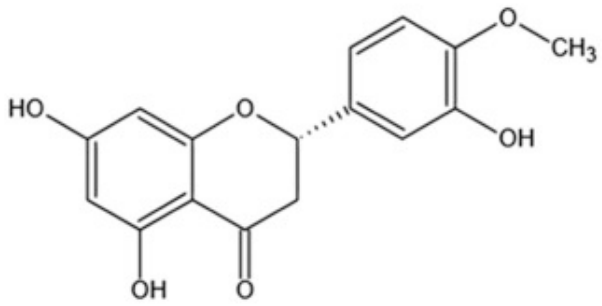

Figure 2.1 Chemical structure of hesperetin.

Obtained from [204]

Hesperetin pharmacokinetics have been studied and demonstrated to possess a low oral bioavailability resulting from the extensive first-pass metabolism, its lipophilic nature, and its low aqueous solubility, this consequently result in low and often subtherapeutic concentrations in the systemic circulation following oral administration [185, 193, 205-210]. Given these limitations to optimal oral bioavailability, the use of transdermal formulation systems for hesperetin may have the potential to deliver higher plasma concentrations than those obtained following oral delivery. However, such studies are currently lacking.

2.1.2 Pharmaceutical semisolid emulsions for topical and transdermal drug delivery

An emulsion is a mixture of two immiscible or partially miscible liquids, in which one is distributed in the form of fine droplets (internal phase), in the other (the external phase) (Figure 2.2). One liquid is nonpolar including oil, lipid, or wax, and the other liquid is polar including water or aqueous solution. Oil-in-water (o/w) emulsions composed of oil droplets distributed in water, and water-in-oil (w/o) emulsions include water droplets distributed in oil. The most commonly used class of emulsions is the semisolid emulsions including creams and lotions for dermatological use [106].

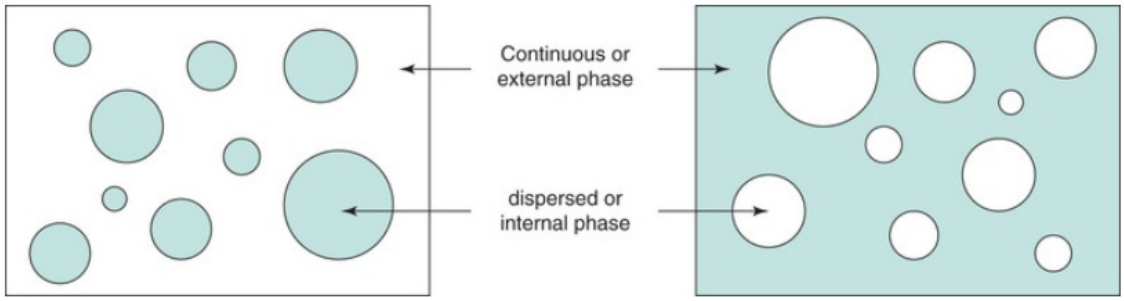

Figure 2.2 The representation of emulsions showing the oil-in-water emulsion (left) and the water-in-oil emulsion (right) with the shaded area representing oil.

Obtained from [106]

2.1.2.1 Composition of pharmaceutical emulsions

Pharmaceutical emulsions are composed of an oil phase, water phase, emulsifiers, and other excipients such as preservatives, antioxidants and humectants. The choice of the components and type of emulsion depends on the administration route, desired physical properties, the solubility of drugs, the desired rheological properties, clinical use, and therapeutic response.

2.1.2.1.1 Oils and emulsifiers

Hydrocarbons-based oils are widely used for emulsions applied externally such as liquid paraffin, benzyl benzoate, turpentine oil, and various silicone oils [211].

Emulsifiers are necessary for controlling the stability of emulsions during shelf life. Without emulsifiers, emulsions will be thermodynamically unstable and will tend to crack by separating the two phases of oil and water through coalescence. Combinations of emulsifying agents are usually used in practice instead of single agents due to the enhanced stability by multiple agents. Emulsifiers control stability by the formation of a barrier at the droplet interface, which is called an interfacial film, or in the external phase as a rheological barrier. These barriers are responsible of preventing the coalescence of the dispersed droplets, hence, the enhanced stability. There are two general groups of emulsifiers: (i) synthetic or semisynthetic surfactants and polymers (including anionic, cationic, non-ionic, polymeric, fatty amphiphiles) and (ii) agents from natural origin [106, 211] (Table 2.1).

Table 2.1 Classes of emulsifying agents for topical administration.

Class	Example	Emulsion type
Anionic	Sodium lauryl sulfate	o/w
	Sodium stearate	o/w

	Calcium oleate	w/o
Cationic	Cetrimide	o/w
Non-ionic	Polyethylene glycol 40 stearate	o/w
	Sorbitan monooleate (Span 80)	w/o
Polymeric	Poloxomers (Pluronic F-68)	o/w
Fatty amphiphiles	Cetostearyl alcohol	o/w
	Commercial cetyl alcohol	o/w
	Commercial stearyl alcohol	o/w
	Triple-pressed stearic acid	o/w
	Glyceryl monostearate	o/w
Natural origin	Sterols (wool fat, choleserol and its esters)	w/o
	Bentonite	o/w, w/o

2.1.2.1.2 Preservatives

The aqueous phase in o/w emulsions are strongly susceptible to contamination by the growth of fungi and bacteria. This contamination could potentially be a health hazard and affect the physiochemical characteristics of the emulsions including pH, colour, or odour changes in addition to phase separation.

w/o emulsions are less prone to contamination due to the enclosure and protection of aqueous phase by the oil phase. Phenoxyethanol, p-hydroxybenzoates, and benzoic acid are commonly used preservatives in topical emulsions [106].

2.1.2.1.3 Antioxidants and humectants

Antioxidants in emulsions are important to prevent oxidative reactions of the components which could cause changes in physical properties. Commonly used antioxidants in pharmaceutical emulsions are butylated hydroxyanisole, butylated hydroxytoluene, the alkyl gallates, and α-tocopherol. Humectants are commonly added to dermatological emulsions to reduce water evaporation during use and storage. Glycerol, propylene glycol, and sorbitol at low concentrations are commonly used humectants [106].

2.1.2.2 Oil-in-water creams

The type of creams that are mostly used pharmaceutically and cosmetically are generally the o/w semisolid emulsions (o/w creams). The structuring and stability of the continuous phase in o/w creams is enabled by either the addition of rheological modifiers including polymeric materials, or, by forming lamellar gel network phases (α-crystalline gel network phase) through the interactions of various emulsifiers and water. In the preparation of o/w creams, soluble fatty amphiphiles mixed with water-soluble surfactants are commonly used (Table 2.2). o/w creams

consist of four phases, a dispersed oil phase stabilised by interfacial film, α-crystalline gel phase consist of bilayers of surfactant and alcohol separated by interlamellar fixed water layers, α-crystalline hydrates, and the continuous water phase (Figure 2.3). These multiple phases ensure the immobility of oil droplets and prevent flocculation and coalescence [106].

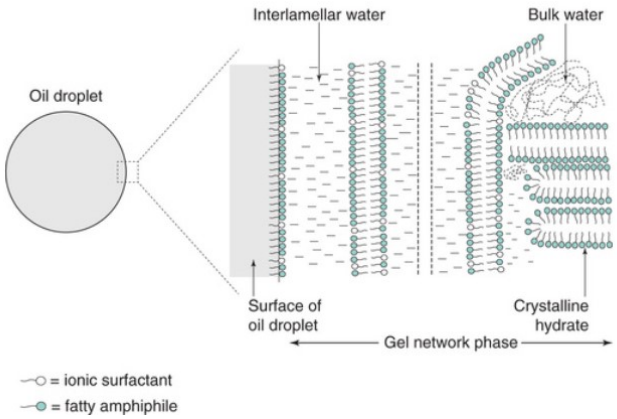

Figure 2.3 The illustration of the complex nature of o/w cream system and it structured gel network phase that ensures the immobility of oil droplets.

Obtained from [106]

2.1.2.3 Compounding pharmaceutical bases

Compounding vehicles that are 'ready-to-use' are developed and designed to suit different skin requirements and compatible with broad range of drugs. These vehicles are easy to use with simple compounding steps and are designed according to the latest knowledge of topical vehicle tolerance and safety. A wide range of pharmaceutical base creams are available for compounding (Table 2.2). Studies have explored the capability of some vehicles to deliver drugs through the skin. The o/w base creams mentioned below are vehicles for both hydrophilic and hydrophobic drugs due to their composition which is oil and water.

Table 2.2 The appearance and description of the evaluated pharmaceutical base creams.

Pharmaceutical Base formulations	Appearance	Description	Notes
Vanish-pen™ cream base by Medisca® [212]	Off-white o/w cream	- Vehicle for hydrophilic and lipophilic drugs. - Pluronic lecithin organogel (PLO) - based.	- PH 5-6 - Stable at 40°C - Stable in the presence of both salt and base forms of active agents. - Penetrating capabilities not available.

PLO transdermal cream by Medisca® [212]	Off-white o/w cream	- Vehicle for hydrophilic and lipophilic drugs. - PLO-based. - Slightly sticky.	- Good penetrating capabilities extrapolated based on *In-vitro* skin penetration of Progesterone
VersaPro™ gel base by Medisca® [213]	Clear to slightly hazy. Viscous gel.	- Vehicle for hydrophilic and lipophilic drugs. - Quick drying, non-greasy.	- Proven target site delivery with Diclofenac Sodium
VersaPro™ cream base by Medisca® [212]	White, shiny, elegant o/w cream	- Vehicle for hydrophilic and lipophilic drugs. - Non-greasy. - Hypoallergenic.	- Excellent penetrating capabilities extrapolated based on *In-vitro* skin penetration of Progesterone
PenDerm™ cream by Medisca® [212]	White o/w cream	- Vehicle for hydrophilic and lipophilic drugs.	- Excellent penetrating capabilities extrapolated based on *In-vitro* skin penetration of Progesterone
Doublebase™ gel by Dermal® [214, 215]	White opaque hydrating gel	- Hydrating gel. - high protective and moisturising properties containing high amount of emollient oils and glycerol.	- Aids in treating chapped or dry skin conditions such as psoriasis, eczema, ichthyosis or elderly dry skin. - The active ingredients are liquid paraffin and isopropyl myristate. Other ingredients: glycerol, carbomer, sorbitan laurate, trolamine, phenoxyethanol, purified water - No freezing - No storage above 25°C
Versatile™ cream base gel by Fagron© [108].	Shiny, white to off-white o/w cream	- Hydrophilic vanishing base cream with excellent hydration effect. - Its consistency is retained with high concentrations and broad range of APIs, solvents, and dermaceutical ingredients.	- PH of 3.5-5.5 - Store below 25°C - The ingredients are purified water, emollient, O/W emulsifiers, lubricant, vitamin E, pro-liposome, silicone, chelating agent, and preservatives. - Free of any harmful and controversial ingredients.
Pentravan® cream base by Fagron© [107].	Yellow o/w emulsion	- Great extent and rate of absorption of the API. - Compatible with a broad range of APIs. - Non-greasy.	- pH of 4-5.5. - Liposomal matrix with penetration enhancing ingredients. - Fragrance free.

Pentravan® was investigated to deliver ketoprofen and testosterone percutaneously and compared to Pluronic Lecithin Organogel (PLO) [216]. In this study, Pentravan® demonstrated 3.8-fold higher ketoprofen absorption than PLO and 1.7-fold higher testosterone absorption than PLO [216]. A study by Kirilov et al. (2016) used Pentravan® and low molecular-mass organic gelator (LMOG) organogel to deliver enrofloxacin but the later provided 3.7 times higher absorption [217]. Polonini et al. (2014a) performed drug release studies on Pentravan® formulation containing human sexual steroids which showed high release rates [218]. In another study by Polonini et al. (2014b) Pentravan® was evaluated to deliver female sexual steroids (progesterone, estradiol, estriol) transdermally. The results demonstrated that Pentravan® provided satisfactory permeation rates through human skin and expected to deliver good efficacy systemically [219]. Two studies used Pentravan® successfully to deliver enrofloxacin transdermally to reptiles' skin [220, 221]. Pentravan® and other ready-to-use transdermal vehicles were compounded with anti-emetic drugs (aprepitant, dexamethasone, ondansetron) and assessed [109]. Pentravan® was one of the most efficient vehicles tested to release aprepitant and dexamethasone in terms of quantity [109].

A few studies have utilised Versatile™ as a vehicle to deliver drugs topically and assessed drugs' percutaneous permeation [222-224]. The percutaneous absorption of some analgesics compounded to Versatile™ versus a reference cream was investigated [224]. The study has shown that Versatile™ formulation had improved characteristics and the authors anticipated that Versatile™ could provide enhanced transdermal delivery of some of the tested analgesic medications (ketamine, bupivacaine, diclofenac, gabapentin, orphenadrine, and pentoxyifylline) compared to the reference cream [224].

The stability of several compounded preparations in Vanish-Pen™ cream base (by Medisca®) was assessed for 30, 60, and/or 90 days at room temperature and at 4°C showing very promising vehicle. The potency (content) of the drugs in the vehicle remained around 100%, this was achieved with progesterone, pentoxifylline, and clonidine reflecting their stability in Vanish-pen™ when stored at both room temperature and at 4°C for 90 days [225].

Additional studies have assessed other Medisca® bases and demonstrated the stability and the reserved potency of different drugs including diclofenac (in VersaPro™ gel base) [226], naproxen (in PLO Gel Mediflo™) [227], estrogens (HRT cream base) [228], and progesterone (in PLO Transdermal Cream™ and HRT Cream™ Base) [229]. A study illustrated the effectiveness of diclofenac gel (using PLO Mediflo 30 gel base by Medisca®) in reducing the

pain in participants with chronic Achilles tendinopathy (CAT) [230]. Studies conducted by Dow Pharmaceuticals for Medisca® showed the good-to-excellent penetrating capabilities of most Medisca® cream bases extrapolated based on *in-vitro* skin penetration of progesterone, these bases include VersaPro™ Cream Base, HRT Cream Base, Transdermal Pain Base, PenDerm™ Cream Base, PLO Transdermal Cream, and Mediderm™ Cream Base [212].

Doublebase™ cream has been used previously to deliver 10 % gabapentin but it did not facilitate skin permeation [222]. No further studies were found on the skin delivery of drugs using Doublebase™.

The o/w base creams mentioned above are vehicles for delivering both hydrophilic and hydrophobic drugs and they are compatible with broad range of drugs due to their composition which is oil and water, thus, they were used in this study to be compounded with the flavonoid hesperetin. In addition, o/w creams are the most commonly used pharmaceutically and they are more accepted by patients due to easy handling and the non-greasy texture, unlike w/o creams.

2.2 Aims and Objectives

The aims of this study are to incorporate hesperetin into pharmaceutical base creams and to identify the most appropriate vehicle in terms of solubility, stability, and release kinetics. In this present study, a range of pharmaceutical base creams were evaluated for the delivery of hesperetin. The evaluated vehicles were Vanish-Pen™ base cream by Medisca®, PLO transdermal cream by Medisca®, VersaPro™ gel base by Medisca®, VersaPro™ cream base by Medisca®, PenDerm™ cream by Medisca®, Doublebase™ gel by Dermal®, Versatile™ by Fagron©, and Pentravan® by Fagron©.

To achieve the aims, the overall objectives were:

- Validation of a HPLC method for the detection of hesperetin in terms of specificity, linearity, accuracy, precision-repeatability, limit of detection, and limit of quantitation.
- Determine homogeneity of hesperetin in the chosen vehicles and explore the requirement of solubilising hesperetin in a solvent carrier.
- Develop hesperetin cream formulations using commercial compounding vehicles.
- Conduct storage studies on the developed formulations stored at both 4°C and 25°C for 10 weeks by morphology characterisation, organoleptic properties assessment, pH investigation, and drug *in-vitro* release studies with kinetic assessment.

2.3 Materials

Hesperetin (Cayman Chemical Company, USA), phosphate buffered saline (PBS) and acetic acid (Sigma-Aldrich®, UK); polyethylene glycol 400 (Alfa Aesar, UK); acetonitrile (Fisher Scientific UK.); Doublebase™ gel (Dermal®, UK); Vanish-pen™ cream base, PLO transdermal cream, VersaPro™ gel base, VersaPro™ cream base and PenDerm™ cream (Medisca®, UK); Versatile™ base cream and Pentravan® transdermal base cream (Fagron©, UK). All other chemicals were obtained from Sigma Aldrich.

2.4 Methods

2.4.1 High Performance Liquid Chromatography (HPLC) detection method for hesperetin

An isocratic HPLC method was utilised to detect hesperetin during *in-vitro* drug release studies. The method previously developed [231] was optimised successfully to detect hesperetin. The HPLC system used was Agilent 1200 Series (Waldbronn, Germany) with a Phenomenex HyperClone C18 LC column of 150 mm x 4.6 mm x 5 µm used for achieving the chromatographic separation at wavelength 288 nm. The mobile phase comprised of a 55:45 ratio of 0.1 % acetic acid in deionised water to acetonitrile at a flow rate of 1 mL/min at ambient temperature, and the injection volume was set at 20 µL. The mobile phase was filtered with 70 mm glass microfibre filters (Whatman ®) and sonicated for 15 minutes before use.

2.4.2 HPLC method validation

The method was validated in terms of specificity, linearity, accuracy, precision-repeatability, limit of detection, and limit of quantitation [232]. Samples were prepared from a hesperetin stock solution (20 mg/mL) in filtered PBS.

2.4.2.1 Specificity

For specificity, PBS was injected to demonstrate the absence of interference with the peak of hesperetin.

2.4.2.2 Linearity

The linearity of precision for hesperetin was determined over six prepared concentrations, 0.469, 0.938, 1.875, 3.75, 7.5, 15 µg/mL. At each concentration, three replicates were prepared individually and analysed by HPLC. The mean ($\bar{x}$), standard deviation (SD) and relative standard deviation (RSD) were calculated for each concentration. The concentration versus the mean response (peak area) for each concentration was plotted to obtain the regression equation and the coefficient of determination (r^2) [232].

2.4.2.3 Accuracy

To assess the accuracy of the method, three samples were prepared and analysed over the range of 50-200 % of the target analyte with three individually prepared replicates for each concentration. The mean response, SD, and RSD for all samples were calculated. The theoretical value and assay value were reported using the equation for regression line, and the percent recovery was calculated for all concentrations. The accuracy of the HPLC method was considered successful when the mean percent recovery of the samples is 100 % ± 2 % [232].

2.4.2.4 Precision and repeatability

To test the precision of the method, ten replicates were made from one prepared sample solution containing the target concentration, 3.75 µg/mL. The peak area, retention time, and peak height for each replicate were recorded and the mean, SD, and RSD determined.

2.4.2.5 The limit of detection (*LOD*) and limit of quantification (*LOQ*)

The limit of detection (*LOD*) and limit of quantification (*LOQ*) were obtained through the standard error (SE) of intercept of the linearity curve (S). The SD of intercept (σ) (Equation 9), *LOD* (Equation 10) and *LOQ* (Equation 11) were subsequently calculated [232].

$$\sigma = SE \,.\sqrt{N} \qquad (9)$$

$$LOD = 3.3\,(\frac{\sigma}{S}) \qquad (10)$$

$$LOQ = 10\,\left(\frac{\sigma}{S}\right) \qquad (11)$$

where σ is the standard deviation of intercept, SE is the standard error of intercept, *N* is the number of samples, and *S* is the slope of the calibration curve.

2.4.3 Preparation of hesperetin cream formulations

Hesperetin was incorporated directly in the tested pharmaceutical base creams (Vanish-Pen™ base cream by Medisca®, PLO transdermal cream by Medisca®, VersaPro™ gel base by Medisca®, VersaPro™ cream base by Medisca®, PenDerm™ cream by Medisca®, Doublebase™ gel by Dermal®, Versatile™ by Fagron©, and Pentravan® by Fagron©) and mixed manually thoroughly for 10 minutes using a spatula on a marble flat plate. In addition, hesperetin was dissolved (0.1 % w/w) in different vehicles (acetone, ethanol, and PEG) prior to combining with the tested bases. O/w bases were utilised due to their non-greasy nature and water absorption ability, also, preparing w/o emulsions is more difficult than developing o/w emulsions which can be prepared by simple compounding steps. W/o emulsions are greasy and less tolerated by patients due to the high oil content.

The prepared formulations were investigated using a Zeiss Primovert (Zeiss,UK) microscope to investigate homogeneity and solubility of the drug in the base creams and to explore the requirement of dissolving hesperetin in a vehicle prior to the incorporation into the creams [109]. The optimal formulations was determined when a homogeneous and clear mixture was observed with no insoluble regions of drug [109]. Morphological analysis using optical microscopy has been used previously to assess the solubility and homogeneity of drugs in similar formulations [109].

2.4.4 Impact of storage temperature on stability

The selected formulations were stored at both 4°C and 25°C for 10 weeks. pH investigation, morphology characterisation, organoleptic properties assessment and drug *in-vitro* release studies were conducted at weeks 0, 2, 4, 8 and 10. Control studies (for all but the *in-vitro* release) were performed by using the selected plain pharmaceutical base creams.

2.4.4.1 pH assessment

The pH of the dermal layer ranges from 4-7.4, therefore, the formulations are expected to remain within this range for the duration of any stability study [233]. Any change in pH may reflect changes in the chemical stability, lipophilicity, or solubility of the drug. The pH was determined by laying a drop of formulation on pH indicator paper (pH 1-14) (Ahlstrom-Munksjö ©).

2.4.4.2 Morphology characterisation and organoleptic properties

To optimise the formulations, morphology characterisation and organoleptic properties assessment were conducted to detect any changes that might occur during the period storage which might detect the degradation and instability of the products. The morphology of the formulations was investigated microscopically to detect any insoluble crystals formation over a period of 10 weeks.

A successful formulation would have stable clear microscope images during the period of storage (up to 10 weeks), and visually within the amorphous form (not crystallised) for effective and safe transdermal delivery [234]. The colour and the visual appearance of the formulations were also assessed and captured to note any changes with storage which could reflect instability or potential chemical degradation.

2.4.4.3 *In-vitro* drug release studies

In-vitro drug release studies were conducted using a Thincert® 12-well plate permeable inserts with a 0.4 µm pore size membrane (Greiner®, UK), representing the barrier function of the skin

following topical delivery of a formulation [235, 236]. A sample of 0.25 g from each of the formulations (containing 250 µg hesperetin) was placed into the donor compartment, with 1 mL PBS placed into the receptor compartment (Figure 2.4). The release study was conducted in an orbital shaker at 100 rpm with the temperature maintained at 37 °C for 24 hours. Samples of 100 µL were withdrawn at 0.25, 0.5, 1, 1.5, 2, 3, 4, 5, 24 hours, and replaced with fresh (pre-warmed) PBS. The withdrawn samples were filtered through a 0.22 µm filter and assessed by the HPLC analysis.

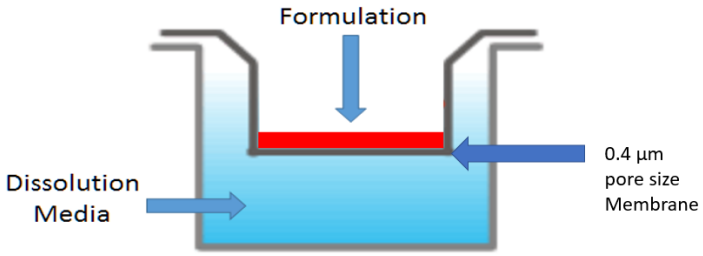

Figure 2.4 The presentation of the donor and receptor compartments in the permeable inserts.

2.4.4.4 Kinetic assessment

To analyse the mechanism of drug release from the formulations, data obtained from *in-vitro* release profiles were quantified in several kinetic models including zero order, first order, Higuchi, and Korsmeyer-Peppas (KP) [237-240].

Models were applied and the best fitted model was determined by computing the coefficient of determination (r^2) and Akaike Information Criteria (AIC) values. The AIC measures the quality of the models for the given data, the lower the AIC value the better the model. The resulting release profiles from the *in-vitro* drug release studies were fitted to the release models to compare the rate of drug release, and to understand the mechanism of drug release from the formulations.

For zero-order models, the release of the drug is at a constant rate independent of the initial concentration (Equation 12).

$$C = C_0 - Kt \qquad (12)$$

where *C* is the concentration, C_0 is the initial concentration, *k* is the release rate constant and *t* is time.

In first-order model, the drug is released at a constant rate proportional to the amount of drug available at a time (*t*) (Equation 13).

$$C = C_0\, e^{-Kt} \qquad (13)$$

where *C* is the concentration, C_0 is the initial concentration, *K* is the release rate constant and *t* is time.

Higuchi developed theoretical models to understand the release of water-soluble drugs and low solubility drugs incorporated into solid and/or semi-solid matrixes [237]. Mathematical expressions were attained for drug particles dispersed in a uniform matrix that behave as the diffusion media (Equation 14):

$$C = C_0\, K\, \sqrt{t} \qquad (14)$$

where *C* is the concentration, C_o is the initial concentration, *K* is the release rate constant and *t* is time.

Korsmeyer-Peppas (KP) Model is a semi-empirical and simple model that relates the drug release exponentially to the fractional release of the drug (Equation 15) [238, 239].

$$\frac{C_t}{C} = Kt^n \qquad (15)$$

where C_t/C is fraction of drug released at a time (*t*), *K* is the release rate constant and n is the release exponent. The n-value is the diffusional exponent which is used to indicate the release for cylindrical shaped matrices, the value of n can be utilised to describe the mechanism of drug release from the formulations (Table 2.3).

Table 2.3 The diffusional exponent n may be used to characterise the mechanism of release of drug from the prepared transdermal formulations.

Diffusional release exponent (n)	**Solute transport mechanism**	**Release controlled by:**
n < 0.5	Fickian diffusion	Diffusion controlled
0.5 < n < 1	Anomalous (Non-Fickian) diffusion	Diffusion and polymer relaxation controlled

1	Case II transport	Zero order release
n> 1	Super case II transport	Erosion controlled (macromolecular relaxation of the polymeric chains)

2.4.5 Data and statistical analysis

Unless otherwise stated, all experiments were conducted in triplicate. Data is presented as mean (standard deviation). Statistical analysis was conducted using paired students t-test with a statistical significance implied with a probability value of < 0.05.

2.5 Results

2.5.1 HPLC method validation

A HPLC method for the detection of hesperetin was validated successfully and detailed in the following sections.

2.5.1.1 Specificity

For specificity, no interfering agents were detected to be overlapping with hesperetin. The blank (PBS only sample) is with a retention time of 1.4-1.5 minutes (Figure 2.5) and hesperetin peak at a retention time of around 3.5 minutes (Figure 2.6).

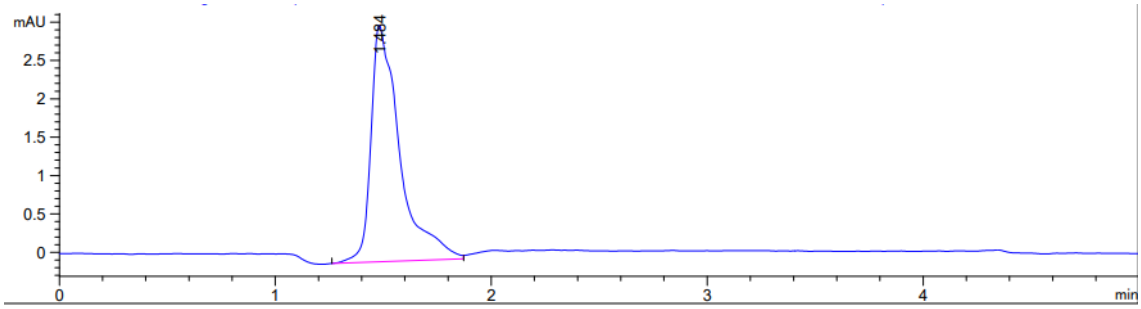

Figure 2.5 PBS only HPLC chromatogram.

PBS was detected with a retention time of 1.484 minutes using reversed phase C18 column and a mobile phase containing 45:55:0.1 acetonitrile: water: acetic acid at 1 mL/min flow rate.

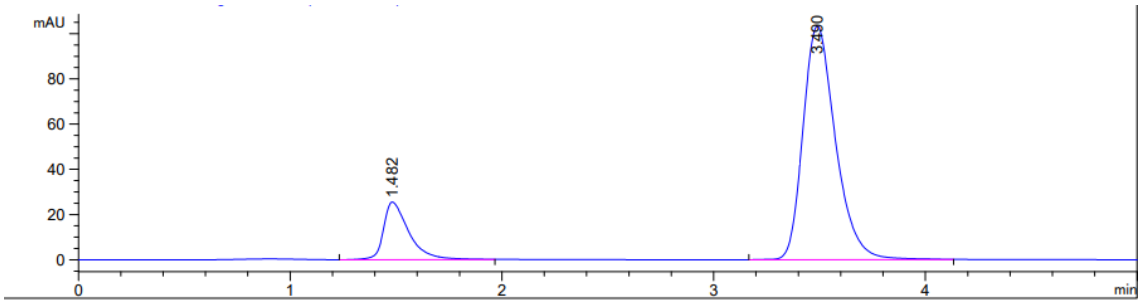

Figure 2.6 Hesperetin HPLC chromatogram.

Hesperetin was detected with a retention time of 3.5 minutes using reversed phase C18 column and a mobile phase containing 45:55:0.1 acetonitrile: water: acetic acid at 1 mL/min flow rate.

2.5.1.2 Linearity

A proportional response was shown versus the concentration range analysed with a linear equation of y = 38.795x + 14.744 and a r^2 value of 0.997, which satisfies the acceptance criteria, $r^2 \geq 0.997$ (Table 2.4) (Figure 2.7).

Table 2.4 The linearity table illustrates the tested concentration of hesperetin providing the linear equation and r^2 value.

Concentration (µg/ml)	**Peak area [Mean of three injections] (mAU)**	**Peak area (% RSD)**
0.469	20.5485 (0.34)	1.638
0.938	41.66531 (0.39)	0.940
1.875	89.81976 (0.07)	0.077
3.75	177.054 (1.399)	0.790
7.5	318.1477 (1.12)	0.352
15	586.9389 (2.69)	0.458
Regression = y = 38.795x + 14.744		**r^2=0.997**

% RSD: Percentage relative standard deviation.

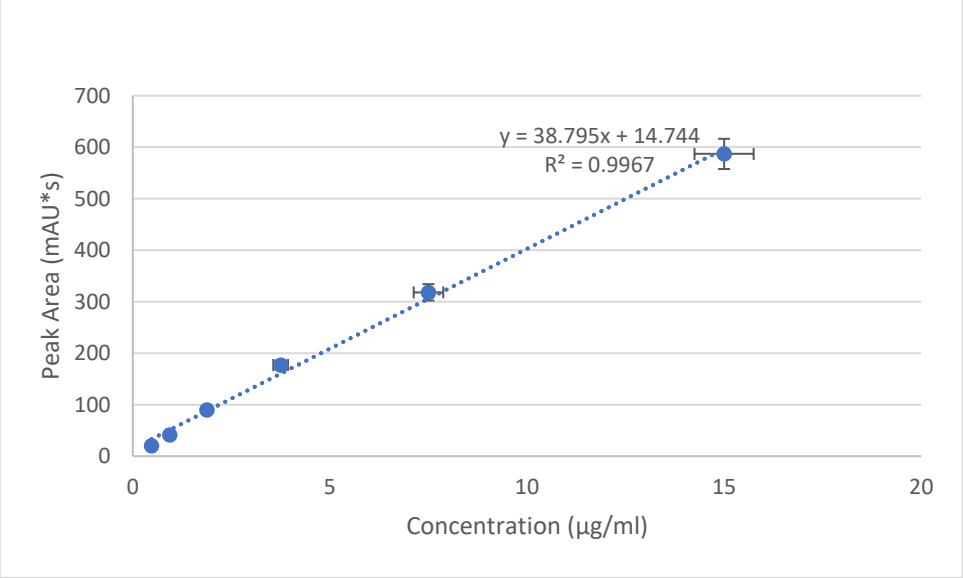

Figure 2.7 Calibration curve of hesperetin showing linear response.

Data represent the mean and error bars are the standard deviation, n=3.

2.5.1.3 Accuracy

The accuracy of the HPLC method was successful following a mean percent recovery of 100.5 % (Table 2.5). RSDs for all samples were also within the acceptable range, ≤1 %.

Table 2.5 Accuracy of the HPLC method for hesperetin using 50-200 % of the target concentration.

	Concentration 1 1.875 µg/mL (50 %)	**Concentration 2 3.75 µg/mL (100 %)**	**Concentration 3 7.5 µg/mL (200 %)**
Injection 1 (mAU)	89.77	176.06	317.36
Injection 2 (mAU)	89.87	178.04	318.94
Injection 3 (mAU)	89.69	178.23	316.55
Mean peak area (mAU)	89.78	177.45	317.61
SD	0.09	1.2	1.22
RSD (%)	0.1	0.68	0.38
Spiked amount (µg/mL)	1.875	3.75	7.5
Found amount (µg/mL)	1.89	3.77	7.52
Recovery (%)	100.8	100.53	100.27

SD: standard deviation. RSD: relative standard deviation.

2.5.1.4 Precision and repeatability

Ten replicates of 3.75 µg/mL were analysed by HPLC. The RSDs calculated for peak area, retention time, and peak height were all ≤ 1 % which is acceptable (Table 2.6). This reflected the precision and repeatability of the method.

2.5.1.5 The limit of detection (LOD) and limit of quantification (LOQ)

The limit of detection (LOD) was determined to be 0.676 µg/mL and limit of quantification (LOQ) to be 2.05 µg/ml.

Table 2.6 Ten replicates of the target analyte analysed by HPLC to test the precision of the method.

Injection No.	Peak area (mAU)	Retention time (min)	Peak height
Replicate 1	176.06	3.50	18.38
Replicate 2	178.04	3.50	18.53
Replicate 3	178.44	3.50	18.45
Replicate 4	177.12	3.50	18.60
Replicate 5	178.23	3.50	18.29
Replicate 6	176.36	3.50	18.57
Replicate 7	177.76	3.51	18.49
Replicate 8	176.67	3.50	18.31
Replicate 9	178.88	3.50	18.56
Replicate 10	178.15	3.50	18.37
Mean	177.57	3.50	18.45
SD	0.96	0.00	0.11
RSD%	0.54	0.11	0.61

SD: standard deviation. RSD%: Percentage relative standard deviation

2.5.2 Preparation of hesperetin cream formulations

Hesperetin (0.05 % w/w) was dissolved in different carriers (acetone, ethanol, or PEG) before mixing it with the base creams or directly added by its own to assess the solubility of hesperetin in the 8 tested base creams and to investigate the need of incorporating a carrier to optimise solubility [109]. The most promising carrier was PEG 400 as hesperetin dissolved fully and showed a clear homogenous formulation under optical microscopy (Zeiss Primovert with 10x objective lens) with no insoluble patches noticed, therefore it was selected. While incorporating hesperetin powder alone or using acetone or ethanol produced formulations with undissolved drug patches under the microscope. VersaPro™ gel base was excluded from the study due to the insolubility of hesperetin in the gel base with all the tested carriers.

2.5.3 Impact of storage temperature on stability

2.5.3.1 pH assessment

The pH of the chosen formulations was assessed at weeks 0, 2, 4, 8, and 10 to ensure that the formulations are stable and suitable for skin application. The pH of each base cream formulation did not change during the 10 weeks of storage at 4 °C and 25 °C (Table 2.7).

Table 2.7 pH of the tested formulations over 10 weeks of storage at 4 °C and 25 °C.

Week	Vanish-Pen™	Doublebase™	Versatile™	Pentravan®
0	6	7	4	7
2	6 to 7	7	4	7
4	6 to 7	7	4	6.5 to 7
8	6 to 7	7	4	6.5 to 7
10	6 to 7	7	4	7

2.5.3.2 Morphological characterisation

Changes in the morphology of the formulations may result in changes in drug efficacy and permeation. The visual morphology of the formulations was investigated microscopically using a light microscope to assess the possibility of crystallisation of hesperetin in the formulations over a period of 10 weeks. Hesperetin was fully dissolved and dispersed in Vanish-Pen™ (Figure 2.8), Doublebase™ (Figure 2.9), Versatile™ (Figure 2.10), and Pentravan® (Figure 2.11), during the whole period of 10 weeks and no significant crystallisation detected when compared to the plain cream bases. The white and dark specks are considered artefacts or bubbles when compared to control.

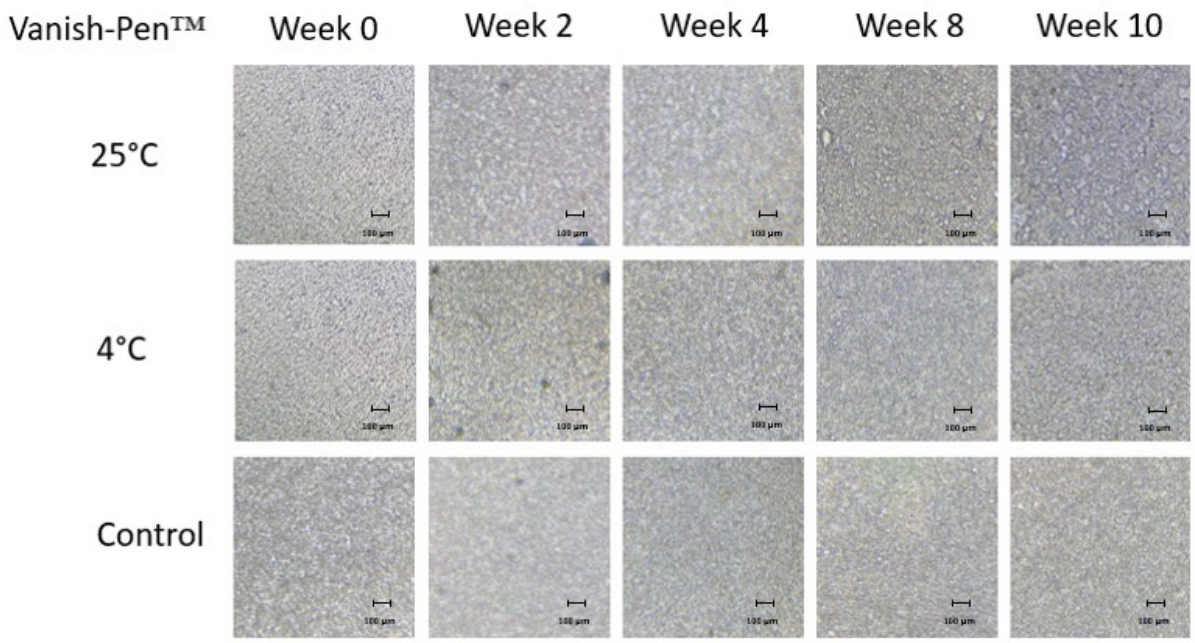

Figure 2.8 Vanish-Pen™ formulations morphology characterisation under the microscope during storage period (10 weeks).

Storage at 4 °C and 25 °C. Images captured using Zeiss Primovert microscope with 10x objective lens. Plain: the storage of Vanish-pen™ plain cream base (no hesperetin) as a baseline of comparison.

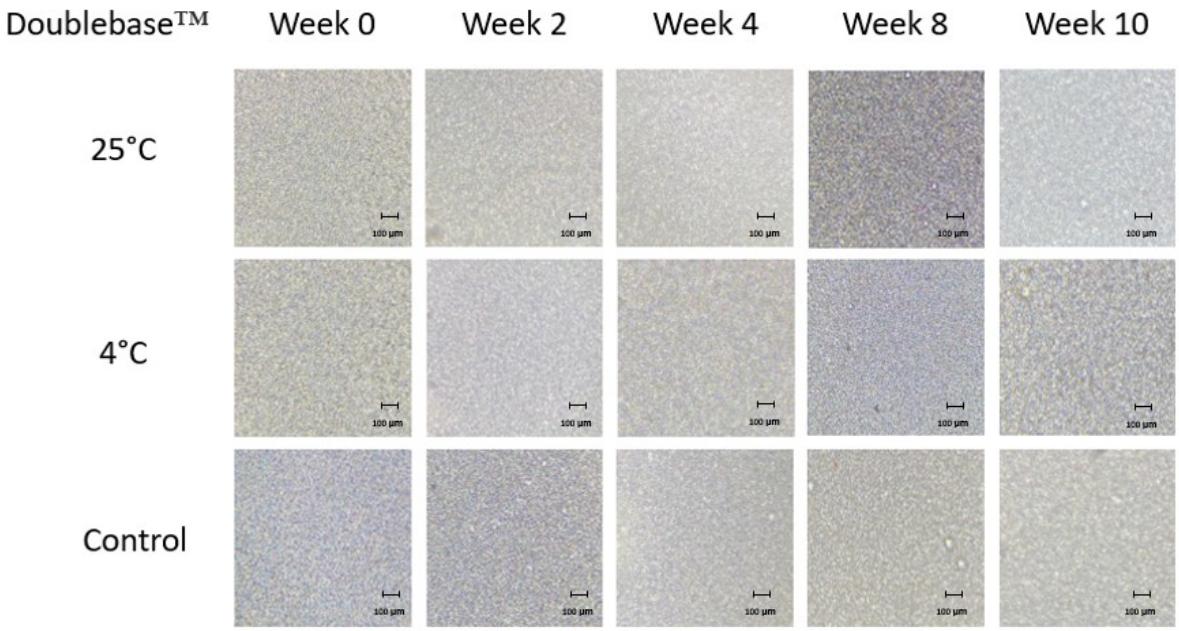

Figure 2.9 Doublebase™ formulations morphology characterisation under the microscope during storage period (10 weeks).

Storage at 4 °C and 25 °C. Images captured using Zeiss Primovert microscope with 10x objective lens. Plain: the storage of Doublebase™ plain cream base (no hesperetin) as a baseline of comparison.

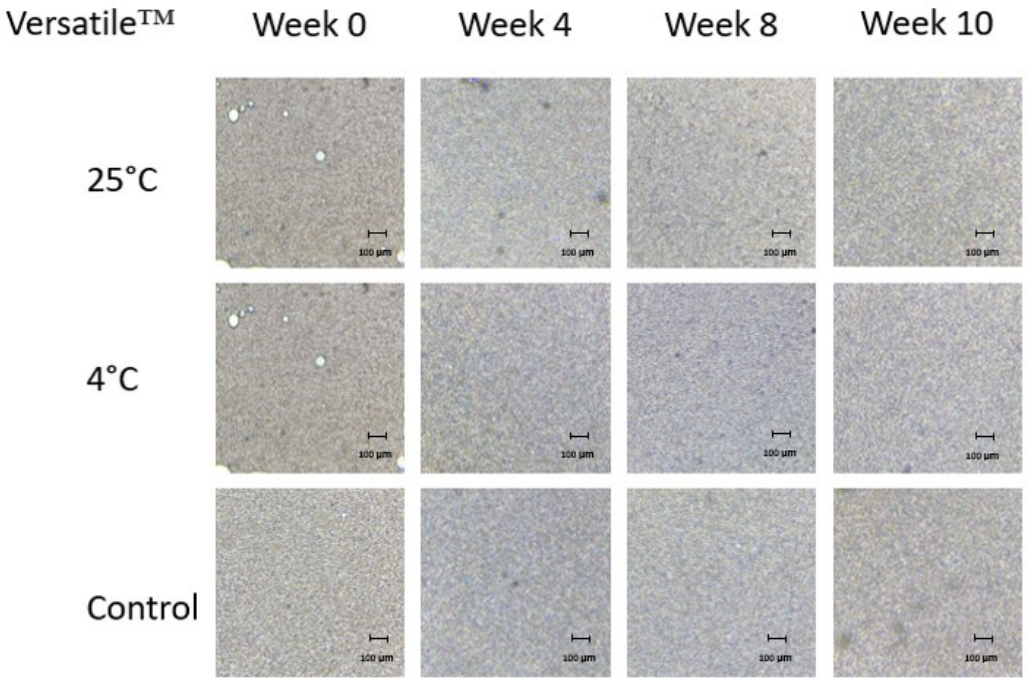

Figure 2.10 Versatile™ formulations morphology characterisation under the microscope during storage period (10 weeks).

Storage at 4 °C and 25 °C. Images captured using Zeiss Primovert microscope with 10x objective lens. Plain: the storage of Versatile™ plain cream base (no hesperetin) as a baseline of comparison.

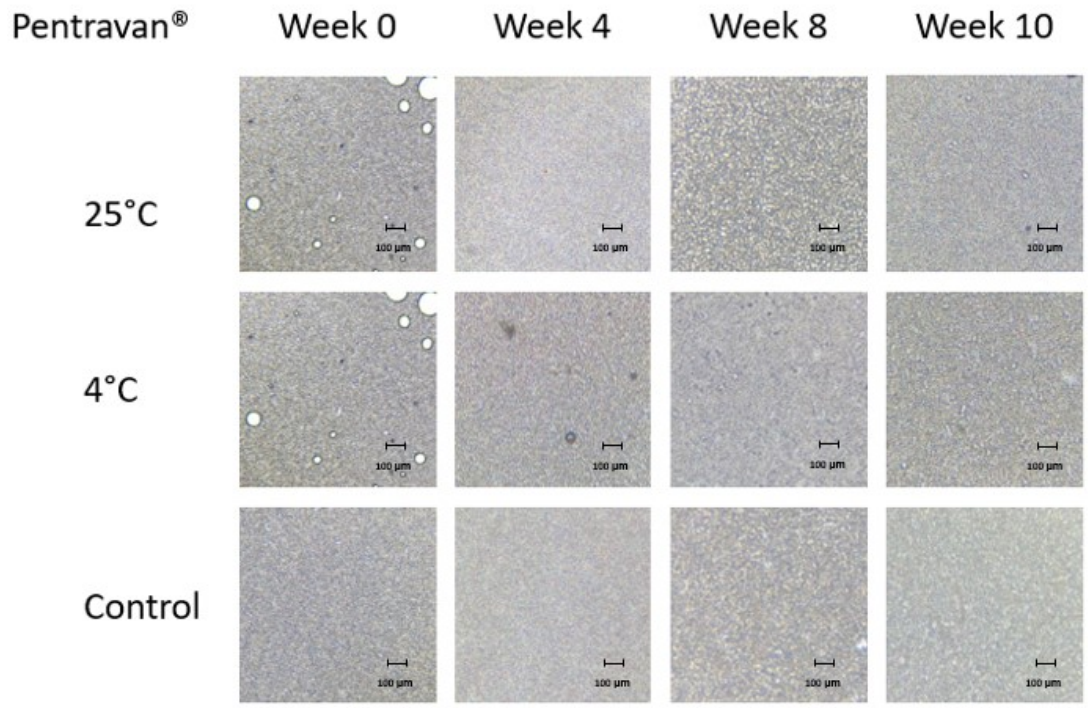

Figure 2.11 Pentravan® formulations morphology characterisation under the microscope during storage period (10 weeks).

Storage at 4 °C and 25 °C. Images captured using Zeiss Primovert microscope with 10x objective lens. Plain: the storage of Pentravan® plain cream base (no hesperetin) as a baseline of comparison.

2.5.3.3 Organoleptic properties

The colour and the visual appearance of the selected formulations were assessed to detect any discoloration or changes noticed in the creams during the period of storage.

No significant change in the colour or visual appearance of Vanish-Pen™ (Figure 2.12), Doublebase™ (Figure 2.13), Versatile™ (Figure 2.14), and Pentravan® (Figure 2.15) formulations during the period of 10 weeks storage at both 4°C and 25°C. The change in colour noticed in Figure 2.15 in week 10 (25°C) for Pentravan® was due to the influence of lighting within the laboratory, no visual changes were observed.

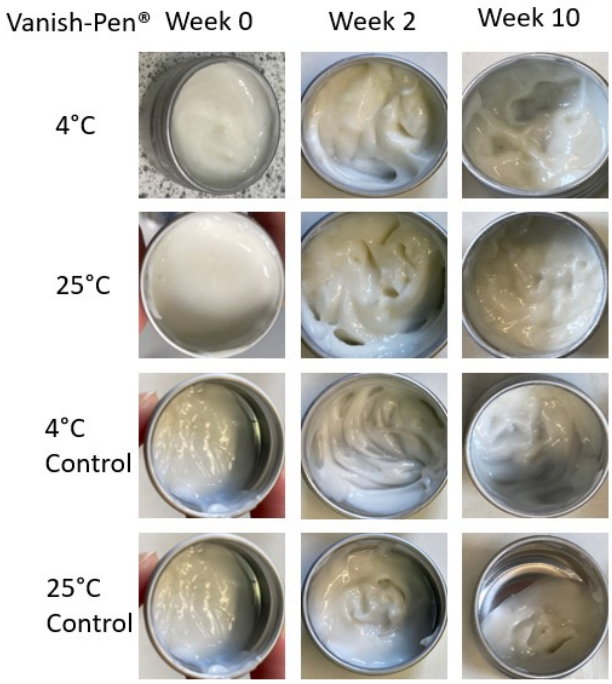

Figure 2.12 The observation of the organoleptic properties of Vanish-Pen™ formulations under storage.

The storage period is 10 weeks at 4°C and 25°C. Plain: the storage of Vanish-pen™ plain cream (no hesperetin) as a baseline of comparison.

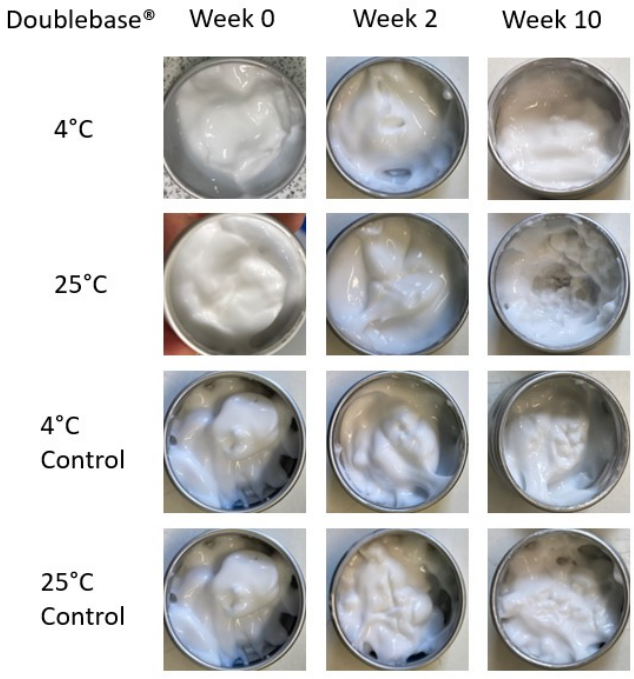

Figure 2.13 The observation of the organoleptic properties of Doublebase™ formulations under storage

The storage period is 10 weeks at 4°C and 25°C. Plain: the storage of Doublebase™ plain cream (no hesperetin) as a baseline of comparison.

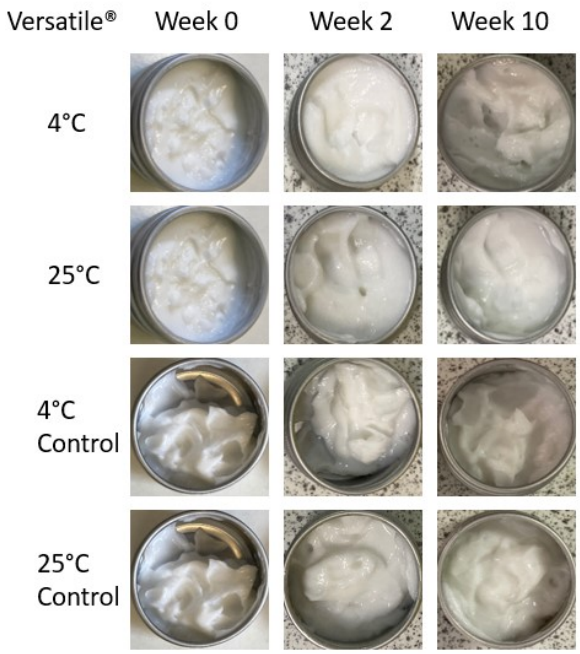

Figure 2.14 The observation of the organoleptic properties of Versatile™ formulations under storage

The storage period is 10 weeks at 4°C and 25°C. Plain: the storage of Versatile™ plain cream (no hesperetin) as a baseline of comparison.

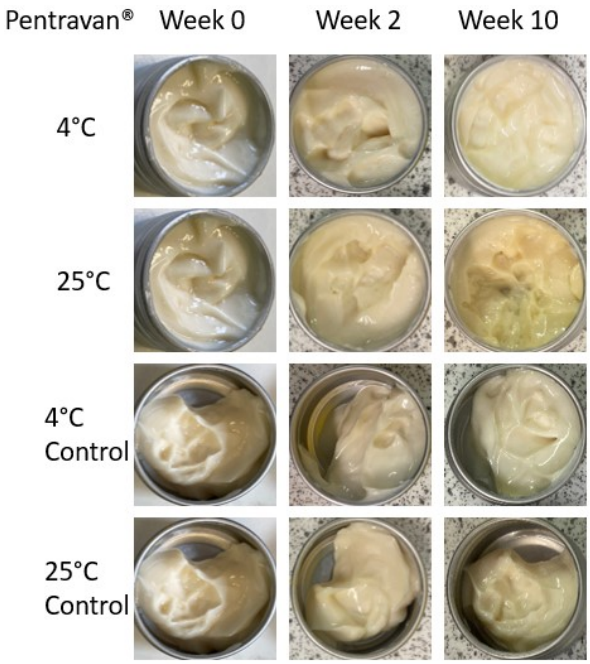

Figure 2.15 The observation of the organoleptic properties of Pentravan® formulations under storage

The storage period is 10 weeks at 4°C and 25°C. Plain: the storage of Pentravan® plain cream (no hesperetin) as a baseline of comparison.

2.5.3.4 *In-vitro* drug release studies

The ability of the prepared formulations to release hesperetin was successfully assessed by *in-vitro* drug release studies using a permeable insert model. Drug release was assessed on weeks 2, 4, 8, and 10 for Vanish-pen™ and Doublebase™ creams, and on weeks 4, 8, and 10 for Versatile® and Pentravan® creams. For all creams, release was assessed following storage at 4°C and 25°C during the stability study period.

The release studies conducted in week 0 was the control release profile of hesperetin. The Medisca® bases PLO transdermal cream, VersaPro™ cream base, and PenDerm™ cream base were discarded due to the poor broad peaks by the HPLC. The HPLC method of hesperetin was not suitable to detect hesperetin released from the above-mentioned bases, hence, no further studies conducted on these bases.

When comparing the freshly prepared formulations, Pentravan® formulation released the highest percentage of hesperetin after 24 hours, 12.69 % (0.68 %), but no significant difference was detected when compared to Vanish-pen™ formulations (12.28 % (0.16 %)). Doublebase™ and Versatile™ formulations released significantly lower percentages of hesperetin of 11.35 % (0.26 %) and 4.53 % (0.65 %), respectively, when compared to Pentravan® ($p<0.05$) (Figure 2.16).

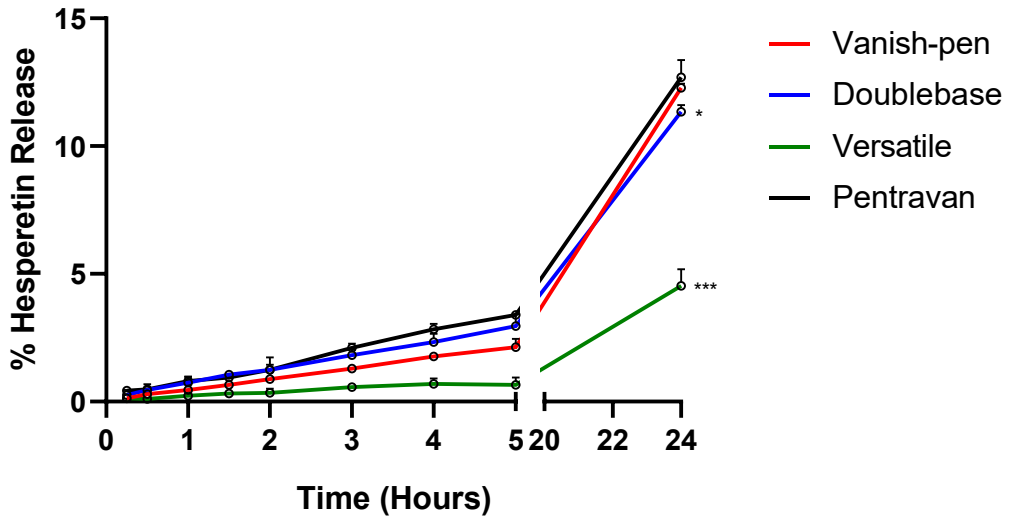

Figure 2.16 *In-vitro* drug release profiles of the tested base creams at preparation.

Open circles reflect the mean percentage hesperetin release. Error bars represent the standard deviation. n=3. Data are represented with open circles. *p<0.05, ***p<0.001 representing the comparison of the % release at 24 hrs of each cream with Pentravan as the control.

No statistically significant changes were detected in the release profiles of Vanish-pen™ formulations when stored for 10 weeks in 4°C storage condition (Figure 2.17A) (Table 2.8). Storing the Vanish-pen™ formulations for 8 weeks at 25°C storage temperature provided consistent release profiles with no statistically significant difference detected when comparing the whole release profiles. While at week 10, significant increase in the release profile of hesperetin was detected ($p<0.05$) and the percentage release of hesperetin reached up to 14.71 % (0.32 %) after 24 hours when compared to week 0 (12.28 % (0.16 %)) (Figure 2.17A) (Table 2.8).

The storage of Doublebase™ formulation at 25°C for 10 weeks resulted in consistent release profiles with no significant changes detected (Figure 2.17B) (Table 2.8). While the storage at 4°C resulted in significant decrease ($p<0.05$) in the release profiles of hesperetin in weeks 2, 8, and 10 (Figure 2.17B) (Table 2.8).

For Versatile™ formulation, the storage at both 4°C and 25°C for 10 weeks provided consistent release profiles with no statistically significant changes detected (Figure 2.18A) (Table 2.8).

The storage of Pentravan® formulations at 4°C and 25°C resulted in statistically significant decrease in the release profiles of hesperetin in weeks 4 and 10 ($p<0.05$). Whilst in week 8, insignificant decrease in the release profiles was detected (Figure 2.18B) (Table 2.8).

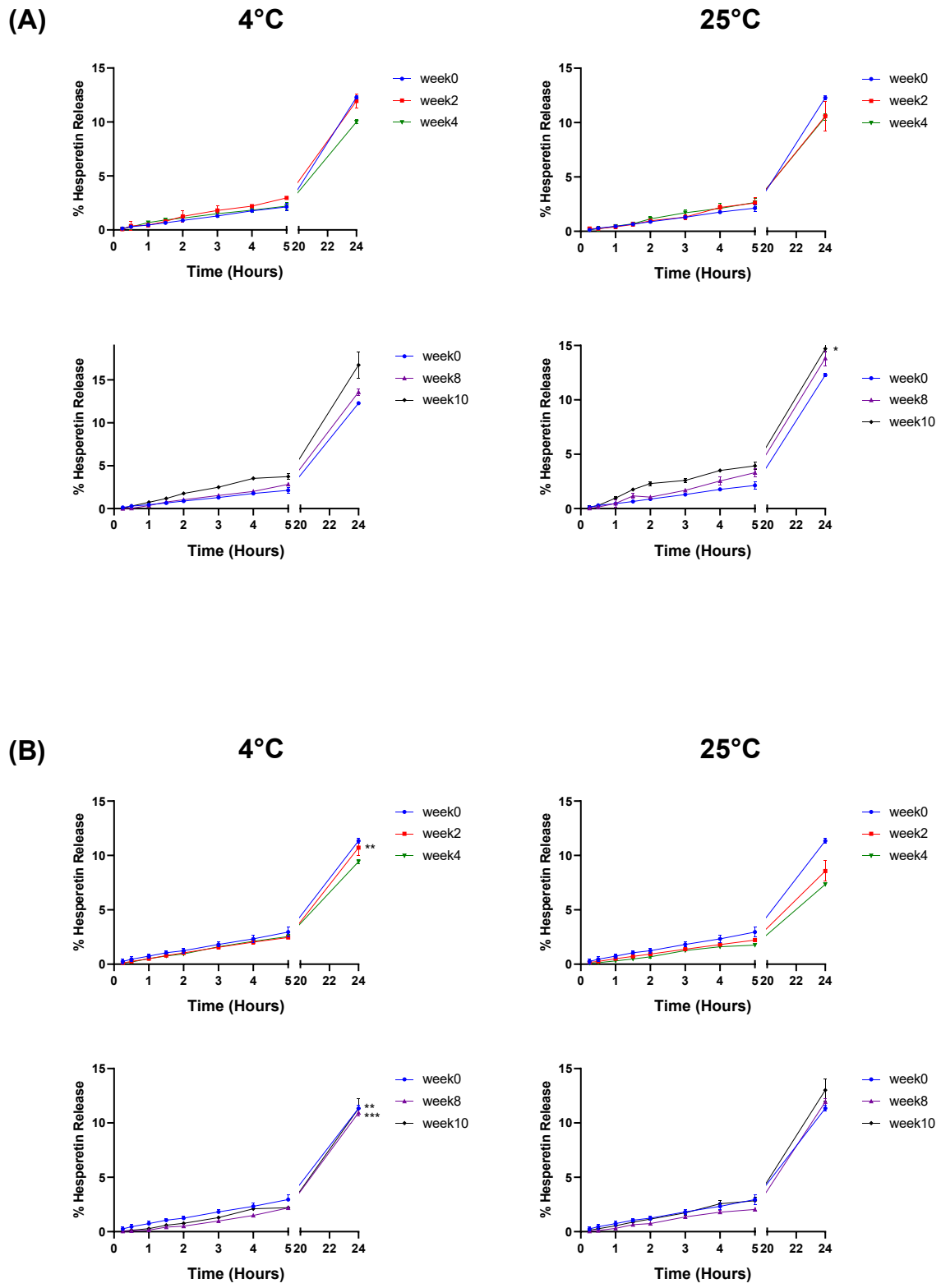

Figure 2.17 *In-vitro* drug release profile at 4°C and 25°C in weeks 0, 2, 4, 8, and 10 for Vanish-Pen™ and Doublebase™ formulations.

(A) Vanish-Pen™ and (B) Doublebase™ formulations. Data represent the mean percentage hesperetin release. Error bars represent the standard deviation. n=3. *p<0.05, **p<0.01, ***p<0.001, ****p<0.0001 representing the comparison of the release profiles with week 0 as the control obtained by one-way ANOVA with Dunnett's post-hoc test.

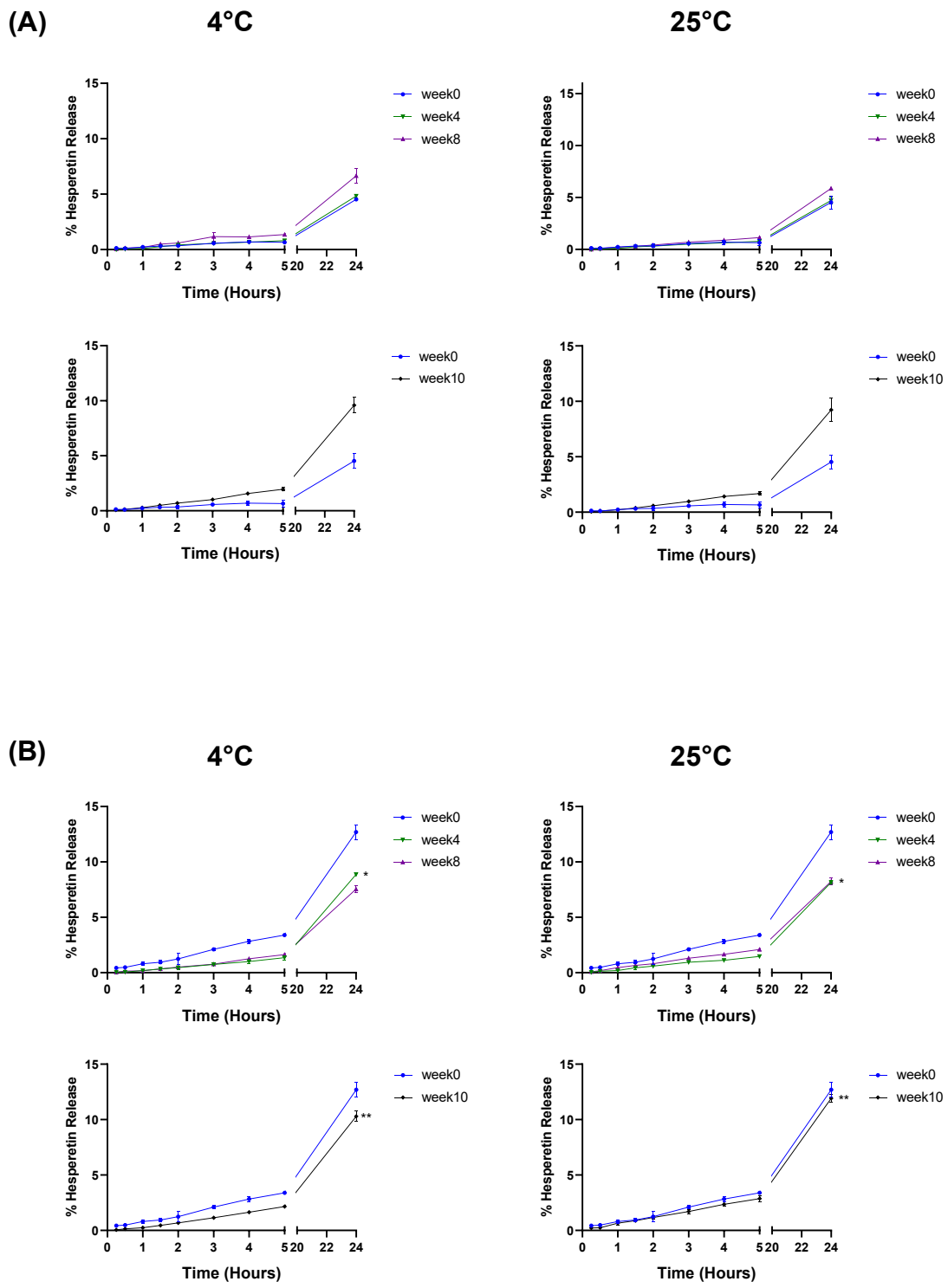

Figure 2.18 *In-vitro* drug release profile at 4°C and 25°C in weeks 0, 4, 8, and 10 for Versatile™ and Pentravan® formulations

(A) Versatile™ and (B) Pentravan® formulations. Data represent the mean percentage hesperetin release. Error bars represent the standard deviation. n=3. *p<0.05, **p<0.01, ***p<0.001 representing the comparison of the release profiles with week 0 as the control obtained by one-way ANOVA with Dunnett's post-hoc test.

Table 2.8 The statistical significance (p-value) of the hesperetin release profiles from the formulations during storage at 4°C and 25°C.

Formulation	Storage Temperature	Week 0 vs. week 2	Week 0 vs. week 4	Week 0 vs. week 8	Week 0 vs. week 10
Vanish-Pen™	**4 °C**	0.271	0.9544	0.3823	0.1013
	25 °C	0.988	0.9999	0.1123	**0.0104**
Doublebase™	**4 °C**	**0.0015**	0.129	**0.0002**	**0.0024**
	25 °C	0.1497	0.1229	0.0821	0.9534
Versatile™	**4 °C**	N/A	0.9835	0.1697	0.2803
	25 °C	N/A	0.7875	0.3675	0.3372
Pentravan®	**4 °C**	N/A	**0.0191**	0.0583	**0.0084**
	25 °C	N/A	**0.0454**	0.1084	**0.0087**

Data represented as p-values obtained by one-way ANOVA with Dunnett's post-hoc test. Bold data represent a p-value<0.05. N/A: data not available. Week 0 used as baseline for comparison.

2.5.3.5 Kinetic assessment

The mechanism of drug release rate from the formulations was analysed by applying several kinetic models on the data obtained from the *in-vitro* drug release profiles. These kinetic models applied include zero order, first order, Higuchi, and KP. Both r^2 and AIC values were utilised to select the optimal kinetic model.

Of all the models tested, the KP release model was selected since it has demonstrated the highest r^2 values and lowest AIC for all the tested formulations in week 0 release studies which reflected a fitted model (Tables 2.9-2.12). The KP model describes the release of the drug from polymeric systems and the n-value (diffusional release exponent) propose different release mechanisms from these systems, as described in the Methods Section 2.4.4.4 Table 2.3.

For Vanish-pen™ cream, the model selection was favouring KP model in all the repeated stability release studies for both 4°C and 25°C storage, except for week 2 and week 8 release studies stored in 25°C. In those exception weeks, the AIC of first order model was lower than KP model but the fitness of the models was further assessed by referring to the fraction dissolved (%) graphs of KP and first order models. One of the "3 hours" samples was slightly deviated from the fitted line of KP model in both week 2 and 8 (Figure 2.19). In addition, the first order rate constant was almost very low through all the weeks for all the formulations tested (Table 2.9).

The n-value of KP model was used to understand the mechanism of drug release from the formulations. The repeated release studies of Vanish-Pen™ base cream formulations stored in 4°C and 25°C showed variable n-values (Table 2.9). Week 0 and week 8 (4°C storage) release studies showed that KP mechanism is ruled by the macromolecular relaxation of the polymeric chains ($n > 1$), Super case II transport. While the n-values obtained from the drug release studies performed in weeks 2, 4, 8 (25°C), and 10 were $0.5 < n < 1$ representing a non-Fickian (anomalous) diffusion mechanism which is controlled by both the Fickian diffusion and the degradation and relaxation of the polymer matrix (Table 2.4) (Table 2.9).

For Doublebase™ gel formulations, all the repeated release studies in both storage conditions (4°C, 25°C) were favouring KP model, $r^2>0.997$. The n-values of KP model showed that two drug transport mechanisms might be involved since week 8 (4°C, 25°C) and week 10 (4°C) release studies showed n-values > 1 (Super case II drug transport), while the rest of the repeated release studies were $0.5 < n < 1$ (Anomalous diffusion) (Table 2.10).

All the repeated drug release studies of Versatile™ formulations were favouring the KP model, except week 8 (4°C). The applied mathematical models on week 8 (4°C) release profile were not conclusive as the r^2 and AIC values of KP, zero order, first order models were comparable (Table 2.12). Referring to the mathematical modelling graphs, samples taken at 3 hours in week 8 (4°C) show a deviation from the fitted line when compared to week 0 KP model fitness graph as illustrated in Figure 2.20 which represent a single time point sample.
The KP n-value for Versatile™ formulations repeated release studies was > 1, except for week 8 (4°C) 0.5 < n < 1 (Table 2.11). The more favourable transport mechanism for Versatile™ formulations is super case II transport (Figure 2.20).

For Pentravan® cream formulations, all the repeated release studies in both storage conditions (4°C, 25°C) were favouring KP model, $r^2 > 0.997$. The n-values showed that two drug transport mechanisms might be involved since week 0, week 8 (25°C), and week 10 (25°C) had 0.5 < n < 1 (Anomalous diffusion), while week 4, week 8 (4°C), and week 10 (4°C) had n > 1 (super case II drug transport) (Table 2.13). The release rate constant values (kKP) were decreasing with storage which is related to the decrease in drug release with storage illustrated by *in-vitro* release studies (Table 2.12).

.

Table 2.9 Kinetic assessment of the release data of Vanish-Pen™ formulations performed during storage at 4°C and 25°C.

Model	Parameter	Week 0		Week 2 (4°C)		Week 2 (25°C)		Week 4 (4°C)		Week 4 (25°C)		Week 8 (4°C)		Week 8 (25°C)		Week 10 (4°C)		Week 10 (25°C)	
		Mean	SD	Mean	SD	Mean	SD	Mean	SD	Mean	SD	Mean	SD	Mean	SD	Mean	SD	Mean	SD
Zero order	k0	0.0080	0.0000	0.008	0	0.007	0.001	0.007	0	0.007	0	0.009	0	0.01	0.001	0.012	0.001	0.011	0
	R^2	0.997	0.003	0.989	0.013	0.994	0.003	0.99	0.004	0.99	0.003	0.998	0.001	0.996	0.002	0.995	0.003	0.974	0.004
	AIC	-8.359	7.311	-1.523	10.217	-3.837	2.588	-3.683	4.568	0.4345	3.997	-9.977	2.44	-4.99	7.212	0.944	3.406	14.845	1.525
First order	k1	<0.0001	<0.0001	<0.0001	<0.0001	<0.0001	<0.0001	<0.0001	<0.0001	<0.0001	<0.0001	<0.0001	<0.0001	<0.0001	<0.0001	0.00013	<0.0001	0.00012	<0.0001
	R^2	0.994	0.004	0.991	0.011	0.995	0.002	0.994	0.003	0.992	0.002	0.997	0.001	0.997	0.001	0.998	0.002	0.981	0.003
	AIC	-2.946	5.491	-3.212	10.217	-5.96	1.555	-5.238	4.277	-1.636	3.219	-4.736	1.42	-6.266	4.03	-6.058	6.032	12.125	1.467
Higuchi	Kh	0.2300	0.0060	0.2380	0.0020	0.21	0.027	0.2000	0.0030	0.212	0.009	0.257	0.008	0.271	0.018	0.334	0.026	0.31	0.009
	R^2	0.739	0.015	0.802	0.045	0.794	0.017	0.804	0.025	0.81	0.014	0.751	0.003	0.783	0.019	0.803	0.012	0.857	0.008
	AIC	32.855	0.429	29.45	3.385	27.762	2.949	26.103	1.37	26.898	0.454	34.318	0.469	33.26	0.421	35.614	2.232	30.143	0.262
Korsmeyer-Peppas	kKP	0.005	0.001	0.0160	0.0100	0.0120	0.0030	0.0130	0.0050	0.0150	0.0040	0.0070	0.0000	0.0130	0.0050	0.0200	0.0020	0.039	0.005
	n	1.086	0.044	0.9250	0.0970	0.9370	0.0350	0.9240	0.0540	0.9030	0.0340	1.0440	0.0060	0.9660	0.0430	0.9240	0.0250	0.816	0.014
	R^2	0.999	0.001	0.997	0.003	0.996	0.001	0.997	0.002	0.995	0.0004	0.999	0.001	0.998	0.001	0.999	0.001	0.997	0.001
	AIC	-24.62	12.184	-7.419	7.065	-5.903	0.738	-9.342	5.126	-4.5	1.192	-12.96	3.935	-5.683	4.262	-7.52	3.715	-2.08	2.632

K0: the rate constant for zero order model; k1: first order rate constant; kh: Higuchi rate constant; kKP: Korsmeyer-Peppas rate constant; r^2: is the coefficient of determination; AIC: the Akaike Information Criteria; n: the diffusional release exponent. SD: Standard deviation.

Table 2.10 Kinetic assessment of the release data of Doublebase™ formulations performed during storage at both 4°C and 25 °C.

Model	Parameter	Week 0		Week 2 (4°C)		Week 2 (25°C)		Week 4 (4°C)		Week 4 (25°C)		Week 8 (4°C)		Week 8 (25°C)		Week 10 (4°C)		Week 10 (25°C)	
		Mean	SD	Mean	SD	Mean	SD	Mean	SD	Mean	SD	Mean	SD	Mean	SD	Mean	SD	Mean	SD
Zero order	k0	0.0081	0.0001	0.0075	0.0005	0.0061	0.0006	0.0067	0.0001	0.0052	0.0001	0.0075	0.0002	0.0082	0.0002	0.0078	0.0006	0.0091	0.0007
	r^2	0.9849	0.0143	0.9961	0.0056	0.9873	0.0099	0.9876	0.0051	0.9923	0.0042	0.9938	0.0008	0.9964	0.0026	0.9978	0.0004	0.9978	0.0021
	AIC	2.6880	7.5030	-16.872	15.9471	-5.9567	11.6010	-0.2198	4.2572	-9.4736	5.9678	-2.6150	1.6527	-7.7365	7.4989	-11.510	3.2524	-12.682	10.8760
First order	k1	<0.0001	<0.0001	<0.0001	<0.0001	<0.0001	<0.0001	<0.0001	<0.0001	<0.0001	<0.0001	<0.0001	<0.0001	<0.0001	<0.0001	<0.0001	<0.0001	<0.0001	<0.0001
	r^2	0.9882	0.0118	0.9974	0.0042	0.9898	0.0084	0.9907	0.0042	0.9939	0.0035	0.9916	0.0011	0.9942	0.0035	0.9970	0.0012	0.9986	0.0010
	AIC	0.0139	8.2814	-24.045	18.5900	-9.8360	15.1760	-2.9442	4.8085	-11.754	6.5778	0.1098	1.7041	-3.1209	6.3258	-9.2306	5.4687	-14.958	5.8706
Higuchi	Kh	0.2323	0.0033	0.2128	0.0110	0.1750	0.0132	0.1938	0.0057	0.1481	0.0043	0.2023	0.0043	0.2229	0.0044	0.2161	0.0144	0.2560	0.0207
	r^2	0.8280	0.0365	0.7995	0.0273	0.8289	0.0329	0.8302	0.0133	0.8105	0.0163	0.7219	0.0058	0.7356	0.0174	0.7571	0.0146	0.7880	0.0152
	AIC	27.0073	2.5360	27.6832	2.4794	21.9585	3.7577	23.9136	0.5488	20.5011	0.7276	31.6427	0.6550	32.5489	1.0544	30.7654	2.0890	31.8089	1.3987
Korsmeyer-Peppas	kKP	0.0213	0.0113	0.0124	0.0048	0.0155	0.0053	0.0174	0.0035	0.0103	0.0026	0.0033	0.0004	0.0045	0.0015	0.0065	0.0012	0.0125	0.0034
	n	0.8748	0.0707	0.9362	0.0583	0.8746	0.0678	0.8678	0.0268	0.9062	0.0332	1.1164	0.0173	1.0895	0.0485	1.0276	0.0354	0.9586	0.0364
	r^2	0.9978	0.0021	0.9998	0.0002	0.9995	0.0004	0.9986	0.0003	0.9977	0.0013	0.9984	0.0004	0.9995	0.0001	0.9984	0.0003	0.9991	0.0005
	AIC	-12.555	8.228	-33.264	6.4062	-29.413	5.3974	-17.451	2.0824	-18.130	4.8849	-12.799	2.1062	-21.982	2.2001	-12.394	1.0947	-16.325	5.7076

K0: the rate constant for zero order model; k1: first order rate constant; kh: Higuchi rate constant; kKP: Korsmeyer-Peppas rate constant; r^2: is the coefficient of determination; AIC: the Akaike Information Criteria; n: the diffusional release exponent. SD: Standard deviation.

Table 2.11 Kinetic assessment of the release data of Versatile™ formulations performed during storage at 4°C and 25 °C.

Model	Parameter	Week 0		Week 4 (4°C)		Week 4 (25°C)		Week 8 (4°C)		Week 8 (25°C)		Week 10 (4°C)		Week 10 (25°C)	
		Mean	SD	Mean	SD	Mean	SD	Mean	SD	Mean	SD	Mean	SD	Mean	SD
Zero order	k0	0.003	0.000	0.003	0.000	0.003	0.000	0.005	0.000	0.004	0.000	0.007	0.000	0.006	0.001
	r^2	0.986	0.009	0.996	0.001	0.995	0.002	0.994	0.008	0.999	0.001	0.998	0.001	0.997	0.001
	AIC	-13.448	9.358	-20.986	1.929	-19.810	1.898	-17.142	12.215	-27.880	3.931	-17.211	7.623	-12.025	3.859
First order	k1	<0.0001	<0.0001	<0.0001	<0.0001	<0.0001	<0.0001	<0.0001	<0.0001	<0.0001	<0.0001	<0.0001	<0.0001	<0.0001	<0.0001
	r^2	0.985	0.010	0.995	0.001	0.994	0.002	0.994	0.007	0.998	0.001	0.997	0.002	0.995	0.001
	AIC	-13.368	10.090	-19.501	1.987	-18.268	1.580	-17.584	12.133	-24.663	3.385	-14.748	9.113	-8.614	4.193
Higuchi	Kh	0.085	0.010	0.090	0.003	0.087	0.007	0.131	0.014	0.111	0.000	0.182	0.010	0.172	0.018
	r^2	0.739	0.038	0.736	0.010	0.725	0.008	0.783	0.012	0.750	0.007	0.754	0.022	0.736	0.007
	AIC	14.534	3.455	16.201	0.962	16.202	0.970	19.946	2.100	19.222	0.464	27.875	2.178	27.878	2.234
Korsmeyer-Peppas	kKP	0.002	0.002	0.002	0.000	0.001	0.000	0.006	0.002	0.003	0.000	0.005	0.002	0.003	0.000
	n	1.077	0.105	1.087	0.025	1.119	0.025	0.963	0.037	1.050	0.018	1.040	0.056	1.085	0.021
	r^2	0.990	0.006	0.998	0.001	0.999	0.000	0.995	0.006	1.000	0.000	0.999	0.000	0.999	0.001
	AIC	-13.879	8.175	-29.306	5.470	-38.499	3.321	-16.735	12.074	-41.450	10.682	-24.505	4.331	-30.718	11.149

K0: the rate constant for zero order model; k1: first order rate constant; kh: Higuchi rate constant; kKP: Korsmeyer-Peppas rate constant; r^2: is the coefficient of determination; AIC: the Akaike Information Criteria; n: the diffusional release exponent. SD: Standard deviation.

Table 2.12 Kinetic assessment of the release data of Pentravan® formulations performed during storage at both 4°C and 25 °C.

Model	Parameter	Week 0		Week 4 (4°C)		Week 4 (25°C)		Week 8 (4°C)		Week 8 (25°C)		Week 10 (4°C)		Week 10 (25°C)	
		Mean	SD	Mean	SD	Mean	SD	Mean	SD	Mean	SD	Mean	SD	Mean	SD
Zero order	k0	0.009	0.000	0.006	0.000	0.006	0.000	0.005	0.000	0.006	0.000	0.007	0.000	0.008	0.000
	r^2	0.985	0.005	0.988	0.008	0.996	0.004	0.998	0.001	0.993	0.003	0.998	0.000	0.996	0.004
	AIC	6.702	2.892	-1.850	7.075	-15.157	8.366	-19.537	2.158	-7.535	3.011	-14.042	1.573	-8.232	10.970
First order	k1	<0.0001	<0.0001	<0.0001	<0.0001	<0.0001	<0.0001	<0.0001	<0.0001	<0.0001	<0.0001	<0.0001	<0.0001	<0.0001	<0.0001
	r^2	0.989	0.004	0.985	0.009	0.995	0.004	0.997	0.000	0.995	0.002	0.997	0.001	0.998	0.003
	AIC	3.802	2.968	0.280	6.235	-12.041	7.539	-17.404	1.004	-10.450	3.646	-10.654	2.133	-15.866	15.286
Higuchi	Kh	0.261	0.012	0.160	0.005	0.152	0.002	0.144	0.005	0.166	0.005	0.195	0.007	0.238	0.012
	r^2	0.831	0.022	0.698	0.029	0.738	0.024	0.753	0.002	0.816	0.013	0.750	0.008	0.805	0.019
	AIC	29.017	2.077	28.570	0.966	25.503	1.346	23.677	0.721	22.180	1.345	29.358	1.064	29.376	0.481
Korsmeyer-Peppas	kKP	0.024	0.006	0.002	0.001	0.003	0.001	0.004	0.000	0.012	0.002	0.005	0.001	0.015	0.005
	n	0.865	0.040	1.206	0.096	1.082	0.063	1.035	0.009	0.897	0.024	1.043	0.024	0.923	0.041
	r^2	0.997	0.002	1.000	0.000	0.999	0.000	0.998	0.001	0.999	0.001	0.999	0.001	1.000	0.000
	AIC	-8.206	9.933	-40.723	10.187	-26.106	3.775	-20.920	5.071	-25.993	10.522	-19.103	7.166	-23.903	4.863

K0: the rate constant for zero order model; k1: first order rate constant; kh: Higuchi rate constant; kKP: Korsmeyer-Peppas rate constant; r^2: is the coefficient of determination; AIC: the Akaike Information Criteria; n: the diffusional release exponent. SD: Standard deviation.

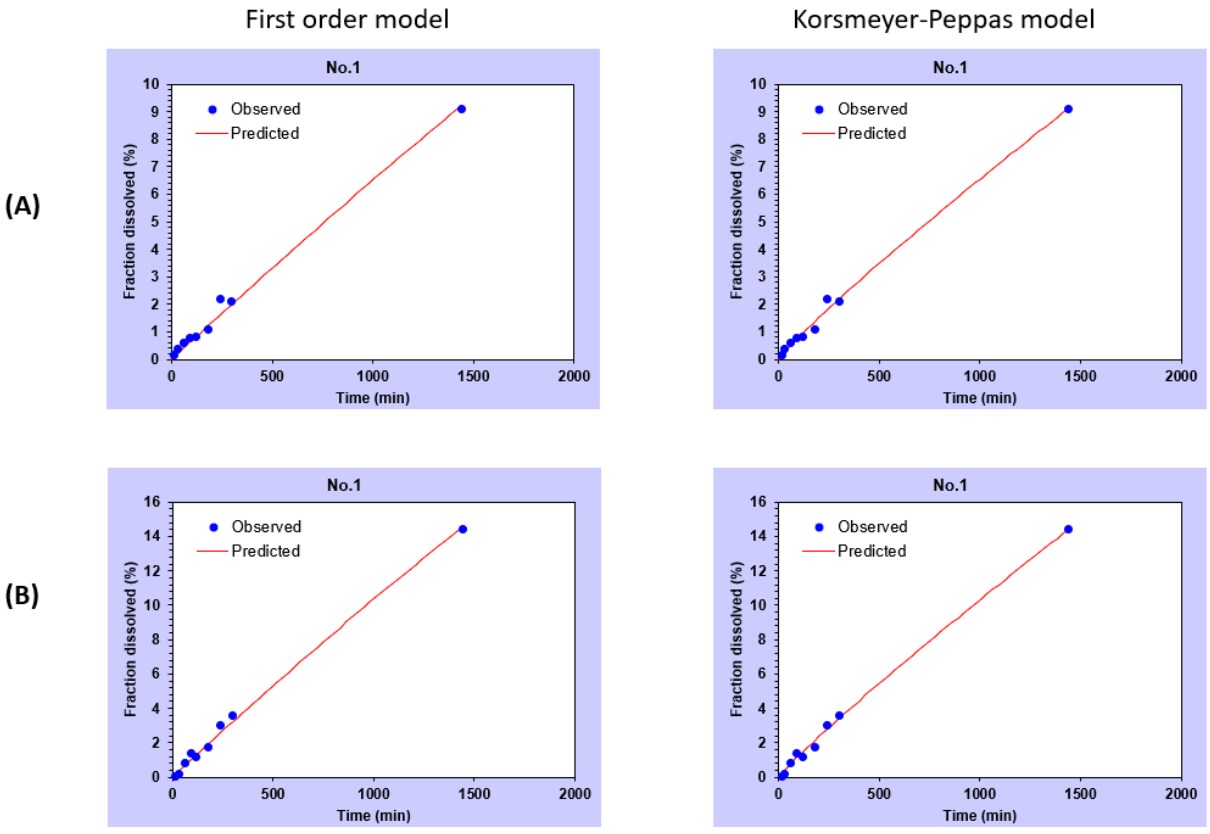

Figure 2.19 Comparison of model fitness between KP and first order models of Vanish-pen™.
(A) week 2, 25°C, and (B) week 8, 25°C. Solid circles represent individual data points.

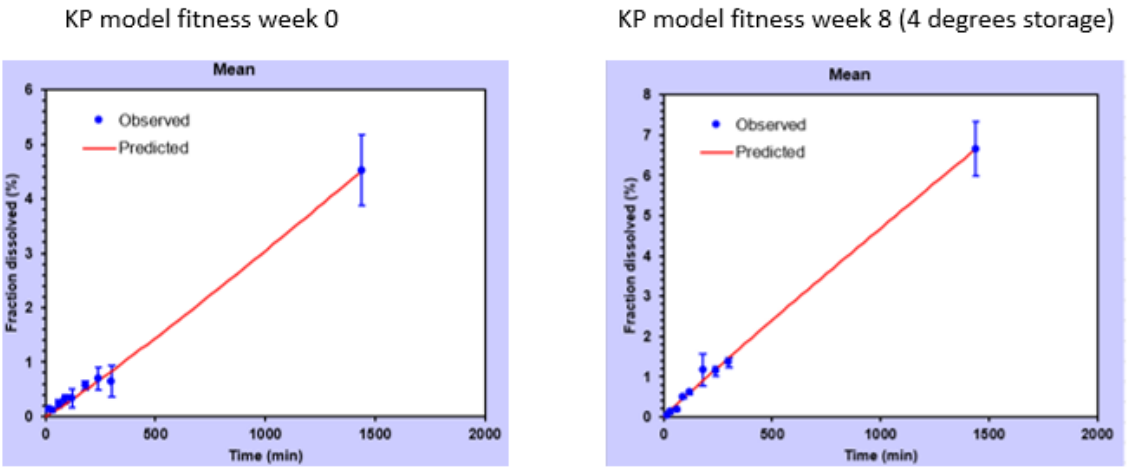

Figure 2.20 Comparison of KP model fitness at week 0 and week 8 of Versatile™ release profile
Solid circles represent the mean and error bars represent the standard deviation.

2.6 Discussion

The flavonoid hesperetin, which is present in citrus fruits [76], was reported to possess several benefits against depression, cancer, neurological diseases, inflammation, oxidation, and convulsions [52, 76, 81, 184-187]. Due to the extensive first-pass metabolism nature, hesperetin has low oral bioavailability [205-207]. Delivering hesperetin systemically through the skin could potentially be achieved by transdermal formulations development including creams, gels, transdermal patches. The use of cream formulation systems is a convenient approach [109], with commercial compounding vehicles that are 'ready-to-use', representing a viable approach to deliver therapeutics. These vehicles are easy to use with simple compounding steps and are designed according to the latest knowledge of topical vehicle tolerance and safety.

The goal of this study was to develop hesperetin transdermal formulations using commercial base creams (Vanish-Pen™ base cream manufactured by Medisca®, Doublebase™ gel by Dermal®, Versatile™ and Pentravan® by Fagron) and assess their ability to release hesperetin efficiently with investigating the stability of the formulations at different storage conditions (4°C and 25°C) for 10 weeks. The formulations were assessed by morphology characterisation, visual organoleptic properties, pH assessments and *in-vitro* drug release studies with kinetic assessment.

Other pharmaceutical bases were assessed including the Medisca® bases: PLO transdermal cream, VersaPro™ cream base, and PenDerm™ cream base, these bases were discarded due to the poor broad peaks by the HPLC. The HPLC method of hesperetin was not suitable to detect hesperetin released from the above-mentioned bases, hence, no further studies conducted on these bases. The interference of the components of the creams with the analytical detection of hesperetin may have hampered the use of these cream bases. A major obstacle encountered in the HPLC analysis of topical and transdermal dosage form is the interference of the additives and preservatives present in the complex cream formulation [241]. The excipients can pass through the column and cause some loss in the chromatographic resolution [241-243]. VersaPro™ gel base was discarded due to insoluble drug patches detected under the microscope reflecting non-homogenous mixture.

2.6.1 Preparation of hesperetin cream formulations

The solubility and homogeneity of hesperetin in the base creams were assessed by optical microscopy and showed the requirement of PEG to dissolve hesperetin (20 mg/mL) in the base creams. Acetone and ethanol did not facilitate the solubilisation of hesperetin in the creams

and showed insoluble patches under the microscope. PEG, is one of the most common cosolvents that are used to solubilise drugs in pharmaceutical formulations and have been used previously with hesperetin creams [244]. In this study by Huang et al., 2010, the solubility of hesperetin in different solvents (including PEG 400) was investigated to obtain the suitable solvent to prepare hesperetin creams. PEG 400 showed the highest solubilising effect on hesperetin when compared to other solvents [244].

2.6.2 Impact of storage temperature on stability

Repeated storage studies on the prepared formulations were conducted at storage temperatures of 4°C and 25°C for a period of 10 weeks. Storage studies included morphology characterisation, organoleptic properties assessment, pH investigation and drug *in-vitro* release studies. All the tested formulations showed consistent morphological characteristics (Figures 2.8 to 2.11), colour, and visual appearance (Figures 2.12 to 2.15) with no crystallisation or changes in colour detected at both storage temperatures over the period of 10 weeks.

2.6.2.1 pH assessment

pH values, ranging from 4 - 7 of all the developed formulations were consistent throughout the storage period of 10 weeks and was not affected with different storage conditions (Table 2.7). The pH of the dermal layer ranges from 4-7.4 reflecting that the formulations were in a satisfying pH ranges for skin application [233]. The composition of the commercial bases (Vanish-Pen™, Versatile™, and Pentravan®) is not available, therefore, it is not known what ingredient is stabilising the pH of the formulations. Frequently used ingredients to adjust or stabilise the pH of the formulations are citric and lactic acid, sodium lactate, sodium acetate, sodium citrate, and diammonium citrate [245]. For Doublebase™, it is believed that the presence of triethanolamine, which is an anionic surfactant, in the mixture can act as a neutraliser and aid in the stability of pH during storage [246] .

2.6.2.2 Morphology characterisation and organoleptic properties

For morphological characterisation, crystallisation in the developed creams was assessed using optical microscopy. No crystal formation was detected at storage temperatures of 4°C and 25°C for a period of 10 weeks (Figures 2.8 to 2.11). Using optical microscopy allows direct observations of the samples and was successfully used previously by several studies to detect crystallisation [247, 248]. The drug must remain diffused or dissolved in its amorphous form for effective transdermal delivery [234]. During storage, however, the drug may crystallise. Supersaturation of the drug is one of the most common reasons of crystallisation, as it produces an increase in thermodynamic activity, which can lead to crystal formation.

Temperature affects crystallisation because higher temperatures generate more diffusion, which causes more crystal formation. This fact emphasises the significance of storage conditions in guaranteeing transdermal formulations stability [249-251].

Differential scanning calorimetry (DSC) has been typically used to understand the thermal characteristics of compounds incorporated into topical and transdermal systems [252-256] by giving an insight into thermal and chemical properties including phase transitions, melting temperatures, degree of crystallinity, heat capacity changes, and homogenous dispersion.

The organoleptic properties of the creams were assessed visually during storage with no visual changes detected in the tested creams during the whole period of storage (Figures 2.12 to 2.15). Changes in colour of creams during storage could reflect instability or potential chemical degradation.

2.6.2.3 *In-vitro* drug release studies and kinetic assessment

An isocratic HPLC method was utilised to detect hesperetin during *in-vitro* drug release studies. The method previously developed (Arya et al., 2015) was optimised successfully to detect hesperetin. In our study, *in-vitro* drug release studies were conducted at week 0 on the freshly prepared formulations showing that Pentravan® formulation released the highest percentage of hesperetin after 24 hours, 12.69 % (0.68 %), but no significant difference was detected when compared to Vanish-Pen™ formulations (12.28 % (0.16 %)). Doublebase™ released significantly lower percentage of hesperetin of 11.35 % (0.26 %) when compared to Pentravan® ($p<0.05$). Versatile™ released the lowest percentage of hesperetin of 4.53 % (0.65 %) ($p<0.05$) (Figure 2.16).

To further assess the stability of the formulations, *in-vitro* drug release studies on the stored Vanish-pen™ and Doublebase™ formulations were repeated in weeks 2, 4, 8, and 10 (Figure 2.17), while for Versatile™ and Pentravan®, studies were conducted in weeks 4, 8, and 10 (Figure 2.18). Week 2 studies for Versatile™ and Pentravan® not conducted.

The subsequent results were further analysed using kinetic assessment and models application, these models are first order, zero order, Higuchi model, and KP model. According to r^2 and AIC values, KP model was selected as the most fitted model to describe the mechanism of hesperetin release from all the formulations during the storage period (Tables 2.9 to 2.12). It is the most appropriate model to reflect drugs release from creams as it can aid in characterising drug release from cylindrical shaped matrices which could describe the

release mechanisms from polymers and could be applied to understand the diffusion of a drug across synthetic membranes [109, 257].
For Vanish-pen™ (week 2 and 8 (25°C)) (Table 2.9) (Figure 2.19) and Versatile™ (week 8 4°C) (Table 2.11) (Figure 2.20), the model selection showed inconclusive data which was attributed to sampling error.

2.6.2.3.1 Vanish-Pen™

Hesperetin release provided by Vanish-Pen™ formulations are likely due to the presence of pluronic lecithin organogel (PLO) in the base components [212]. Due to the amphiphilic nature of PLO systems, they facilitate the delivery of various drugs and enhance their permeation across the skin [258]. Pluronic lecithin organogel (PLO) has been used for hydrophilic and hydrophobic APIs for topical and transdermal delivery [259].

No statistically significant changes were detected in the release profiles of Vanish-pen™ formulations when stored for 10 weeks in 4°C storage condition (Figure 2.17A) (Table 2.8). For 25°C storage temperature, consistent release profiles were detected for 8 weeks with no statistically significant changes, while at week 10, significant increase in the release profile of hesperetin was detected ($p<0.05$) (Figure 2.17A) (Table 2.8). However, the release rate constant increased with storage (Table 2.9). Two mechanisms are suggested to be responsible of the release of hesperetin, these mechanisms are super case II drug transport and anomalous diffusion. Having multiple release mechanisms is not uncommon because the formulation could include multiple polymer matrices, including PLO, that could be affected during storage [260, 261].

Factors that could relate to the changes in the release profiles during storage at 25 °C is the possible change in the viscosity of PLO during storage which could lead to either decrease or increase in drug release profile [262], this could also be related to polymeric chains relaxation and changes in size leading to interrupted efficiency in controlling or improving drug release.

Vanish-Pen™ cream base provided a consistent release profile of hesperetin when stored in 4°C for 10 weeks but the percentage release is still minimum and could to be improved with the addition of penetration enhancers that could facilitate more hesperetin release from the formulation.

2.6.2.3.2 Doublebase™

The percentages of hesperetin released during the study over weeks 2-10 ranged from 9-12 % at 4 °C and 7-14 % at 25 °C (Figure 2.17B). Two mechanisms are suggested to be responsible of the release of hesperetin, namely super case II drug transport and anomalous diffusion. This demonstrate that the predominant molecular mechanism of drug release from Doublebase™ is drug diffusion governed by concentration gradient in addition to macromolecular relaxation of the polymer chains of carbomer.

The storage of Doublebase™ formulation at 25°C for 10 weeks resulted in consistent release profiles with no significant changes detected (Figure 2.17B) (Table 2.8). While the storage at 4°C resulted in significant decrease ($p<0.05$) in the release profiles of hesperetin in weeks 2, 8, and 10 (Figure 2.17B) (Table 2.8). The release rate constant (kKP) decreased during storage in both temperatures (Table 2.10). Doublebase™ gel contains the polymer carbomer which is used previously in transdermal delivery [263-265]. In addition to its potential use as a sustained release system, previous reports have showed that increasing the amount of carbomer polymers in gel formulations could reduce drug release due to its swelling capacity that could aid in controlling drug release [265].

In addition, Doublebase™ contains surfactants and penetration enhancers, including sorbitan laurate (non-anionic), trolamine (anionic), and glycerol that could potentially influence drug release. It has been shown that increasing the amount of trolamine in gel formulations can decrease drug release by creating more viscous matrix that hinder drug molecules to be released out of the systems [265]. Glycerol is widely used as a penetration enhancer and it could potentially increase drug release in gel formulations [265]. Sorbitan laurate could impact the release as it can provide more sustained release by reducing the amount of drug released from the system [266]. These components reflect the release obtained by Doublebase™ formulations which suggest the potential of its usage as a compounding base for topical/transdermal drug delivery although it has not been extensively investigated by studies.

The decrease in the release at 4°C also could be related to the change in the carbomer polymer matrix integrity which can be influenced by the physiochemical properties of the drug and the interaction between the drug and the polymer provoked by temperature [260, 267]. This could subsequently lead to the resistance of polymer to swell and relax due to the increased network cross-link density and increased viscosity, thus, prevent the release of the drug.

Storage temperature of 25°C for 10 weeks is optimum for providing consistent hesperetin release from Doublebase™ but more experimentations are needed to improve the percentage release.

2.6.2.3.3 Versatile™

Versatile® formulations demonstrated the lowest release of hesperetin in week 0, potentially reflecting its ability to delay release and provide possible sustained release properties. The release of hesperetin from Versatile™ formulation stored at n both 4 °C and 25 °C ranged from 4-10 % over weeks 4-10 (Figure 2.18A). The most favourable transport mechanism according to the KP model was the super case II transport governed by macromolecular relaxation of the polymeric chains.

The storage of Versatile™ formulations at both 4°C and 25°C for 10 weeks provided consistent release profiles with no statistically significant changes detected (Figure 2.18A) (Table 2.8). While the release rate constants increased with storage (Table 2.11).

Versatile™ cream base contain proliposome technology [108] which has been investigated widely for its potential as a sustained transdermal dosage form [268-272]. This technology is reflected by the low release noticed in 24 hours from Versatile™ formulations (Figure 2.16). Proliposomes are composed of phospholipids, steroids, water soluble carriers, and solvents [273]. Increasing the concentration of the lipid in the proliposome could enhance the control of drug release for longer periods reflecting sustained release [274]. Proliposomes have been developed as an approach to avoid the physiochemical instability encountered by conventional liposomes. When applying proliposomes to mucosal membrane, they are expected to form liposomes when in contact with mucosal fluids and the resulting liposomes act as sustained release dosage form for the loaded drugs [273].

The increase in the release rate constants during storage noticed in our study is suggested to be caused by polymeric changes and relaxation of the proliposomal matrix. Versatile™ components are trade secrets, but polymers are common components of cream bases. A potential explanation for the increased drug release with Versatile™ formulations are that polymers changes (e.g. swelling, relaxation, and erosion) during storage, could lead to reduced polymer efficacy and easier route for drug diffusion through the polymer matrix into the release media [260].

2.6.2.3.4 Pentravan®

The storage of Pentravan® formulations at both 4°C and 25°C resulted in statistically significant decrease in the release profiles of hesperetin in weeks 4 and 10 ($p<0.05$). Whilst in week 8, insignificant decrease in the release profiles was detected (Figure 2.18B) (Table 2.8).

The release rate constant values were decreasing with storage which is related to the decrease in drug release with storage illustrated by *in-vitro* release studies (Table 2.12).

The percentages of hesperetin released in 24 hours in weeks 4, 8, and 10 from Pentravan® formulation stored in 4°C ranged from 7-10.5 %, In the contrary, the formulation stored in 25°C released 8-12 % of hesperetin (Figure 2.18B). Two release mechanisms are suggested to be responsible of the release of hesperetin in 24 hours during the 10 weeks storage period, these mechanisms are super case II drug transport and anomalous diffusion demonstrating that the predominant molecular mechanism of drug release from Pentravan® is drug diffusion governed by concentration gradient in addition to macromolecular relaxation of the polymeric and liposomal matrices. Having multiple release mechanisms is normal because the formulation could include multiple polymer matrices that could be affected during storage [260, 261].

Pentravan® is an o/w emulsion base that contains a liposomal matrix with penetration enhancers that could be the reason of the greater drug release than other bases shown in week 0 (Figure 2.16) [107]. Penetration enhancers could promote drug release and reduce the resistance of skin barrier by interacting with the constituents of the skin. Liposomes have been frequently used in studies to improve and control percutaneous absorption of various compounds like diclofenac [275], betahistidine [276], tetracaine [277] and triamcinolone [278, 279]. The details of Pentravan® components are trade secret. Liposomes with smaller diameter (up to 600 nm) penetrate the skin more easily than the bigger diameter liposomes (1000 nm and more) [280]. Several factors can influence the chemical and physical stability of liposomes during storage including pH, temperature, and the presence of degradation substances. Liposomes could consequently exhibit disadvantages such as self-aggregation, coalescence, flocculation, and particle fusion which could result in precipitation and the formation of larger vesicles with increased size due to the loosening of the bilayer structure of liposomes. This will eventually decrease the efficacy of liposomes in controlling and improving drug delivery [281].

The mechanism of drug release from liposomal matrices occurs by forming transient pores in the lipid bilayer in which drugs transport from the inner core of liposomes to the external medium followed by the diffusion across the membrane. Another mechanism could be the initial transport of liposomes through the membrane followed by the release of drug from the liposomes core into the release media, this mechanism can be governed by the pore size of the membrane [282, 283].

The decrease in drug release with storage of Pentravan® formulation could be related to several factors: (i) reversible binding of the released drug from the liposome which prevents the transport of the drug through the membrane into the release media [283]; (ii) liposomes usually increase in size with storage resulting in aggregation which could render the passage of liposomes through the pores of the release membrane [284, 285]; (iii) the polymer used in the commercial base is not known but the inclusion of polymers with liposomal matrix is common. Pentravan® base has penetration enhancers which could include polymers, such as Carbapol and PEG [286]. The polymer matrix integrity can be influenced by the physiochemical properties of the drug and the interaction between the drug and the polymer [260, 267], which could subsequently lead to the resistance of polymer to swell. The swelling of polymers aids in drug release, therefore the resistance to swell will eventually result in decreasing drug release; (iv) some penetration enhancers can be affected by temperature and lose their penetration properties in specific temperatures, an example of that is Tween® 20 which has a freezing point of 7°C [287].

Using pharmaceutical base creams to deliver hesperetin through or into the skin is a convenient way for the developer and the patient. Vanish-pen™ (4°C), Doublebase™ (25°C), and Versatile™ (4°C and 25°C) formulations were showing consistent storage studies at specific storage temperatures for 10 weeks.

The limitations encountered during this work were the short period of release studies, stability issues, low amounts of drug released, and storage temperatures. The release studies were conducted for 24 hours only due to the leakage of the creams into the release media when studies are conducted for more than 24 hours. This could be improved by using different release procedure such as using Franz cells, however Franz cells were not feasible in this study because of using low amounts of hesperetin. With higher amounts, Franz cells could be used. Also, solubility enhancement could be beneficial to improve the release as hesperetin has low aqueous solubility. Solubility enhancement techniques include particle size reduction, nanotechnology, and using different surfactants or penetration enhancers. Although the manufacturers of the base creams confirmed the instability of the creams at high temperatures (40°C), assessing the formulations at this storage temperature would be beneficial to explore the behaviour and stability of hesperetin formulations at higher temperatures.

.

2.7 Conclusion

Transdermal delivery of drugs using creams is a very promising and convenient while several challenges can be faced such as the stratum corneum barrier, the formulation optimisation, and the stability of drugs in the formulations during storage.

The main goal of this study is to incorporate the flavonoid hesperetin into the 'ready-to-use' pharmaceutical base creams and evaluate it by morphological characterisation, physical properties, release studies and storage conditions.

For consistent hesperetin release profiles for 10 weeks, it is suggested for Vanish-pen™ formulations to be stored at 4°C, Doublebase™ formulations at 25°C, and Versatile™ formulations at both 4°C and 25°C. while Pentravan® formulations stored at both 4°C and 25°C resulted in inconsistent release profiles.

The tested vehicles (except Pentravan®) showed good potential to be used clinically owing to their easy compounding steps, morphological and physical stability with storage, consistent release profiles at specific storage temperatures, and simple development of semi solid topical/transdermal formulations. However, in our study, the storage conditions affected the amount of hesperetin released from Pentravan® and the kinetic assessments showed that polymer matrices were potentially contributing to the release mechanisms. Also, the release obtained from all the tested vehicles was not optimum and could potentially be further improved by using different drug release methods and more penetration and solubility enhancers.

Hesperetin creams could be beneficial for topical and localised purposes for the treatment of skin disorders including skin cancer. More studies are required in this area to assess the delivery and permeation of hesperetin into the skin.

Chapter 3

Transdermal delivery of hesperetin for CNS disorders using transdermal patches

3.1 Introduction

In Chapter 2, we highlighted the application of compound base creams for the topical and transdermal delivery of hesperetin with demonstrating hesperetin's CNS and anti-carcinogenic properties, pharmacokinetics, and physiochemical properties. In this chapter, we considered the use of transdermal patch systems for hesperetin. It has been shown that hesperetin possesses low oral bioavailability owing to its lipophilic nature, extensive first-pass metabolism, and low aqueous solubility, this consequently resulted in low and often subtherapeutic concentrations in the systemic circulation following oral administration [185, 193, 205-210].

Transdermal patches are designed to efficiently treat targeted diseases by delivering a therapeutically effective amount of drug through the skin into the systemic circulation. Using transdermal patches to deliver drugs is convenient for patients due to the ease of application and improved patient compliance, in addition to the reversibility of treatment by patch removal. Transdermal patch exhibits numerous advantages over oral drug delivery as it avoids the first-pass metabolism associated with oral drug delivery. Therefore, transdermal administration is a proven way to improve drug's bioavailability [88].

Transdermal patches can be formulated in two common types, either as a liquid/gel reservoir patch or a solid matrix (drug-in-adhesive) patch (Figure 1.5). In liquid/gel reservoir, a fluid or a semisolid that contain the drug is sequestered in a cavity formed between a permeable film and an impermeable backing film. The permeable membrane separates the reservoir from the adhesive layer. Matrix patches are more flexible, thinner, more comfortable and adhering. In matrix patches, the drug is mixed with a polymeric or viscous adhesive in the same layer to deliver the drug and to adhere to the skin [90].

In transdermal patches drug delivery, polymers (adhesives) are necessary as they act as the backbone for the system and promote drug release, while plasticisers are required to prevent brittle patches, improve flexibility, and enhance or modify drug release [288].

3.1.1 Transdermal delivery of flavonoids

The delivery of flavonoids using transdermal patches has been explored by few studies to overcome the problems associated with oral delivery [289-291]. Bhalerao et al. (2019), developed hesperidin transdermal patches using hydroxy methylcellulose (HPMC) and Eudragit S100 as polymers, and Dibutyl phthalate as plasticiser. Their patches demonstrated high hesperidin release (93.7 %) in 6 hours and good physiochemical properties [289].

Another study developed quercetin transdermal patches using the polymers HPMC and ethyl cellulose with PEG as a plasticiser. This study showed that the release of the drug from the patches reached up to 85.8 % in 24 hours and significant anti-inflammatory activities were employed by the patches [290].

Ermawati et al, (2021), developed quercetin transdermal matrix patch using the combination of hydrophilic-hydrophilic polymers such as HPMC and carboxymethylcellulose natrium (CMC-Na) which resulted in a release of 37 % in 5 hours and followed Higuchi model with diffusion mechanism [291].

However, no pressure sensitive adhesives were used in Ermawati et al, (2021) study and Kharia et al, (2020), only cellulose polymers. They did not include a pressure sensitive adhesive which is an essential component when developing a transdermal patch. Inadequate water resistance, low mechanical strength, and compatibility with the hydrophobic matrix are some of the drawbacks of natural polymer cellulose. All the FDA approved patches in the market are made of pressure sensitive adhesives.

3.1.2 Pressure sensitive adhesives (PSA)

For a transdermal patch to adhere efficiently to the skin a proper adhesive is needed. The pressure sensitive adhesives (PSA) in transdermal patches aid in maintaining the adhesiveness of the patch to the skin, furthermore, PSAs affect drug delivery, drug permeation, and physical and chemical stability [90, 111]. PSAs adhere to surfaces via Van der Waals interactions under the application of external pressure [292]. There are three commonly used pressure sensitive adhesives for transdermal drug delivery patches, these are silicone polymers, acrylates, and rubber-based adhesives [112, 293].

3.1.2.1 Silicone PSAs

DuPont™ Liveo™ offers a wide range of silicone-based adhesive solutions including BIO-PSA silicone adhesives that are intended for transdermal and controlled drug delivery [294]. The advantages of these BIO-PSA silicone adhesives are their high delivery, low irritation, non-cytotoxic, non-sensitising, and low reactivity (stable). In the other hand, they have low solubility with drugs, their cost is high, and their tendency of crystallisation is high [90, 112, 295]. Silicone PSAs are produced through condensation reaction of the long chain polymer, polydimethylsiloxane (PDMS), with a silicate resin (Figure 3.1). The ratio of the polymer/resin determines the viscosity of the adhesive which could impact the rate of drug release [295, 296].

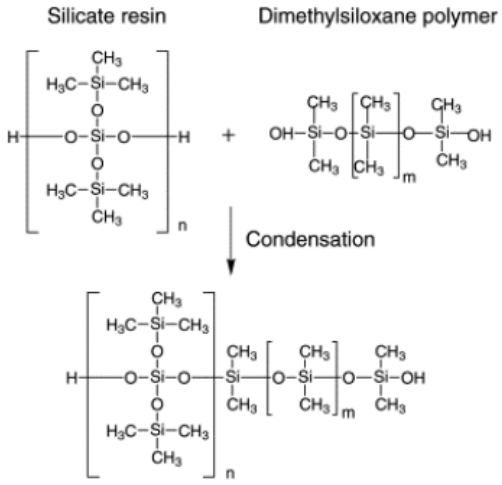

Figure 3.1 The chemical structure and the condensation reaction to produce silicone pressure sensitive adhesives.

Obtained from [296].

The use of silicone adhesives for transdermal patch drug delivery has been widely researched previously and reviewed [293, 297-304]. Silicone adhesive transdermal patch successfully released lidocaine rapidly in higher percentage when compared to the acrylate and Polyisobutylene (PIB) adhesives transdermal patches [297]. A further study demonstrated that silicone adhesive matrices provide the highest permeability and flux of physostigmine when compared to the PIB and acrylate matrices [298]. The pharmacokinetic parameters of tolterodine obtained from silicone and acrylate-based patches were compared and showed that silicone-based patch showed 2-fold higher steady-state concentration and higher bioavailability than the acrylate-based patch [300]. Silicone adhesives have been used in commercial transdermal systems successfully, examples are Transderm-Nitro® nitroglycerin system manufactured by ALZA Corporation for Novartis, Duragesic® fentanyl system manufactured by ALZA Corporation for Janssen Pharmaceutical, and FemPatch® estradiol patch made by Cygnus, Inc. for Parke-Davis [296].

3.1.2.2 Acrylic PSAs

Acrylic based PSAs are copolymers obtained by the combination of ‘hard’ and ‘soft’ monomers at different ratios which provide the optimal characteristics of the PSA [305]. The advantages of acrylic PSAs are their low cost and their excellent affinity for pharmaceutical compounds. The main disadvantage is the presence of monomers that are unreacted and can be toxic [90].

An example of the acrylic PSAs is the methyl methacrylate copolymer (Eudragit®) (Figure 3.2) that is currently used in transdermal drug delivery systems by being formulated as hydrophilic or amphiphilic adhesive, when combined with the proper plasticisers [306]. Eudragit polymers have high drug loading capacity, and they are well tolerated by the skin and non-irritant [307, 308]. Eudragit® E100 formulations are resistant to thermal degradation and oxidation, they are of moderate cost, self-adhesiveness, and suitable with wide range of hydrophilic and hydrophobic plasticisers, these properties make them commercially highly accepted [308].

The ability of Eudragit® E100 transdermal patches to deliver various drugs (metronidazole, ondansetron, chlorpheniramine, losartan, atorvastatin, donepezil, fentanyl) and herbal compounds transdermally was successfully studied and explored by several studies [288, 307-316].

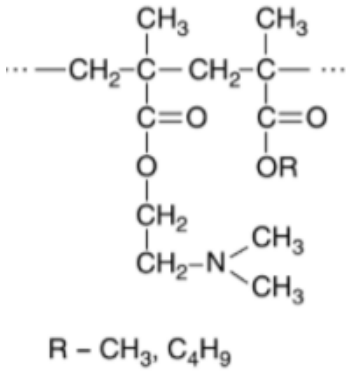

Figure 3.2 The chemical structure of Eudragit® E100

Obtained from [317].

3.1.2.3 Rubber-based PSAs

Rubber-based adhesives have properties of interest for transdermal drug delivery systems, including its high mechanical resistance, biocompatibility, easy film forming with good flexibility, low cost, and being chemically inert [318]. The poor affinity of rubber adhesive for drugs and excipients and their low solvents solubility are the disadvantages [90, 112]. Styrene-butadiene (SBR), and styrenic block copolymers (SBC) including polystyrene-polybutadiene-polystyrene (SBS) or polystyrene-polyisoprene-polystyrene (SIS) are examples of synthetic rubber PSAs that are widely used for transdermal patch systems [318].

3.1.3 Plasticisers in transdermal patch systems

Plasticisers are one of the basic components used for developing transdermal patches. They are resins or liquids with low molecular weight that reduce the secondary bonds of polymer-

polymers chains, instead, they form secondary bonding with polymer chains and increase molecular space [319, 320]. The plasticiser will attach between the polymer chain creating secondary hydrogen bonds which provide molecular flexibility, less rigidity, and more molecular space. The addition of the plasticiser reduces the glass transition temperature resulting in more flexible polymer chains. They improve the film forming mechanical properties, prevent cracking and brittleness of the patch, increase flexibility, and control drug release rate from the transdermal system [320, 321]. Examples of commonly used plasticisers are polyvinylpyrrolidone 30 (PVP 30), Tween® 20, glycerol, and triacetin.

3.1.3.1 Glycerol

Glycerol was utilised frequently by several studies as a plasticiser of biodegradable and edible films [320, 322-339]. Glycerol-filled silicone adhesive patches were developed previously through simple mixing method with high shear forces [340]. Glycerol enhances the water absorption of the polymer in silicone adhesives, provide gentle skin adherence, and low peel forces, which makes them ideal for sensitive skin types [340]. Glycerol, which is highly hygroscopic, was added in most of the hydrocolloid films and film-forming solutions to reduce brittleness of the film [341-343].

Films containing glycerol achieved more water adsorption and at an increased rate during storage when compared to other films [320]. It was suggested that 5-10 % of glycerol in transdermal patches is optimal to maintain mechanical flexibility and resistance while using 3 % glycerol results in brittle films and using 12 % causes phase separation on the film surface [344]. Water can penetrate easily into the pressure sensitive adhesive structure with the presence of glycerol as highly mobile channels are created in the adhesive matrix influencing the adhesive physicochemical properties [345]. Glycerol increased ketoprofen penetration rate from the patch when used as a penetration enhancer. The *in-vitro* penetration study on rat skin showed that the patch flux is significantly higher when the concentration of glycerol is higher [346].

3.1.3.2 Tween®20

Tween®20 has been previously formulated into transdermal patches as a permeation enhancer or as a plasticiser [347, 348]. The effect of Tween® 20 on drug permeation through rabbit skin was tested [347]. Several studies reported the effectiveness of Tween®20 in increasing skin penetration of certain compounds [349-351], while in another study they demonstrated the ineffectiveness of Tween®20 on specific compounds [352]. An amount of 1 and 5 % w/v of Tween® 20 were used as a permeation enhancer of 5-flurouracil and achieved a two-fold increase in the permeability with 5 % amount [353]. It was observed that Tween®

20 exerts its permeability enhancement effect mostly on hydrophilic molecules. It was hypothesised that Tween® 20 allows polar molecules to easily partition across the skin barrier due to increasing stratum corneum water content or due to forming large micelles that extract skin lipids, thus favouring hydrophilic molecules permeation [353] [354].

3.1.3.3 PVP 30

PVP 30 is a hydrophilic and hygroscopic polymer which impacts moisture content in transdermal patches. PVP can increase the moisture content by allowing easy water diffusion into the matrix [355]. The addition of PVP into insoluble films can enhance the release rate constants by the formation of pores which decrease the length of the diffusion path of drug molecules to diffuse into the dissolution medium resulting in higher dissolution rates. PVP is able to improve the solubility of the drug into the matrix by retarding crystallisation and sustaining the amorphous form of the drug [356]. Several studies showed that increased PVP amounts in different types of transdermal patches (including PSA) inhibited crystallisation and enhanced drug permeation and release [288, 357-361].

3.1.3.4 Triacetin

The plasticiser triacetin was researched and investigated widely when incorporated into Eudragit® E100 patches, it was found that triacetin is an effective first plasticiser for Eudragit polymers [309, 312]. The use of triacetin in atorvastatin Eudragit® E100 transdermal patches had a positive effect on flexibility and bioadhesion due to the interaction of the organic ester bonds of triacetin with Eudragit® E100. Furthermore, triacetin allowed better and higher release of atorvastatin compared to PEG E400 [313].

3.1.4 Crystallisation in transdermal patch systems

Crystallisation in transdermal patches is a major problem that results in unstable patch and impacts drug release. The solid-state drug concentration in a transdermal patch system can reach a saturation limit, resulting in the possibility of crystallisation, which causes stability issues [249]. The initiation of crystallisation occurs through the collisions of single drug molecules forming a nucleus. The frequent continuous collisions between the molecules of drug result in increased critical radius of the formed nucleus that is not easy to re-dissolve, resulting in drug crystals formation. Until a saturation state is achieved, the growth of crystals continues. The formation of crystals in transdermal patches leads to the delivery of dangerous or ineffective amounts of drug, makes them unstable, negatively impacts skin permeation, reduces patient's acceptability of the product because of the reduced aesthetic appeal of the product [249, 362].

The crystallisation of the drug in the patch can be eliminated or reduced by several approaches including the reduction of drug loading to below the saturation solubility, the usage of pro-drug which has higher solubility in the formulation, the usage of co-solvents which increase solubility, the modification of the adhesive, and the usage of crystallisation inhibitors. Crystallisation inhibitors and solubilisers include PVP 30, polyethylene glycol, copovidone, crospovidone, mannitol, dextrin derivatives, polypropylene glycol, glycerine, poloxamer, Labrasol ® and Tween® 80 [249].

The drug must remain diffused or dissolved in its amorphous form for effective transdermal patch delivery [234]. During storage, however, the drug often crystallises. Supersaturation of the drug is one of the most common reasons of crystallisation, as it produces an increase in thermodynamic activity, which can lead to crystal formation. Temperature affects crystallisation because higher temperatures generate more diffusion, which causes more crystal formation. As a result, a higher temperature promotes crystallisation. This fact emphasises the significance of storage conditions in guaranteeing transdermal patch stability [249, 250].

3.2 Aims and objectives

The primary aim of this study is the development of hesperetin matrix transdermal patch systems with optimal mechanical properties, efficient drug release, and storage stability with understanding the release mechanisms and kinetics.

To achieve the aims, the overall objectives were:

- Prepare different hesperetin transdermal patches using either Dow Corning® BIO-PSA 7-4501 silicone adhesive or Eudragit® E100 copolymer as an acrylic-based PSA.
- To assess the impact of plasticisers (PVP 30, Tween® 20, glycerol, or triacetin) on drug release from the patches.
- Evaluate the properties of the developed patches preliminarily through *in-vitro* drug release studies, thickness measurements and visual mechanical properties (stickiness and peel).
- Assess the stability of the formulations for 3 weeks storage at 4°C and 25°C by morphology characterisation, pH investigation, and *in-vitro* drug release.
- Assess the impact of 3 weeks storage on the release kinetics of hesperetin from patches.

3.3 Materials

Kollidon® 30 (Polyvinylpyrrolidone 30) (*BASF*, Ludwigshafen, Germany), Tween® 20 (Sigma-Aldrich®, UK), Eudragit® E100 (Evonik, Germany), Glycerol (Sigma-Aldrich®, UK), Succinic acid (Sigma-Aldrich®, UK), Triacetin (Sigma-Aldrich®, UK), Dow Corning® BIO-PSA 7-4501 silicone adhesive (DuPont™, UK), Scotchpak™ 9741 Release Liner (3M™, UK), Ethyl acetate (Fisher Scientific, UK), Isopropanol (Fisher Scientific, UK).

3.4 Methods

3.4.1 High Performance Liquid Chromatography (HPLC) Method for hesperetin

The HPLC method utilised was previously described in Section 2.4.1.

3.4.2 HPLC method Validation

The HPLC method validation was previously described in Section 2.4.2.

3.4.3 Preliminary studies

3.4.3.1 The development of hesperetin matrix transdermal patches

Hesperetin matrix transdermal patch systems developed using Dow Corning® BIO-PSA 7-4501 as a silicone adhesive and Eudragit® E100 as an acrylic adhesive with different plasticisers incorporated (polyvinylpyrrolidone 30 (PVP 30), Tween® 20, glycerol, triacetin).

3.4.3.1.1 Dow Corning® BIO-PSA 7-4501 silicone adhesive patches

Hesperetin powder was dissolved thoroughly in acetone (10 mg/mL) and then added into the silicone adhesive with or without adding the required additives (PVP 30, Tween® 20 [353], or Glycerol [344]) (Table 3.1) [297]. The addition of hesperetin powder directly into the adhesive formed heterogeneous mixture which necessitated the solubilisation of hesperetin in acetone. The mixture was then vortex mixed [340] for 60 minutes until a homogenous mixture is apparent and was then casted slowly on a release liner (Scotchpak 9741 (3M™, UK)) using an Elcometer 4340 Automatic Film Applicator to form a thin film. The film was then left to dry for 24 hours at room temperature. The backing layer were placed over the film, patches were cut into 2 cm^2 squares.

Table 3.1 Composition of hesperetin silicone-based adhesive patches.

	F1	F2	F3	F4	F5	F6	F7
PVP 30	0	5 %	10 %	-	-	-	-
Tween® 20	0	-	-	2.5 %	5.0 %	-	-
Glycerol	0	-	-	-	-	2.5 %	5.5 %
Hesperetin	0.05 %	0.05 %	0.05 %	0.05 %	0.05 %	0.05 %	0.05 %

Compositions are reported as % w/w.

Dow Corning® BIO-PSA 7-4501 silicone adhesive is designed for transdermal drug delivery systems [294]. The use of silicone adhesives for transdermal patch drug delivery has been widely researched previously and reviewed [293, 297-304]. The resin/polymer ratio in Dow Corning® BIO-PSA 7-4501 is 60/40, the silanol content is high with 70 % solid content, the solvent used is heptane, and the viscosity is 1800 mPa.s [295]. Glycerol-filled silicone adhesive patches were developed previously through simple mixing method with high shear forces [340].

3.4.3.1.2 Acrylic-based PSA (Eudragit® E100)

To prepare the Eudragit E100-based transdermal patches, a previously studied method for patch development was used [309]. In their patch development no glycerol added while in this study glycerol was added to facilitate the release. Succinic acid was dissolved in 10:5 ethyl acetate/isopropanol then 10 g Eudragit® E100 was added to the mixture and mixed thoroughly by vortex mixing for 90 minutes until a clear yellow dense solution is formed. An amount of 3 g of this polymer mixture was mixed with hesperetin and the required additives [344] (Table 3.2) then casted slowly on the release liner (Scotchpak 9741 3M™) using Elcometer 4340 Automatic Film Applicator to form a thin film. The film was then left to dry for 24 hours at room temperature. The backing layer were placed over the film and patches were cut. Succinic acid was incorporated into the formulations as a cohesion promoter and triacetin was needed to provide plasticising action [309].

Table 3.2 Composition of hesperetin Eudragit® E100 patches.

	F8	F9	F10	F11	F12	F13
Triacetin	45 %	45 %	-	-	-	45 %
Glycerol	-	5 %	2 %	5 %	10 %	10 %
Succinic acid	1.75 %	1.75 %	1.75 %	1.75 %	1.75 %	1.75 %
Hesperetin	0.17 %	0.17 %	0.17 %	0.17 %	0.17 %	0.17 %
Eudragit® E100	66 %	66 %	66 %	66 %	66 %	66 %

Compositions are reported as % w/w.

The additives used with Eudragit® E100 in this study were necessary for optimising the formulations and obtaining the required mechanical properties and flexibility. Succinic acid was incorporated into the formulations as a cohesion promoter and triacetin was needed to provide plasticising action [309]. The effect of those two additives together alters the mechanical properties of Eudragit® as succinic acid allow the polymer chains to cross-link into layers that

smoothly glide by the action of triacetin over one another [309, 311]. Succinic acid has been used previously with Eudragit® E100 transdermal patches as a cohesion promoter and a cross-linking agent to deliver metronidazole, losartan, and herbal molecules [307, 309-311, 314], and further as a release modifier to influence the release of ondansetron and losartan [288, 311]. Glycerol has been previously incorporated into Eudragit® E100 patches as a plasticiser for the delivery of donepezil, fentanyl, and herbal molecules [307, 314-316].

3.4.3.2 Measurement of patch thickness

The thickness of the developed patches was measured using a digital micrometre with an average of three readings for each patch.

3.4.3.3 Morphology and mechanical characterisation

For optimum patches formulation, the drug should be dissolved and homogeneously dispersed in the polymer matrix. Hesperetin powder was either mixed directly in the adhesive matrix or dissolved in acetone before mixing to assess the need of solvent incorporation. The morphology of the initial formulations was assessed using optical microscopy (Zeiss Primovert [Zeiss,UK] with 10x objective lens) to detect the possible formation of insoluble drug crystals which would reflect the insolubility and inhomogeneity of contents together in the developed formulations [249, 297]. Using optical microscopy allows direct observations of the samples and was successfully used by several studies to detect crystallisation [247, 248].

The formulations were further assessed visually in terms of regular handling, stickiness, and peel-ability or detachability from the release liner. This was achieved if the patch is peeled off the release liner easily without leaving visual traces on the liner and by adhering efficiently on the release studies glass jars and not detach after adding the release media. The formulations that were not homogenous under the microscope, too sticky, hard to detach from the liner, and do not stick properly on the bottom of the glass jars were discarded. Accurate mechanical tests are necessary such as tensile strength test, uniformity testing, and peel adhesion test [112, 297].

3.4.3.4 *In-vitro* drug release studies

The *in-vitro* drug release studies were conducted using cylindrical screw top jars (15 mL). The patch was placed inside at the bottom of the jar and the release media used was PBS. The release study was conducted in an orbital shaker at 100 rpm and temperature maintained at 37°C for 24 hours. Samples of 100 µL were withdrawn (n=3) at 1 and 24 hours and replaced with fresh (pre-warmed) phosphate buffered saline (PBS), pH 7.4. The withdrawn samples were filtered through a 0.22 µm filter and assessed by the HPLC analysis. One formulation

from each of the two different types of patches (silicone and acrylic PSAs) was selected for further storage studies. The selection of the optimal formulation was based upon the formulation causing the highest drug release.

3.4.4 Storage studies at different temperatures

The selected formulations were stored at 4°C and 25°C and assessed by morphology and mechanical characterisation, pH assessment, *in-vitro* drug release studies, and kinetic assessments. All storage studies were performed for the selected formulations at weeks 0, 2, and 3.

3.4.4.1 Morphology and mechanical characterisation

Morphological characterisation studies (see Section 3.4.3.3) were repeated on the selected formulations during a storage period of 3 weeks at 4°C and 25°C, in airtight glass jars, to observe any morphological changes throughout storage [363]. In addition, visual mechanical properties were assessed (see Section 3.4.3.3) during storage which may detect the degradation and incompatibility of the products.

3.4.4.2 pH assessment

The pH of the dermal layer ranges from 4-7.4, therefore, the formulations are expected to be in this range [233]. The pH in this study was assessed by applying a drop of the formulation (un-casted and undried) on pH indicator paper (pH 1-14) (Ahlstrom-Munksjö ©).

3.4.4.3 *In-vitro* drug release studies

The *in-vitro* drug release studies were conducted on the selected formulations (see Section 3.4.3.3). Samples of 100 µL (n=3) were withdrawn at 0.25, 0.5, 1, 1.5, 2, 3, 4, 5, 24 hours.

3.4.4.4 Kinetic assessment

Drug release kinetics were assessed as described in Section 2.4.4.4.

3.4.5 Data and statistical analysis

Unless otherwise stated, all experiments were conducted in triplicate. Data is presented as mean (standard deviation). Statistical analysis was conducted using one-way ANOVA with Dunnett's post-hoc test and paired t-test with a statistical significance implied with a probability value of < 0.05.

3.5 Results

3.5.1 Preliminary assessments

3.5.1.1 Formulation development and morphology/mechanical characterisation,

Hesperetin was required to be dissolved in acetone to be mixed homogeneously with the adhesive or the polymer matrix. Mixing hesperetin powder directly into the adhesive or polymer matrix formed undissolved hesperetin patches detected using optical microscopy. The initial formulations F1-F12 were successfully developed with good visual mechanical properties as the patches were peeled off the liner easily with no traces on the liner and adhered efficiently on the release jars with no detachment detected when adding the release media. F13 patch, which contained 10% glycerol and 45% triacetin in Eudragit®E100 polymer, was too sticky and was unable to detach from the release liner, hence, discarded.

3.5.1.2 Measurement of patch thickness

The mean thickness of the patches ranged from 0.29-0.33mm (Table 3.3).

Table 3.3 Thickness measurement of the developed patches (F1-F12).

Formulation	Thickness (mm)
F1	0.30 (0.009)
F2	0.29 (0.008)
F3	0.29 (0.009)
F4	0.32 (0.008)
F5	0.32 (0.007)
F6	0.31 (0.008)
F7	0.31 (0.009)
F8	0.31 (0.006)
F9	0.32 (0.007)
F10	0.33 (0.009)
F11	0.33 (0.009)
F12	0.33 (0.007)

Data presented as mean (standard deviation).

3.5.1.3 *In-vitro* drug release studies

The initial formulations F1-F12 were assessed according to their ability to release hesperetin through *in-vitro* drug release studies (Figures 3.3 and 3.4) (Table 3.4).

For the silicone PSA patches (F1-F7) (Figure 3.3), F7 with 5.5 % glycerol provided the highest mean percentage of hesperetin dissolved in 24 hours, 39.9 % (0.37 %) (Figure 3.3B). While F6 patch with 2.5 % glycerol released 13 % of hesperetin (Figure 3.3B). F1 patch, which has no plasticiser incorporated, had the lowest percentage of hesperetin released in 24 hours, 4.25 % (0.04 %) (Figure 3.3A).

Using 10 % PVP 30 (F3) did not influence the release when compared to 5 % PVP 30 patch (F2), both patches released approximately 13 % of hesperetin after 24 hours (Figure 3.3A). Lower concentration of Tween® 20 (2.5 %) in F4 patch produced higher release than the patch with 10 % Tween® 20 (Figure 3.3).

For the Eudragit® E100 based patches (Figure 3.4), F9 with both triacetin and 5 % glycerol dissolved the highest percentage of hesperetin after 24 hours, 8 % (0.06 %), while F10 with 2 % glycerol and no triacetin provided the lowest mean percentage of hesperetin dissolved in 24 hours, 0.76 % (0.01 %).

Using glycerol alone at different concentrations without triacetin produced low release profiles in 24 hours for F10, F11, and F12, ranging from 0.76-1.35 % (Figure 3.4). For the further assessments and storage studies, F7 and F9 were selected due to their highest hesperetin release in 24 hours when compared to the remaining formulations in each type of adhesive.

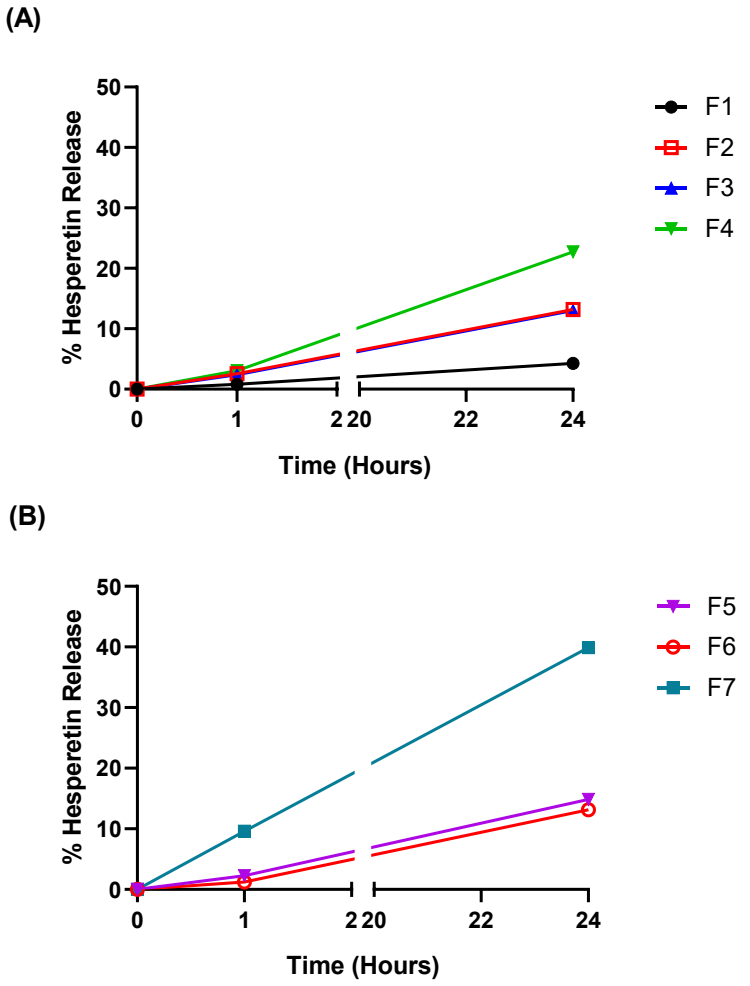

Figure 3.3 The *in-vitro* drug release profile of the Dow Corning® BIO-PSA 7-4501 patches (F1-F7) at 1 and 24 hours.

(A) F1 - F4 patches; (B) F5 - F7 patches. Data represents mean of each sampling point. n=3.

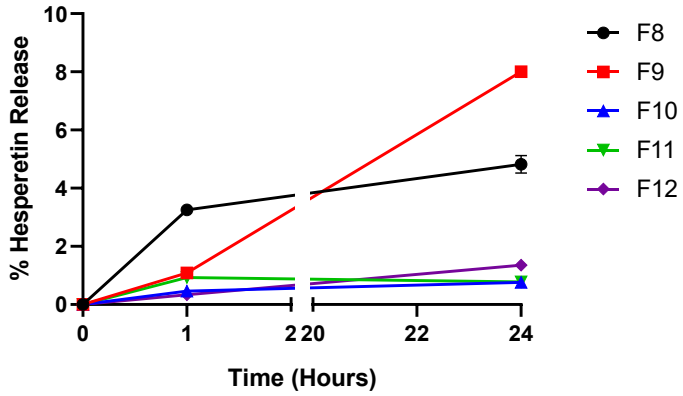

Figure 3.4 The *in-vitro* drug release profile of the Eudragit® E-100 patches (F8-F13) at 1 and 24 hours.

Date represented as mean percentage hesperetin release. n=3.

Table 3.4 The percentage of hesperetin released from the formulations (F1-F12) at 1 and 24 hours. F1 – F7 are silicone-based patches. F8 – F12 are acrylic-based patches.

	1 hour (%)	**24 hours (%)**
F1	0.82 (0.03)	4.25 (0.04)
F2	2.56 (0.18)	13.17 (0.33)
F3	2.41 (0.20)	13.04 (0.19)
F4	3.07 (0.13)	22.71 (0.39)
F5	2.26 (0.02)	14.86 (0.15)
F6	1.24 (0.09)	13.13 (0.24)
F7	9.62 (0.20)	39.91 (0.37)
F8	3.25 (0.12)	4.82 (0.30)
F9	1.09 (0.06)	8 (0.06)
F10	0.46 (0.01)	0.76 (0.01)
F11	0.93 (0.01)	0.78 (0.03)
F12	0.34 (0.02)	1.35 (0.03)

Data reported as mean (standard deviation).

3.5.2 Storage studies at different temperatures

The selected Formulations (F7 and F9) were stored at both 4°C and 25°C for 3 weeks. Morphology characterisation, pH assessment and drug *in-vitro* release studies were conducted at weeks 0, 2, and 3.

3.5.2.1 Morphology and mechanical characterisation

The morphology of the formulations was investigated by optical microscopy to assess the solubility and the possibility of crystallisation of hesperetin in the formulations over a period of 3 weeks. Hesperetin was fully dissolved and dispersed in F7 patch during the whole period of 3 weeks and no significant crystallisation observed under the microscope except for visible air bubbles (Figure 3.5). F7 retained its good mechanical properties during the storage period at both temperatures.

Formulation F9 was also homogeneous, and no insoluble drug patches detected for week 0, however was subsequently discarded due to the poor detachability, poor handling and stickiness noticed after 2 weeks of storage at both 4°C and 25°C.

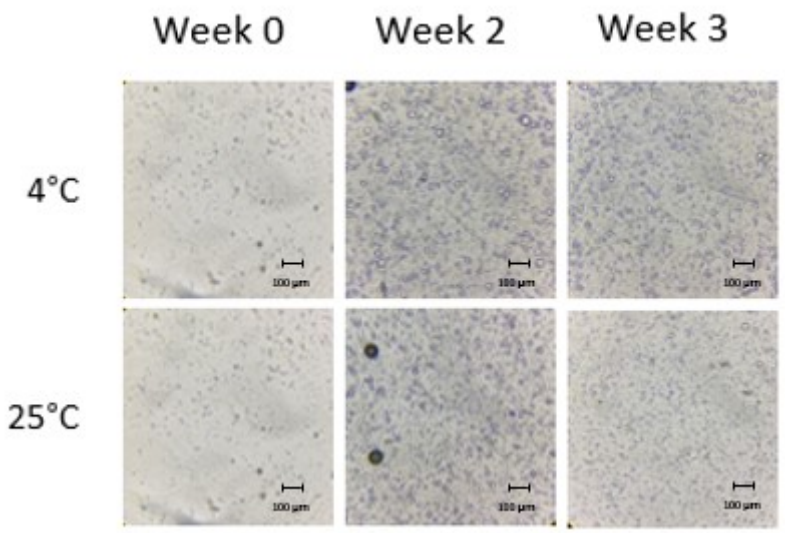

Figure 3.5 Morphology characterisation of F7 patch during the period of stability studies (3 weeks) under storage conditions 4°C and 25°C.

Images captured using Zeiss Primovert microscope with 10x objective lens. F7 patch composed of silicone PSA with 5.5% glycerol.

3.5.2.2 pH assessment

The pH of the selected formulations was assessed at weeks 0, 2 and 3 to ensure that the formulations are stable and suitable for skin application. The pH of each formulation (F7, F9) did not change during the 3 weeks of storage at both 4 °C and 25 °C (Table 3.5).

Table 3.5 pH of the tested formulations (F7, F9) at weeks 0, 2, and 3 stored in 4 °C and 25 °C.

	F7	**F9**
Week 0	5	7
Week 2	5	7
Week 3	5	7

3.5.2.3 *In-vitro* drug release studies

The ability of the prepared patches to release hesperetin was successfully assessed by *in-vitro* drug release studies using a cylindrical screw top glass jars (15 mL) where the patch was placed at the bottom of the jar then removing the release liner with thin tweezer and then the jars were filled with PBS as a receptor medium. The studies were conducted on weeks 0, 2, and 3 for F7 patch to observe the stability over the 3 weeks period when storing the formulation

in both 4°C and 25°C (Figure 3.6, 3.7). For F9 (Figure 3.8), only week 0 release profile was obtained due to stickiness and changes in mechanical properties of the patch during storage at both 4°C and 25°C as discussed above.

The mean percentage of hesperetin released by F7 after 24 hours in week 0 was 40.50 % (6.18 %), which was significantly higher when compared to F9 release profile, 3.64 % (0.54 %) ($p<0.001$) (Figure 3.6). Storage of F7 at 4°C for 2 - 3 weeks resulted in significantly lower drug release profile reaching 18 - 21 % in 24 hours ($p<0.01$) (Figure 3.7A). Concurrently, the storage at 25°C resulted in further significant reductions in drug release with a range of 13 - 16 % ($p<0.01$) (Figure 3.7B). Compared with baseline (week 0), drug release profiles in all subsequent weeks were statistically significantly lower and in both storage conditions (Table 3.6).

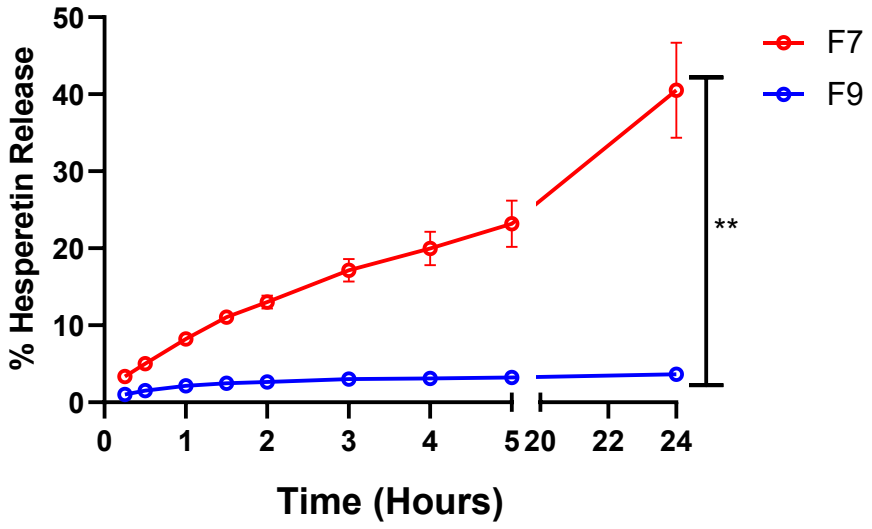

Figure 3.6 Comparing the *in-vitro* drug release profiles of silicone-based (F7) and acrylic-based (F9) patches at week 0.

Open circles represent the mean. Error bars reflect the standard deviation (SD). n=3. ***p<0.001 representing the comparison of the release time point at 24 hrs.

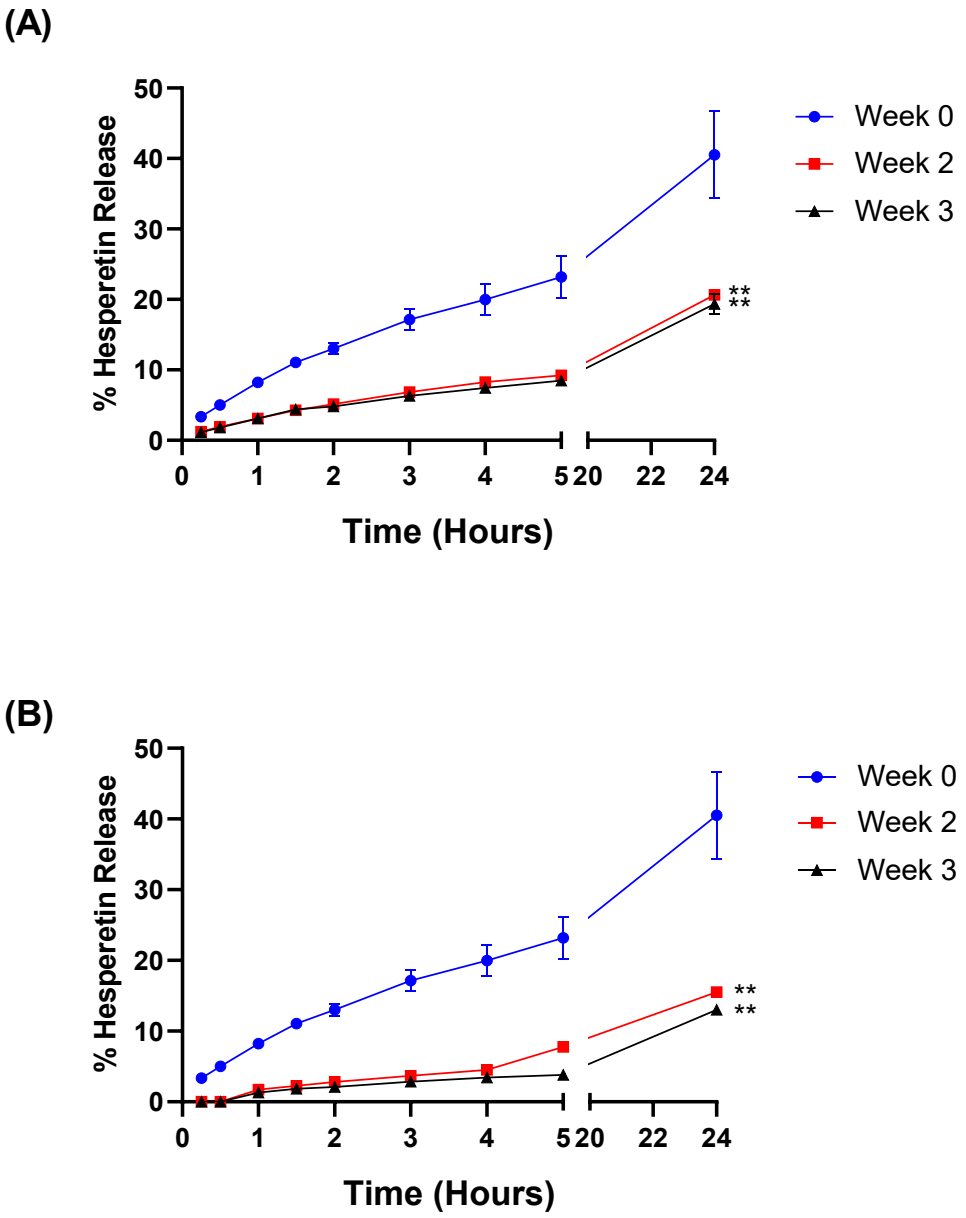

Figure 3.7 The *in-vitro* drug release profile of F7 patch in weeks 0, 2, and 3.

Storage at (A) 4°C and (B) 25°C. Data represented as mean percentage hesperetin release. Error bars reflect the standard deviation. n=3. F7 patch composed of silicone PSA with 5.5% glycerol. **p<0.01 representing the comparison of the release profiles with week 0 as the control.

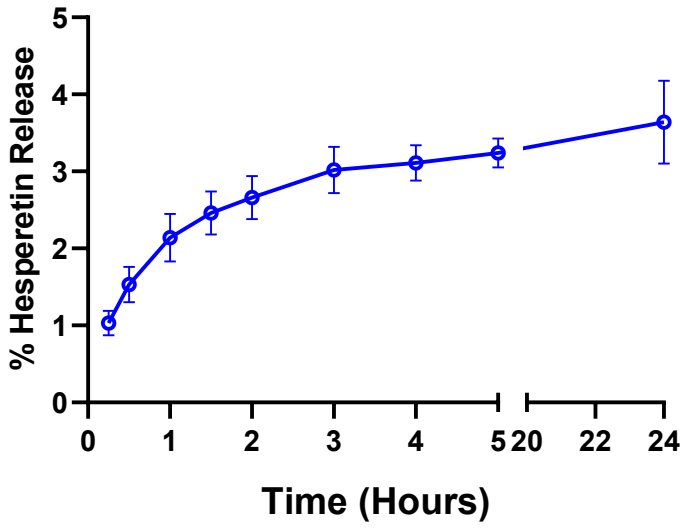

Figure 3.8 The *in-vitro* drug release profile of F9 at week 0.

Open circles represent the mean. Error bars reflect the standard deviation (SD). N=3.

Table 3.6 Statistical significance in the *in-vitro* drug release studies profiles on F7 (silicone-based patch) during storage at 4°C and 25°C

	4 °C	25 °C
Week 0 vs. week 2	0.0045	0.0029
Week 0 vs. week 3	0.0054	0.0039

Data represented as individual p-values of each time point. All the data shows significant difference using one-way ANOVA with Dunnett's post-hoc test, statistical significance implied with a p-value of < 0.05. Week 0 values used as the baseline of comparison.

Hesperetin release profile from F7 patch significantly decreased during both storage conditions (Table 3.6). To confirm the absence of chemical degradation occurred to hesperetin in F7 patch during both storage conditions, HPLC chromatograms obtained in week 0 and week 3 (24 hours sample) were compared showing that hesperetin peak is still present reflecting the absence of chemical degradation (Figure 3.9). Differential scanning calorimetry (DSC) has been typically used to understand the thermal and chemical characteristics of compounds incorporated into topical and transdermal systems [252-256].

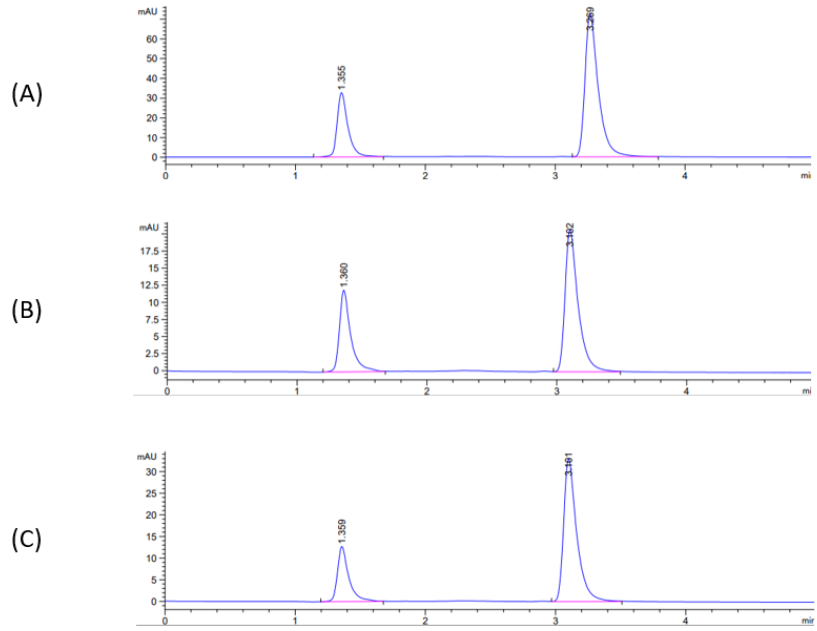

Figure 3.9 HPLC chromatogram of hesperetin from F7 patch release studies (24 hours sample) over 3 weeks

(A) week 0, (B) week 3, 25 °C storage, (C) week 3, 4 °C storage. F7 patch composed of silicone PSA with 5.5% glycerol.

3.5.2.4 Kinetic assessment

Drug release kinetic models were applied to assess the mechanism of drug release for formulations F7 and F9. The KP model was selected for F7 since it has shown the highest r^2 values and lowest AIC in weeks 0, 2, and 3 release studies which reflected a fitted model across both 4°C and 25°C storage temperatures (Table 3.7). For F9, KP model was also the best fitted model on week 0 release profile (Table 3.8).

For F7, the KP diffusional release exponent (n) value was < 0.5 in week 0 release profile representing release controlled by drug diffusion (Fickian diffusion). While at weeks 2 and 3 with both storage temperatures, the n-values were 0.5 < n < 1 reflecting that the release is controlled by both drug diffusion and polymer relaxation (anomalous diffusion) (Table 3.7). This elucidates the decrease in the release profile of hesperetin with storage affected by polymer relaxation. For F9, The KP n-value obtained for week 0 release profile was < 0.5 representing Fickian diffusion (Table 3.8)

Table 3.7 Kinetic assessment of release data of F7 performed at weeks 0, 2, 3 at both 4°C and 25°C storage conditions.

Model	Parameter	Week 0		Week 2 (4C)		Week 2 (25C)		Week 3 (4C)		Week 3 (25C)	
		Mean	SD	Mean	SD	Mean	SD	Mean	SD	Mean	SD
Zero order	k0	0.034	0.005	0.016	0.000	0.012	0.001	0.015	0.001	0.010	0.000
	r^2	0.300	0.147	0.689	0.025	0.829	0.024	0.687	0.036	0.928	0.046
	AIC	61.030	1.232	42.114	0.184	24.255	0.473	40.782	0.498	14.613	4.503
First order	k1	0.001	0.000	0.000	0.000	0.000	0.000	0.000	0.000	0.000	0.000
	r^2	0.506	0.155	0.739	0.024	0.853	0.024	0.733	0.036	0.940	0.040
	AIC	57.710	0.500	40.516	0.256	23.188	0.627	39.319	0.333	13.160	4.911
Higuchi	kh	1.143	0.143	0.525	0.007	0.358	0.013	0.491	0.031	0.289	0.009
	r^2	0.965	0.012	0.985	0.005	0.898	0.008	0.988	0.004	0.891	0.039
	AIC	33.790	1.536	14.296	4.194	20.653	0.104	11.350	4.469	18.321	3.061
Korsmeyer-Peppas (KP)	kKP	1.502	0.121	0.368	0.021	0.120	0.003	0.347	0.012	0.063	0.028
	n	0.457	0.028	0.556	0.011	0.667	0.010	0.554	0.015	0.744	0.067
	r^2	0.977	0.001	0.995	0.002	0.961	0.014	0.997	0.000	0.999	0.001
	AIC	32.446	3.284	6.589	5.030	15.681	2.032	1.129	0.838	-10.843	5.561

K0: the rate constant for zero order model; k1: first order rate constant; kh: Higuchi rate constant; kKP: Korsmeyer-Peppas rate constant; r^2: is the coefficient of determination; AIC: the Akaike Information Criteria; n: the diffusional release exponent. SD: Standard deviation.

Table 3.8 Kinetic assessment of release data of F9 performed at week 0.

Model	Parameter	Week 0	
		Mean	SD
Zero order	k0	0.004	0.000
	r^2	-4.913	0.871
	AIC	33.666	1.680
First order	k1	0.000	0.000
	r^2	-4.847	0.864
	AIC	33.565	1.668
Higuchi	kh	0.147	0.016
	r^2	-0.759	0.349
	AIC	22.709	1.558
Korsmeyer-Peppas	kKP	0.935	0.114
	n	0.203	0.014
	r^2	0.822	0.054
	AIC	3.870	1.514

k0: the rate constant for zero order model; k1: first order rate constant; kh: Higuchi rate constant; kKP: Korsmeyer-Peppas rate constant; r^2: is the coefficient of determination; AIC: the Akaike Information Criteria; n: the diffusional release exponent; SD: Standard deviation.

3.6 Discussion

Transdermal patch systems exhibit numerous advantages over oral drug delivery, primarily through avoiding first-pass metabolism associated with oral drug delivery and improving bioavailability [88]. Using transdermal patches to deliver drugs is convenient for patients as they are easy and simple to apply, thus, improve patient compliance. Transdermal drug delivery could be used for sustained drug release for chronic disorders that need long term doses to maintain the required therapeutic drug concentration [289].

The flavonoid hesperetin possesses various benefits against depression, cancer, neurological diseases, inflammation, oxidation, and convulsions [52, 76, 81, 184-187], however, the therapeutic potential is affected with oral delivery due to the extensive first-pass metabolism of hesperetin which results in a reduced oral bioavailability. The low bioavailability challenge was highlighted for all dietary flavonoids due to the insufficient plasma concentrations after dietary intake which hinder their therapeutic potential [364, 365]. It has been suggested that the transdermal delivery of flavonoids is one of the most advantageous routes to overcome the challenges of flavonoid administration [289-291, 364].

For hesperetin specific, a previous study formulated hesperidin using transdermal patch systems using a combination of two polymers, Eudragit S100 and HPMC E5. *In-vitro* drug release studies were conducted using Franz diffusion cell resulted in 93.7% hesperidin released in 6 hours [289]. Another study developed quercetin transdermal patches and showed that the release of the drug from the patches reached up to 85.8 % in 24 hours and significant anti-inflammatory activities were demonstrated by the patches [290].

The aim of this study was to develop a range of hesperetin matrix transdermal patches using silicone (Dow Corning® BIO-PSA 7-4501) and acrylic (Eudragit® E100) pressure sensitive adhesives with incorporating different plasticisers such as PVP 30 (5 % and 10 %), glycerol (2% - 10%), Tween® 20 (2.5 % and 5 %), and triacetin (45%) (Tables 3.1, 3.2). The preliminarily developed patches were evaluated through morphology and visual mechanical assessments, thickness measurement, and *in-vitro* drug release studies. The formulations with best release profiles (F7, F9) were selected for further storage studies.

The stability of the selected patches in both 4°C and 25°C were assessed and evaluated for 3 weeks period. Stability studies included morphology and visual mechanical characterisation, pH investigation, and *in-vitro* drug release studies with kinetic assessments. Assessments during storage is an important step to evaluate the formulations as storage conditions can potentially influence the efficiency and safety of the formulations.

3.6.1 Preliminary assessments

3.6.1.1 Measurement of patch thickness

The thickness of transdermal patches is an important parameter to assess because increased patch thickness can reduce the ability of drug molecules to become mobile and hence reduce overall drug release, moreover, it can impact the folding endurance, moisture uptake and moisture content [308, 366]. The thickness of the developed hesperetin patches in our study (F1-F12) ranged from 0.29-0.33mm (Table 3.3), which is within the range obtained by previous studies [112, 288, 308, 311, 359, 366].

3.6.1.2 Morphology and mechanical characterisation

The incorporation of hesperetin powder directly into the adhesives matrices resulted in inhomogeneous mixture with insoluble drug spots detected under the microscope. Hesperetin was required to be dissolved in acetone to be mixed homogeneously with the adhesive or the polymer matrix. The preliminary formulations F1-F12 were successfully developed with good

visual mechanical properties assessed visually in terms of regular handling, stickiness, and peel-ability or detachability from the release liner. The patches were peeled off the liner easily with no visual traces on the liner and adhered efficiently on the release jars with no detachment detected when adding the release media. F13 patch, which contained 10% glycerol and 45% triacetin in Eudragit®E100 polymer, was too sticky and was unable to detach from the release liner, hence, discarded. Accurate mechanical tests are necessary such as tensile strength test and peel adhesion test as they will assist in better understanding of mechanical differences between the developed patches [112, 297, 367].

3.6.1.3 *In-vitro* drug release studies

The formulations F1-F12 were assessed according to their ability to release hesperetin in 24 hours (Figure 3.3 and 3.4) (Table 3.4). For the silicone PSA patches (F1-F7), F7 with 5.5 % glycerol provided the highest mean percentage of hesperetin dissolved in 24 hours, 39.9 % (0.37 %), 2-fold higher than the release obtained from F6 patch (2.5 % glycerol) (Figure 3.3B). Glycerol was utilised frequently by several studies as a plasticiser of biodegradable and edible films [320, 322-339]. Water can penetrate easily into the pressure sensitive adhesive structure with the presence of glycerol as highly mobile channels are created in the adhesive matrix influencing the adhesive physicochemical properties and the penetration rate of the drug which is increased with higher glycerol concentrations [345, 346]. Without the use of a plasticiser (formulation F1), hesperetin release was the lowest, 4.25 % (0.04 %) (Figure 3.3A). This emphasises the need of plasticiser incorporation into silicone adhesives to facilitate drug release

Using 10 % PVP 30 (F3) did not statistically significantly enhance hesperetin release when compared to the 5 % PVP 30 patch (F2), with both patches releasing approximately 13 % of hesperetin after 24 hours (Figure 3.3A). However, several studies showed that increased PVP amounts in different types of transdermal patches inhibited crystallisation and enhanced drug permeation and release [288, 357-361].

Lower concentration of Tween® 20 (2.5 %) in the F4 patch produced higher hesperetin release when compared to patch incorporating 5 % Tween® 20 (F5) (Figure 3.3). This concentration dependant effect could be related to the fact that Tween® 20 exerts its permeability enhancement effect mostly on hydrophilic molecules, while hesperetin is a lipophilic compound, however, it could potentially reflect a good option for sustained release system with higher Tween® 20 concentrations [353, 354]. Several studies reported the effectiveness of Tween® 20 in increasing skin penetration of certain compounds [349-351], while in another study they demonstrated the ineffectiveness of Tween® 20 on specific compounds [352].

For the Eudragit® E100 based patches, F9 with both triacetin and 5 % glycerol released the highest percentage of hesperetin after 24 hours, 8 % (0.06 %) (Figure 3.4). However, formulation F10 with 2 % glycerol and no triacetin, provided the lowest mean percentage hesperetin release in 24 hours, 0.76 % (0.01 %) (Figure 3.4). Using glycerol alone at different concentrations without triacetin produced low release profiles in 24 hours ranging from 0.76-1.35 % (Figure 3.4). Triacetin was required in Eudragit® patches for providing optimised drug release as it improves flexibility between polymer chains [309, 312, 313].

F7 and F9 were selected for storage studies due to their highest hesperetin release in 24 hours when compared to the rest of the formulations in each type of adhesive matrix (Figure 3.3 and 3.4) (Table 3.4).

3.6.2 Storage studies at different temperatures

3.6.2.1 Morphology and mechanical characterisation

Regarding morphology characterisation, F7 patches stored at 4°C and 25°C were investigated under optical microscopy at weeks 0, 2, and 3 and demonstrated that hesperetin was fully dissolved and dispersed during the whole period of 3 weeks and no significant crystallisation detected (Figure 3.5). Using optical microscopy allows direct observations of the samples and was successfully used by several studies to detect crystallisation [247, 248].

Visual mechanical assessments were implied during the storage period on F7 and F9 patches. F7 retained its mechanical properties such visual peelability and proper stickiness during the storage period at both temperatures, while F9 has been discarded as it has lost its mechanical properties with storage.

The mechanical instability of Eudragit® patch (F9) could be related to the changes in the interchain Van der Waals forces that could be either weakened or strengthened with temperature changes due to the increased or decreased mobility between polymer chains [292]. Furthermore, a physical aging phenomenon could be the reason of the physical changes observed during storage. Physical ageing emerges when a polymer is out of equilibrium, and it is prompted by molecular relaxations that are driven in the direction expected to put the polymer system closer to equilibrium [368]. This is monitored by determining the elongation of the polymeric patches represented by coalescence of the colloidal acrylic particles and entanglement, which can be characterised by the relaxation of the polymer at equilibrium and can be impacted by several factors including plasticiser amount, temperature, and humidity. This could also be reflected by changes in tensile strength and drug release and could be

better understood with the conduction of accurate mechanical tests such as tensile strength test and peel adhesion test [369-371].

3.6.2.2 pH assessment

The assessment of pH on F7 patches showed that the pH was consistent and unchanged with storage in 4°C and 25°C for 3 weeks and was maintained at pH 5 (Table 3.5). The pH of F9 was maintained at 7 for 3 weeks. It is necessary to assess the pH of any formulation intended to be used on the skin because acidic or alkaline pH of transdermal formulations can cause skin damage and irritation. The pH of the dermal layer ranges from 4-7.4 reflecting that the formulation is in a satisfying pH range for skin application [233].

3.6.2.3 *In-vitro* drug release studies

The storage of F7 patches at 4 °C for 3 weeks resulted in a significant reduction in the release by around 20 % after 24 hours (Figure 3.7A) (Table 3.6). Concurrently, the storage at 25 °C resulted in further significant reductions in drug release by around 26 % when compared to week 0 baseline after 24 hours (Figure 3.7B) (Table 3.6). This could be due to the polymer matrix integrity which can be influenced by the physiochemical properties of the drug and the interaction between the drug and the polymer [260, 267], which could subsequently lead to the resistance of polymer to swell. Polymers swelling aid in the release of drug; thus, the resistance of swelling will eventually decrease drug release.

To rule out any chemical changes reflected by the decreased release from F7 patch during storage, the HPLC chromatograms of hesperetin released in 24 hours from F7 in week 0 and week 3 were compared and demonstrated no change in detecting peak properties (Figure 3.9). Differential scanning calorimetry (DSC) is commonly used for understanding the thermal characteristics of compounds incorporated into topical and transdermal systems [252-256] by giving an insight into thermal and chemical properties including phase transitions, melting temperatures, heat capacity changes, or any chemical changes [372].

Without the proper adhesion to the skin, the drug release will not occur. The adhesion properties of PSA could be affected by temperature which could also contribute to the decreased drug release with storage, and this reflect the changes in the intermolecular links of the polymer. The interchain Van der Waals forces could be either weaken or strengthen with temperature changes due to the increased or decreased mobility between polymer chains [292]. Accurate mechanical tests are necessary such as tensile strength test and peel adhesion test as they will assist in understanding any potential changes during storage [112, 297, 367].

The Eudragit® E100 based patch, F9, which released only 3.6 % of hesperetin at week 0 (Figure 3.8), was physically unstable during storage due to its stickiness corrupted as explained above, therefore, no further stability studies were conducted (except for pH assessments).

3.6.2.4 Kinetic assessment

The application of drug release kinetics and mathematical models illustrated that F7 followed KP model with a release mechanism controlled by Fickian diffusion in week 0 (Table 3.7). While with storage, the release mechanism was controlled by both Fickian diffusion and non-Fickian (anomalous) diffusion. Having multiple release mechanisms for one formulation is common (Table 3.7) [260, 261]. A previous study by Ritger and Peppas demonstrated both Fickian and anomalous behaviours from swellable matrices [261].

Fickian diffusion is described by drug flux due to molecular diffusion and the concentration gradient. Fickian diffusion in polymer networks is often observed when the temperature is above the glass transition temperature of the polymer (Tg) reflecting the rubbery state of the polymer. In this rubbery state, polymer chains have higher mobility and elongations under relatively low load that allows an easier penetration of the solvent [373]. In non-Fickian (anomalous) behaviour, both drug diffusion and polymer relaxation control the release of drug from the formulation [261].

The predominant molecular mechanism of drug release from F7 during storage is a coupling of drug diffusion and macromolecular relaxation of the polymer chains in which the drug diffuses outward [261, 374, 375]. If the temperature is below the Tg, the chains of the polymer will be restricted in which the penetration of the solvent to the core of the polymer is harder [373]. The storage of the patch at different temperatures could affect the rubbery state of the polymer affecting the mobility of polymer chains and networks. This could also be related to the decrease noticed in hesperetin release and the change in the release mechanism from Fickian diffusion in week 0 to both Fickian and non-Fickian diffusion during storage (Figure 3.7).

The Eudragit® E100 based patch, F9, also followed a KP model in week 0 with a release mechanism controlled by Fickian diffusion representing a concentration gradient drug diffusion (Table 3.8).

Silicone PSA based patches produced better performance, higher release, better stability, and good physical handling with easier preparation when compared to Eudragit E100 films which

were time consuming, provided low release and instable mechanical properties during storage (Figure 3.6). However, the effect of the adhesive matrices on the release of different drugs is variable and cannot be generalised due to the variable physiochemical properties of drugs and plasticisers that would influence the thermodynamic activity and the intermolecular interactions between the drug and the PSA [297].

3.7 Pharmaceutical base creams vs. transdermal patches system

Using Dow Corning ® BIO-PSA 7-4501 adhesive for the development of patches with glycerol (5.5%) have shown the highest percentage of hesperetin release of 40 % in 24 hours, while the highest percentage obtained from the developed creams was about 13 % from Pentravan® formulation.

Creams were easier and faster to develop by simple compounding steps when compared to transdermal patches which require 24 hours drying. Both formulation systems showed consistent pH values and morphological characterisation during the storage period at 4ºC and 25ºC. Base creams showed consistent release profiles (except Pentravan®) at specific storage temperatures, however, the developed transdermal patch have shown inconsistent release profiles during storage with significantly decreasing profile.

The application of both patches and creams are considered easy and convenient for patients but the stickiness of the patches should be assessed as some patches could leave residues on the skin or are resistant to peel off and that would be inconvenient for the patients. The patches would be more suitable for transdermal and sustained release as the creams can be easily washed of by water.

Hesperetin pharmaceutical base creams could be used for topical and localised purposes for the treatment of skin disorders including skin cancer. Also, the topical delivery of hesperetin as a photoprotective agent using creams has been explored previously [244, 376]. Dow Corning ® BIO-PSA 7-4501 hesperetin patches demonstrate a potential candidate to release hesperetin systemically owing to the high release profile. However, more studies are required in this area to assess the stability of the formulations during storage and to improve the release.

3.8 Conclusion

The delivery of hesperetin to the systemic circulation through the skin by transdermal patches could be a potential solution for its reduced oral bioavailability. The objective of this study is to formulate and evaluate hesperetin transdermal matrix patch systems using Dow Corning ® BIO-PSA 7-4501 adhesive or Eudragit® E100 with different plasticisers. The developed patches were subjected to preliminary evaluation studies including thickness measurement, morphological characterisation, visual mechanical properties, and *in-vitro* drug release studies. The most successful patches with highest drug release were further evaluated during storage.

Using Dow Corning ® BIO-PSA 7-4501 adhesive showed good potential with good hesperetin release profile and simple and easy development process. Glycerol (5.5 %) was the best plasticiser to be used with Dow Corning ® BIO-PSA 7-4501 adhesive (F7 patch) as it significantly facilitated hesperetin release (~40 %), showed stable visual mechanical properties, and demonstrated consistent morphological characterisation during storage. However, the percentages of hesperetin released from F7 patches with storage at 4°C and 25°C for 3 weeks were decreased significantly which could be attributed to polymer relaxation or drug-polymer interactions. Further studies are required to better understand the reasons behind the changes in release profiles during storage.

Dow Corning ® BIO-PSA 7-4501 adhesive is a potential candidate for the development of transdermal patches attributed to its easy use, flexibility, compatibility with wide range of APIs, and safety profile. While according to this study, Eudragit® E100 patches produced low release, lost its mechanical properties with storage, and were time consuming and not easy to develop.

Chapter 4

Precision dosing-based optimisation of paroxetine during pregnancy for poor and ultra-rapid CYP2D6 metabolisers: a virtual clinical trial pharmacokinetics study

Disclaimer

Elements of this chapter have been published as follows:

Almurjan, A., Macfarlane, H., & Badhan, R. K. S. Precision dosing-based optimisation of paroxetine during pregnancy for poor and ultrarapid CYP2D6 metabolisers: a virtual clinical trial pharmacokinetics study. Journal of Pharmacy and Pharmacology, 72(8):1049-1060. doi:10.1111/jphp.13281

4.1 Introduction

Depression in pregnancy is a serious and prevalent condition with incidence rates as high as 20% [29]. Selective Serotonin Reuptake Inhibitors (SSRIs) are the first-line antidepressant medications and now regarded as an alternative to TCAs [377]. The superior toleration of SSRIs compared to the older antidepressants is due to their selective inhibition of serotonin reuptake and their reduced effect on cholinergic, adrenergic, and histaminergic receptors. SSRIs exert their effect at the presynaptic axon terminal by inhibiting the serotonin transporter (SERT) resulting in increased amount of serotonin neurotransmitter in the synaptic cleft [378].

SSRIs are considered safe in overdose, and they are better tolerated than the older antidepressants including TCAs. SSRIs adverse effects are troublesome but in general not life-threatening, these include gastrointestinal disturbances such as nausea and diarrhoea, agitation, sleep disturbances, anorexia, anxiety, myalgia, sexual dysfunction, and headaches [20, 379]. SSRIs include antidepressants such as citalopram, fluoxetine, sertraline, paroxetine, and fluvoxamine.

Paroxetine is used to treat several conditions including major depressive disorder, anxiety disorder, posttraumatic stress disorder, panic disorder, and obsessive-compulsive disorder [22, 380]. It is the most potent clinically available serotonin reuptake inhibitor with less selectivity for the site of serotonin reuptake when compared to sertraline. Despite this, anticholinergic adverse effects are not apparent until administering toxic paroxetine doses that are significantly higher than the regular therapeutic doses [377].

Paroxetine is primarily metabolised by Cytochrome P450 2D6 (CYP 2D6) and to a lesser extent (but equally important) by CYP 3A4, with minor roles for CYP 1A2, C219 and 3A5 (Figure 4.1) [381]. Further, paroxetine is also a mechanism-based inhibitor of CYP 2D6 [382, 383], which results in a significant decrease in clearance under multiple-dosing (steady-state) conditions and could give rise to drug-drug interactions [377, 384].

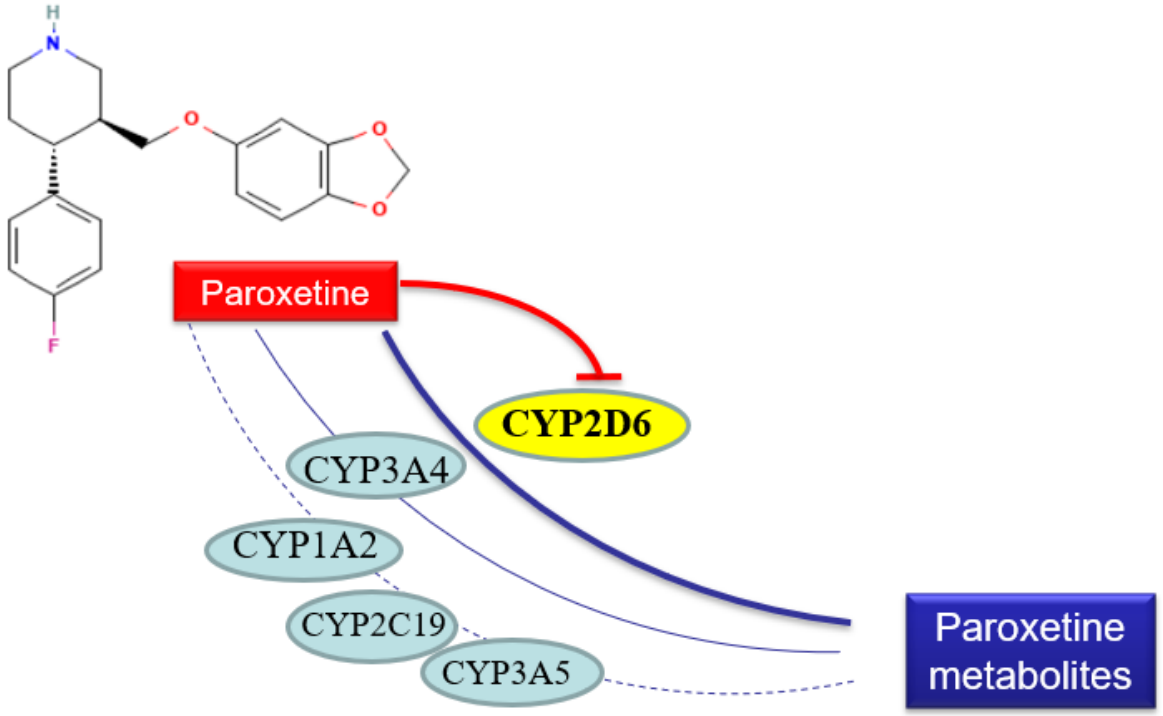

Figure 4.1 Paroxetine hepatic metabolism pathway showing the main metabolism by CYP2D6.

Due to its non-linear pharmacokinetics, the half-life ($t_{1/2}$) of paroxetine is variable as it depends on the duration and the dose administered, ranging from approximately 15 - 20 hours [385, 386]. Moreover, the AUC after a single dose of 20 mg is much lower to that of multiple dosing, 191 ng/hr/mL for single dosing and 1481 ng/hr/mL for multiple dosing [387, 388].

Several studies have noticed an apparent increase in the activity of CYP 2D6 during gestation which results in an approximate 50 % decrease in paroxetine plasma concentrations compared to pre-pregnancy levels [380, 389-393]. The underlying mechanisms of CYP2D6 induction during pregnancy is suggested to be related to the increase in the key female hormones estradiol and progesterone throughout pregnancy, with concentrations reaching up to 100 nM and 1 μM for estradiol and progesterone, respectively. These levels are significantly greater than those during menstruation (< 50 nM) [394, 395]. Such female hormones are known to be activators for basic helix-loop-helix transcription factors (e.g. aryl hydrocarbon receptor; AhR) or nuclear hormone transcriptional regulators (constitutive androstane receptor, CAR; pregnane X receptor, PXR; estrogen receptor, ER), which contribute to the induction of a variety of CYP isoforms and enhanced drug clearances [396, 397].

However, perhaps complicating the use of paroxetine during gestation, is the fact that CYP 2D6 is extensively polymorphic with at least a 7-fold difference in the median total clearance between the extensive metabolism (EM) and poor metaboliser (PM) phenotypes [384, 388]. In poor metabolisers (PM), high plasma concentrations may provoke anticholinergic side effects [398]. Furthermore, the therapeutic window was assumed to be in the range of 20-60 ng/mL [399, 400]. However, therapeutic blood concentrations for paroxetine can range from 10 ng/mL to 120 ng/mL [401], with toxicity reported to commence at approximately 350 ng/mL [402].

Paroxetine has been given a category D banding by the FDA because of its increased risk of causing birth defects when taken during the first trimester, in addition to being associated with neonatal withdrawal syndrome when administered later in pregnancy [403]. Nevertheless, the potential harms of using paroxetine during pregnancy should be weighed carefully against the potential for serious risks of untreated maternal depression. This is particularly important given that recent reports in the UK have suggested that 1 in 25 women (aged 20-35 years) who die by suicide, do so during the perinatal periods (conception-pregnancy and post-natal) [404]. And further, that poor mental health during gestation is a highly correlated with poor mental health postnatally [405]. A poor treatment response or intolerable side effects frequently requires an intervention and to switch from one antidepressant to another. Conservative switching techniques involve tapering off the initial antidepressant gradually, followed by a sufficient washout period before beginning the new antidepressant. This can take a long time and may involve intervals without medical attention, which carries the risk of exacerbations of the condition that could be fatal to the mother and the foetus. If antidepressants are abruptly stopped after a long period of use, withdrawal syndromes may develop. Additionally, depression can relapse or worsen [406].

There are no well-controlled, large scale reliable studies of paroxetine use throughout gestation. However, the clinical toxicology database TOXBASE® (https://www.toxbase.org) [407], from the National Poisons Information Service Unit has published guidance for paroxetine use throughout pregnancy and suggest that paroxetine can be continued where an SSRI is considered clinically necessary and where paroxetine has been found to be the only effective agent. Further, the risks of continuing must be weighed against the possible negative outcomes associated with relapse [408]. It is important to consider the risks associated with any relapse as well as the risk of relapse itself and recommendations are to use the lowest effective dose and for clinicians to follow this advice without risking relapse [408]. With this in mind, it is important that clinicians are aware of likely gestation-related variation in paroxetine levels [409].

In the context of post-natal period, paroxetine has been reported to lead to neonatal withdrawal syndrome, particularly persistent pulmonary hypertension of the new-born (PPHN) when paroxetine is used beyond 20 weeks gestation, but not amongst infants of mothers who used the drug prior to eight weeks [410]. However, this risk is thought to be small for the SSRI group as a whole [411].

Given that poor mental health during gestation is a highly correlated with poor mental health postnatally [405], the benefit of therapy should be weighed against the potential risk of cessation of therapy and the associated consequence for the mother and child [405, 412]. However, the requirement for adjustments of daily dosing during gestation is uncertain.

In light of the paucity in pharmacokinetic data for paroxetine during gestation, we have, for the first time, applied the concept of pharmacokinetics-based virtual clinical trials dosing to elucidate possible dose adjustments that could be implemented in both EM and polymorphic CYP 2D6 subjects throughout gestation.

4.2 Aims and objectives

The primary aim of this study was to use the principles of mechanistic pharmacokinetic modelling and virtual clinical trials to elucidate the causative effects of the decrease in plasma paroxetine levels during gestation and to provide a clinically relevant dosing adjustment strategy that could be implemented to maintain plasma paroxetine levels during gestation, when taking into consideration the CYP 2D6 phenotype status patients.

To achieve the aims, the overall objectives were:

- To validate the previously developed paroxetine PBPK model using published single and multiple dose studies in healthy population.
- To further validate the model in pregnant population
- To assess the impact of CYP 2D6 polymorphism on paroxetine plasma concentration during pregnancy
- To explore approaches to paroxetine dose titration during gestation for CYP 2D6 phenotypes.

4.3 Methods

The physiologically based pharmacokinetic (PBPK) modelling tool Simcyp was utilised to conduct virtual clinical trials simulations in subjects (Simcyp Ltd, a Certara company, Sheffield, UK, Version 17). For studies in Step 1, simulations incorporated mixed genders (50:50), with studies in Step 2-4 utilising females only. A four-stage workflow approach was applied for the development, validation, and simulation studies with paroxetine (Figure 4.2).
Adaptations to both the paroxetine 'compound file' and the Pregnancy 'population group' were made and described below.

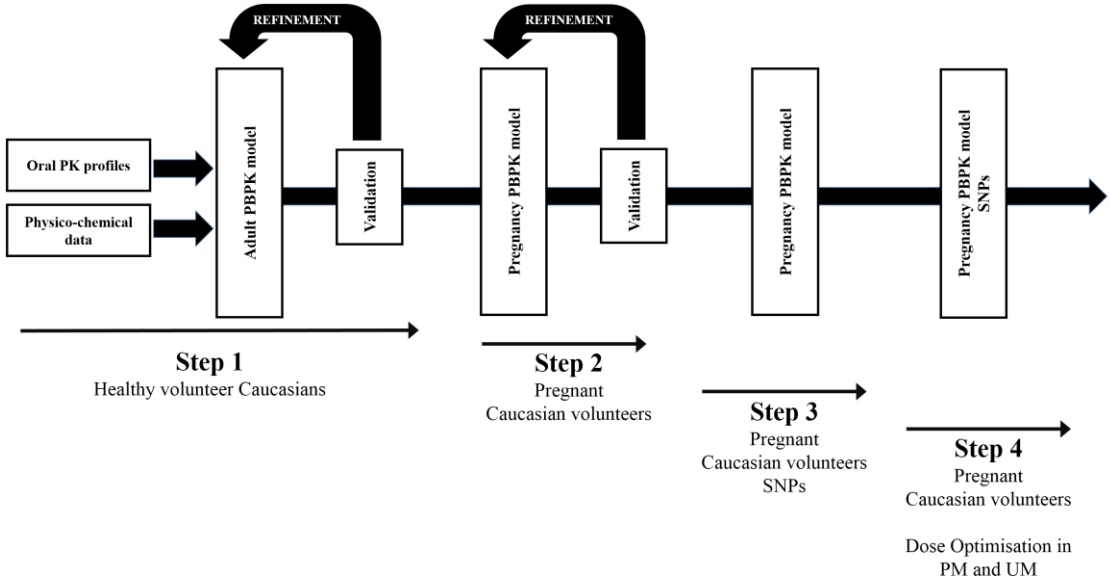

Figure 4.2 A four-stage workflow-based approach to paroxetine modelling

4.3.1 Step 1: Validation of paroxetine

Within the virtual clinical trial simulator Simcyp, the 'healthy volunteer' (HV) population group was used to simulate 'non-pregnant' females as a baseline, with the 'pregnancy' population group utilised for all gestational studies. The pregnancy population group was developed by Simcyp, to include necessary gestational dependant changes in physiology, such as blood volume and organ/tissue perfusion and enzyme/protein expression thought to play a role in altering the pharmacokinetics of drugs [413-416].

Paroxetine has been previously developed by Simcyp and incorporated into the Simcyp simulator [381]. However, to account for the impact of physiological alterations during gestation on paroxetine pharmacokinetics, a modification to the prediction of the volume of distribution at steady-state (Vss) was required, from a pre-set minimal-PBPK model to a full-body PBPK distribution model. This required the application of a Weighted Least Square (WLS) approach and the Nelder-Mead minimisation method to the calculation of Vss from a tissue-partition

coefficient scaler (Kp scalar) [417]. The pharmacokinetics parameters used for paroxetine model are detailed in Appendix A (Table A1).

Validation of the revision made to the paroxetine compound file employed three single dose studies and two multiple dose studies: (i) 28 male healthy volunteers (18-50 years old) dosed a single oral dose of 20 mg [418]; (ii) 9 healthy male subjects administered a single 20 mg oral dose of paroxetine [419]; (iii) 12 healthy volunteers aged between 20-35 years old (9 males, 3 females) administered a 20 mg single dose of paroxetine [420]; (iv) 28 healthy volunteers administered a 20 mg daily for 13 days, with sampling on days 12 and 13 [421]; (v) 7 healthy males administered a 20 mg oral dose of paroxetine daily for 3 days, with sampling on day 1 and 3 [422]. Simulation trial designs were run to match clinical studies used in validation.

4.3.2 Step 2: Validation of paroxetine during gestation

Paroxetine plasma concentrations have been reported during gestation from a retrospective analysis of therapeutic drug monitoring services in Norway [380], consisting of 29 serum drug concentrations during pregnancy and 31 drug concentrations at baseline (non-pregnancy females) obtained from 19 women taking an oral dose of 20 mg daily. This data was extracted and utilised as 'observed' data for validation purposes. The Simcyp Pregnancy population group was adapted to incorporate CYP 2C19 activity modifications during gestation, details of which can be found in the Appendix A. Further, the optimised Vss predicted from Step 1 was applied here, which was allowed to alter in line with maternal physiological changes during gestation.

In simulating paroxetine pharmacokinetics during gestation, a 38-week trial design was utilised, with simulations conducted using a 3x10 trial design with a daily oral dose of 20 mg for all subjects. Data was collected over the final 24 hours of every fifth week. The trial design was also replicated for healthy volunteer population of non-pregnant females (baseline) dosed under the same dosing strategy for comparison. Furthermore, changes in AUC and total *in-vivo* clearance were quantified during gestation.

4.3.3 Step 3: Phenotype simulation

To assess the impact of CYP 2D6 phenotypes on maternal paroxetine plasma concentrations, data was extracted from an observational cohort study in 74 pregnant women aged from 25 to 45 years who used paroxetine during pregnancy and where data was reported for gestational weeks 16–20, 27–31 and 36–40 [423]. The study included data from 43 extensive metabolisers (EM), 5 poor metabolisers (PM) and 1 ultra-rapid metaboliser (UM).

Simulations were conducted using a 10x10 trial design at GW 20, 30 and 38, with EM, UM and PM populations dosed 20 mg daily during gestation and compared to results obtained from Simcyp.

4.3.4 Step 4: Dose adjustment during gestation

In order to identify the requirement for a dose adjustment during gestation, we examined the impact of dose escalation on paroxetine plasma concentrations. Doses were escalated in 5 mg increments every 3 days to 15-50 mg daily doses during gestation, with trough plasma concentrations analysed for the final day of each trimester. Data was collected and reported for the EM, PM and UM phenotype. The percentage of subjects with trough plasma concentrations below 20 ng/mL and above 60 ng/mL were quantified for each trimester and each phenotype.

4.3.5 Predictive performance

For all simulations in steps 1-3, a prediction of a pharmacokinetic metric to within two-fold (0.5-2.0-fold) of that published clinical data was generally accepted as part of the 'optimal' predictive performance [424-426].

4.3.6 Visual predictive checks

Model predictions in step 1-3 were compared to clinical studies using a visual predictive checking (VPC) strategy [427]. In this approach, the predicted mean/median and 5^{th} and 95^{th} percentiles of the concentration–time profiles (generated from Simcyp) were compared against the observed data for any validation data sets. The prediction was assumed to be valid when the predicted data points overlapped with the observed data sets.

4.3.7 Data and statistical analysis

All observed data obtained from clinical studies were extracted using WebPlotDigitizer v.3.10 (http://arohatgi.info/WebPlotDigitizer/). Statistical analysis was conducted using a non-parametric Kruskal-Wallis with a Dunn's multiple comparison post-hoc test. Statistical significance was confirmed where $p < 0.05$ was determined. All statistical analysis was performed using GraphPad Prism version 7.00 for Windows (GraphPad Software, La Jolla California USA, www.graphpad.com).

4.4 Results

4.4.1 Step 1: Validation of a revised paroxetine full-body PBPK model

A validated paroxetine model, developed and incorporated into the Simcyp Simulator, was utilised with adaptations to include a full-PBPK model for determination of appropriate Vss and

to model physiological changes during gestation. The model was validated against a range of published clinical studies using the Simcyp healthy volunteer population group (Table 4.1). For all single dose studies (Figure 4.3A and 4.3B) and multi-dose studies (Figure 4.3C), the simulated plasma concentration-time profiles were successfully predicted to within the observed range for each study and model-predicted t_{max}, C_{max}, and AUC were predicted to within 2-fold of the reported parameters for each study, confirming successful validation (Table 4.1).

Table 4.1 Summary of pharmacokinetics parameters from the single and multiple-dose studies

Dosing		PK Parameters	Observed	Predicted
Single	Segura *et al* (2003)[419]	$AUC_{(0\text{-}24\ h)}$	96.50 (65.90)	156.83 (138.69)
		C_{max}	8.60 (5.50)	11.10 (8.87)
		tmax	5 (3-5)	3.9 (1.72)
	Yasui-Furukori *et al* (2007)[420]	$AUC_{(0\text{-}48\ h)}$	127 (67)	230.3 (222.34)
		C_{max}	6.5 (2.4)	11.10 (8.87)
		tmax	5 (4-10)	3.9 (1.71)
	Massaroti *et al* (2005)[418]	$AUC_{(0\text{-}120\ h)}$	225.04 (291.91)	312.34 (347.90)
		C_{max}	9.02 (8.82)	11.10 (8.87)
		tmax	5.03 (1.91)	3.89 (1.71)
Multiple	Segura *et al* (2005)[422]	$AUC_{(0\text{-}8\ h)}$ [Day 1]	53.8 (26.7)	65.37 (53.52)
		$AUC_{(0\text{-}8\ h)}$ [Day 8]	159.8 (49.8)	205.76 (104.80)
		C_{max} [Day 1]	10.4 (4.8)	11.09 (8.87)
		C_{max} [Day 8]	26.1 (7.1)	31.61 (15.18)
		tmax [Day 1]	3 (3–5)	3.87 (1.62)
		tmax [Day 8]	8 (3–8)	4.15 (0.83)

AUC, area under the curve; C_{max}, maximum plasma concentration and tmax, time at maximum plasma concentration. Data represent mean (standard deviation). AUC: ng/ml h; C_{max}: ng/ml; and tmax: h.

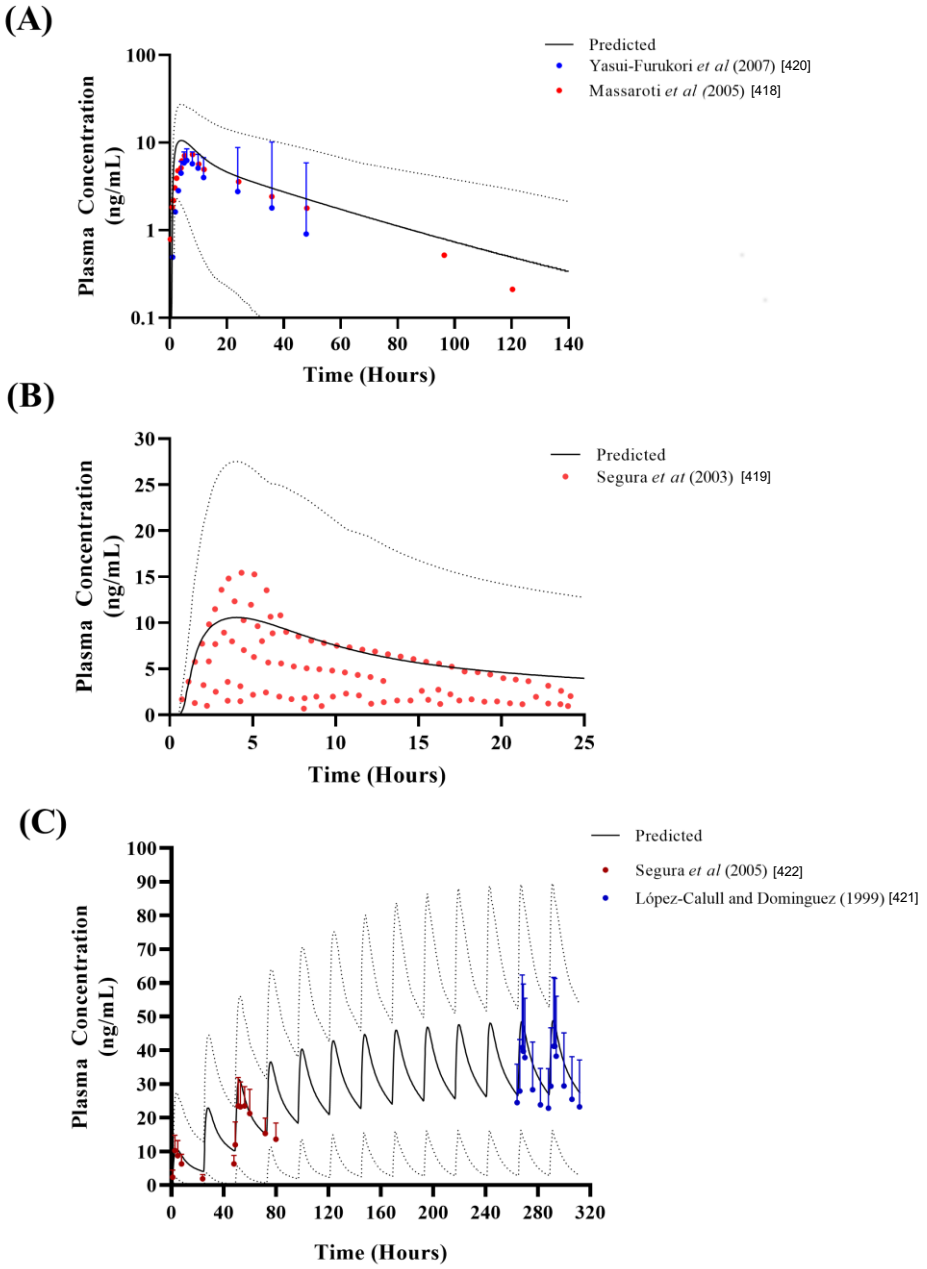

Figure 4.3 Simulated paroxetine plasma concentrations following single and multiple dosing.

(A) Single 20 mg oral dose of paroxetine; (B) single oral 20 mg dose with observed data presented as multiple sampling; and (C) multiple daily 20 mg oral dose. Solid lines represent mean predicted concentration–time profile with dotted lines representing 5th and 95th percentile range. Solid circles represent observed clinical data from each study with error bars indicating standard deviation.

4.4.2 Step 2: Validation of paroxetine during gestation

Model predicted plasma concentrations during gestation overlapped with the range of observations reported [380] during the entire period of gestation (Figure 4.4). The mean at baseline, 24.05 ng/mL ± 15.45 ng/mL, decreased for trimesters 1 (week 5: 21.51 ng/mL ± 12.93

ng/mL), 2 (week 20: 18.09 ng/mL ± 11.72 ng/mL) and 3 (week 30: 17.16 ng/mL ± 11.05 ng/mL), with a statistically significant decrease from week 15 onwards to week 35 ($p < 0.05$).

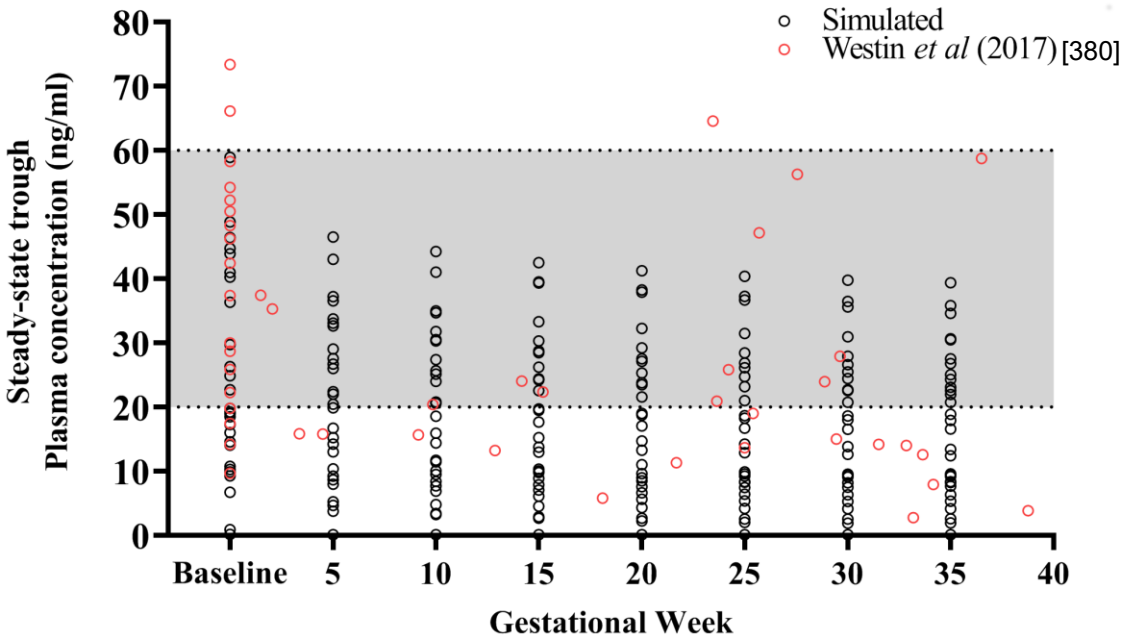

Figure 4.4 Simulated paroxetine plasma concentrations during gestation.

Paroxetine plasma concentrations were simulated during gestation (n = 30). Simulated concentrations represent postdose trough concentrations (sampled at 24 h after dosing) and collated at 5-week intervals over the gestation period (black open circles). Subjects were administered a 20 mg daily dose. 'Baseline' refers to non-pregnant females. Red open circles represent observed (pooled) plasma concentrations obtained from a total of 19 subjects. Shaded regions between 20–60 ng/ml represents the therapeutic window.

Given the polymorphic nature of the primary metabolic pathway of paroxetine (CYP 2D6), the changes in both clearance and AUC were further assessed during gestation for EM, PM and UM phenotype subjects within the heterogeneous healthy volunteer population generated by Simcyp (default Caucasian frequencies: EM: 86.5 %, PM: 8.2 % and UM: 5.3 %).

For both EM and PM, statistically significant differences in the AUC were apparent from gestational week (GW) 15 (EM) and GW10 (PM) onwards, respectively and GW25 for UM when compared to baseline subjects (Figure 4.5A) (Appendix A: Table A2 and A3). For CL, statistically significant differences for both EM and PM were evident from GW10 onwards and week 20 for UM (Figure 4.5B) (Appendix A: Table A2 and A3).

For UM the AUC and CL demonstrated a 70-80 % decrease and 450-480 % increase in trimester 3 when compared to baseline, respectively (Figure 4.5). This is in comparison to EM where a 19-22 % decrease and 16-18 % increase in AUC and CL were noted from baseline, in trimester 3, respectively (Figure 4.5) (Appendix A: Table A2).

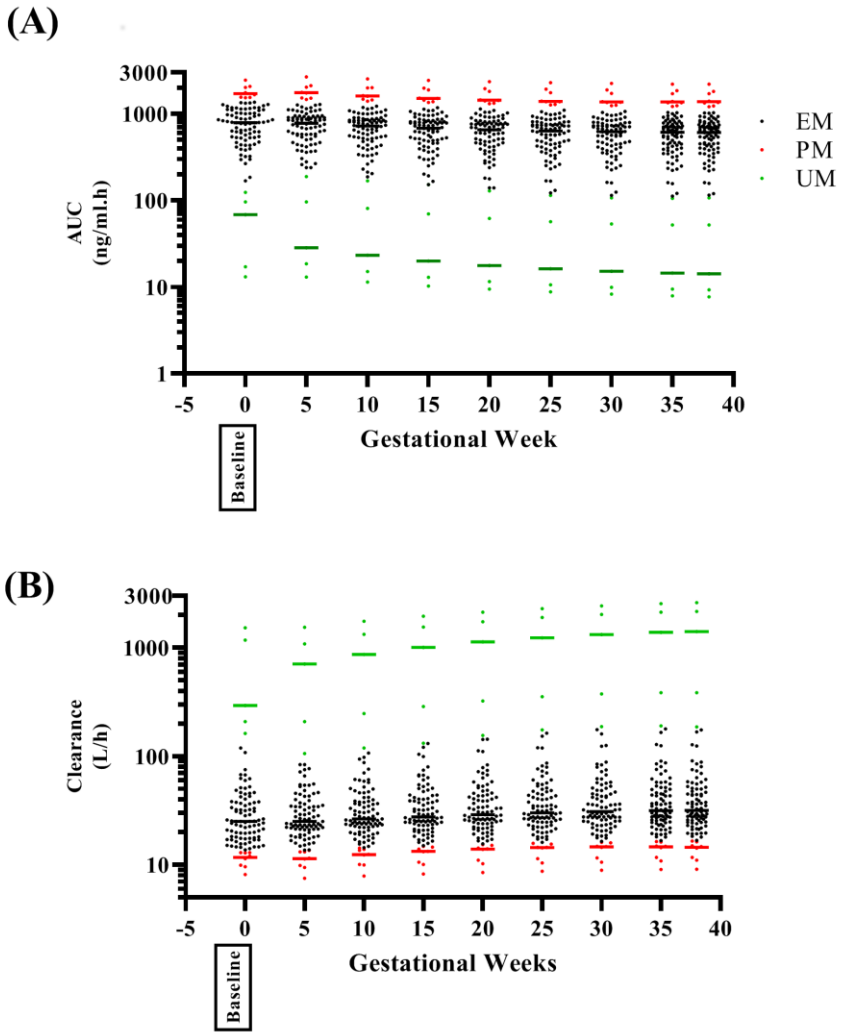

Figure 4.5 Impact of gestation on paroxetine pharmacokinetics demarked by CYP 2D6 population phenotype status.

The impact of gestation on paroxetine (A) area under the curve (AUC) and (B) clearance at baseline (non-pregnant females) and during gestation. Data are demarked for the population (n = 100) phenotype status with black circles representing EM, red circles representing UM and green circles represented PM. Solid coloured line represents median value.

4.4.3 Step 3: The impact of CYP 2D6 phenotypes on paroxetine levels during gestation

The effect of CYP 2D6 phenotypes on maternal paroxetine plasma concentrations during pregnancy were subsequently directly explored. Paroxetine plasma concentrations have previously been reported in CYP 2D6 phenotyped subjects [423]. To validate the ability of the

model of recapitulate the impact of CYP 2D6 phenotypes (EM, PM and UM) on paroxetine levels, we compared model predictions of uniform singular phenotype population to those reported [423]. For EM, the predicted range of paroxetine plasma concentration (determined from the range of simulated maximum and minimum values), where within the range reported (Figure 4.6A). For PM (Figure 4.6B) and UM (Figure 4.6C), despites there being a limited number of reported values plasma concentration measurements available, predicted paroxetine vales were generally within or spanning the range reported [423] (Figure 4.6).

Within each phenotype, a decrease in both peak and trough concentrations were noted (Table 4.2), with the UM phenotype resulted in a significant number of subjects possessing trough levels below 20 ng/mL (73-76 %) compared to EM (51-53 %) (Table 4.2).

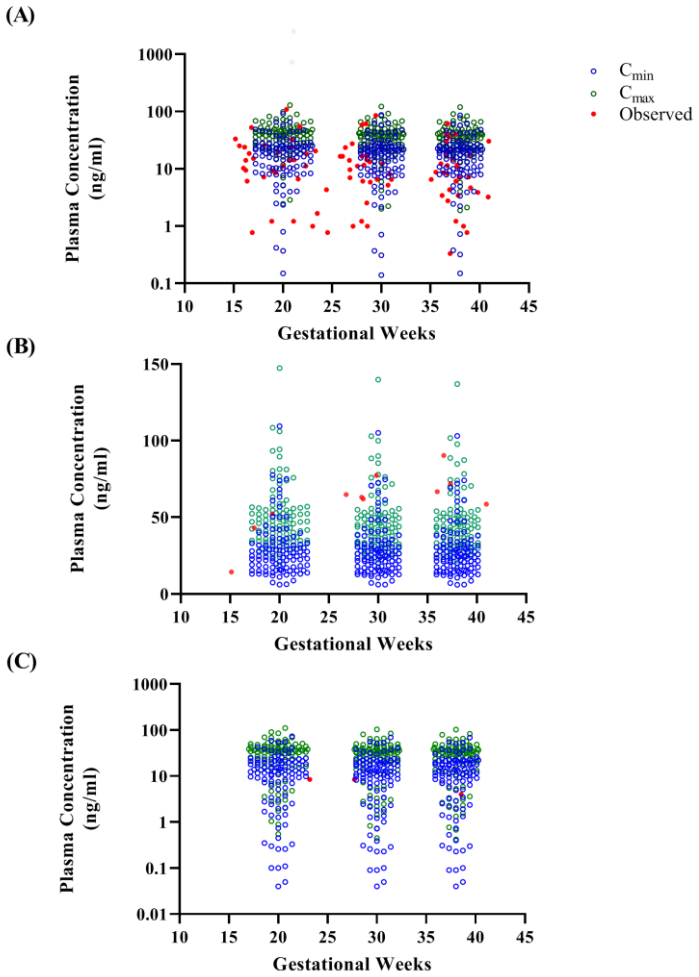

Figure 4.6 Simulated paroxetine plasma concentrations for CYP 2D6 polymorphs.

Paroxetine peak (C_{max}) and trough (C_{min}) plasma concentration were simulated in CYP 2D6 EM (A), PM (B) and UM (C) subjects at gestations week 20, 30 and 38. Simulation concentrations were

compared to reported plasma concentration (red open circles) for each phenotype. Blue circles: C_{min} of each subject; green circles: C_{max} of each subject.

Table 4.2 Simulated paroxetine plasma concentrations during gestation

	Week	C_{max} (ng/mL)	C_{min} (ng/mL)	Trough concentration < 20 ng/mL (% subjects)
EM	**20**	39.875 (129.6-2.45)	19.63 (0.15-91.87)	51
	30	37.235 (2.01-122.28)	18.765 (0.14-87.64)	53
	38	36.56 (1.88-120.04)	18.82 (0.15-86.16)	53
PM	**20**	46.535 (18.95-147.25)	25.225 (6.06-109.49)	34
	30	43.77 (17.62-139.78)	24.345 (6-105.09)	34
	38	42.85 (17.21-136.98)	24.435 (5.99-103.05)	34
UM	**20**	34.4 (0.55-110.91)	12.465 (0.04-73.3)	73
	30	31.69 (0.45-103.66)	11.665 (0.04-69.13)	76
	38	30.84 (0.42-102)	11.985 (0.04-68.22)	76

C_{max}, maximum plasma concentration; C_{min}, minimum plasma concentration; EM, extensive metabolises; PM, poor metabolisers; UM, ultra-rapid metabolisers. Data represent mean (range).

4.4.4 Step 4: Paroxetine dose optimisation

To identify appropriate dose adjustments during gestation for CYP 2D6 phenotypes, the number of subjects with trough concentration below 20 ng/mL and above 60 ng/mL were quantified over the dosing range of 15-50 mg daily.

In all phenotypes studies (EM, PM and UM), the daily dose required was in excess of the standard 20 mg/day throughout gestation. The choice of optimal dose was based around ensuring a balance of a low percentages of subjects with plasma levels below 20 ng/mL or above 60 ng/mL. In order to accomplish this, a suggested indicator of 20 % was used to ensure, where possible, as many subjects as possible had trough concentration above 20 ng/mL in addition to being below 60 ng/mL (Figure 4.7) (Appendix A: Table A4).

For EM, a dose of 30 mg daily in trimester 1 followed by 40 mg daily in trimesters 2 and 3 is suggested to be optimal. For PM a 20 mg daily dose in trimester 1 followed by 30 mg daily in trimesters 2 and 3 is suggested to be optimal. For UM, a 40 mg daily dose throughout gestation is suggested to be optimal

In determining the appropriate dose, the 40-50 mg/d doses resulted in the highest individual trough concentration in the range of 200-300 ng/mL for the trial group (Appendix A: Table A4).

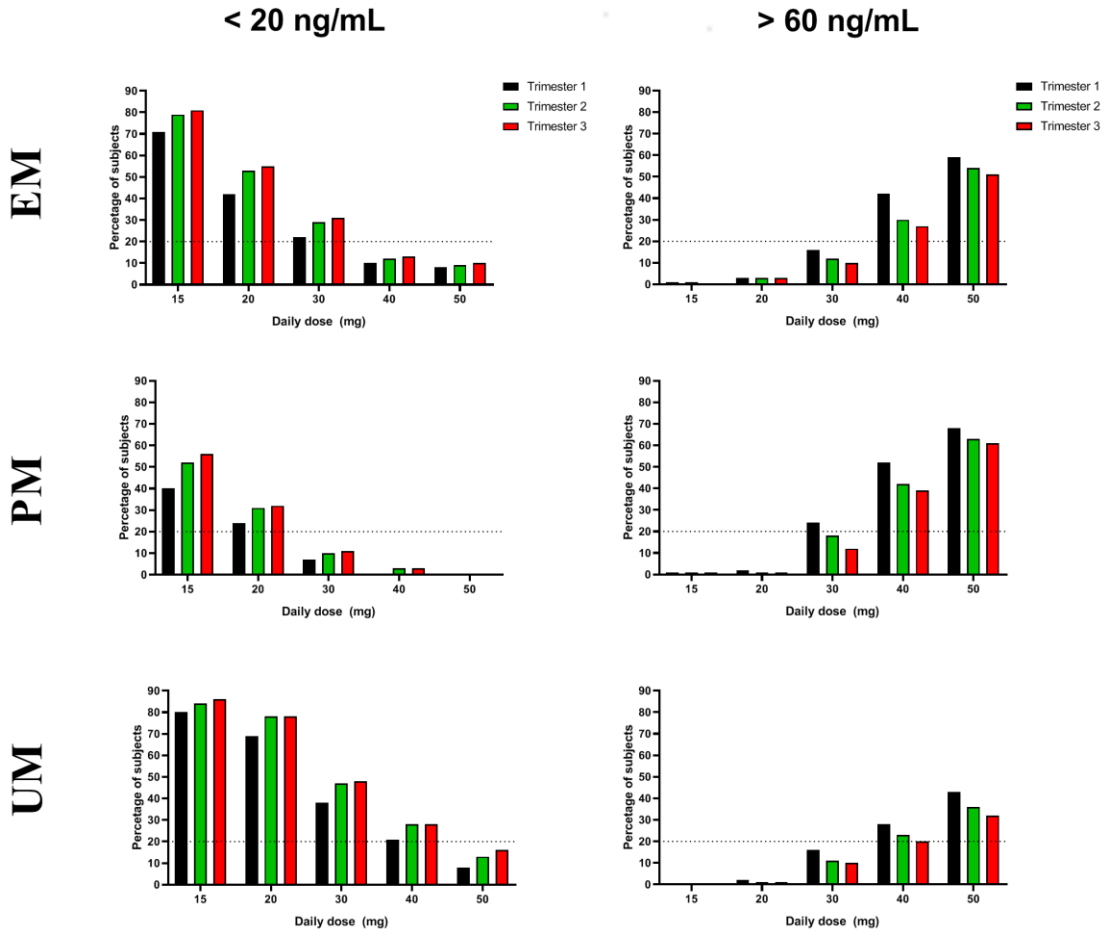

Figure 4.7 Phenotype-based dose optimisation of paroxetine during gestation.

Paroxetine doses were escalated in 5 mg increments every 3 days to 15–50 mg daily dose during gestation, with trough plasma concentrations analysed for the final day of each trimester in entirely EM, PM or UM pregnancy population groups. The number of subjects with trough plasma concentration below 20 ng/ml (left panels) or above 60 ng/ml (right panels) is reported.

4.5 Discussion

Depression is far more prevalent in women than men [428, 429], and is the leading cause of disability worldwide [430]. Furthermore, the prevalence of depression during pregnancy is thought to be in excess of 10 % [431], however the use of mental health services by pregnant women is low, approximately 14 %, when compared to non-pregnant women, approximately 25 % [432]. The use of pharmacological treatment for mental health disorders during pregnancy is governed by balancing the risk to the foetus alongside the risk of relapse in the mental health of the mother.

The gestation related alterations in maternal physiology, in addition to the treatment itself, can impact upon the pharmacokinetics of drugs. These alterations include the reduction in intestinal motility, increased gastric pH, increased cardiac output, reduced plasma albumin concentrations, and increased glomerular filtration rate [433]. However, the consequences of such alterations are often difficult to ascertain in controlled trials for obvious ethical reasons, which leaves prescribers to empirically treat pregnant patients according to their understanding of the changes in biochemical and physiologic functions [392].

However, to assess the potential impact of pregnancy on antidepressant therapy, the use of robust and validated mechanistic pharmacokinetic models provides an opportunity to prospectively assess the potential changes in a drugs pharmacokinetics to support medicines optimisation.

Paroxetine is primarily metabolised by CYP 2D6 and to a lesser extent by CYPs 3A4, 1A2, C219 and 3A5 [381]. Further, paroxetine is also a mechanism-based inhibitor of CYP 2D6 [382, 383], which results in a significant decrease in clearance under steady-state conditions [384]. The use of paroxetine during gestation is complicated by the fact that several studies have noticed an apparent increase in the activity of CYP 2D6 during gestation [389-393], with an associated decrease in paroxetine plasma concentration during gestation, by up to 50 %, in comparison to non-pregnant females [380].

Given the lack of more detailed clinical studies examining this phenomenon, for the first time this study applied the principle of pharmacokinetic modelling to prospectively assess the use of paroxetine in pregnancy population groups and attempted to relate changes in plasma concentrations during gestation to a potential therapeutic window region. The Simcyp pregnancy PBPK model has been utilised by our group and others for prediction of the impact

of changes in plasma concentrations associated with gestation [414, 417, 434], however this is the first time it has been utilised in the context of paroxetine.

The development of the model utilised an existing, validated, and published model of paroxetine within the Simcyp Simulator, with minor modification to allow it to be used in the context of pregnancy, particularly to account for the impact physiological changes in gestation on paroxetine pharmacokinetics. This was accomplished by utilising paroxetine within a full-body physiologically based pharmacokinetics (PBPK) model. This adaptation required validation against single and multiple dose studies in non-pregnant subjects (Step 1) followed by pregnant subjects (Step 2). Resulting predictions in non-pregnant subjects, were within 2-fold of those reported along with appropriate visual predictive checking (VPC) strategy confirming population level variability in plasma concentrations (Figure 4.3) were appropriately predicted in relation to the clinically reported variability (Table 4.1).

There is currently a paucity of pharmacokinetics data examining the impact of gestation on paroxetine plasma concentrations. To our knowledge, Westin *et al* [380] is the only publication (to date) containing paroxetine plasma concentrations sampled in patients throughout gestation. This was therefore used as the basis for validating the paroxetine pregnancy PBPK model. Simulations were conducted for the entire gestation period (38 weeks) and sampling and quantification conducted on the final day of each week for every 5th week during gestation (Weeks 0-35) (Figure 4.4). In non-pregnant subjects ('baseline'), the predicted plasma concentrations (24.05 ng/mL ± 15.45 ng/mL) were within 2-fold of those reported by Westin *et al* [435] (33.5 ng/mL) and further spanned across a similar range of reported values. Westin *et al* [380] reported a 12 %, 34 % and 51 % decrease in mean plasma concentration at for trimesters 1-3, respectively. Using the PBPK model we demonstrated a similar decrease of up to 30 % by trimester 3 (Figure 4.4).

To understand the rationale for the decrease in paroxetine plasma levels during gestation, we further assessed changes in total (*in-vivo*) clearance and AUC (Figure 4.5). This was demarked for the CYP 2D6 phenotype of each subject. In all phenotypes, the clearance increased during gestation, which mirror the increase in 2D6 activity reported during gestation [392], with the greatest difference in clearance occurring in trimester 3 (Appendix A: Table A2). This increase in clearance would therefore reduce the overall bioavailability within subjects, as demonstrated by the statistically significant difference in the AUC in trimester 3 for all phenotypes (Appendix A: Table A3). Within each phenotype, the UM subjects demonstrated the greatest difference in both clearance and AUC during gestation (Appendix A: Table A2 and A3).

The decrease in plasma concentrations noted in our study concurs with previous reports [392, 423], and may be associated with temporal changes in CYP 2D6 expression (induction) noted throughout gestation [393]. Ververs [423] reported an increase in PM plasma concentration [423] during gestation, which is in contrast to the reduction modelled within our studies. However, the number of PM subjects in their study, n=1, is low making it difficult to extrapolate to a larger cohort of PM subjects in a generalised fashion.

Given the importance of the phenotype of the subject on gestational paroxetine levels, we next explored the ability of the model to correctly capture phenotype levels and to examine the trough levels in the context of the therapeutic window. Paroxetine plasma concentrations have previously been reported in CYP 2D6 phenotyped subjects [423], of which the EM, PM and UM were investigated using uniform singular phenotype populations. Ververs reported single point levels which were sampling at non-specific intervals post-dosing [423] and therefore comparison were made to C_{max} and C_{min} levels in each subject simulated in our studies. For both EM (Figure 4.6A) and PM (Figure 4.6B), model predicted levels spanned the range of reported levels across gestational weeks. For the UM phenotype population, only 3 observed samples were available across gestation (Figure 4.6C). Although the predicted levels spanned some of the reported levels (Figure 4.6C), the lack of UM data precludes a full comparison to be made.

For the PM phenotype, as a result of a loss of function alleles, gestational changes in paroxetine pharmacokinetics would be primarily governed by maternal physiological alterations or alternative clearance pathways, e.g. CYP 3A4, whose activity is known to increase during gestation [436], rather than direct changes in CYP 2D6 expression. Thus, the combined impact of minimal CYP 2D6 mediated clearance (in PM phenotypes), but enhanced CYP 3A4 clearance due to gestational induction, may result in a potential net minimal changes in plasma levels during gestation [434].

To assess the potential impact of these polymorphic subjects on possible sub therapeutic levels, we quantified the percentage of subjects with trough concentration below the lower therapeutic window (20 ng/mL) for the standard 20 mg dose (Table 4.2). The UM group demonstrated significantly larger percentages below 20 ng/mL when compared to the EM group (Table 4.2), > 70 % from week 20 onwards. Whereas for the PM group, this remained at 34 % from week 20 onwards. Given this variability, we next examined how a dose adjustment could be made for EM, PM and UM subjects throughout gestation.

For all phenotypes studies (EM, PM and UM), there was a requirement for daily doses in-excess of the standard 20 mg dose throughout gestation. Whilst there is some uncertainty as to the upper most limit of the therapeutic window (60-350 ng/mL) [401, 402, 437], the lower window was used as a reference point for dose optimisation with trough levels (Figure 4.7) (Appendix A: Table A4).
For EM, a dose of 30 mg daily in trimester 1 followed by 40 mg daily in trimesters 2 and 3 is suggested to be optimal. For PM, a 20 mg daily dose in trimester 1 followed by 30 mg daily in trimesters 2 and 3 is suggested to be optimal. For UM, a 40 mg daily dose throughout gestation is suggested to be optimal (Figure 4.7) (Appendix A: Table A4).

The PM phenotype has been shown to require more frequent switches and dose modification [438] due to an increase in the frequency and severity of associated concentration-dependent adverse effects [439], resulting in an approximate 4-fold increase in the risk of discontinuation during pregnancy [440]. This makes appropriate dose modification difficult in women who are already experiencing adverse effects during gestation, such as nausea from morning sickness in addition to nausea as an SSRI adverse drug reaction. Further, for the UM group, this cohort would be at greater risk of sub-therapeutic paroxetine plasma concentration without a dose adjustment, resulting in an increase in depressive symptoms, as has been recently noted in a retrospective analysis of phenotyped pregnant women taking anti-depressant drugs during gestation [440].

The outcomes of the dose optimisation study identified that a dose increase would be required throughout gestation, irrespective of the phenotype. With EM requiring an increase to 30-40 mg daily, PM 20-30 mg daily and UM 40 mg daily. In all of these cases, the percentage of subjects with sub-therapeutic concentrations (<20 ng/mL) would be less than 20 % (Figure 4.7). Post-natal dose tapering would be required to return maternal plasma levels to those in the pre-natal period. Whilst the capability of simulating the return of maternal physiology to the pre-natal period is not possible within Simcyp, Nagai *et al* (2013) [441] have suggested a tapering dose decrease of 10 mg per week commenced before delivery, based upon transplacental paroxetine transfer and pharmacokinetic modelling, may be effective in reducing the incidence of withdrawal symptoms in the neonate and mother. However, paroxetine has a very short half-life (compared to other SSRIs), and discontinuation phenomena are a concern. Clinicians should be encouraged to be alert for these during dose tapering as they would in any other dose-reduction phase with SSRIs.

It should be noted that given paroxetine is administered orally, changes in gestational gastric physiology such as delayed gastric emptying [442, 443] and alterations in gastric pH [444] may

alter the oral absorption of paroxetine, studies have demonstrated that given paroxetine is completely absorbed [386, 445], changes in GI-physiology during gestation are likely to have a minimal effect. Further, paroxetine oral absorption is unaffected by changes in gastric pH [446] neglecting the potential impact of changes in paroxetine ionization and dissolution when administered orally during gestation. However gestational related changes in material GI-physiology are not currently incorporated in the Simcyp Simulator utilised within this study. Nevertheless, the utilising of robust validation approaches allowed for the pragmatic assessment of the need for dose adjustment during gestation, however further confirmatory clinical studies are warranted to confirm the results presented within this study.

4.6 Conclusion

The decision to continue or withdraw antidepressants during pregnancy is challenging when considering the paramount importance of both maternal and neonatal health. The prescriber must actively decide whether the benefit of continuing treatment outweighs any risk of the drug to the developing embryo/foetus. If treatment is continued throughout pregnancy, the changes in maternal physiology should be considered in dosing strategies. With paroxetine, this is further confounded given its susceptibility to CYP 2D6 polymorphism. Based upon modelling studies, our findings suggest that optimisation of paroxetine during pregnancy requires dose increase when compared to non-pregnant patients, driven by changes in tissue physiology and its impact on the volume of distribution, in addition to gestation related alterations in CYP isozyme abundance. For UM phenotypes, at least a doubling in the dose is required to provide a plasma concentration within the therapeutic range.

Although there is no requirement for genetic testing prior to initiation for SSRIs, our approach highlights the opportunity for pharmacokinetics to bring precision dosing into clinical practice. Pre-emptive genotyping may be an approach to support precision dosing in pregnancy to optimise drug therapy and to reduce the risk of relapse due to inadequate dosing.
However, further studies are required to assess both the extent of this gestational change on plasma concentrations and any associated requirement for dose adjustment, in addition to also identifying a more accurate therapeutic range to more precisely define the necessary dose adjustments.

Chapter 5

The application of precision dosing in the use of sertraline throughout pregnancy for poor and ultra-rapid metaboliser CYP 2C19 subjects: a virtual clinical trial pharmacokinetics study

Disclaimer

Elements of this chapter have been published as follows:

Almurjan, A., Macfarlane, H., & Badhan, R. K. S. The application of precision dosing in the use of sertraline throughout pregnancy for poor and ultra-rapid metaboliser CYP 2C19 subjects: a virtual clinical trial pharmacokinetics study. Biopharmaceutics and Drug Disposition. 2021 June, 42(6):252-262.
doi:10.1002/bdd.2278

5.1 Introduction

Depression throughout pregnancy is known to affect up to 20 % of women [447, 448], although fewer than 20 % of pregnant women will actually receive suitable treatment [449, 450]. The risk of untreated depression is particularly important given that death associated with suicide can affect 1 in every 25 women aged 20-35 years, from conception through to the post-natal period [404]. In addition, antenatal depression is a major risk factor for developing postnatal depression [405]. A key strategy in the management of moderate-to-severe depression is the use of selective serotonin reuptake inhibitors (SSRIs) as first-line agents which include sertraline, citalopram, fluoxetine, paroxetine and fluvoxamine.

Sertraline is one of the most frequently used SSRIs globally, particularly during pregnancy [451-457], and is commonly used to manage, amongst others, anxiety and panic disorders and obsessive-compulsive disorders [22, 380]. It is the second most potent serotonin reuptake inhibitor and is the only SSRI that could bind to dopamine transporters [377]. Furthermore, SSRIs have been demonstrated to lead to very few birth defects [458].

Sertraline is metabolised by multiple Cytochrome P450 enzymes, including primarily CYP 2C19 and 2B6 [459] along with contributions from CYP 2C9, CYP 2D6 and CYP 3A4 [460] and is a moderate inhibitor of CYP 2D6 (Figure 5.1) [461, 462]. Due to its linear pharmacokinetics [463], doses ranging between 50 and 200 mg have similar half-life ($t_{1/2}$) for both single and multiple dosing [377].

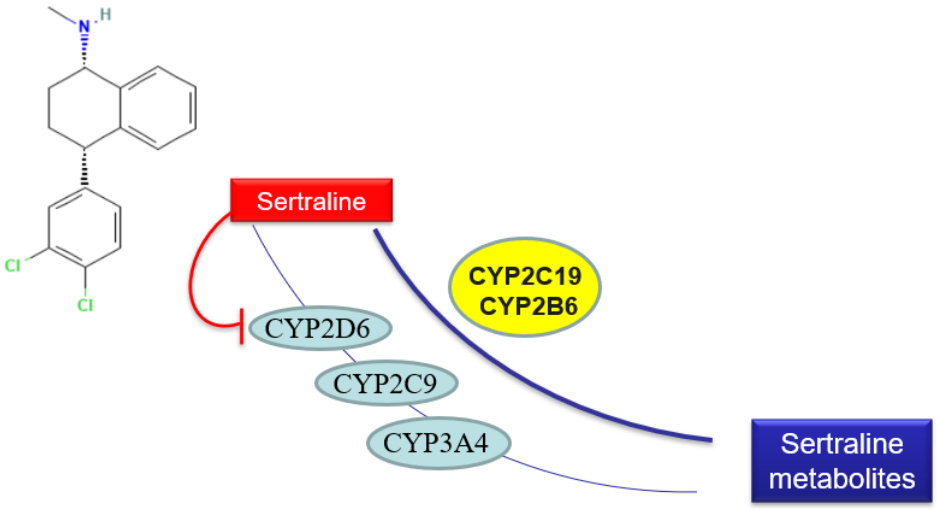

Figure 5.1 Sertraline hepatic metabolism pathway showing the primary metabolism by CYP2C19 and CYP2B6.

Differences between various populations could impact the pharmacokinetics of sertraline. Patients with liver dysfunction have markedly reduced clearance of sertraline [377]. Young males have higher elimination rate constant than females and elderly. Furthermore, the $t_{1/2}$ is approximately 30 % shorter in young males (22.4 hours) than in females and elderly (32.1 – 36.7 hours) [464].

Confounding the use of sertraline in pregnancy are the longitudinal changes in CYP isozyme expression during gestation, where expression increases for 2B6 [465], 2D6 [393, 466, 467] and 3A4 [468, 469] and decreases for 2C19 [470-472].

The implications of such changes during gestation make dose optimisation challenging, and this is confounded by the paucity of the pharmacokinetic studies for sertraline use during pregnancy. In those that have reported plasma concentrations during gestation, conflicting results indicate either an increase in trough plasma levels [380] necessitating possible dose reduction, or a decrease in plasma concentrations requiring a possible dose increase [473-477]. The conflicting reports may, in part, be due to the complex metabolism route and longitudinal changes in the abundance of these enzyme pathways during gestation and often small sample (patient) sizes within studies. Nevertheless, the consensus within all of these studies highlights the need for careful monitoring of depressive symptoms during the perinatal period.

Furthermore, CYP 2C19 is highly polymorphic and these genetic variabilities have been implicated in the requirement for dose adjustment in use of sertraline and other SSRIs with phenotypes of CYP 2C19 [478, 479]. Over 30 allelic variants have been identified for CYP 2C19 with the majority of patients being carriers of *CYP 2C19 *1* (extensive metaboliser [EM] trait), **2* (poor metaboliser [PM] trait), *or *17* (ultra-rapid metaboliser [UM] trait) alleles. Further, guidelines from the Clinical Pharmacogenetics Implementation Consortium (CPIC) (https://cpicpgx.org) detail the allele definitions and phenotypic interpretations of CYP 2C19 and their clinical relevance alongside providing recommendations for genotype-guided dosing of sertraline, namely advocating a dose increase of at least 50 % in PM but no dose adjustment for UM phenotype patients. However, conflicting reports on the impact of specific CYP 2C19 genotypes/phenotypes on sertraline have highlighted the need to investigate the impact of this further on dose adjustments [479].

In the context of post-natal period, SSRIs have been reported to lead to Post Natal Adaptation Syndrome (PNAS). This is, in part, due to their ability to cross the placenta which may result

in increased serotonin concentrations in the developing foetus, thus, impacting foetal respiratory, cardiovascular and neurological development [451, 452, 458].

A recent study implemented a pharmacokinetic modelling approach to explore the changes in sertraline concentrations through gestation [480]. Whilst they also simulated a decrease in sertraline levels, their study lacked both the use of full body physiological model with a dedicated gestational-age dynamic foetal model and used a limited dataset for validation purposes. Given the limited pharmacokinetic data throughout pregnancy, the predominantly reported decrease in sertraline concentrations, coupled with its complex elimination pathways, we have applied, for the first time, a full body virtual clinical trials pharmacokinetic model to assess the dosing of sertraline throughout gestation to identity necessary dose titrations.

5.2 Aims and objectives

With a focus on the existing guidelines for use of sertraline in CYP 2C19 phenotypes, the primary aim of this study was to evaluate the influence of gestation on plasma sertraline levels and to provide a clinically relevant dosing titration strategy for CYP 2C19 phenotype status during gestation.

To achieve the aims, the overall objectives were:

- To validate the revised sertraline PBPK model using published single and multiple dose studies in healthy population.
- To further validate the model in pregnant population
- To assess the impact of CYP 2C19 polymorphism on sertraline plasma concentration during pregnancy
- To explore approaches to sertraline dose titration during gestation for CYP 2C19 phenotypes.

5.3 Methods

Simcyp Simulator was utilised, which is a physiologically based pharmacokinetic (PBPK) modelling tool, to conduct virtual clinical trials simulations (Simcyp Ltd, a Certara company, Sheffield, UK, Version 17). Unless otherwise stated, mixed genders (50:50) into all simulations were incorporated. A four-stage workflow was utilised (Figure 5.2).

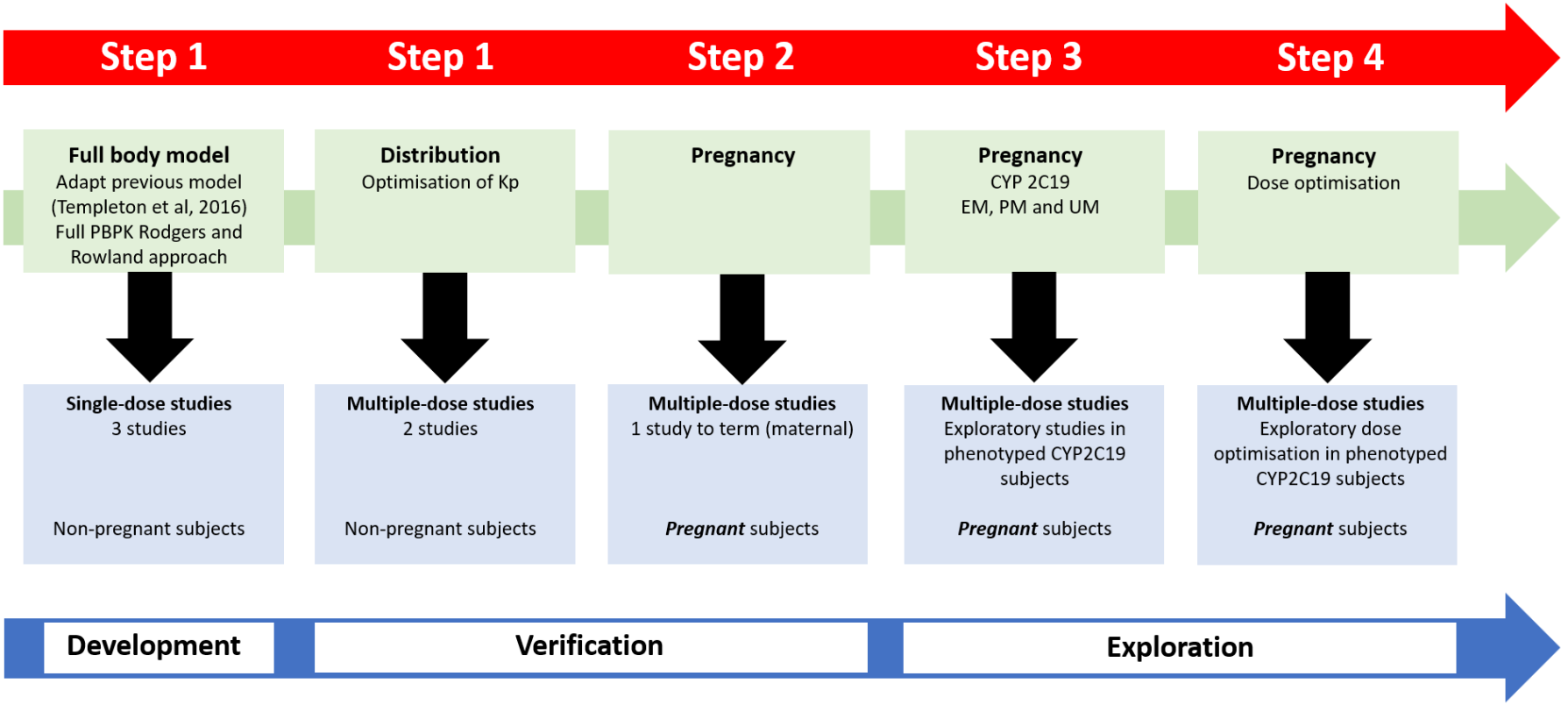

Figure 5.2 A workflow modelling approach for sertraline

5.3.1 Step 1: Validation of sertraline

The Simcyp 'healthy volunteer' (HV) population group was utilised for studies with baseline populations consisting of non-pregnant females. For pregnant population groups, the Simcyp 'pregnancy' population was used. This population was developed previously by Simcyp researchers and includes gestation dependant changes in physiology, cardiac output, tissue perfusion, blood volume alongside biochemistry modification (e.g. human serum albumin) and enzyme/protein expression [413-416]. Sertraline is not available within the Simcyp Simulator; however, a previous study developed and validated a sertraline compound for use within the Simcyp simulator [481], with modifications made by our group to allow its use during gestation.

In order to apply this previously validated model within the context of our studies, 5 retrospective clinical studies were employed, 4 single dose studies and 1 multiple dose studies: (i) 24 healthy adults (12 male and 12 female) aged between 18-45 years old dosed a single oral dose of 50 mg sertraline [482] (ii) 18 healthy subjects administered a single 50 mg oral dose of sertraline [483]; (iii) 5 healthy male volunteers, mean age 26.1 years ± 4.2 years, administered a 50 mg single dose of sertraline [484]; (iv) 5 male and 5 female (19-31 years) dosed 100, 200 and 400 mg as a single dose with C_{max} reported [485] and (v) 11 male and 11 female healthy volunteers aged between 18-45 years old administered a 200 mg daily for 30 days, with sampling on day 30 [486]; The design of trials within Simcyp were matched to these clinical studies. Simcyp Simulator parameters for sertraline are detailed in Appendix B (Section 1: Table B1).

5.3.2 Step 2: Validation of sertraline during pregnancy

In order to apply the developed sertraline model during pregnancy, we conducted further validation using data extracted from a retrospective analysis of therapeutic drug monitoring services in Norway [380]. This study included 56 pregnant and 52 non-pregnant (female) sertraline plasma concentrations, obtained from 34 women taking an oral dose of 50 mg daily. Importantly, this study reported individualised sample data throughout gestation rather than a central tendency without variance [477], missing patient sample data throughout study or poor sample sizes [473].

The Simcyp Pregnancy model has been utilised previously to assess changes in plasma concentration in pregnant women [414, 417, 434] and this study represents its application in the context of sertraline for the first time. The Simcyp Pregnancy model changes the physiology of the mother (e.g. tissue volumes) throughout the study period, which allows the model to operate in a dynamic nature, updating the prediction of V_{ss} through the study as a

result of updated estimates of the tissue-partition coefficient (Kp), as opposed to using fixed estimates of Kp and Vss.

The Simcyp Pregnancy model does not inherently include longitudinal changes in CYPs 2C19 and 2B6, and these were incorporated based on previous reports of successful implementation within the Simcyp Simulator [434] (Appendix B (Section 2)). In order to replicate the study by Westin *et al* [380] we utilised a 38-week gestation and 10 x 10 (n=100 subject) study design with sertraline doses of 50 mg daily. Data was collected for every 5th week and presented as the final 24 hours of that period. A similar trial design was implemented for non-pregnant females (baseline).

5.3.3 Step 3: Impact of CYP 2C19 polymorphism on sertraline plasma concentration during pregnancy

Sertraline plasma concentrations are known to be altered in different CYP 2C19 phenotypes [478]. In order to simulate the impact of CYP 2C19 phenotypes in pregnant women, we simulated entirely extensive metaboliser (EM), poor metaboliser (PM) and ultra-rapid metaboliser (UM) populations through revision of the default phenotype distribution to ensure uniform phenotype populations. For each phenotype, CYP 2C19 enzyme abundance was also incorporated and detailed in Appendix B (Section 2) (Figure B1).

Study design implemented a 10x10 trial design with a daily dose of 50 mg once daily throughout gestation and sampling (of plasma concentration) conducted for every 5th week and presented as the final 24 hours of that period. Where appropriate, data was also presented on the final dosing day of the week during trimester 1 (T1: week 10), trimester 2 (T2: week 20) and trimester 3 (T3: week 30).

In the absence of any published data, the default value of 0 pmol/mg was used for CYP 2C19 PM phenotypes within the Simcyp Simulator [487, 488].

5.3.4 Step 4: Dose adjustment during gestation

To explore approaches to sertraline dose titration during gestation on resultant plasma concentrations, dosing was initiated at 50 mg once daily and increased in weekly increments by 50 mg to a maximum of 300 mg once daily. A proposed therapeutic range was set at 10-75 ng/mL [479]. This was based on reports from the Arbeitsgemeinschaft für Neuropsychopharmakologie und Pharmakopsychiatrie' (AGNP) suggesting a range of 30-500 nM [489], equating to a lower limit of approximately 10 ng/mL. The upper limited was

defined by Bråten *et al* in relation to the concentration of sertraline occurring the serotonin transporter (SERT) and being approximately 250 nM (~75 ng/mL) [479, 490].

Data was reported for each phenotype studied, namely EM, PM and UM subjects, on the final day of each trimester and presented as the percentage of subjects possessing trough plasma concentrations outside of the therapeutic range (i.e. below 10 ng/mL and above 75 ng/mL).

5.3.5 Predictive performance

To ensure appropriate predictive performance (Steps 1-2), predictions of pharmacokinetic metrics that were within two-fold (0.5-2.0-fold) of published data was accepted as part of the 'optimal' predictive performance [424-426]. Furthermore, predictions in step 1-2 were also validated using a visual predictive checking (VPC) strategy [427] when compared to reported data. This approach compared the Simcyp Simulator predicted concentration–time profiles, which consisted of either a mean or median and the 5th and 95th percentiles, against the observed data. A successful validation approach was assumed when Simcyp-predicted results overlapped with the observed data sets [417].

5.3.6 Data and statistical analysis

Retrospective (observed) clinical data was extracted from reported studies using WebPlotDigitizer v.3.10 (http://arohatgi.info/WebPlotDigitizer/). Tabulated (observed) clinical data was utilised as reported in studies, namely mean and standard deviation (Step 1 and 2). Exploratory studies (Step 3 and 4) were reported as median and range, unless otherwise stated. Statistical analysis was conducted using a non-parametric Kruskal-Wallis test with a Dunn's multiple comparison post-hoc test. Significance was confirmed with a $p < 0.05$. All statistical testing was conducted using GraphPad Prism version 8.00 for Windows (GraphPad Software, La Jolla California USA, www.graphpad.com).

5.4 Results

5.4.1 Step 1: Validation of sertraline

A previously reported sertraline model [481] was adapted, implementing a full-PBPK model to appropriately model physiological changes during gestation and their impact upon Vss. The model was validated against 4 single dose studies, 1 multiple dose study and a dose escalation study. The resulting predicted plasma concentration-time profiles successfully predicted single dose (Figure 5.3A), multiple dose (Figure 5.3B) and dose escalation studies (Figure 5.3C). Furthermore, the resultant Simcyp predicted t_{max}, C_{max}, and AUC were within 2-fold of the reported values (Figure 5.3D) (See Appendix B: Table B2).

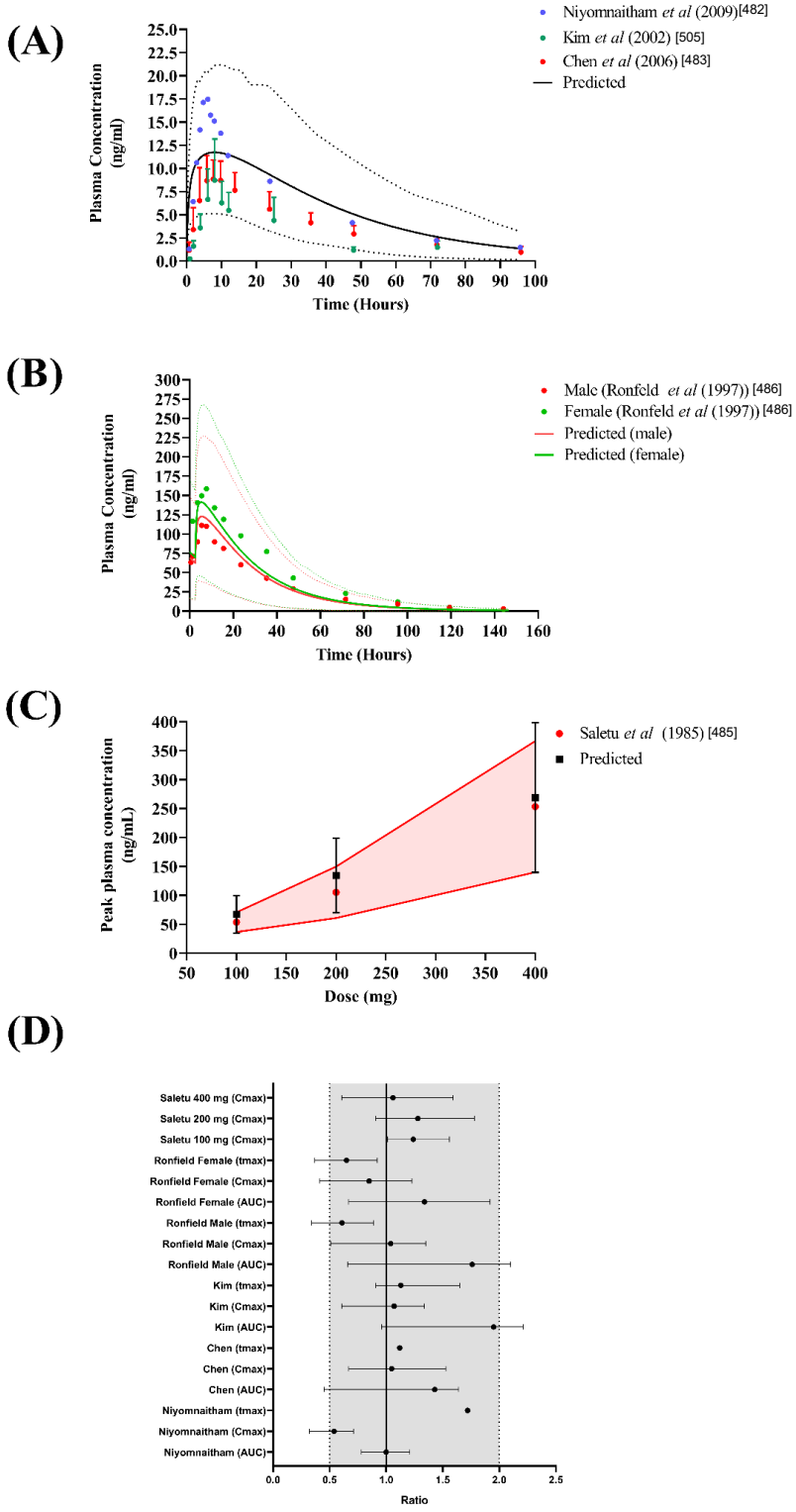

Figure 5.3 Simulated sertraline plasma concentrations

(A) Single 50 mg oral doses of sertraline [482-484]; (B) Multiple daily 50 mg oral doses reported on day 30 [486] for males (red) and females (green); (C) 100, 200 and 400 mg single doses of sertraline [485]; (D) Forest plot showing the predicted mean ± SD over the observed ratio of pharmacokinetic parameters in subjects, with the dotted and shaded area representing the 2-fold range [0.5 to 2] and

solid black line the line of unity. For (A) and (B) solid circles represent observed clinical data with error bars indicating standard deviation, solid lines represent predicted mean concentration-time profile and the 5th and 95th percentile range represented by dotted lines. For (C), solid red circles represent observed clinical data with upper and lower red lines indicating standard deviation. Solid black square and error bars indicate mean and standard deviation respectively.

5.4.2 Step 2: Validation of sertraline during pregnancy

The distribution of simulated sertraline plasma concentrations were similar to the range of observations reported [380] during pregnancy (Figure 5.4). The predicted mean plasma concentration in non-pregnant females (baseline), 16.20 ng/mL ± 10.32 ng/mL, was within 2-fold of that reported, 11.1 ng/mL ± 7.02 ng/mL [380].

Further when compared to baseline, plasma concentrations decreased for trimester 2 (week 15: 16.13 ng/mL ± 9.71 ng/mL, week 20: 15.01 ng/mL ± 9 ng/mL) and trimester 3 (week 30: 14.41 ng/mL ± 8.59 ng/mL, week 35, 13.68 ng/mL ± 8.13 ng/mL). The decrease from baseline was only statistically significant for week 35 ($p = 0.021$).

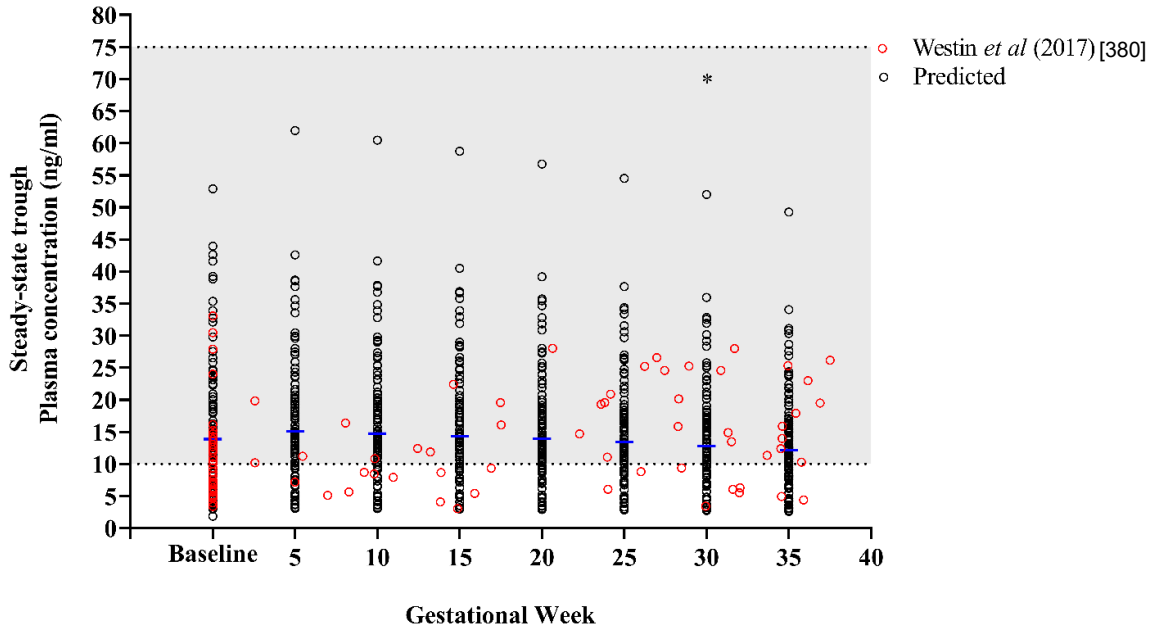

Figure 5.4 Model predicted and observed plasma concentrations of sertraline throughout pregnancy

Predicted concentrations were obtained from subjects (n=100) administered a 50 mg daily dose and data collected as post-dose (trough concentrations) sampled on the final 24 hours period after dosing and collated every 5-weeks (black open circles). Sertraline concentrations in non-pregnant female are illustrated as 'Baseline'. Red open circles represent pooled (observed) plasma concentrations obtained from a total of 34 subjects. The therapeutic window is represented by the shaded regions between 10 ng/mL to 75 ng/mL. Blue horizontal lines represent mean plasma concentration for the simulated dataset.

5.4.3 Step 3: Impact of CYP 2C19 polymorphism on sertraline plasma concentrations during pregnancy

CYP 2C19 is highly polymorphic and the primary metabolic pathway for sertraline. Changes in trough concentrations and intrinsic clearance was assessed for baseline and during gestation for CYP 2C19 phenotype subjects, using frequencies reported within Simcyp Simulator (EM: 59 %, PM: 9.2 % and UM: 31.8 %).

The median trough plasma concentration decreased for by 17.2 % (EM, $p < 0.05$), 14.4 % (PM, $p > 0.05$) and 20 % (UM, $p < 0.001$) by week 30 when compared to baseline (Figure 5.5) (Appendix B: Table B3).

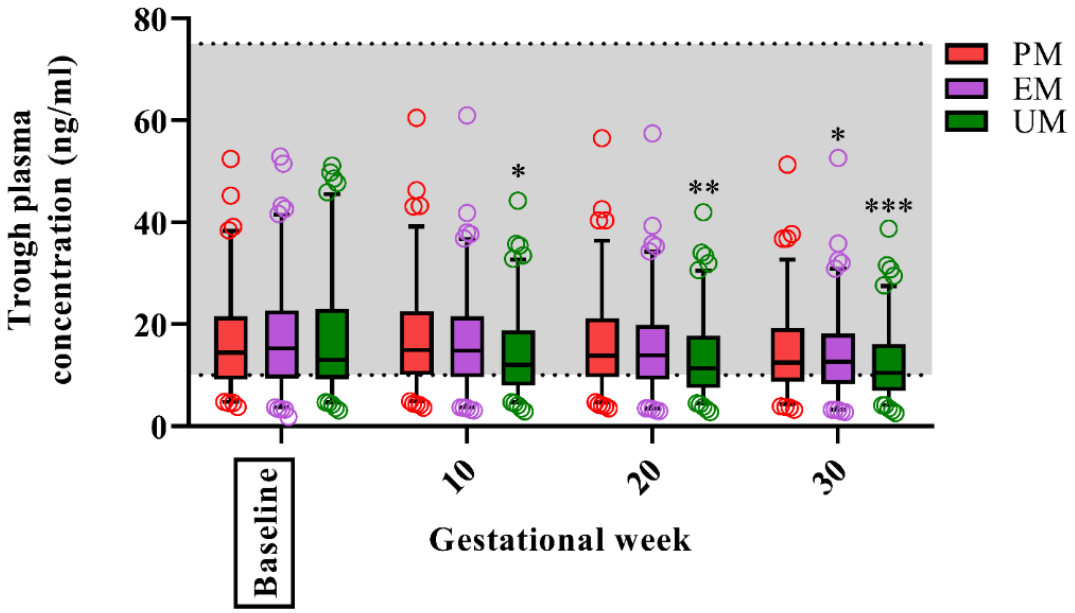

Figure 5.5 Simulated sertraline trough plasma concentrations for CYP 2C19 polymorphs.

The impact of pregnancy on sertraline trough (C_{min}) plasma concentrations for CYP 2C19 extensive metabolisers (EM) and poor metabolisers (UM) in non-pregnant females (baseline) and throughout pregnancy following a 50 mg once daily dose to 100 subjects per phenotype. Data represented by box and whisker plots with median, 5th and 95th percentiles detailed. *p<0.05, **p<0.01, ***p<0.001.

Despite decreases in trough plasma concentrations throughout gestation, CYP 2C19 intrinsic clearance also decreased. For EMs, a decrease in the median Clint by CYP 2C19 was noticed from the 1st trimester (week 5: 78.4 L/h [17.5-611 L/h]) and continued to decrease in weeks 10 and 15: 68.5 L/h [13.8-533.8 L/h], 63.8 L/h [13.3-513.7 L/h], respectively, when compared to the baseline Clint, 78.4 L/h [17.5-622.1 L/h]. Statistically significant decreases in Clint were

apparent from gestational week (GW) 20 onwards when compared to baseline subjects ($p<0.05$) (Figure 5.6) (Appendix B: Table B4).

For UMs, a decrease in the median Clint by CYP 2C19 was also noticed from the 1st trimester (week 5: 97.5 L/h [21.7-721.6 L/h] and continued to decrease in weeks 10 and 15, 90.4 L/h [20.1-671.7 L/h] and 83.3 L/h [18.5-618.7 L/h], respectively, when compared to the baseline Clint, 105.17 L/h [24.5-776.3 L/h]. Statistically significant decrease in Clint was apparent from gestational week (GW) 20 onwards when compared to non-pregnant subjects ($p<0.05$) (Figure 5.6) (Appendix B: Table B4).

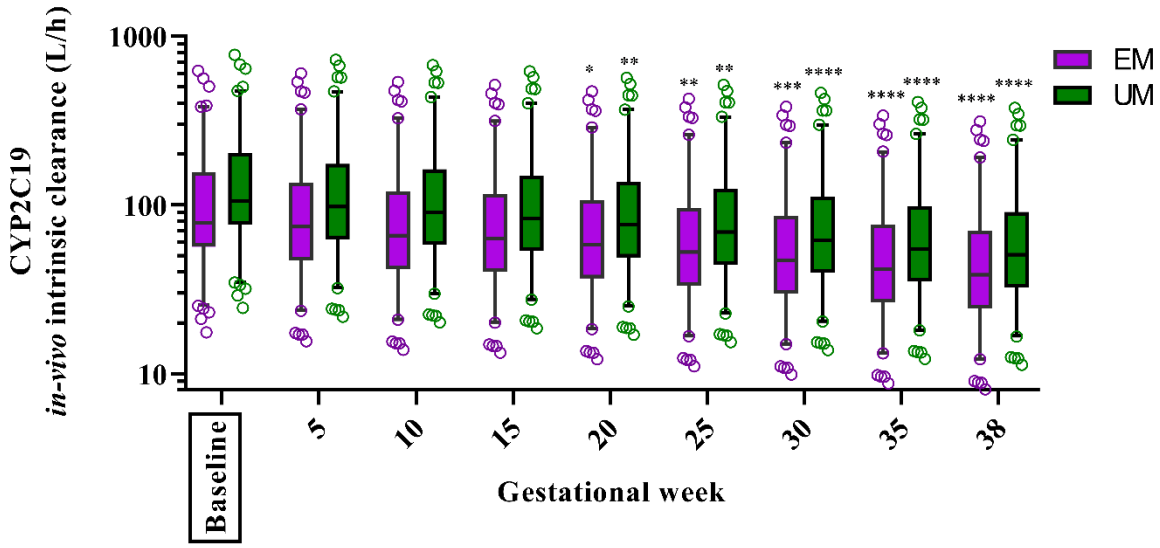

Figure 5.6 The impact of CYP 2C19 polymorphism on sertraline clearance throughout pregnancy

The impact of CYP 2C19 extensive metaboliser (EM) and ultra-rapid metaboliser (UM) phenotypes on Simcyp predicted sertraline *in-vivo* intrinsic clearance for non-pregnant females (baseline) and during pregnancy, following a 50 mg once daily dose to 100 subjects per phenotype. Data represented by box and whisker plots with median, 5th and 95th percentiles detailed. *p<0.05, **p<0.01, ***p<0.001, ****p<0.0001.

5.4.4 Step 4: Sertraline dose optimisation

In order to address changes in sertraline concentrations during gestation for CYP 2C19 phenotype subjects, we quantified the percentage of subjects with plasma concentrations outside of the therapeutic range (i.e. below 10 ng/mL and above 75 ng/mL) across a dosing range of 50-300 mg daily.

Regardless of the phenotype, the daily sertraline dose required to maintain trough concentrations within the therapeutic window was above the usual 50 mg/day throughout

pregnancy. When attempting to identify an optimal dose, we ensured a balance of a low percentages of subjects outside of this window, with an optimal dose defined as where no more than 20 % of subjects possessed concentrations outside of the window (Figure 5.7) (Appendix B: Table B5).

For EM and UM, a dose of 100-150 mg daily is suggested to be optimal throughout pregnancy. For PM, a starting dose of 25 mg once daily resulted in a > 60 % of subjects with trough levels below 10 ng/mL across pregnancy (Figure 5.7). However, a dose of 50 mg once daily resulted in 24 % of subjects possessing trough levels below 10 ng/mL (Figure 5.7). During trimesters 2 and 3, an increase in dose to 100 mg once daily resulted in less than 10 % of the subjects demonstrating trough levels below 10 ng/mL (Figure 5.7) (Appendix B: Table B5).

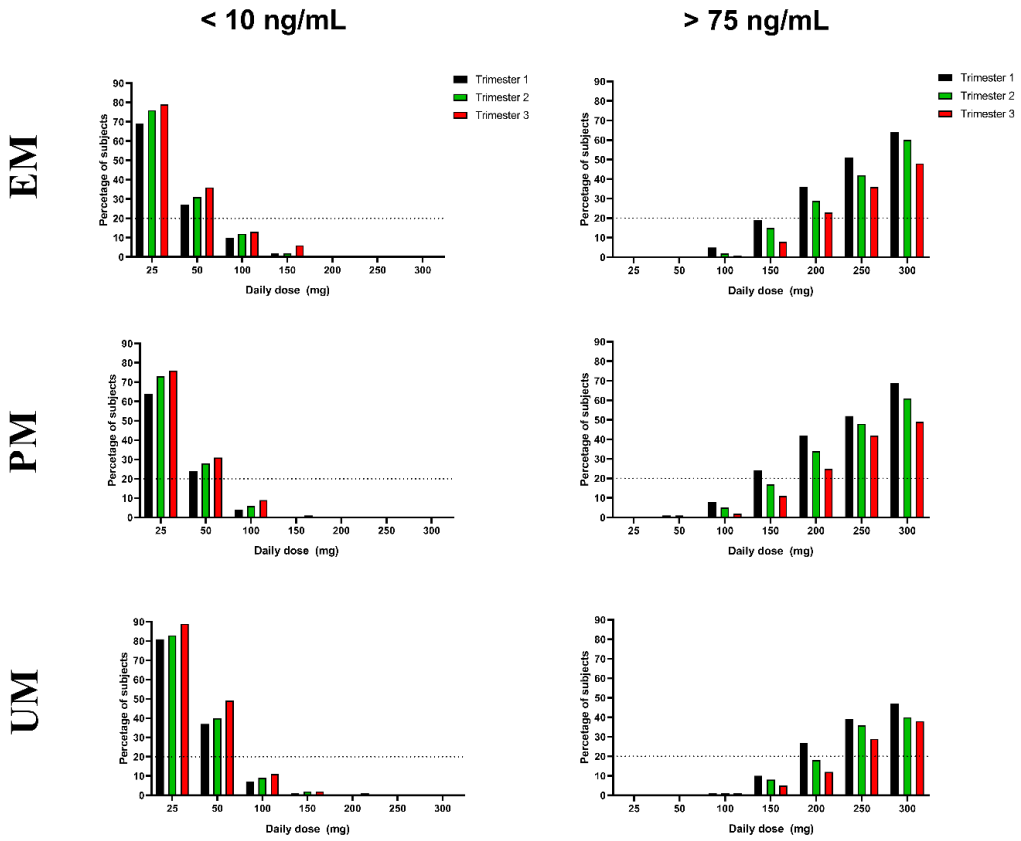

Figure 5.7 Dose optimisation of sertraline during pregnancy in CYP 2C19 phenotyped subjects

Doses were titrated in increments of 50 mg every 3 days over a range of 50 mg to 300 mg once daily throughout pregnancy. Trough plasma concentrations were reported for the final dosing day of each trimester in specific EM, PM or UM pregnancy population groups. Percentages of subjects with plasma concentration (trough) outside of the therapeutic range (below 10 ng/mL [left panels] and above 75 ng/mL [right panels]) are reported.

5.5 Discussion

Depression is a leading cause of disability worldwide [430], and is thought to affect more than 20 % of pregnant women [431, 447, 448]. A key challenge for healthcare professional is the use of pharmacological interventions during pregnancy, which is often informed by balancing the expected benefits for the mother's mental health with the possible risks to the foetus. This decision is further complicated by gestational related alterations in maternal physiology [433] which can impact upon the pharmacokinetics of drugs. Often the combined impact of these, in additional to the longitudinal nature of these alterations, make it difficult to extrapolate their impact during clinical practice [392]. To augment the existing empirical approaches to treatment interventions, the application of robust and well validated pharmacokinetic models offers a unique opportunity to apply virtual clinical trials to support medicines optimisation in mental health for special population groups.

Sertraline is metabolised by multiple enzymes, including CYPs 2C19, 2B6, 2C9, 3A4 and 2D6. Confounding the use of sertraline in pregnancy, is the gestational alterations in maternal CYP 2C19 activity, which has been determined to decrease by 62 % and 68 % during trimester 2 and 3 respectively [470-472]. Despite this decrease, several confounding studies have noticed either an apparent decrease [473-475] or increase [380] in sertraline plasma concentrations during gestation.

In this study, we have applied virtual clinical trials dosing of sertraline throughout pregnancy, to identity suitable dose titration necessary to support therapeutically maintained sertraline plasma concentrations in the mother throughout pregnancy.

We adapted a previously published sertraline model [481] to allow its use within the context of gestation, and this was fully validated with both single and multiple dose studies in both pregnant and non-pregnant subjects, with predictions to 2-fold of those reported (Figures 5.3 and 5.4) (Appendix B: Section 1 Table B1 and B2) and spanning a similar range within the population studies. However, a wider AUC range in the predicted-observed ratios (Figure 5.3D), although still within 2-fold, are thought to reflect the complexity associated with the metabolism of sertraline, namely CYPs 2C9, 2C129, 2B6, 2D6 and 3A4 and hence the associated contribution towards inter-individual variability. The variance in AUC from clinical studies (measured as mainly the standard deviation) was broadly similar to those simulated within our studies (Appendix B: Section 3).

A recent report by Westin *et al* [380] highlighted sertraline plasma concentration throughout gestation in 34 subjects. This was used as the basis for validation of the pregnancy PBPK model. The resulting mean plasma concentrations in non-pregnant subjects (16.20 ng/mL ± 10.32 ng/mL) were within 2-fold of those reported [491] and demonstrated a similar predicted range to that reported (Figure 5.4). Furthermore, we demonstrated a decrease in mean plasma concentration throughout pregnancy with a significant decrease in GW35 ($p<0.05$) compared to baseline (Figure 5.4). On the contrary, a 10 %, 36 % and 68 % increase in plasma concentration were reported by Westin *et al* [380] during trimesters 1-3 respectively. Other studies have identified a similar decrease to that reported here [473] [477], however Westin *et al* [380] included individualised sample data throughout gestation rather than a central tendency without variance [477], missing patient sample data throughout the study or utilising poor sample sizes [473]. Nonetheless, to further examine the reported disparity in clinical observations, we assessed changes in trough plasma concentrations (Figure 5.5) and intrinsic clearance (Figure 5.6) because of population variability in the phenotypes of one of the primary CYP isozyme responsible for sertraline metabolism, namely CYP 2C19. In all tested phenotypes, the intrinsic clearance decreased throughout pregnancy, mirroring decreases in CYP 2C19 activity, the largest significant difference in clearance being noticed in trimester 3 (Figure 5.6) (Appendix B: Table B4).

This decrease in clearance was expected to increase sertraline trough plasma concentrations as observed by Westin *et al* [380]. On the contrary, trough plasma concentrations for EMs and UMs decreased during gestation with the greatest significant decrease occurring in trimester 3 (Figure 5.5) (Appendix B: Table B4), which concurred with a range of other reports [392, 423, 473, 475, 492]. This decrease has been associated with an increase in the key female hormones estradiol and progesterone throughout pregnancy, with concentrations reaching up to 100 nM and 1 μM for estradiol and progesterone, respectively, at term. These levels are significantly greater than those during menstruation (< 50 nM) [394, 395]. Such female hormones are known to be activators for basic helix-loop-helix transcription factors (e.g. aryl hydrocarbon receptor; AhR) or nuclear hormone transcriptional regulators (constitutive androstane receptor, CAR; pregnane X receptor, PXR; estrogen receptor, ER), which contribute to the induction of a variety of CYP isoforms and enhanced drug clearances [396, 397]. However, the metabolic breakdown of sertraline is complicated, and includes CYPs 2B6, 2C9, 2C19, 2D6, and 3A4. The contribution of each isozyme has proven difficult to determine *in-vivo*, however the variable up- or down-regulation of CYP isozyme expression during gestation [493] may contribute to the disparity observed in some studies [380]. For example, the approximate 2-fold decrease in 2C19 activity coupled with approximately 2-fold increase

in 2B6 activity by trimester 3 may negate the overall impact of each pathway, in preference to changes in other physiological factors such as increases in total body water.

Furthermore, the concomitant decrease in albumin is likely to cause the observed increase in sertraline plasma unbound fraction and hence increase the volume of distribution, extending the half-life and reducing sertraline plasma levels. To confirm this, a global sensitivity analysis (GSA) was implemented to examine the combined influence of albumin levels, CYPs 2C19 and 2B6 abundance on C_{max}, AUC, Cl and V_{ss} (Appendix B: Section 3 Table B6 to B8) within the model. The resulting model sensitivity rankings (Appendix B: Section 3 Table B6), confirmed the sensitivity of the model to changes in human serum albumin levels throughout gestation and primarily in trimester 3 (Appendix B: Section 3 Table B7 and B8). Given that sertraline is highly protein bound, the decrease in albumin during pregnancy would be significant driver for reduced plasma levels and an extension of the half-life [494], potentially more so that the impact of CYP isozyme gestational changes.

At present, there is a paucity of studies exploring the impact of CYP 2C19 phenotypes on sertraline levels during pregnancy. A recent dosing guideline for sertraline which considered CYP 2C19 phenotypes has been published [478]. However, it is not clear whether the proposed guidelines are relevant to pregnant women. Given the importance of the phenotype of the subject on gestational sertraline levels, we next examined the changes in the trough levels in relation to the therapeutic range of sertraline under a standard 50 mg daily dosage of sertraline [479]. As expected, the UM phenotypes demonstrated the largest number of subjects below 10 ng/mL (Appendix B: Table B5), whereas for the PM group, this was predicted to be in the range of 24-31 %.

Finally, for all phenotypes (EM, PM and UM), dose titrations were required to daily doses that were typically in excess of the 50 mg dose throughout pregnancy (Figure 5.7) (Appendix B: Table B5). For EM and UM, a dose escalation to 100-150 mg daily is suggested to be optimal through pregnancy. For PM, a dose of 50 mg during the first trimester followed by a dose increase in trimesters 2 and 3 to 100 mg is suggested to be optimal. Furthermore, the doses suggested within this study are within the range clinically utilised and significantly below the known toxicity range in adults (> 4000 mg/daily) [495]. The return of maternal sertraline plasma levels would be needed post-natally and although this is not possible to simulate within Simcyp, tapering the dose of sertraline by 50 mg per 5-7 days is recommended to avoid withdrawal syndrome [496]. Furthermore, although there is very little published studies reporting pharmacodynamic changes during pregnancy for sertraline, the current approaches for the

studies during pregnancy focus primarily on the clinicians role in the dose titration based on empirical changes in the psychiatric state of the patient [497].

In addition, although clinicians routinely monitor drug pharmacodynamics by directly measuring physiological indices of therapeutic responses, the link between (unbound) plasma levels and clinical response is not well established for sertraline [498-500]. Further, any attempt to relate unbound levels to a pharmacodynamic effect would need to further consider that the resultant central effects would be governed by the blood-brain barrier, which acts as a permeability barrier to any resultant central effects on reuptake of monoamines into the presynaptic neurones. Further work is needed to address the reductions in sertraline plasma concentration through gestation on the resultant maternal pharmacodynamic effects on mood stability, in order to fully translate the results presented within this manuscript to clinical practice.

A key benefit of the pregnancy PBPK approach highlighted within our study, is the ability to incorporate key gestational changes in the physiology of the mother, for example the highlight reduction in plasma albumin and increase in maternal volume, which can be coupled with a mechanistic description of the activities of metabolising enzymes to enable disentangling what would otherwise be clinically complicated relationships.

5.6 Conclusion

Any decision to withdraw or continue with antidepressant therapy perinatally is challenging for both maternal and foetal health. A key paradigm is the balance between the benefit of continuing treatment and the risk drug-related toxicity to the developing embryo/foetus.
Confounding treatment during gestation, are longitudinal maternal physiological alternations which alter the requirements for dosing. Furthermore, the susceptibility of CYP 2C19 to polymorphisms only increases the complexity in prescribing decisions.
Our results demonstrated that dose titrations are required throughout pregnancy, with UM subjects being of concern and requiring at least double the standard dose by trimester 3, to support on-going maintenance of plasma sertraline concentrations to within the therapeutic range.

This study has highlighted a key role for the use of pharmacokinetics to allow pragmatic exploration of dosing regimens within a perinatal setting, to support the reduction in risk of treatment relapse due to inappropriate dosing.

Chapter 6

General conclusions and future work

6.1 General conclusions

This thesis aimed to improve the clinical outcomes in CNS (mental) disorders through pharmaceutical and pharmacokinetic approaches with focusing on major depression.
We have highlighted the use of flavonoids, which are chemicals derived from natural extracts of plants and vegetables, as possible novel non-pharmacological approach for the treatment of depression. It has been shown by several studies the ability of flavonoids to cross the blood brain barrier and exert their CNS related effects. The flavonoid hesperetin has been studied widely and demonstrated several pharmacological effects including neuroprotection, anticancer, anti-inflammatory, antioxidant, antidepressant, hypolipidemic, and anticonvulsant properties. The safety, efficacy, and cheap availability of hesperetin make it a candidate drug for pre-clinical and clinical studies for the management of CNS disorders. However, hesperetin possess a low oral bioavailability resulting from the extensive first-pass metabolism, its lipophilic nature, and its low aqueous solubility, this consequently result in low and often subtherapeutic concentrations in the systemic circulation following oral administration [185, 193, 205-210]. Given these limitations to optimal oral bioavailability, in chapters 2 and 3, the use of transdermal formulation systems for hesperetin have been explored due to their possible potential to deliver higher plasma concentrations than those obtained following oral delivery.

Chapter 2 focused on the development and assessment of hesperetin creams using pharmaceutical base creams including Vanish-pen™, Doublebase™ gel, Versatile™, and Pentravan® bases. The developed cream formulations were found to have consistent morphological characteristics, organoleptic properties, and pH values during storage at 4°C and 25°C for 10 weeks. In-vitro drug release studies in week 0 showed that Pentravan® formulation released the highest percentage of hesperetin after 24 hours (12.69 % (0.68 %)), while Versatile™ released the lowest amount. For consistent hesperetin release profiles for 10 weeks, we suggested for Vanish-pen™ formulations to be stored at 4°C, Doublebase™ formulations at 25°C, and Versatile™ formulations at both 4°C and 25°C. While Pentravan® formulations stored at both 4°C and 25°C resulted in inconsistent release profiles. However, the release obtained from all the tested vehicles was not optimum and could be further improved by using different drug release methods and more penetration and solubility enhancers. Pharmaceutical base creams illustrate good potential for the topical and localised delivery of hesperetin to treat skin disorders while more studies are needed to investigate the ability to reach the systemic circulation.

Chapter 3 concerned the development of hesperetin transdermal patch systems using silicone-based adhesive (Dow Corning ® BIO-PSA 7-4501) or acrylic-based adhesive (Eudragit® E100) with the incorporation of different plasticisers (PVP 30, Tween® 20, glycerol, triacetin). The selected patches were evaluated under storage for 3 weeks at temperatures 4ºC and 25ºC using morphological characterisation, visual mechanical properties assessment, pH assessment, in-vitro drug release studies, and kinetics assessment. The silicone-based patch (F7) that contain 5.5 % glycerol provided the highest release, 39.9 % (0.37 %). During storage, F7 patch showed consistent morphological characteristics and pH assessment, however, the release profile was significantly decreased. In the other hand, the Eudragit®-based patch resulted in physical and mechanical changes during storage which prevented the conduction of further studies. More studies are needed to understand the reasons behind the changes during storage. Dow Corning ® BIO-PSA 7-4501 adhesive is a potential candidate for the development transdermal patches attributed to its easy use, flexibility, compatibility with wide range of APIs, and safety profile. Dow Corning ® BIO-PSA 7-4501 patch demonstrate a potential candidate to release hesperetin systemically owing to its release profile, however, more studies are needed to assess the release through the skin. The release through the skin could be further assessed in excised human or animal skin tissue using Franz cell diffusion in conjunction with Strat-M® membrane as an alternative to human skin. Strat-M® is a synthetic membrane-based model with diffusion characteristics well-correlated to human skin [504].

In chapters 2 and 3, we focused on the possible non-pharmacological approaches to treat depression transdermally which could aid in overcoming the limitations associated with conventional antidepressants by using phytochemicals, while in chapters 4 and 5, the aim was to improve the therapeutic outcomes obtained by the commonly prescribed antidepressants, paroxetine and sertraline, through using in-silico PBPK modelling to optimise dosing in challenging populations such as pregnant women.

Chapter 4 focused on using PBPK modelling approach to examine gestational changes in trough plasma concentrations of paroxetine for CYP 2D6 phenotypes, followed by necessary dose adjustment strategies to maintain paroxetine levels within a therapeutic range of 20-60 ng/mL. This study highlighted the decrease in trough plasma concentrations throughout gestation for all phenotypes and the requirement of dose adjustment in-excess of the standard 20 mg dose. The following doses were suggested to be optimal: for EM, 30 mg daily in trimester 1 followed by 40 mg daily in trimesters 2 and 3, for poor-metabolisers (PM), 20 mg daily dose in trimester 1 followed by 30 mg daily in trimesters 2 and 3, and for UM, a 40 mg daily dose throughout gestation.

In Chapter 5, PBPK modelling was implemented to assess gestational changes in trough plasma concentrations of sertraline for CYP 2C19 phenotypes and to highlight appropriate dose titration strategies to stabilise sertraline levels within a defined therapeutic range throughout gestation. This study highlighted the decrease of sertraline trough plasma concentrations during pregnancy which has been attributed to maternal volume expansion and reduction in plasma albumin as possible causative reasons. All CYP 2C19 phenotypes required dose increase throughout gestation. For extensive metaboliser (EM) and ultra-rapid metaboliser (UM) phenotypes, doses of 100-150 mg daily are suggested to be optimal throughout gestation. For poor metabolisers (PM), 50 mg daily during the first trimester followed by a dose of 100 mg daily in trimesters 2 and 3 are required.

Approximately 280 million people in the world are suffering from depression [16].
Although most patients are able to recover with treatment, the rate of recurrence is high and in 70% of depressed patients whom are taking an adequate course of one antidepressant, remission is not achieved [23, 24]. There is a serious need to better manage depression or discover new antidepressants to treat the unresolved conditions or to follow approaches that could improve clinical response. Poor therapeutic outcomes are usually related to patient non-adherence to antidepressants with about 50% of patients discontinue the treatment of depression prematurely [32]. The reasons for non-adherence and discontinuation of antidepressants were side effects, high cost, delayed onset of action, complicated dosing or titration of the drug, poor instruction by the clinician, lack of follow up, and misperceptions about antidepressants [32]. The use of Phytochemicals for depression is a novel approach that have been recently explored by several studies, however, they lack the necessary concrete scientific solidity to be safely carried forward into clinical levels of research, simply because they have not been studied sufficiently. Despite efforts, studies on the precise functions of phytochemicals encountered a number of obstacles as *in-vitro* testing was used for the majority of studies. For instance, techniques for in vitro screening were employed to validate the biological activities of extracted phytochemicals. However, there are a lot of considered phytochemicals to be explored and several potential health effects that require large-scale experiments, which is very expensive.

This thesis aimed to reduce the knowledge gap regarding the possibility of incorporating the phytochemical hesperetin into transdermal systems to improve its bioavailability, which will eventually improve its pharmacological effect. When the bioavailability barrier is resolved, phytochemicals could possibly be studied clinically more efficiently and that could lead to the availability of more studies that could convince the scientific community that these chemicals are worth progressing.

The thesis also highlighted that PBPK modelling can be used to optimise and understand the pharmacokinetics of antidepressants in special populations (pregnant women). This could clinically improve treatment outcomes in pregnant women with mental CNS disorders (depression). Moreover, the need of close monitoring of antidepressants when used in this special population is highlighted.

The gestation related alterations in maternal physiology, in addition to the treatment itself, can impact the pharmacokinetics of drugs. These alterations include the reduction in intestinal motility, increased gastric pH, increased cardiac output, reduced plasma albumin concentrations, and increased glomerular filtration rate [433]. However, the consequences of such alterations are often difficult to ascertain in controlled trials for obvious ethical reasons, which leaves prescribers to empirically treat pregnant patients according to their understanding of the changes in biochemical and physiologic functions and undergo dose titration based on empirical changes in the psychiatric state of the patient [392].
To augment the existing empirical approaches to treatment interventions, the application of robust and well validated pharmacokinetic models offers a unique opportunity to apply virtual clinical trials to support medicines optimisation in mental health for special population groups. Unlike empirical approaches, PBPK is a system biology approach that uses a mechanistic method to predict drug's pharmacokinetics using both mathematical models and drug specific properties including the metabolic, physicochemical, and pharmacogenomic data achieved by preclinical or *in-vitro* pharmaceutical experiments and species-specific physiological, anatomical and pathophysiological parameters [152].

Providing a well-studied dosing strategy for clinicians would prevent the empirical approaches that clinicians use with knowing that the toxic plasma concentration is not reached and the safety of the mother and the foetus is attained by continuous monitoring. Yet the suggested dose optimisation strategies for paroxetine and sertraline provided by this thesis cannot be used clinically at the moment because the knowledge gap in the maternal physiology and the multifactorial effects on drugs pharmacokinetics is still unclear and needs to be studied more intensively until the confidence in using PBPK in this special population group is high. This thesis reduces the knowledge gap which is a step forward for increasing the scientific confidence in using PBPK for pregnancy-related interventions.

6.2 Future work

Future work would focus more extensively on the limitations encountered during this work such as the short period of release studies, stability issues, low amounts of drug, and storage temperatures. The release studies were conducted for 24 hours only due to the leakage of the creams into the release media when studies are conducted for more than 24 hours. This could be improved by using different release procedure such as using Franz cells, however Franz cells were not feasible in this study because of using low amounts of hesperetin. With higher amounts, Franz cells could be used and the percentage release could also be improved when assessing the formulations release for longer period. Also, solubility enhancers could be beneficial to improve the release as hesperetin has low aqueous solubility. Although the manufacturers of the base creams confirmed the instability of the creams at high temperatures (40°C), assessing the formulations at this storage temperature would be beneficial to explore the behaviour and stability of hesperetin formulations at higher temperatures.

More studies are required to be conducted on the cream formulations including *in-vitro/in-vivo* permeation studies on human/animal skin and on mice. This will allow us to reflect the release of hesperetin into or through the skin. Measuring the viscosity using viscometer is required to detect any changes during storage which could be attributed to changes in release profiles. Robustness determination (spreadability) is also required to highlight physical changes during storage. Differential scanning calorimetry (DSC) is required which is typically used for understanding the thermal characteristics of compounds incorporated into topical and transdermal systems [252-256] by giving an insight into thermal and chemical properties including homogenous dispersion, phase transitions, melting temperatures and heat capacity changes that might occur during storage.

Further work is needed with the most promising Dow Corning® BIO-PSA 7-4501 based patch. Accurate mechanical tests are necessary such as tensile strength test, uniformity testing, and peel adhesion test. Also, permeation studies on human/animal skin and mice are required to reflect the efficiency of the formulations to deliver hesperetin systemically. To understand the changes occurring during storage, differential scanning calorimetry (DSC) is required. The usage of more plasticisers and permeation enhancers needs to be explored to enhance the release of hesperetin from the patches [501].

Simcyp's PBPK Simulator now includes a comprehensive dermal model. The multi-phase, multi-dimensional dermal absorption model, known as MPML MechDermA™, is based on skin physiology that includes SC, viable epidermis, dermis, deep tissue, subcutis, and skin appendages (Figure 6.1). The mechanistic MPML-MechDermA skin absorption model

accounts for the drug, formulation, environmental parameters, and physiology, allowing simulation of sophisticated drug diffusion through the SC from different formulations including emulsions, patches, and gels, as well as APIs with variable physicochemical properties [502].

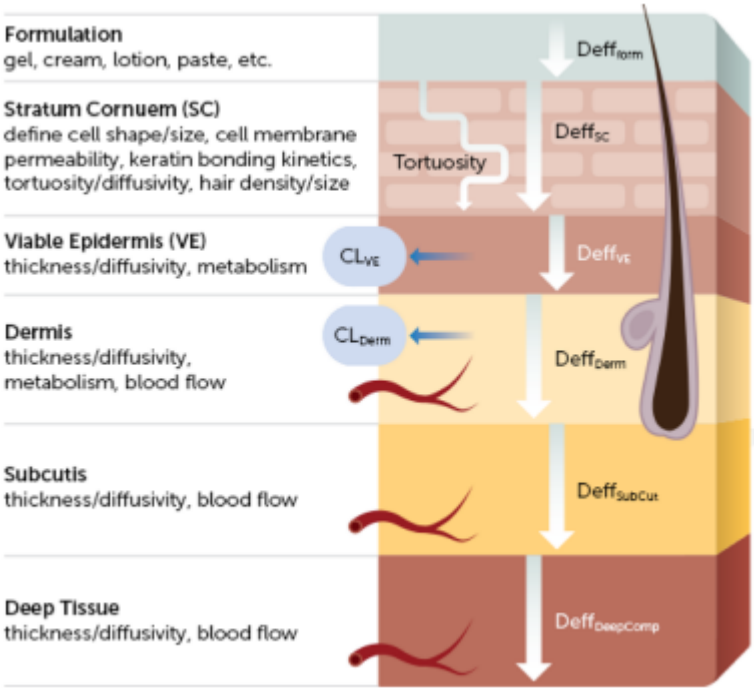

Figure 6.1 MechDermA model Compartments

CL: Clearance. Deff: Diffusion coefficient. Obtained from [502]

The dermal model in Simcyp was utilised previously for PBPK modelling of the transdermal delivery of the antidepressant selegiline along with its metabolites to evaluate their disposition in healthy and special populations [503]. Their validated model predicted variability in drug and metabolites exposure after selegiline transdermal patch application that could potentially result in side effects in depressed patients with hepatic and renal disorders [503].

The Simcyp simulator will be used to translate the obtained *in-vitro* release profiles of hesperetin into *in-vivo* dermal deposition, systemic plasma concentration and target tissue concentrations (i.e. brain tissue). In this approach, hesperetin literature published and model predicted pharmacokinetic parameters will be gathered and utilised within the Simcyp Simulator, this will include estimates of partition coefficients and diffusion coefficients within derma layers. The resulting dermal and systemic concentration profiles will provide a pragmatic understanding of the translation of *in-vitro* formulation release performance to *in-vivo* temporal levels and hence guide further formulation develop to obtain the require target plasma concentration or potential brain tissue accumulation levels. However, to conduct virtual

clinical trials, data from real clinical trials on hesperetin are needed to be able to develop a validated hesperetin compound for PBPK modelling, but these clinical trials are still lacking.

PBPK modelling will also be used to explore other antidepressants disposition in different special populations such as geriatrics, renal and hepatic patients.

References

1. WHO, *Neurological Disorders: Public Health Challenges.* 2006, World Health Organisation. p. 232.

2. Nguyen, T.T., et al., *Nanotechnology-based drug delivery for central nervous system disorders.* Biomedicine & Pharmacotherapy, 2021. **143**.

3. Pardridge, W.M., *CNS drug design based on principles of blood-brain barrier transport.* Journal of Neurochemistry, 1998. **70**(5): p. 1781-1792.

4. Warren, K.E., *Beyond the Blood: Brain Barrier: The Importance of Central Nervous System (CNS) Pharmacokinetics for the Treatment of CNS Tumors, Including Diffuse Intrinsic Pontine Glioma.* Frontiers in Oncology, 2018. **8**.

5. Bagchi, S., et al., *In-vitro blood-brain barrier models for drug screening and permeation studies: an overview.* Drug Design Development and Therapy, 2019. **13**: p. 3591-3605.

6. Delsing, L., et al., *Models of the blood-brain barrier using iPSC-derived cells.* Molecular and Cellular Neuroscience, 2020. **107**.

7. Pardridge, W.M., *Biopharmaceutical drug targeting to the brain.* Journal of Drug Targeting, 2010. **18**(3): p. 157-167.

8. Pardridge, W.M., *Drug targeting to the brain.* Pharmaceutical Research, 2007. **24**(9): p. 1733-1744.

9. Pardridge, W.M., *Drug transport across the blood-brain barrier.* Journal of Cerebral Blood Flow and Metabolism, 2012. **32**(11): p. 1959-1972.

10. Neuwelt, E., et al., *Strategies to advance translational research into brain barriers.* Lancet Neurology, 2008. **7**(1): p. 84-96.

11. Abbott, N.J., et al., *Structure and function of the blood-brain barrier.* Neurobiology of Disease, 2010. **37**(1): p. 13-25.

12. Dutheil, F., et al., *ABC transporters and cytochromes P450 in the human central nervous system: influence on brain pharmacokinetics and contribution to neurodegenerative disorders.* Expert Opinion on Drug Metabolism & Toxicology, 2010. **6**(10): p. 1161-1174.

13. Dauchy, S., et al., *ABC transporters, cytochromes P450 and their main transcription factors: expression at the human blood-brain barrier.* Journal of Neurochemistry, 2008. **107**(6): p. 1518-1528.

14. Kessler, R.C. and E.J. Bromet, *The Epidemiology of Depression Across Cultures.* Annual Review of Public Health, Vol 34, 2013. **34**: p. 119-138.

15. Brigitta, B., *Pathophysiology of depression and mechanisms of treatment* Dialogues Clin Neurosci., 2002. **4**(1): p. 7 - 20.

16. GHDx. *Global Health Data Exchange (GHDx)*. 2019 [cited 2021 24 Oct 2021]; Available from: GHDx (healthdata.org).

17. Reddy, M.S., *Depression: The Disorder and the Burden.* Indian J Psychol Med., 2010. **32**(1): p. 1-2.

18. Gerontoukou, E.I., et al., *Investigation of anxiety and depression in patients with chronic diseases.* Health Psychology Research, 2015. **3**(2): p. 36-40.

19. Rogers, D. and R. Pies, *General Medical Drugs Associated with Depression.* Psychiatry (Edgmont), 2008. **5**(12): p. 28–41.

20. Duval, F., B.D. Lebowitz, and J.-P. Macher, *Treatments in depression.* Dialogues Clin Neurosci., 2006. **8**(2): p. 191–206.

21. Trivedi, M.H., *Tools and Strategies for Ongoing Assessment of Depression: A Measurement-Based Approach to Remission*. 2009, Physicians Postgraduate Press: United States. p. 26-31.

22. Pae, C.U. and A.A. Patkar, *Paroxetine: current status in psychiatry.* Expert Rev Neurother, 2007. **7**(2): p. 107-20.

23. Nelson, C., A. Pikalov, and R. Berman, *Augmentation treatment in major depressive disorder: focus on aripiprazole.* Neuropsychiatr Dis Treat., 2008. **4**(5): p. 937–948.

24. Fava, M., *Diagnosis and definition of treatment-resistant depression.* Biological Psychiatry, 2003. **53**(8): p. 649-659.

25. Greden, J.F., *The burden of recurrent depression: Causes, consequences, and future prospects.* Journal of Clinical Psychiatry, 2001. **62**: p. 5-9.

26. Wilson, S., et al., *Premorbid risk factors for major depressive disorder: Are they associated with early onset and recurrent course?* Development and Psychopathology, 2014. **26**(4): p. 1477-1493.

27. van Loo, H.M., et al., *Multiple risk factors predict recurrence of major depressive disorder in women.* Journal of Affective Disorders, 2015. **180**: p. 52-61.

28. Wang, J.L., et al., *Development and validation of a prediction algorithm for use by health professionals in prediction of recurrence of major depression.* Depress Anxiety, 2014. **31**(5): p. 451-7.

29. Ryan, D., L. Milis, and N. Misri, *Depression during pregnancy.* Can Fam Physician, 2005. **51**: p. 1087-93.

30. Kim, J.J. and R.K. Silver, *Perinatal suicide associated with depression diagnosis and absence of active treatment in 15-year UK national inquiry.* Evidence-Based Mental Health, 2016. **19**(4): p. 122-122.

31. Button, S., et al., *Seeking help for perinatal psychological distress: a meta-synthesis of women's experiences.* BRITISH JOURNAL OF GENERAL PRACTICE, 2017. **67**(663): p. E692-E699.

32. Sansone, R.A. and L.A. Sansone, *Antidepressant Adherence. Are Patients Taking Their Medications?* . Innov Clin Neurosci., 2012. **9**(5-6): p. 41–46.

33. Miret, M., et al., *Depressive disorders and suicide: Epidemiology, risk factors, and burden.* Neuroscience and Biobehavioral Reviews, 2013. **37**(10): p. 2372-2374.

34. Panche, A.N., A.D. Diwan, and S.R. Chandra, *Flavonoids: an overview.* Journal of Nutritional Science, 2016. **5**.

35. Kong, Y., et al., *Cytotoxic Activity of Curcumin towards CCRF-CEM Leukemia Cells and Its Effect on DNA Damage.* Molecules, 2009. **14**(12): p. 5328-5338.

36. Yao, L.H., et al., *Flavonoids in food and their health benefits.* Plant Foods for Human Nutrition, 2004. **59**(3): p. 113-122.

37. Lakhanpal, P. and D.K. Rai, *Quercetin: A Versatile Flavonoid.* Internet Journal of Medical Update., 2007. **2**(2): p. 22-37.

38. Wasowski, C. and M. Marder, *Flavonoids as GABAA receptor ligands: the whole story?.* J Exp Pharmacol., 2012. **4**: p. 9–24.

39. Arts, I.C.W., B. van de Putte, and P.C.H. Hollman, *Catechin contents of foods commonly consumed in The Netherlands. 2. Tea, wine, fruit juices, and chocolate milk.* Journal of Agricultural and Food Chemistry, 2000. **48**(5): p. 1752-1757.

40. Zand, R.S.R., D.J.A. Jenkins, and E.P. Diamandis, *Flavonoids and steroid hormone-dependent cancers.* Journal of Chromatography B-Analytical Technologies in the Biomedical and Life Sciences, 2002. **777**(1-2): p. 219-232.

41. Hertog, M.G.L., P.C.H. Hollman, and B. Vandeputte, *Content of Potentially Anticarcinogenic Flavonoids of Tea Infusions, Wines, and Fruit Juices.* Journal of Agricultural and Food Chemistry, 1993. **41**(8): p. 1242-1246.

42. Williams, R.J. and J.P.E. Spencer, *Flavonoids, cognition, and dementia: Actions, mechanisms, and potential therapeutic utility for Alzheimer disease.* Free Radical Biology and Medicine, 2012. **52**(1): p. 35-45.

43. Solanki, L., et al., *Flavonoid-Based Therapies in the Early Management of Neurodegenerative Diseases.* Advances in Nutrition, 2015. **6**(1): p. 64-72.

44. Shukitt-Hale, B., *Blueberries and Neuronal Aging.* Gerontology, 2012. **58**(6): p. 518-523.

45. Mecocci, P., et al., *Nutraceuticals in cognitive impairment and Alzheimer's disease.* Frontiers in Pharmacology, 2014. **5**.

46. Macready, A.L., et al., *Flavonoids and cognitive function: a review of human randomized controlled trial studies and recommendations for future studies.* Genes and Nutrition, 2009. **4**(4): p. 227-242.

47. Cherniack, E.P., *A berry thought-provoking idea: the potential role of plant polyphenols in the treatment of age-related cognitive disorders.* British Journal of Nutrition, 2012. **108**(5): p. 794-800.

48. Blumberg, J.B., et al., *The Science of Cocoa Flavanols: Bioavailability, Emerging Evidence, and Proposed Mechanisms.* Advances in Nutrition, 2014. **5**(5): p. 547-549.

49. Mercer, L.D., et al., *Dietary polyphenols protect dopamine neurons from oxidative insults and apoptosis: investigations in primary rat mesencephalic cultures.* Biochemical Pharmacology, 2005. **69**(2): p. 339-345.

50. Meng, X.Y., et al., *Molecular Mechanisms Underlying the Flavonoid-Induced Inhibition of alpha-Synuclein Fibrillation.* Biochemistry, 2009. **48**(34): p. 8206-8224.

51. Wasowski, C., et al., *Isolation and identification of 6-methylapigenin, a competitive ligand for the brain GABA(A) receptors, from Valeriana wallichii.* Planta Medica, 2002. **68**(10): p. 934-936.

52. Kwon, J.Y., et al., *Beneficial Effects of Hesperetin in a Mouse Model of Temporal Lobe Epilepsy.* Journal of Medicinal Food, 2018. **21**(12): p. 1306-1309.

53. Medina, J.H., et al., *Chrysin (5,7-di-OH-flavone), a naturally-occurring ligand for benzodiazepine receptors, with anticonvulsant properties.* Biochem Pharmacol, 1990. **40**(10): p. 2227-31.

54. Wolfman, C., et al., *Possible Anxiolytic Effects of Chrysin, a Central Benzodiazepine Receptor-Ligand Isolated from Passiflora-Coerulea.* Pharmacology Biochemistry and Behavior, 1994. **47**(1): p. 1-4.

55. Guan, L.P. and B.Y. Liu, *Antidepressant-like effects and mechanisms of flavonoids and related analogues.* European Journal of Medicinal Chemistry, 2016. **121**: p. 47-57.

56. Sun, J.H., et al., *Rutin attenuates H2O2-induced oxidation damage and apoptosis in Leydig cells by activating PI3K/Akt signal pathways.* Biomedicine & Pharmacotherapy, 2017. **88**: p. 500-506.

57. Kanimozhi, S., P. Bhavani, and P. Subramanian, *Influence of the Flavonoid, Quercetin on Antioxidant Status, Lipid Peroxidation and Histopathological Changes in Hyperammonemic Rats.* Indian Journal of Clinical Biochemistry, 2017. **32**(3): p. 275-284.

58. Ekeanyanwu, R.C. and O.U. Njoku, *Flavonoid-rich fraction of the Monodora tenuifolia seed extract attenuates behavioural alterations and oxidative damage in forced-swim stressed rats.* Chinese Journal of Natural Medicines, 2015. **13**(3): p. 183-191.

59. Herrera-Ruiz, M., et al., *Antidepressant effect and pharmacological evaluation of standardized extract of flavonoids from Byrsonima crassifolia.* Phytomedicine, 2011. **18**(14): p. 1255-1261.

60. Ahmadi, A. and A. Shadboorestan, *Oxidative stress and cancer; the role of hesperidin, a citrus natural bioflavonoid, as a cancer chemoprotective agent.* Nutrition and Cancer-an International Journal, 2016. **68**(1): p. 29-39.

61. Freitas, M., et al., *Synthesis of chlorinated flavonoids with anti-inflammatory and proapoptotic activities in human neutrophils.* European Journal of Medicinal Chemistry, 2014. **86**: p. 153-164.

62. Mai, L.H., et al., *Antivascular and anti-parasite activities of natural and hemisynthetic flavonoids from New Caledonian Gardenia species (Rubiaceae).* European Journal of Medicinal Chemistry, 2015. **93**: p. 93-100.

63. Yi, L.T., et al., *Antidepressant-like behavioral, neurochemical and neuroendocrine effects of naringenin in the mouse repeated tail suspension test.* Progress in Neuro-Psychopharmacology & Biological Psychiatry, 2012. **39**(1): p. 175-181.

64. Haas, J.S., et al., *The Anti-Immobility Effect of Hyperoside on the Forced Swimming Test in Rats is Mediated by the D2-Like Receptors Activation.* Planta Medica, 2011. **77**(4): p. 334-339.

65. Du, B., et al., *Antidepressant-like effects of the hydroalcoholic extracts of Hemerocallis citrina and its potential active components.* BMC Complementary and Alternative Medicine., 2014. **14**(1).

66. Can, O.D., U.D. Ozkay, and U.I. Ucel, *Anti-depressant-like effect of vitexin in BALB/c mice and evidence for the involvement of monoaminergic mechanisms.* European Journal of Pharmacology, 2013. **699**(1-3): p. 250-257.

67. Souza, L.C., et al., *Evidence for the involvement of the serotonergic 5-HT-(1A) receptors in the antidepressant-like effect caused by hesperidin in mice.* Progress in Neuro-Psychopharmacology & Biological Psychiatry, 2013. **40**: p. 103-109.

68. Cassani, J., et al., *Anti-Depressant-Like Effect of Kaempferitrin Isolated from Justicia spicigera Schltdl (Acanthaceae) in Two Behavior Models in Mice: Evidence for the Involvement of the Serotonergic System.* Molecules, 2014. **19**(12): p. 21442-21461.

69. Filho, C.B., et al., *Kappa-opioid receptors mediate the antidepressant-like activity of hesperidin in the mouse forced swimming test.* European Journal of Pharmacology, 2013. **698**(1-3): p. 286-291.

70. Krishnan, V. and E.J. Nestler, *The molecular neurobiology of depression.* Nature, 2008. **455**(7215): p. 894-902.

71. Sawamoto, A., et al., *3,5,6,7,8,3 ',4 '-Heptamethoxyflavone, a Citrus Flavonoid, Ameliorates Corticosterone-Induced Depression-like Behavior and Restores Brain-Derived Neurotrophic Factor Expression, Neurogenesis, and Neuroplasticity in the Hippocampus.* Molecules, 2016. **21**(4).

72. Xiong, Z., et al., *Antidepressant Effects of a Plant-Derived Flavonoid Baicalein Involving Extracellular Signal-Regulated Kinases Cascade.* Biological & Pharmaceutical Bulletin, 2011. **34**(2): p. 253-259.

73. Zheng, M.Z., et al., *Antidepressant-like effect of hyperoside isolated from Apocynum venetum leaves: Possible cellular mechanisms.* Phytomedicine, 2012. **19**(2): p. 145-149.

74. Donato, F., et al., *Hesperidin exerts antidepressant-like effects in acute and chronic treatments in mice: Possible role of L-arginine-NO-cGMP pathway and BDNF levels.* Brain Research Bulletin, 2014. **104**: p. 19-26.

75. Yi, L.T., et al., *BDNF signaling is necessary for the antidepressant-like effect of naringenin.* Progress in Neuro-Psychopharmacology & Biological Psychiatry, 2014. **48**: p. 135-141.

76. Khan, A., et al., *Antioxidant and Anti-Inflammatory Effects ofCitrusFlavonoid Hesperetin: Special Focus on Neurological Disorders.* Antioxidants, 2020. **9**(7).

77. Ikram, M., et al., *Hesperetin Confers Neuroprotection by Regulating Nrf2/TLR4/NF-kappa B Signaling in an A beta Mouse Model.* Molecular Neurobiology, 2019. **56**(9): p. 6293-6309.

78. Muhammad, T., et al., *Hesperetin, a Citrus Flavonoid, Attenuates LPS-Induced Neuroinflammation, Apoptosis and Memory Impairments by Modulating TLR4/NF-kappa B Signaling.* Nutrients, 2019. **11**(3).

79. Kiasalari, Z., et al., *Protective Effect of Oral Hesperetin Against Unilateral Striatal 6-Hydroxydopamine Damage in the Rat.* Neurochemical Research, 2016. **41**(5): p. 1065-1072.

80. Shagirtha, K., N. Bashir, and S. MiltonPrabu, *Neuroprotective efficacy of hesperetin against cadmium induced oxidative stress in the brain of rats.* Toxicology and Industrial Health, 2017. **33**(5): p. 454-468.

81. Choi, E.J. and W.S. Ahn, *Neuroprotective Effects of Chronic Hesperetin Administration in Mice.* Archives of Pharmacal Research, 2008. **31**(11): p. 1457-1462.

82. Hwang, S.L. and G.C. Yen, *Effect of Hesperetin against Oxidative Stress via ER- and TrkA-Mediated Actions in PC12 Cells.* Journal of Agricultural and Food Chemistry, 2011. **59**(10): p. 5779-5785.

83. Rainey-Smith, S., et al., *Neuroprotective effects of hesperetin in mouse primary neurones are independent of CREB activation.* Neuroscience Letters, 2008. **438**(1): p. 29-33.

84. Vauzour, D., et al., *Activation of pro-survival Akt and ERK1/2 signalling pathways underlie the anti-apoptotic effects of flavanones in cortical neurons.* Journal of Neurochemistry, 2007. **103**(4): p. 1355-1367.

85. Hwang, S.L. and G.C. Yen, *Neuroprotective effects of the citrus flavanones against H2O2-induced cytotoxicity in PC12 cells.* Journal of Agricultural and Food Chemistry, 2008. **56**(3): p. 859-864.

86. Ikram, M., et al., *Natural Dietary Supplementation of Curcumin Protects Mice Brains against Ethanol-Induced Oxidative Stress-Mediated Neurodegeneration and Memory Impairment via Nrf2/TLR4/RAGE Signaling.* Nutrients, 2019. **11**(5).

87. Alkilani, A.Z., M.T.C. McCrudden, and R.F. Donnelly, *Transdermal Drug Delivery: Innovative Pharmaceutical Developments Based on Disruption of the Barrier Properties of the stratum corneum.* Pharmaceutics, 2015. **7**(4): p. 438-470.

88. Prausnitz, M.R. and R. Langer, *Transdermal drug delivery.* Nature Biotechnology, 2008. **26**(11): p. 1261-1268.

89. Kaestli, L.Z., et al., *Use of transdermal drug formulations in the elderly.* Drugs & Aging, 2008. **25**(4): p. 269-280.

90. Benson, H.A.E. and A.C. Watkinson, *Topical and Transdermal Drug Delivery: Principles and Practice*. 2011, Canada: A John Wiley & Sons, Inc. 409.

91. Abdo, J.M., N.A. Sopko, and S.M. Milner, *The applied anatomy of human skin: A model for regeneration.* Wound Medicine., 2020. **28**.

92. Alves, M.C., et al., *Green tea in transdermal formulation: HPLC method for quality control and in vitro drug release assays.* Quimica Nova, 2014. **37**(4): p. 728-U217.

93. WHO, *6, Physiology of normal skin.*, in *WHO Guidelines on Hand Hygiene in Health Care: First Global Patient Safety Challenge Clean Care Is Safer Care.* 2009, World Health Organization.: Geneva.

94. Wong, R., et al., *The dynamic anatomy and patterning of skin.* Experimental Dermatology, 2016. **25**(2): p. 92-98.

95. Margetts, L. and R. Sawyer, *Transdermal drug delivery: principles and opioid therapy.* Continuing Education in Anaesthesia Critical Care & Pain, 2007. **7**(5): p. 171–176.

96. Bolzinger, M.A., et al., *Penetration of drugs through skin, a complex rate-controlling membrane.* Current Opinion in Colloid & Interface Science, 2012. **17**(3): p. 156-165.

97. Dayan, N., *Pathways for Skin Penetration.* Lipo Chemicals Inc., 2005. **120**(6): p. 67-76.

98. Szunerits, S. and R. Boukherroub, *Heat: A Highly efficient Skin enhancer for Transdermal Drug Delivery.* Frontiers in Bioengineering and Biotechnology, 2018. **6**.

99. Gibaldi, M., M. Lee, and A. Desai, *Gibaldi's drug delivery systems in pharmaceutical care,*. 2007, Bethesda, Maryland.: American society of health-system pharmacists.

100. Thomas, B.J. and B.C. Finnin, *The transdermal revolution.* Drug Discovery Today, 2004. **9**(16): p. 697-703.

101. Alexander, A., et al., *Approaches for breaking the barriers of drug permeation through transdermal drug delivery.* Journal of Controlled Release, 2012. **164**(1): p. 26-40.

102. Jorge, L.L., C.C. Feres, and V.E. Teles, *Topical preparations for pain relief: efficacy and patient adherence.* J Pain Res. , 2010. **4**: p. 11–24.

103. Guy, R.H. and J. Hadgraft, *Transdermal Drug Delivery - a Simplified Pharmacokinetic Approach.* International Journal of Pharmaceutics, 1985. **24**(2-3): p. 267-274.

104. Magner, L., *A history of medicine.* 2nd edition. ed. 2005.: Boca Raton, FL: Taylor & Francis Group.

105. Geller, M., *Ancient Babylonian medicine: theory and practice.* 2010, Malden, MA.: Wiley-Blackwell.

106. Aulton, M.E. and K.M.G. Taylor, *Emulsions and creams*, in *Aulton's Pharmaceutics E-Book : The Design and Manufacture of Medicines*. 2018, Elsevier: Edinburgh, Scotland. p. 446-474.

107. Fagron. *Pentravan® Transdermal cream base.* 2012-2019. [cited 2021 12/08/2021]; Available from: https://fagron.com/en/concept/pentravanr.

108. Fagron. *Versatile™ Vanishing O/w Cream Base.* 2013-2019 [cited 2021 12/08/2021]; Available from: https://fagron.com/en/product/versatiletm.

109. Bourdon, F., et al., *Evaluation of Pentravan (R), Pentravan (R) Plus, Phytobase (R), Lipovan (R) and Pluronic Lecithin Organogel for the transdermal administration of antiemetic drugs to treat chemotherapy-induced nausea and vomiting at the hospital.* International Journal of Pharmaceutics, 2016. **515**(1-2): p. 774-787.

110. Citrome, L., C.M. Zeni, and C.U. Correll, *Patches: Established and Emerging Transdermal Treatments in Psychiatry.* Journal of Clinical Psychiatry, 2019. **80**(4).

111. Pastore, M.N., et al., *Transdermal patches: history, development and pharmacology.* British Journal of Pharmacology, 2015. **172**(9): p. 2179-2209.

112. Cilurzo, F., C.G.M. Gennari, and P. Minghetti, *Adhesive properties: a critical issue in transdermal patch development.* Expert Opinion on Drug Delivery, 2012. **9**(1): p. 33-45.

113. Peterson, T.A., S.M. Wick, and C. Ko, *Design, Development, Manufacturing, and Testing of Transdermal Drug Delivery Systems.*, in *Dermal Drug Delivery*. 2020, CRC Press.

114. Peterson, T.A. *Transdermal Drug Formulation and Process Development.* 2003; Available from: https://alfresco-static-files.s3.amazonaws.com/alfresco_images/pharma/2014/08/22/a50aec24-9082-4d08-b2e8-3d6f91d914a7/article-59304.pdf.

115. Tijani, A.O., et al., *Transdermal Route: A Viable Option for Systemic Delivery of Antidepressants.* Journal of Pharmaceutical Sciences, 2021. **110**(9): p. 3129-3149.

116. Azzaro, A.J., et al., *Pharmacokinetics and absolute bioavailability of selegiline following treatment of healthy subjects with the selegiline transdermal system (6 mg/24 h): A comparison with oral selegiline capsules.* Journal of Clinical Pharmacology, 2007. **47**(10): p. 1256-1267.

117. Farlow, M.R. and M. Somogyi, *Transdermal Patches for the Treatment of Neurologic Conditions in Elderly Patients: A Review.* Prim Care Companion CNS Disord., 2011. **13**(6).

118. Schoretsanitis, G., et al., *TDM in psychiatry and neurology: A comprehensive summary of the consensus guidelines for therapeutic drug monitoring in neuropsychopharmacology, update 2017; a tool for clinicians.* World Journal of Biological Psychiatry, 2018. **19**(3): p. 162-174.

119. Pichini, S., et al., *Pharmacokinetics and Therapeutic Drug Monitoring of Psychotropic Drugs in Pediatrics.* Therapeutic Drug Monitoring, 2009. **31**(3): p. 283-318.

120. Hiemke, C., et al., *Therapeutic drug monitoring in psychiatry. Consensus guidelines of the AGNP/TDM expert group.* Psychopharmakotherapie, 2005. **12**(5): p. 166-182.

121. Eilers, R., *Therapeutic drug monitoring for the treatment of psychiatric disorders - Clinical use and cost effectiveness.* Clinical Pharmacokinetics, 1995. **29**(6): p. 442-450.

122. Fan, J.H. and I.A.M. de Lannoy, *Pharmacokinetics.* Biochemical Pharmacology, 2014. **87**(1): p. 93-120.

123. Urso, R., P. Blardi, and G. Giorgi, *A short introduction to pharmacokinetics.* Eur Rev Med Pharmacol Sci., 2002. **6**: p. 33-44.

124. Markl, D. and J.A. Zeitler, *A Review of Disintegration Mechanisms and Measurement Techniques.* Pharmaceutical Research, 2017. **34**(5): p. 890-917.

125. Noyes, A. and W. Whitney, *The rate of solution of solid substances in their own solutions.* Journal of American Chemistry Society., 1897. **19**(12): p. 930–934.

126. Gavhane, Y.N. and A.V. Yadav, *Loss of orally administered drugs in GI tract.* Saudi Pharmaceutical Journal, 2012. **20**(4): p. 331-344.

127. Alqahtani, M.S., et al., *Advances in Oral Drug Delivery.* Front. Pharmacol., 2021.

128. Urso, R., P. Blardi, and G. Giorgi, *A short introduction to pharmacokinetics.* Eur Rev Med Pharmacol Sci., 2002. **6**(2-3): p. 33-44.

129. Schmidt, S., D. Gonzalez, and H. Derendorf, *Significance of Protein Binding in Pharmacokinetics and Pharmacodynamics.* Journal of Pharmaceutical Sciences, 2010. **99**(3): p. 1107-1122.

130. Nebert, D.W. and D.W. Russell, *Clinical importance of the cytochromes P450.* Lancet, 2002. **360**(9340): p. 1155-1162.

131. Gan, J.P., S.G. Ma, and D.L. Zhang, *Non-cytochrome P450-mediated bioactivation and its toxicological relevance.* Drug Metabolism Reviews, 2016. **48**(4): p. 473-501.

132. Jhajra, S., et al., *Extrahepatic Drug-Metabolizing Enzymes and Their Significance.* Drug Metabolism and Interactions., 2012. **6**: p. 1-97.

133. Krishna, D.R. and U. Klotz, *Extrahepatic metabolism of drugs in humans.* Clin Pharmacokinet, 1994. **26**(2): p. 144-60.

134. Zanger, U.M. and M. Schwab, *Cytochrome P450 enzymes in drug metabolism: Regulation of gene expression, enzyme activities, and impact of genetic variation.* Pharmacology & Therapeutics, 2013. **138**(1): p. 103-141.

135. Glatt, H., *Sulfotransferases in the bioactivation of xenobiotics.* Chemico-Biological Interactions, 2000. **129**(1-2): p. 141-170.

136. Ritter, J.K., *Roles of glucuronidation and UDP-glucuronosyltransferases in xenobiotic bioactivation reactions.* Chemico-Biological Interactions, 2000. **129**(1-2): p. 171-193.

137. Dresser, M.J., M.K. Leabman, and K.M. Giacomini, *Transporters involved in the elimination of drugs in the kidney: Organic anion transporters and organic cation transporters.* Journal of Pharmaceutical Sciences, 2001. **90**(4): p. 397-421.

138. Taft, D., *Pharmacology: Principles and practice.*, ed. M. Hacker, W. Messer, and K. Bachmann. 2009, Burlington MA 01803, USA.: Elsevier.

139. Benet, L.Z. and P. Ziaamirhosseini, *Basic principles of pharmacokinetics.* Toxicol Pathol, 1995. **23**(2): p. 115-23.

140. Benet, L.Z., *Pharmacokinetic Parameters - Which Are Necessary to Define a Drug Substance.* European Journal of Respiratory Diseases., 1984. **65**: p. 45-61.

141. Gardmark, M., et al., *Interchangeability and predictive performance of empirical tolerance models.* Clinical Pharmacokinetics, 1999. **36**(2): p. 145-167.

142. Ito, K. and J.B. Houston, *Prediction of human drug clearance from in vitro and preclinical data using physiologically based and empirical approaches.* Pharmaceutical Research, 2005. **22**(1): p. 103-112.

143. Shargel, L. and A.B.C. Yu, *Applied Biopharmaceutics & Pharmacokinetics*. 2005, New York: McGraw-Hill.

144. Savic, R.M., et al., *Implementation of a transit compartment model for describing drug absorption in pharmacokinetic studies.* Journal of Pharmacokinetics and Pharmacodynamics, 2007. **34**(5): p. 711-726.

145. Gabrielsson, J. and D. Weiner, *Non-compartmental analysis.* Methods Mol Biol. , 2012. **929**: p. 377-389.

146. Gillespie, W.R., *Noncompartmental versus compartmental modelling in clinical pharmacokinetics.* Clinical Pharmacokinetics, 1991. **20**(4): p. 253-262.

147. Jamei, M., et al., *Population-Based Mechanistic Prediction of Oral Drug Absorption.* Aaps Journal, 2009. **11**(2): p. 225-237.

148. Jones, H.M., et al., *A novel strategy for physiologically based predictions of human pharmacokinetics.* Clinical Pharmacokinetics, 2006. **45**(5): p. 511-542.

149. Bischoff, K.B., *Physiological pharmacokinetics.* Bull Math Biol, 1986. **48**(3-4): p. 309-22.

150. Barrett, J.S., et al., *Physiologically Based Pharmacokinetic (PBPK) Modeling in Children.* Clinical Pharmacology & Therapeutics, 2012. **92**(1): p. 40-49.

151. Miyagi, S. and J. Long-Boyle, *Predicting Pediatric Drug Disposition - Present and Future Directions of Pediatric Physiologically-Based Pharmacokinetics.* . Drug Metabolism Letters, 2015. **9**(2): p. 80-87.

152. Jones, H. and K. Rowland-Yeo, *Basic concepts in physiologically based pharmacokinetic modeling in drug discovery and development.* CPT Pharmacometrics Syst Pharmacol., 2013. **2**(8): p. e63.

153. Whiting, B., A.W. Kelman, and J. Grevel, *Population pharmacokinetics. Theory and clinical application.* Clin Pharmacokinet, 1986. **11**(5): p. 387-401.

154. Samara, E. and R. Granneman, *Role of population pharmacokinetics in drug development - A pharmaceutical industry perspective.* Clinical Pharmacokinetics, 1997. **32**(4): p. 294-312.

155. Dahiya, R., *Application of PBPK models in personalized healthcare.* Journal of Pharmacokinet Exp Ther., 2016. **1**(1): p. e004.

156. Peters, S., *Physiologically-based pharmacokinetic (PBPK) modeling and simulations: principles, methods, and applications in the pharmaceutical industry*. 2012: John Wiley & Sons.

157. Khalil, F. and S. Laer, *Physiologically Based Pharmacokinetic Modeling: Methodology, Applications, and Limitations with a Focus on Its Role in Pediatric Drug Development.* Journal of Biomedicine and Biotechnology, 2011.

158. Conner, T.M., et al., *Physiologically based pharmacokinetic modeling of disposition and drug-drug interactions for valproic acid and divalproex.* European Journal of Pharmaceutical Sciences, 2018. **111**: p. 465-481.

159. Conner, T.M., R.C. Reed, and T. Zhang, *A Physiologically Based Pharmacokinetic Model for Optimally Profiling Lamotrigine Disposition and Drug-Drug Interactions.* European Journal of Drug Metabolism and Pharmacokinetics, 2019. **44**(3): p. 389-408.

160. Huang, W.Z., et al., *Physiologically Based Pharmacokinetic Model of the CYP2D6 Probe Atomoxetine: Extrapolation to Special Populations and Drug-Drug Interactions.* Drug Metabolism and Disposition, 2017. **45**(11): p. 1156-1165.

161. Badhan, R.K.S., R. Gittins, and D. Al Zabit, *The optimization of methadone dosing whilst treating with rifampicin: A pharmacokinetic modeling study.* Drug and Alcohol Dependence, 2019. **200**: p. 168-180.

162. Kneller, L.A., et al., *Influence of CYP2D6 Phenotypes on the Pharmacokinetics of Aripiprazole and Dehydro-Aripiprazole Using a Physiologically Based Pharmacokinetic Approach.* Clinical Pharmacokinetics, 2021.

163. Polasek, T.M., et al., *Predicted metabolic drug clearance with increasing adult age.* British Journal of Clinical Pharmacology, 2013. **75**(4): p. 1019-1028.

164. Li, J., et al., *Prediction of Drug Disposition in Diabetic Patients by Means of a Physiologically Based Pharmacokinetic Model.* Clinical Pharmacokinetics, 2015. **54**(2): p. 179-193.

165. Zhao, P., et al., *Evaluation of Exposure Change of Nonrenally Eliminated Drugs in Patients With Chronic Kidney Disease Using Physiologically Based Pharmacokinetic Modeling and Simulation.* Journal of Clinical Pharmacology, 2012. **52**: p. 91S-108S.

166. Mendes, M.D., et al., *Physiologically-based pharmacokinetic modeling of renally excreted antiretroviral drugs in pregnant women.* British Journal of Clinical Pharmacology, 2015. **80**(5): p. 1031-1041.

167. Alqahtani, S. and A. Kaddoumi, *Development of Physiologically Based Pharmacokinetic/Pharmacodynamic Model for Indomethacin Disposition in Pregnancy.* Plos One, 2015. **10**(10).

168. Walsh, C., et al., *Development of a physiologically based pharmacokinetic model of actinomycin D in children with cancer.* British Journal of Clinical Pharmacology, 2016. **81**(5): p. 989-998.

169. Jogiraju, V.K., et al., *Application of physiologically based pharmacokinetic modeling to predict drug disposition in pregnant populations.* Biopharmaceutics & Drug Disposition, 2017. **38**(7): p. 426-438.

170. Zhou, L., et al., *Physiologically based pharmacokinetic modelling to predict exposure differences in healthy volunteers and subjects with renal impairment: Ceftazidime case study.* Basic & Clinical Pharmacology & Toxicology, 2019. **125**(2): p. 100-107.

171. Zakaria, Z.H., A.Y.Y. Fong, and R.K.S. Badhan, *Clopidogrel Pharmacokinetics in Malaysian Population Groups: The Impact of Inter-Ethnic Variability.* Pharmaceuticals, 2018. **11**(3).

172. Olafuyi, O., M. Coleman, and R.K.S. Badhan, *Development of a paediatric physiologically based pharmacokinetic model to assess the impact of drug-drug interactions in tuberculosis co-infected malaria subjects: A case study with artemether-lumefantrine and the CYP3A4-inducer rifampicin.* European Journal of Pharmaceutical Sciences, 2017. **106**: p. 20-33.

173. Olafuyi, O., M. Coleman, and R.K.S. Badhan, *The application of physiologically based pharmacokinetic modelling to assess the impact of antiretroviral-mediated drug-drug interactions on piperaquine antimalarial therapy during pregnancy.* Biopharmaceutics & Drug Disposition, 2017. **38**(8): p. 464-478.

174. Jamei, M., *Recent Advances in Development and Application of Physiologically-Based Pharmacokinetic (PBPK) Models: a Transition from Academic Curiosity to Regulatory Acceptance.* Curr Pharmacol Rep., 2016. **2**(3): p. 161–169.

175. Li, A.Q., et al., *Development of Guanfacine Extended-Release Dosing Strategies in Children and Adolescents with ADHD Using a Physiologically Based Pharmacokinetic Model to Predict Drug-Drug Interactions with Moderate CYP3A4 Inhibitors or Inducers.* Pediatric Drugs, 2018. **20**(2): p. 181-194.

176. Johnson, T.N., D.S. Zhou, and K.H. Bui, *Development of physiologically based pharmacokinetic model to evaluate the relative systemic exposure to quetiapine after administration of IR and XR formulations to adults, children and adolescents.* Biopharmaceutics & Drug Disposition, 2014. **35**(6): p. 341-352.

177. Yeo, K.R. and T. Johnson, *Advancing Pediatric Drug Development Using Simcyp PBPK*. 2021. p. 1-15.

178. Tangden, T., et al., *The role of infection models and PK/PD modelling for optimising care of critically ill patients with severe infections.* Intensive Care Medicine, 2017. **43**(7): p. 1021-1032.

179. Duong, J.K., et al., *A dosing algorithm for metformin based on the relationships between exposure and renal clearance of metformin in patients with varying degrees of kidney function.* European Journal of Clinical Pharmacology, 2017. **73**(8): p. 981-990.

180. Polasek, T.M., S. Shakib, and A. Rostami-Hodjegan, *Precision dosing in clinical medicine: present and future.* Expert Review of Clinical Pharmacology, 2018. **11**(8): p. 743-746.

181. Vinks, A.A., C. Emoto, and T. Fukuda, *Modeling and Simulation in Pediatric Drug Therapy: Application of Pharmacometrics to Define the Right Dose for Children.* Clinical Pharmacology & Therapeutics, 2015. **98**(3): p. 298-308.

182. Darwich, A.S., et al., *Role of pharmacokinetic modeling and simulation in precision dosing of anticancer drugs.* Translational Cancer Research, 2017. **6**: p. S1512-+.

183. Benavente-Garcia, O. and J. Castillo, *Update on uses and properties of Citrus flavonolds: New findings in anticancer, cardiovascular, and anti-inflammatory activity.* Journal of Agricultural and Food Chemistry, 2008. **56**(15): p. 6185-6205.

184. Jo, S.H., et al., *Hesperetin inhibits neuroinflammation on microglia by suppressing inflammatory cytokines and MAPK pathways.* Archives of Pharmacal Research, 2019. **42**(8): p. 695-703.

185. Roohbakhsh, A., et al., *Neuropharmacological properties and pharmacokinetics of the citrus flavonoids hesperidin and hesperetin - A mini-review.* Life Sciences, 2014. **113**(1-2): p. 1-6.

186. Zhu, X., et al., *Hesperetin ameliorates diabetes-associated anxiety and depression-like behaviors in rats via activating Nrf2/ARE pathway.* Metabolic Brain Disease.

187. Dimpfel, W., *Different anticonvulsive effects of hesperidin and its aglycone hesperetin on electrical activity in the rat hippocampus in-vitro.* Journal of Pharmacy and Pharmacology, 2006. **58**(3): p. 375-379.

188. Zhu, X., et al., *The Antidepressant-Like Effects of Hesperidin in Streptozotocin-Induced Diabetic Rats by Activating Nrf2/ARE/Glyoxalase 1 Pathway.* Frontiers in Pharmacology, 2020. **11**.

189. Zhu, X., et al., *Hesperetin ameliorates diabetes-associated anxiety and depression-like behaviors in rats via activating Nrf2/ARE pathway.* Metabolic Brain Disease, 2021.

190. Wolfram, J., et al., *Hesperetin Liposomes for Cancer Therapy.* Current Drug Delivery, 2016. **13**(5): p. 711-719.

191. Smina, T.P., et al., *Hesperetin exerts apoptotic effect on A431 skin carcinoma cells by regulating mitogen activated protein kinases and cyclins.* Cellular and Molecular Biology, 2015. **61**(6): p. 92-99.

192. Babukumar, S., et al., *Molecular effects of hesperetin, a citrus flavanone on 7,12-dimethylbenz(a)anthracene induced buccal pouch squamous cell carcinoma in golden Syrian hamsters.* Archives of Physiology and Biochemistry, 2017. **123**(4): p. 265-278.

193. Zarebczan, B., et al., *Hesperetin, a potential therapy for carcinoid cancer.* American Journal of Surgery, 2011. **201**(3): p. 329-333.

194. Choi, S.Y., et al., *Correlation between flavonoid content and the NO production inhibitory activity of peel extracts from various citrus fruits.* Biological & Pharmaceutical Bulletin, 2007. **30**(4): p. 772-778.

195. Ye, L., et al., *The citrus flavonone hesperetin inhibits growth of aromatase-expressing MCF-7 tumor in ovariectomized athymic mice.* Journal of Nutritional Biochemistry, 2012. **23**(10): p. 1230-1237.

196. Park, K.I., et al., *Induction of the cell cycle arrest and apoptosis by flavonoids isolated from Korean Citrus aurantium L. in non-small-cell lung cancer cells.* Food Chemistry, 2012. **135**(4): p. 2728-2735.

197. Nagappan, A., et al., *Flavonoids isolated from Citrus platymamma induced G2/M cell cycle arrest and apoptosis in A549 human lung cancer cells.* Oncology Letters, 2016. **12**(2): p. 1394-1402.

198. Sak, K., et al., *Suppression of Taxanes Cytotoxicity by Citrus Flavonoid Hesperetin in PPC-1 Human Prostate Cancer Cells.* Anticancer Research, 2018. **38**(11): p. 6209-6215.

199. Zhang, J.X., et al., *Hesperetin Induces the Apoptosis of Gastric Cancer Cells via Activating Mitochondrial Pathway by Increasing Reactive Oxygen Species.* Digestive Diseases and Sciences, 2015. **60**(10): p. 2985-2995.

200. Shimoda, K. and H. Hamada, *Production of Hesperetin Glycosides by Xanthomonas campestris and Cyclodextrin Glucanotransferase and Their Anti-allergic Activities.* Nutrients, 2010. **2**(2): p. 171-180.

201. Sangpheak, W., et al., *Physical properties and biological activities of hesperetin and naringenin in complex with methylated beta-cyclodextrin.* Beilstein Journal of Organic Chemistry, 2015. **11**: p. 2763-2773.

202. He, Y.J., et al., *Chemical Profiles and Simultaneous Quantification of Aurantii fructus by Use of HPLC-Q-TOF-MS Combined with GC-MS and HPLC Methods.* Molecules, 2018. **23**(9).

203. Brand, W., et al., *Metabolism and transport of the citrus flavonoid hesperetin in Caco-2 cell monolayers.* Drug Metabolism and Disposition, 2008. **36**(9): p. 1794-1802.

204. Usach, I., et al., *Hesperetin induces melanin production in adult human epidermal melanocytes.* Food and Chemical Toxicology, 2015. **80**: p. 80-84.

205. Erlund, I., et al., *Plasma kinetics and urinary excretion of the flavanones naringenin and hesperetin in humans after ingestion of orange juice and grapefruit juice.* Journal of Nutrition, 2001. **131**(2): p. 235-241.

206. Kanaze, F.I., et al., *.Pharmacokinetics of the citrus flavanone aglycones hesperetin and naringenin after single oral administration in human subjects.* European Journal of Clinical Nutrition, 2007. **61**(4): p. 472-477.

207. Manach, C., et al., *Bioavailability in humans of the flavanones hesperidin and narirutin after the ingestion of two doses of orange juice.* European Journal of Clinical Nutrition, 2003. **57**(2): p. 235-242.

208. Ferreira, O., B. Schroder, and S.P. Pinho, *Solubility of Hesperetin in Mixed Solvents.* Journal of Chemical and Engineering Data, 2013. **58**(9): p. 2616-2621.

209. Erlund, I., et al., *Plasma concentrations of the flavonoids hesperetin, naringenin and quercetin in human subjects following their habitual diets, and diets high or low in fruit and vegetables.* European Journal of Clinical Nutrition, 2002. **56**(9): p. 891-898.

210. Shete, G., et al., *Oral Bioavailability and Pharmacodynamic Activity of Hesperetin Nanocrystals Generated Using a Novel Bottom-up Technology.* Molecular Pharmaceutics, 2015. **12**(4): p. 1158-1170.

211. Jones, D.S., *Pharmaceutical disperse systems: ointments, pastes, lotions, gels, and related formulations*, in *Pharmaceutics [electronic resource] : dosage form and design*. 2016, Pharmaceutical Press: London. p. 93-128.

212. Medisca, *Cream base reference chart*, in *pdf*. 2021, Medisca Pharmaceutique Inc.: online.

213. Medisca, *Gel base reference chart*, in *pdf.* 2021, Medisca Pharmaceutique Inc.: online.

214. Dermal, L.L., *Doublebase Gel*, D. Laboratories, Editor. 2006, The electronic medicines compendium (emc): online.

215. Wynne, A., et al., *An effective, cosmetically acceptable, novel hydro-gel emollient for the management of dry skin conditions.* Journal of Dermatological Treatment, 2002. **13**(2): p. 61-66.

216. Lehman, P.A. and S.G. Raney, *In vitro percutaneous absorption of ketoprofen and testosterone: comparison of pluronic lecithin organogel vs. pentravan cream.* International Journal of Pharmaceutical Compounding (IJPC), 2012. **16**(3): p. 248-52.

217. Kirilov, P., et al., *Ex-Vivo percutaneous absorption of enrofloxacin: Comparison of LMOG organogel vs. pentravan cream.* International Journal of Pharmaceutics, 2016. **498**(1-2): p. 170-177.

218. Polonini, H.C., et al., *Transdermal Formulations Containing Human Sexual Steroids: Development and Validation of Methods and in Vitro Drug Release.* Quimica Nova, 2014. **37**(4): p. 720-U208.

219. Polonini, H.C., et al., *Evaluation of percutaneous absorption performance for human female sexual steroids into pentravan cream.* International Journal of Pharmaceutical Compounding (IJPC), 2014. **18**(4): p. 332-40.

220. Ducrotte-Tassel, A., et al., *Detection of Enrofloxacin after Single-Dose Percutaneous Administration in Python Regius, Boa Constrictor Imperator, and Acrantophis Dltmerili.* Journal of Exotic Pet Medicine, 2017. **26**(4): p. 263-269.

221. Ducrotte-Tassel, A., et al., *Ex-vivo permeation of enrofloxacin through shed skin of Python molurus bivittatus, as evaluated with a Franz cell.* Journal of Drug Delivery Science and Technology, 2016. **36**: p. 89-94.

222. Martin, C.J., et al., *Development and Evaluation of Topical Gabapentin Formulations.* Pharmaceutics, 2017. **9**(3).

223. Taofiq, O., et al., *Mushroom ethanolic extracts as cosmeceuticals ingredients: Safety and ex vivo skin permeation studies.* Food and Chemical Toxicology, 2019. **127**: p. 228-236.

224. Wang, X. and L. Black, *Ex Vivo Percutaneous Absorption of Ketamine, Bupivacaine, Diclofenac, Gabapentin, Orphenadrine, and Pentoxyifylline: Comparison of Versatile Cream vs. Reference Cream.* International Journal of Pharmaceutical Compounding (IJPC), 2013. **17**(6): p. 520-5.

225. Medisca, *Stability of Compounded Preparations (buds) Medisca's Vanish-pen™ Cream Base*, in *pdf*. 2021, Medisca,.

226. Tarbox, T., et al., *Development and Validation of HPLC Assay Method for Stability Testing of a High-Potency Diclofenac Sodium Gel*, in *AAPS National Biotechnology Conference.* 2016: Colorado convention center, Denver.

227. Sarkar, A.B., C. Sekar, and R.D. Paruchiri, *Stability studies on naproxen cream.* International Journal of Applied Science and Technology., 2011. **1**(5): p. 28-30.

228. BasuSarkar, A., A. Kandimalla, and R. Dudley, *Ninety day Chemical Stability of Compounded Estradiol, Estrone and Estriol combination and Beyond Use Date.* JPSI., 2012. **1**(5): p. 23-26.

229. Sarkar, A.B., A. Kandimalla, and R. Dudley, *Chemical Stability of Progesterone in Compounded Topical Preparations using PLO Transdermal Cream™ and HRT Cream™ Base over a 90-Day Period at Two Controlled Temperatures* J Steroids Horm Sci., 2013. **4**(2).

230. Bussin, E.R., et al., *Randomised controlled trial evaluating the short-term analgesic effect of topical diclofenac on chronic Achilles tendon pain: a pilot study.* Bmj Open, 2017. **7**(4).

231. Arya, A., et al., *Validation of RP-HPLC Method for Simultaneous Quantification of Bicalutamide and Hesperetin in Polycaprolactone-Bicalutamide-Hesperetin-Chitosan Nanoparticles.* Journal of Chromatographic Science, 2015. **53**(9): p. 1485-1490.

232. Shabir, G.A., *Systematic Strategies in High-Performance Liquid Chromatography Method Development and Validation.* Separation Science and Technology, 2010. **45**(5): p. 670-680.

233. Cordero, J.A., et al., *A comparative study of the transdermal penetration of a series of nonsteroidal antiinflammatory drugs.* Journal of Pharmaceutical Sciences, 1997. **86**(4): p. 503-508.

234. Brown, M.B., et al., *Dermal and transdermal drug delivery systems: Current and future prospects.* Drug Delivery, 2006. **13**(3): p. 175-187.

235. Marwah, M., et al., *Intracellular uptake of EGCG-loaded deformable controlled release liposomes for skin cancer.* Journal of Liposome Research, 2020. **30**(2): p. 136-149.

236. Marwah, M., R.K.S. Badhan, and D. Lowry, *Development of a novel polymer-based carrier for deformable liposomes for the controlled dermal delivery of naringenin.* Journal of Liposome Research.

237. Higuchi, T., *Mechanism of sustained-action medication. Theoretical analysis of rate of release of solid drugs dispersed in solid matrices.* Journal of Pharmaceutical Sciences, 1963. **52**(12): p. 1145-1149.

238. Korsmeyer, R.W., et al., *Mechanisms of Solute Release from Porous Hydrophilic Polymers.* International Journal of Pharmaceutics, 1983. **15**(1): p. 25-35.

239. Peppas, N.A., *Analysis of Fickian and non-Fickian drug release from polymers.* Pharm Acta Helv, 1985. **60**(4): p. 110-1.

240. Siepmann, J. and N.A. Peppas, *Modeling of drug release from delivery systems based on hydroxypropyl methylcellulose (HPMC).* Advanced Drug Delivery Reviews, 2012. **64**: p. 163-174.

241. Smith, E.W., J.M. Haigh, and I. Kanfer, *A Stability-Indicating Hplc Assay with Online Cleanup for Betamethasone 17-Valerate in Topical Dosage Forms.* International Journal of Pharmaceutics, 1985. **27**(2-3): p. 185-192.

242. Lake, O.A., et al., *Analysis of creams. IV. Application of high performance liquid chromatography. Part I.* Pharmaceutisch Weekblad-Scientific Edition, 1983. **5**(1): p. 15-21.

243. Olson, M.C., *Analysis of adrenocortical steroids in pharmaceutical preparations by high-pressure liquid--liquid chromatography.* Journal of Pharmaceutical Sciences, 1973. **62**(12): p. 2001-2007.

244. Huang, Y.B., et al., *The Effect of Component of Cream for Topical Delivery of Hesperetin.* Chemical & Pharmaceutical Bulletin, 2010. **58**(5): p. 611-614.

245. Lukic, M., I. Pantelic, and S.D. Savic, *Towards Optimal pH of the Skin and Topical Formulations: From the Current State of the Art to Tailored Products.* Cosmetics, 2021. **8**(3).

246. Islam, M.T., et al., *Rheological characterization of topical carbomer gels neutralized to different pH.* Pharmaceutical Research, 2004. **21**(7): p. 1192-1199.

247. Ma, X.G., J. Taw, and C.M. Chiang, *Control of drug crystallization in transdermal matrix system.* International Journal of Pharmaceutics, 1996. **142**(1): p. 115-119.

248. Ravula, R., et al., *Formulation optimization of a drug in adhesive transdermal analgesic patch.* Drug Development and Industrial Pharmacy, 2016. **42**(6): p. 862-870.

249. Sharma, P.K., et al., *Solid-State Stability Issues of Drugs in Transdermal Patch Formulations.* Aaps Pharmscitech, 2018. **19**(1): p. 27-35.

250. Kitamura, M., *Controlling factors and mechanism of polymorphic crystallization.* Crystal Growth & Design, 2004. **4**(6): p. 1153-1159.

251. Hadgraft, J. and M.E. Lane, *Drug crystallization - implications for topical and transdermal delivery.* Expert Opinion on Drug Delivery, 2016. **13**(6): p. 817-830.

252. Schnitzler, E., et al., *Application of differential scanning calorimetry (DSC) in the thermal characterization of dexamethasone acetate, excipients and dexamethasone cream.* Ecletica Quimica, 2001. **26**: p. 41-52.

253. Seif, M., et al., *Topical Cream-Based Dosage Forms of the Macrocyclic Drug Delivery Vehicle Cucurbit 6 uril.* Plos One, 2014. **9**(1).

254. Woo, J.O., et al., *Development of a Controlled Release of Salicylic Acid Loaded Stearic Acid-Oleic Acid Nanoparticles in Cream for Topical Delivery.* Scientific World Journal, 2014.

255. Banerjee, S., et al., *Accelerated stability testing of a transdermal patch composed of eserine and pralidoxime chloride for prophylaxis against (+/-)-anatoxin A poisoning.* Journal of Food and Drug Analysis, 2014. **22**(2): p. 264-270.

256. Parhi, R. and S. Padilam, *In vitro permeation and stability studies on developed drug-in-adhesive transdermal patch of simvastatin.* Bulletin of Faculty of Pharmacy, Cairo University., 2018. **56**(2018): p. 26-33.

257. Obluchinskaya, E.D., et al., *Formulation, Optimization and In Vivo Evaluation of Fucoidan-Based Cream with Anti-Inflammatory Properties* Mar. Drugs, 2021. **19**(11).

258. Pandey, M., et al., *Pluronic lecithin organogel as a topical drug delivery system.* Drug Delivery, 2010. **17**(1): p. 38-47.

259. Sahoo, S., et al., *Organogels: Properties and Applications in Drug Delivery.* Designed Monomers and Polymers, 2011. **14**(2): p. 95-108.

260. Rao, K.V.R. and K.P. Devi, *Swelling Controlled-Release Systems - Recent Developments and Applications.* International Journal of Pharmaceutics, 1988. **48**(1-3): p. 1-13.

261. Ritger, P.L. and N.A. Peppas, *A simple equation for description of solute release II. Fickian and anomalous release from swellable devices.* Journal of Controlled Release., 1987. **5**(1): p. 37-42.

262. Mady, F.M., et al., *Formulation and clinical evaluation of silymarin pluronic-lecithin organogels for treatment of atopic dermatitis.* Drug Design Development and Therapy, 2016. **10**: p. 1101-1110.

263. Kashyap, A., A. Das, and A.B. Ahmed, *Formulation and Evaluation of Transdermal Topical Gel of Ibuprofen.* Journal of Drug Delivery and Therapeutics, 2020. **10**(2): p. 20-25.

264. Lee, S.G., et al., *Enhanced topical delivery of tacrolimus by a carbomer hydrogel formulation with transcutol P.* Drug Development and Industrial Pharmacy, 2016. **42**(10): p. 1636-1642.

265. Yen, W.F., et al., *Formulation and Evaluation of Galantamine Gel as Drug Reservoir in Transdermal Patch Delivery System.* ScientificWorldJournal., 2015. **2015**.

266. Pravilovic, R.N., et al., *Comparative Effects of Span 20 and Span 40 on Liposomes Release Properties.* International Journal of Food Engineering, 2017. **13**(12).

267. Nafee, N.A., et al., *Mucoadhesive buccal patches of miconazole nitrate: in vitro/in vivo performance and effect of ageing.* International Journal of Pharmaceutics, 2003. **264**(1-2): p. 1-14.

268. Shruthi, M., et al., *Evaluation of potential hypoglycemic activity of proliposomal gel containing metformin hydrochloride.* Asian J Res Biol Pharm Sci, 2014. **2**(2): p. 77-88.

269. Hwang, B.Y., et al., *In vitro skin permeation of nicotine from proliposomes.* Journal of Controlled Release, 1997. **49**(2-3): p. 177-184.

270. Kumara, B., et al., *Formulation and Evaluation of Proliposomal Gel Containing Repaglinide Using Mannitol as Water Soluble Carrier* Imperial Journal of Interdisciplinary Research, 2016. **2**(5): p. 1777-1786.

271. Kurakula, M., et al., *Formulation and Evaluation of Prednisolone Proliposomal Gel for Effective Topical Pharmacotherapy.* International Journal of Pharmaceutical Sciences and Drug Research, 2012. **4**(1): p. 35-43.

272. Kurakula, M. and N. Pasula, *Piroxicam proliposomal gel: A novel approach for topical delivery.* J Pharm Res, 2012. **5**(3): p. 1755.

273. Singh, N., et al., *Proliposomes: An Approach for the Development of Stable Liposome.* Ars Pharmaceutica, 2019. **60**(4): p. 231-240.

274. Gupta, V., A.K. Barupal, and S. Ramteke, *Formulation Development and in vitro Characterization of Proliposomes for Topical Delivery of Aceclofenac.* Indian Journal of Pharmaceutical Sciences, 2008. **70**(6): p. 768-775.

275. Nishihata, T., et al., *Rat percutaneous transport of diclofenac and influence of hydrogenated soya phospholipids.* Chem Pharm Bull (Tokyo), 1987. **35**(9): p. 3807-12.

276. Ogiso, T., N. Niinaka, and M. Iwaki, *Mechanism for enhancement effect of lipid disperse system on percutaneous absorption.* Journal of Pharmaceutical Sciences, 1996. **85**(1): p. 57-64.

277. Foldvari, M., *In vitro cutaneous and percutaneous delivery and in vivo efficacy of tetracaine from liposomal and conventional vehicles.* Pharm Res, 1994. **11**(11): p. 1593-8.

278. El Maghraby, G.M. and A.C. Williams, *Vesicular systems for delivering conventional small organic molecules and larger macromolecules to and through human skin.* Expert Opinion on Drug Delivery, 2009. **6**(2): p. 149-163.

279. Yu, H.Y. and H.M. Liao, *Triamcinolone permeation from different liposome formulations through rat skin in vitro.* International Journal of Pharmaceutics, 1996. **127**(1): p. 1-7.

280. Schramlova, J., et al., *Electron microscopic demonstration of the penetration of liposomes through skin.* Folia Biologica, 1997. **43**(4): p. 165-169.

281. Yu, J.Y., et al., *Post-Processing Techniques for the Improvement of Liposome Stability.* Pharmaceutics, 2021. **13**(7).

282. Wang, Y.W., et al., *Enhanced Solubility and Bioavailability of Naringenin via Liposomal Nanoformulation: Preparation and In Vitro and In Vivo Evaluations.* Aaps Pharmscitech, 2017. **18**(3): p. 586-594.

283. Modi, S. and B.D. Anderson, *Determination of Drug Release Kinetics from Nanoparticles: Overcoming Pitfalls of the Dynamic Dialysis Method.* Molecular Pharmaceutics, 2013. **10**(8): p. 3076-3089.

284. Heurtault, B., et al., *Physico-chemical stability of colloidal lipid particles.* Biomaterials, 2003. **24**(23): p. 4283-4300.

285. Rashidinejad, A., et al., *Delivery of green tea catechin and epigallocatechin gallate in liposomes incorporated into low-fat hard cheese.* Food Chemistry, 2014. **156**: p. 176-183.

286. Bajgrowicz, M., J. Detyna, and M. Langner, *Liposomes in polymer matrix. Stability of liposomes in PEG 400 and PEG 8000 solutions.* Proceedings Iwbbio 2014: International Work-Conference on Bioinformatics and Biomedical Engineering, Vols 1 and 2, 2014: p. 1313-1322.

287. Natural-Sourcing, *Material safety data sheet, Polysorbate 20.* 2017, Natural Sourcing.: 341 Christian Street, Oxford, CT 06478, USA. .

288. David, S.R.N., R. Rajabalaya, and E.S. Zhia, *Development and In vitro Evaluation of Self-Adhesive Matrix-Type Transdermal Delivery System of Ondansetron Hydrochloride.* Tropical Journal of Pharmaceutical Research, 2015. **14**(2): p. 211-218.

289. Bhalerao, R.A., M.R. Bhalekar, and M.C. Damle, *Formulation and Evaluation Transdermal Patch of Hesperidin.* Journal of Drug Delivery & Therapeutics, 2019. **9**(4): p. 311-317.

290. Kharia, A., A.K. Singhai, and R. Gilhotra, *Formualtion and evalaution of transdermal patch for the treatment of inflammation.* J. Pharm. Sci. & Res., 2020. **12**(6): p. 780-788.

291. Ermawati, D.E., et al., *Study of kinetics model of flavonoid total release in patch of antihypertensive herbs.* Journal of Pharmaceutical Sciences and Community, 2021. **18**(1): p. 7-14.

292. Beharaj, A., et al., *Sustainable polycarbonate adhesives for dry and aqueous conditions with thermoresponsive properties.* Nature Communications, 2019. **10**.

293. Ganti, S.S., et al., *Formulation and evaluation of 4-benzylpiperidine drug-in-adhesive matrix type transdermal patch.* International Journal of Pharmaceutics, 2018. **550**(1-2): p. 71-78.

294. DuPont™. *DuPont™ Liveo™ Silicone Skin Adhesives*. The right adhesive for the right application 2021 [cited 2021 14/12/2021]; Available from: https://www.dupont.com/products/Liveo-silicone-adhesives.html.

295. Toddywala, R.D., et al., *Effect of Physicochemical Properties of Adhesive on the Release, Skin Permeation and Adhesiveness of Adhesive-Type Transdermal Drug Delivery Systems (a-Tdd) Containing Silicone-Based Pressure-Sensitive Adhesives.* International Journal of Pharmaceutics, 1991. **76**(1-2): p. 77-89.

296. Tan, H.S. and W.R. Pfister, *Pressure-sensitive adhesives for transdermal drug delivery systems.* Pharmaceutical Science & Technology Today, 1999. **2**(2): p. 60-69.

297. Bozorg, B.D. and A.K. Banga, *Effect of Different Pressure-Sensitive Adhesives on Performance Parameters of Matrix-Type Transdermal Delivery Systems.* Pharmaceutics, 2020. **12**(3).

298. Kim, J.H., C.H. Lee, and H.K. Choi, *Transdermal delivery of physostigmine: Effects of enhancers and pressure-sensitive adhesives.* Drug Development and Industrial Pharmacy, 2002. **28**(7): p. 833-839.

299. Roy, S.D., et al., *Controlled transdermal delivery of fentanyl: Characterizations of pressure-sensitive adhesives for matrix patch design.* Journal of Pharmaceutical Sciences, 1996. **85**(5): p. 491-495.

300. Liu, J., et al., *Silicone adhesive, a better matrix for tolterodine patches-a research based on in vitro/in vivo studies.* Drug Development and Industrial Pharmacy, 2012. **38**(8): p. 1008-1014.

301. Pfister, W.R., *Silicone Adhesives for Transdermal Drug Delivery Systems.* Drug & Cosmetic Industry, 1988. **143**(4): p. 44-&.

302. Pfister, W.R., J.T. Woodard, and S. Grigoras, *Silicone Adhesives for Transdermal Drug Delivery.* Chemistry in Britain, 1991. **27**(1): p. 43-46.

303. Minghetti, P., et al., *Formulation study of oxybutynin patches.* Pharmaceutical Development and Technology, 2007. **12**(3): p. 239-246.

304. Ulman, K.L. and C.L. Lee, *Drug Permeability of Modified Silicone Polymers .3. Hydrophilic Pressure-Sensitive Adhesives for Transdermal Controlled Drug Release Applications.* Journal of Controlled Release, 1989. **10**(3): p. 273-281.

305. Venkatraman, S. and R. Gale, *Skin adhesives and skin adhesion 1. Transdermal drug delivery systems.* Biomaterials, 1998. **19**(13): p. 1119-1136.

306. Akhtar, N., et al., *Non-invasive drug delivery technology: development and current status of transdermal drug delivery devices, techniques and biomedical applications.* Biomedical Engineering-Biomedizinische Technik, 2020. **65**(3): p. 243-272.

307. Minghetti, P., et al., *Development of local patches containing melilot extract and ex vivo-in vivo evaluation of skin permeation.* European Journal of Pharmaceutical Sciences, 2000. **10**(2): p. 111-117.

308. Rajabalaya, R., et al., *Studies on the effect of plasticizer on in vitro release and ex vivo permeation from Eudragit E 100 based chlorpheniramine maleate matrix type transdermal delivery system.* Journal of Excipients and Food Chemicals, 2010. **1**(2).

309. Elgindy, N. and W. Samy, *Evaluation of the mechanical properties and drug release of cross-linked Eudragit films containing metronidazole.* International Journal of Pharmaceutics, 2009. **376**(1-2): p. 1-6.

310. Hu, Y., et al., *Development of drug-in-adhesive transdermal patch for alpha-asarone and in vivo pharmacokinetics and efficacy evaluation.* Drug Delivery, 2011. **18**(1): p. 84-89.

311. Almazan, E.A., et al., *Design and Evaluation of Losartan Transdermal Patch by Using Solid Microneedles as A Physical Permeation Enhancer.* Iranian Journal of Pharmaceutical Research, 2020. **19**(1): p. 138-152.

312. Lin, S.Y., C.J. Lee, and Y.Y. Lin, *The effect of plasticizers on compatibility, mechanical properties, and adhesion strength of drug-free Eudragit E films.* Pharm Res, 1991. **8**(9): p. 1137-43.

313. Castaneda, P.S., et al., *Design and Evaluation of a Transdermal Patch with Atorvastatin.* Farmacia, 2017. **65**(6): p. 908-916.

314. Zhang, K., et al., *Preparation of Cangai oil transfersomes patches and its in vitro evaluation.* China Journal of Chinese Materia Medica, 2020. **45**(4): p. 854-860.

315. Madan, J., N. Argade, and K. Dua, *Formulation and evaluation of transdermal patches of donepezil.* Recent Patents on Drug Delivery & Formulation, 2015. **9**(1): p. 95-103.

316. Mehdizadeh, A., et al., *Design and in vitro evaluation of new drug-in-adhesive formulations of fentanyl transdermal patches.* Acta Pharm., 2004. **54**(4): p. 301-317.

317. Nguyen, C.A., et al., *Preparation of surfactant-free nanoparticles of methacrylic acid copolymers used for film coating.* Aaps Pharmscitech, 2006. **7**(3).

318. Suksaeree, J., et al., *Rubber Polymers for Transdermal Drug Delivery Systems.* Industrial & Engineering Chemistry Research, 2014. **53**(2): p. 507-513.

319. Gal, A. and A. Nussinovitch, *Plasticizers in the manufacture of novel skin-bioadhesive patches.* International Journal of Pharmaceutics, 2009. **370**(1-2): p. 103-109.

320. Mali, S., et al., *Water sorption and mechanical properties of cassava starch films and their relation to plasticizing effect.* Carbohydrate Polymers, 2005. **60**(3): p. 283-289.

321. Rahman, M. and C.S. Brazel, *The plasticizer market: an assessment of traditional plasticizers and research trends to meet new challenges.* Progress in Polymer Science, 2004. **29**(12): p. 1223-1248.

322. Cheng, L.H., A. Abd Karim, and C.C. Seow, *Effects of water-glycerol and water-sorbitol interactions on the physical properties of konjac glucomannan films.* Journal of Food Science, 2006. **71**(2): p. E62-E67.

323. Bergo, P.V.A., et al., *Physical properties of edible films based on cassava starch as affected by the plasticizer concentration.* Packaging Technology and Science, 2008. **21**(2): p. 85-89.

324. Suyatma, N.E., L. Tighzert, and A. Copinet, *Effects of hydrophilic plasticizers on mechanical, thermal, and surface properties of chitosan films.* Journal of Agricultural and Food Chemistry, 2005. **53**(10): p. 3950-3957.

325. Bergo, P. and P.J.A. Sobral, *Effects of plasticizer on physical properties of pigskin gelatin films.* Food Hydrocolloids, 2007. **21**(8): p. 1285-1289.

326. Audic, J.L. and B. Chaufer, *Influence of plasticizers and crosslinking on the properties of biodegradable films made from sodium caseinate.* European Polymer Journal, 2005. **41**(8): p. 1934-1942.

327. Galietta, G., et al., *Mechanical and thermomechanical properties of films based on whey proteins as affected by plasticizer and crosslinking agents.* Journal of Dairy Science, 1998. **81**(12): p. 3123-3130.

328. Jangchud, A. and M.S. Chinnan, *Properties of peanut protein film: Sorption isotherm and plasticizer effect.* Food Science and Technology-Lebensmittel-Wissenschaft & Technologie, 1999. **32**(2): p. 89-94.

329. Sobral, P.J.A., E.S. Monterrey-Q, and A. Habitante, *Glass transition study of Nile Tilapia myofibrillar protein films plasticized by glycerin and water.* Journal of Thermal Analysis and Calorimetry, 2002. **67**(2): p. 499-504.

330. Kim, S.J. and Z. Ustunol, *Solubility and moisture sorption isotherms of whey-protein-based edible films as influenced by lipid and plasticizer incorporation.* Journal of Agricultural and Food Chemistry, 2001. **49**(9): p. 4388-4391.

331. Zhang, Y.C. and J.H. Han, *Mechanical and thermal characteristics of pea starch films plasticized with monosaccharides and polyols.* Journal of Food Science, 2006. **71**(2): p. E109-E118.

332. Moore, G.R., et al., *Influence of the glycerol concentration on some physical properties of feather keratin films.* Food Hydrocolloids, 2006. **20**(7): p. 975-982.

333. Thomazine, M., R.A. Carvalho, and P.J.A. Sobral, *Physical properties of gelatin films plasticized by blends of glycerol and sorbitol.* Journal of Food Science, 2005. **70**(3): p. E172-E176.

334. Talja, R.A., et al., *Effect of various polyols and polyol contents on physical and mechanical properties of potato starch-based films.* Carbohydrate Polymers, 2007. **67**(3): p. 288-295.

335. Muller, C.M.O., F. Yamashita, and J.B. Laurindo, *Evaluation of the effects of glycerol and sorbitol concentration and water activity on the water barrier properties of cassava starch films through a solubility approach.* Carbohydrate Polymers, 2008. **72**(1): p. 82-87.

336. Fishman, M.L., et al., *Extrusion of pectin/starch blends plasticized with glycerol.* Carbohydrate Polymers, 2000. **41**(4): p. 317-325.

337. Colla, E., P.J.A. Sobral, and F.C. Menegalli, *Amaranthus cruentus flour edible films: Influence of stearic acid addition, plasticizer concentration, and emulsion stirring speed on water vapor permeability and mechanical properties.* Journal of Agricultural and Food Chemistry, 2006. **54**(18): p. 6645-6653.

338. Galdeano, M.C., et al., *Effects of production process and plasticizers on stability of films and sheets of oat starch.* Materials Science & Engineering C-Biomimetic and Supramolecular Systems, 2009. **29**(2): p. 492-498.

339. Galdeano, M.C., et al., *Effects of plasticizers on the properties of oat starch films.* Materials Science & Engineering C-Biomimetic and Supramolecular Systems, 2009. **29**(2): p. 532-538.

340. Yu, L.Y., et al., *Glycerol-Filled Silicone Adhesive Patches with Excellent Sun Protection.* Macromolecular Materials and Engineering, 2021. **306**(5).

341. Cuq, B., et al., *Selected functional properties of fish myofibrillar protein-based films as affected by hydrophilic plasticizers.* Journal of Agricultural and Food Chemistry, 1997. **45**(3): p. 622-626.

342. Karbowiak, T., et al., *Effect of plasticizers (water and glycerol) on the diffusion of a small molecule in iota-carrageenan biopolymer films for edible coating application.* Biomacromolecules, 2006. **7**(6): p. 2011-2019.

343. Kristo, E. and C.G. Biliaderis, *Water sorption and thermo-mechanical properties of water/sorbitol-plasticized composite biopolymer films: Caseinate-pullulan bilayers and blends.* Food Hydrocolloids, 2006. **20**(7): p. 1057-1071.

344. da Silva, M.A., A.C.K. Bierhalz, and T.G. Kieckbusch, *Alginate and pectin composite films crosslinked with Ca2+ ions: Effect of the plasticizer concentration.* Carbohydrate Polymers, 2009. **77**(4): p. 736-742.

345. Sartori, T., et al., *Biodegradable pressure sensitive adhesives produced from vital wheat gluten: Effect of glycerol as plasticizer.* Colloids and Surfaces a-Physicochemical and Engineering Aspects, 2019. **560**: p. 42-49.

346. Pratama, F.N. and U.C.A. Nurahmanto, *The effect of glycerin as penetration enhancer in a ketoprofen solid preparation–patch on in vitro penetration study through rat skin.* Annals of Tropical Medicine and Public Health, 2020. **23**(3): p. 71-83.

347. Idrees, A., et al., *In Vitro Evaluation of Transdermal Patches of Flurbiprofen with Ethyl Cellulose.* Acta Poloniae Pharmaceutica, 2014. **71**(2): p. 287-295.

348. J, P.H., et al., *Permeability studies of anti hypertensive drug amlodipine besilate for transdermal delivery.* Asian Journal of Pharmaceutical and Clinical Research, 2010. **3**(1): p. 31-34.

349. Sarpotdar, P.P. and J.L. Zatz, *Evaluation of penetration enhancement of lidocaine by nonionic surfactants through hairless mouse skin in vitro.* Journal of Pharmaceutical Sciences, 1986. **75**(2): p. 176-181.

350. Sarpotdar, P.P. and J.L. Zatz, *Percutaneous Absorption Enhancement by Nonionic Surfactants.* Drug Development and Industrial Pharmacy, 1987. **13**(1): p. 15-37.

351. Shahi, V. and J.L. Zatz, *Effect of formulation factors on penetration of hydrocortisone through mouse skin.* Journal of Pharmaceutical Sciences, 1978. **67**(6): p. 789-792.

352. Aungst, B.J., N.J. Rogers, and E. Shefter, *Enhancement of naloxone penetration through human skin in vitro using fatty acids, fatty alcohols, surfactants, sulfoxides and amides.* International Journal of Pharmaceutics, 1986. **33**(1-3): p. 225-234.

353. Lopez, A., et al., *Comparative enhancer effects of Span (R) 20 with Tween (R) 20 and Azone (R) on the in vitro percutaneous penetration of compounds with different lipophilicities.* International Journal of Pharmaceutics, 2000. **202**(1-2): p. 133-140.

354. Ridout, G., et al., *The effects of zwitterionic surfactants on skin barrier function.* Fundam Appl Toxicol, 1991. **16**(1): p. 41-50.

355. David, S.R., et al., *Development of controlled release silicone adhesive-based mupirocin patch demonstrates antibacterial activity on live rat skin against Staphylococcus aureus.* Drug Design Development and Therapy, 2018. **12**: p. 481-494.

356. Rao, P.R. and P.V. Diwan, *Formulation and in vitro evaluation of polymeric films of diltiazem hydrochloride and indomethacin for transdermal administration.* Drug Development and Industrial Pharmacy, 1998. **24**(4): p. 327-336.

357. Swain, K., et al., *Feasibility Assessment of Ondansetron Hydrochloride Transdermal Systems: Physicochemical Characterization and In vitro Permeation Studies.* Latin American Journal of Pharmacy, 2009. **28**(5): p. 706-714.

358. Jain, P. and A.K. Banga, *Inhibition of crystallization in drug-in-adhesive-type transdermal patches.* International Journal of Pharmaceutics, 2010. **394**(1-2): p. 68-74.

359. Prajapati, S.T., C.G. Patel, and C.N. Patel, *Formulation and Evaluation of Transdermal Patch of Repaglinide.* ISRN Pharmaceutics, 2011. **2011**: p. 651909.

360. Mita, S.R., P. Husni, and D. Setiyowati, *In vitro Permeation Study of Ketoprofen Patch with Combination of Ethylcellulose and Polyvynil Pyrrolidone as Matrix Polymers.* Journal of Young Pharmacists, 2018. **10**(2): p. S101-S105.

361. Feldstein, M.M., et al., *Hydrophilic polymeric matrices for enhanced transdermal drug delivery.* International Journal of Pharmaceutics, 1996. **131**(2): p. 229-242.

362. Chaudhuri, K.R., *Crystallisation within transdermal rotigotine patch: is there cause for concern?* Expert Opinion on Drug Delivery, 2008. **5**(11): p. 1169-1171.

363. Puri, A., et al., *Development of a Transdermal Delivery System for Tenofovir Alafenamide, a Prodrug of Tenofovir with Potent Antiviral Activity Against HIV and HBV.* Pharmaceutics, 2019. **11**(4).

364. Costa, R., et al., *On the Development of a Cutaneous Flavonoid Delivery System: Advances and Limitations.* Antioxidants, 2021. **10**(9).

365. Yang, B.Y., et al., *Nanoformulations to Enhance the Bioavailability and Physiological Functions of Polyphenols.* Molecules, 2020. **25**(20).

366. Shinde, A.J., A.L. Shinde, and H.N. More, *Design and evaluation transdermal drug delivery system of gliclazide.* Asian Journal of Pharmaceutics, 2010. **4**(2): p. 121-129.

367. Schalau II, G.K., et al., *Silicone Adhesives in Medical Applications.*, in *Applied Adhesive Bonding in Science and Technology.* 2017, Intechopen.

368. White, J.R., *Polymer ageing: physics, chemistry or engineering? Time to reflect.* Comptes Rendus Chimie, 2006. **9**(11-12): p. 1396-1408.

369. Kucera, S., et al., *Influence of an Acrylic Polymer Blend on the Physical Stability of Film-Coated Theophylline Pellets.* Aaps Pharmscitech, 2009. **10**(3): p. 864-871.

370. Gutierrezrocca, J.C. and J.W. Mcginity, *Influence of Aging on the Physical-Mechanical Properties of Acrylic Resin Films Cast from Aqueous Dispersions and Organic Solutions.* Drug Development and Industrial Pharmacy, 1993. **19**(3): p. 315-332.

371. Zheng, W.J., D. Sauer, and J.W. McGinity, *Influence of hydroxyethylcellulose on the drug release properties of theophylline pellets coated with Eudragit (R) RS 30 D.* European Journal of Pharmaceutics and Biopharmaceutics, 2005. **59**(1): p. 147-154.

372. Suksaeree, J., P. Siripornpinyo, and S. Chaiprasit, *Formulation, Characterization, and In Vitro Evaluation of Transdermal Patches for Inhibiting Crystallization of Mefenamic Acid.* Journal of Drug Delivery, 2017. **2017**.

373. Masaro, L. and X.X. Zhu, *Physical models of diffusion for polymer solutions, gels and solids.* Progress in Polymer Science, 1999. **24**(5): p. 731-775.

374. Lee, P.I., *Kinetics of drug release from hydrogel matrices.* Journal of Controlled Release, 1985. **2**: p. 277-288.

375. Peppas, N.A. and J.J. Sahlin, *A Simple Equation for the Description of Solute Release .3. Coupling of Diffusion and Relaxation.* International Journal of Pharmaceutics, 1989. **57**(2): p. 169-172.

376. Tsai, Y.H., et al., *In vitro permeation and in vivo whitening effect of topical hesperetin microemulsion delivery system.* International Journal of Pharmaceutics, 2010. **388**(1-2): p. 257-262.

377. Hiemke, C. and S. Härtter, *Pharmacokinetics of selective serotonin reuptake inhibitors.* Pharmacology & Therapeutics, 2000. **85**(1): p. 11-28.

378. Feighner, J.P., *Mechanism of action of antidepressant medications.* Journal of Clinical Psychiatry, 1999. **60**: p. 4-13.

379. Ferguson, J.M., *SSRI Antidepressant Medications: Adverse Effects and Tolerability.* Prim Care Companion J Clin Psychiatry, 2001. **3**(1): p. 22–27.

380. Westin, A.A., et al., *Selective serotonin reuptake inhibitors and venlafaxine in pregnancy: Changes in drug disposition.* PLoS One, 2017. **12**(7): p. e0181082.

381. Jornil, J., et al., *Identification of cytochrome P450 isoforms involved in the metabolism of paroxetine and estimation of their importance for human paroxetine metabolism using a population-based simulator.* Drug Metab Dispos, 2010. **38**(3): p. 376-85.

382. Bertelsen, K.M., et al., *Apparent mechanism-based inhibition of human CYP2D6 in vitro by paroxetine: comparison with fluoxetine and quinidine.* Drug Metab Dispos, 2003. **31**(3): p. 289-93.

383. Zhao, S.X., et al., *NADPH-dependent covalent binding of [3H]paroxetine to human liver microsomes and S-9 fractions: identification of an electrophilic quinone metabolite of paroxetine.* Chem Res Toxicol, 2007. **20**(11): p. 1649-57.

384. Sindrup, S.H., et al., *The relationship between paroxetine and the sparteine oxidation polymorphism.* Clin Pharmacol Ther, 1992. **51**(3): p. 278-87.

385. Harten, V.J., *Clinical pharmacokinetics of selective serotonin reuptake inhibitors.* Clinical Pharmacokinetics, 1993. **24**(3): p. 203-220.

386. Kaye, C., et al., *A review of the metabolism and pharmacokinetics of paroxetine in man.* Acta Psychiatrica Scandinavica, 1989. **80**(S350): p. 60-75.

387. Lund, J., et al., *Paroxetine: pharmacokinetics, tolerance and depletion of blood 5-HT in man.* Acta Pharmacol Toxicol (Copenh), 1979. **44**(4): p. 289-95.

388. Sindrup, S.H., K. Brosen, and L.F. Gram, *Pharmacokinetics of the selective serotonin reuptake inhibitor paroxetine: nonlinearity and relation to the sparteine oxidation polymorphism.* Clin Pharmacol Ther, 1992. **51**(3): p. 288-95.

389. Buchanan, M.L., et al., *Clonidine pharmacokinetics in pregnancy.* Drug Metab Dispos, 2009. **37**(4): p. 702-5.

390. Claessens, A.J., et al., *CYP2D6 mediates 4-hydroxylation of clonidine in vitro: implication for pregnancy-induced changes in clonidine clearance.* Drug Metab Dispos, 2010. **38**(9): p. 1393-6.

391. Högstedt, S., et al., *Pregnancy-induced increase in metoprolol metabolism.* Clin Pharmacol Ther, 1985. **37**(6): p. 688-92.

392. Tracy, T.S., et al., *Temporal changes in drug metabolism (CYP1A2, CYP2D6 and CYP3A Activity) during pregnancy.* Am J Obstet Gynecol, 2005. **192**(2): p. 633-9.

393. Wadelius, M., et al., *Induction of CYP2D6 in pregnancy.* Clin Pharmacol Ther, 1997. **62**(4): p. 400-7.

394. Holinka, C.F., et al., *Estetrol: a unique steroid in human pregnancy.* 2008. **110**(1-2): p. 138-143.

395. Cunningham, F., et al., *Williams obstetrics, 24e*. 2014: Mcgraw-hill.

396. Jeong, H., et al., *Regulation of UDP-glucuronosyltransferase (UGT) 1A1 by progesterone and its impact on labetalol elimination.* Xenobiotica, 2008. **38**(1): p. 62-75.

397. Chen, H., et al., *Up-regulation of UDP-glucuronosyltransferase (UGT) 1A4 by 17beta-estradiol: a potential mechanism of increased lamotrigine elimination in pregnancy.* Drug Metab Dispos, 2009. **37**(9): p. 1841-7.

398. Vandenberg, S.J., *Comparing SSRIs: From chemistry to clinical choice.* Human Psychopharmacology-Clinical and Experimental, 1995. **10**: p. S199-S209.

399. Tomita, T., et al., *Therapeutic reference range for plasma concentrations of paroxetine in patients with major depressive disorders.* Ther Drug Monit, 2014. **36**(4): p. 480-5.

400. Hiemke, C., et al., *Consensus Guidelines for Therapeutic Drug Monitoring in Neuropsychopharmacology: Update 2017.* Pharmacopsychiatry, 2018. **51**(01/02): p. 9-62.

401. Schulz, M., et al., *Therapeutic and toxic blood concentrations of nearly 1,000 drugs and other xenobiotics.* Crit Care, 2012. **16**(4): p. R136.

402. Lewis, R., P.M. Kemp, and R.D. Johnson, *Distribution of Paroxetine in Postmortem Fluids and Tissues*. 2015, Federal Aviation Administration: Washington, USA.

403. Nevels, R.M., S.T. Gontkovsky, and B.E. Williams, *Paroxetine-The Antidepressant from Hell? Probably Not, But Caution Required.* Psychopharmacol Bull, 2016. **46**(1): p. 77-104.

404. Kim, J.J. and R.K. Silver, *Perinatal suicide associated with depression diagnosis and absence of active treatment in 15-year UK national inquiry.* Evid Based Ment Health, 2016. **19**(4): p. 122.

405. McAllister-Williams, R.H., et al., *British Association for Psychopharmacology consensus guidance on the use of psychotropic medication preconception, in pregnancy and postpartum 2017.* Journal of Psychopharmacology, 2017. **31**(5): p. 519-552.

406. Keks, N., J. Hope, and S. Keogh, *Switching and stopping antidepressants.* Australian prescriber, 2016. **39**(3): p. 76-83.

407. Bateman, D.N., et al., *TOXBASE: poisons information on the internet.* Emerg Med J, 2002. **19**(1): p. 31-4.

408. Briggs, G.G., R.K. Freeman, and S.J. Yaffe, *Drugs in pregnancy and lactation: a reference guide to fetal and neonatal risk*. 11 ed. 2017: Wolters Kluwer.

409. Service, U.T.I. *Use of paroxetine in pregnancy*. 2017 [cited 2019 25th November]; Available from: https://www.medicinesinpregnancy.org/bumps/monographs/USE-OF-PAROXETINE-IN-PREGNANCY/.

410. Kieler, H., et al., *Selective serotonin reuptake inhibitors during pregnancy and risk of persistent pulmonary hypertension in the newborn: population based cohort study from the five Nordic countries.* BMJ, 2012. **344**: p. d8012.

411. Huybrechts, K.F., et al., *Antidepressant use late in pregnancy and risk of persistent pulmonary hypertension of the newborn.* JAMA, 2015. **313**(21): p. 2142-51.

412. National Institute for Health and Care Excellence. *Antenatal and postnatal mental health: clinical management and service guidance (Clinical guideline [CG192])*. 2018 [cited 2019 May]; Available from: https://www.nice.org.uk/guidance/cg192/chapter/1-Recommendations.

413. De Sousa Mendes, M., et al., *Physiologically-based pharmacokinetic modeling of renally excreted antiretroviral drugs in pregnant women.* Br J Clin Pharmacol, 2015. **80**(5): p. 1031-41.

414. Jogiraju, V.K., et al., *Application of physiologically based pharmacokinetic modeling to predict drug disposition in pregnant populations.* Biopharm Drug Dispos, 2017. **38**(7): p. 426-438.

415. Abduljalil, K., et al., *Anatomical, physiological and metabolic changes with gestational age during normal pregnancy: a database for parameters required in physiologically based pharmacokinetic modelling.* Clin Pharmacokinet, 2012. **51**(6): p. 365-96.

416. Lu, G., et al., *Physiologically-based pharmacokinetic (PBPK) models for assessing the kinetics of xenobiotics during pregnancy: achievements and shortcomings.* Curr Drug Metab, 2012. **13**(6): p. 695-720.

417. Olafuyi, O. and R.K.S. Badhan, *Dose Optimization of Chloroquine by Pharmacokinetic Modeling During Pregnancy for the Treatment of Zika Virus Infection.* J Pharm Sci, 2019. **108**(1): p. 661-673.

418. Massaroti, P., et al., *Validation of a selective method for determination of paroxetine in human plasma by LC-MS/MS.* J Pharm Pharm Sci, 2005. **8**(2): p. 340-7.

419. Segura, M., et al., *Quantitative determination of paroxetine and its 4-hydroxy-3-methoxy metabolite in plasma by high-performance liquid chromatography/electrospray ion trap mass spectrometry: application to pharmacokinetic studies.* Rapid Commun Mass Spectrom, 2003. **17**(13): p. 1455-61.

420. Yasui-Furukori, N., et al., *Terbinafine increases the plasma concentration of paroxetine after a single oral administration of paroxetine in healthy subjects.* Eur J Clin Pharmacol, 2007. **63**(1): p. 51-6.

421. López-Calull, C. and N. Dominguez, *Determination of paroxetine in plasma by high-performance liquid chromatography for bioequivalence studies.* J Chromatogr B Biomed Sci Appl, 1999. **724**(2): p. 393-8.

422. Segura, M., et al., *Contribution of cytochrome P450 2D6 to 3,4-methylenedioxymethamphetamine disposition in humans - Use of paroxetine as a metabolic inhibitor probe.* Clinical Pharmacokinetics, 2005. **44**(6): p. 649-660.

423. Ververs, F.F., et al., *Effect of cytochrome P450 2D6 genotype on maternal paroxetine plasma concentrations during pregnancy.* Clin Pharmacokinet, 2009. **48**(10): p. 677-83.

424. Edginton, A.N., W. Schmitt, and S. Willmann, *Development and evaluation of a generic physiologically based pharmacokinetic model for children.* Clin Pharmacokinet, 2006. **45**(10): p. 1013-34.

425. Ginsberg, G., et al., *Physiologically based pharmacokinetic (PBPK) modeling of caffeine and theophylline in neonates and adults: implications for assessing children's risks from environmental agents.* J Toxicol Environ Health A, 2004. **67**(4): p. 297-329.

426. Parrott, N., et al., *Development of a physiologically based model for oseltamivir and simulation of pharmacokinetics in neonates and infants.* Clin Pharmacokinet, 2011. **50**(9): p. 613-23.

427. U.S. Food and Drug Administration. *Summary Minutes of the Advisory Committee for Pharmaceutical Science and Clinical Pharmacology*. 2012 [cited 2018 29th May]; Available from: https://wayback.archive-it.org/7993/20170403224110/https://www.fda.gov/AdvisoryCommittees/CommitteesMeetingMaterials/Drugs/AdvisoryCommitteeforPharmaceuticalScienceandClinicalPharmacology/ucm286697.htm.

428. Ford, D.E. and T.P. Erlinger, *Depression and C-reactive protein in US adults: data from the Third National Health and Nutrition Examination Survey.* Archives of internal medicine, 2004. **164**(9): p. 1010-1014.

429. Cyranowski, J.M., et al., *Adolescent onset of the gender difference in lifetime rates of major depression: a theoretical model.* Archives of general psychiatry, 2000. **57**(1): p. 21-27.

430. World Health Organization, *The global burden of disease: 2004 update.* 2008.

431. Gaynes, B.N., et al., *Perinatal depression: prevalence, screening accuracy, and screening outcomes.* Evid Rep Technol Assess (Summ), 2005(119): p. 1-8.

432. Vesga-Lopez, O., et al., *Psychiatric disorders in pregnant and postpartum women in the United States.* Arch Gen Psychiatry, 2008. **65**(7): p. 805-15.

433. Isoherranen, N. and K.E. Thummel, *Drug metabolism and transport during pregnancy: how does drug disposition change during pregnancy and what are the mechanisms that cause such changes?* Drug Metab Dispos, 2013. **41**(2): p. 256-62.

434. Ke, A.B., R. Greupink, and K. Abduljalil, *Drug Dosing in Pregnant Women: Challenges and Opportunities in Using Physiologically Based Pharmacokinetic Modeling and Simulations.* CPT Pharmacometrics Syst Pharmacol, 2018. **7**(2): p. 103-110.

435. Westin, A.A., et al., *Treatment With Antipsychotics in Pregnancy: Changes in Drug Disposition.* Clinical pharmacology and therapeutics, 2018. **103**(3): p. 477-484.

436. Feghali, M., R. Venkataramanan, and S. Caritis, *Pharmacokinetics of drugs in pregnancy.* Seminars in perinatology, 2015. **39**(7): p. 512-519.

437. Fatemi, S.H. and P.J. Clayton, *The Medical Basis of Psychiatry*, Springer, Editor. 2016, Springer.

438. Mulder, H., et al., *The association between cytochrome P450 2D6 genotype and prescription patterns of antipsychotic and antidepressant drugs in hospitalized psychiatric patients: a retrospective follow-up study.* Journal of clinical psychopharmacology, 2005. **25**(2): p. 188-191.

439. Rau, T., et al., *CYP2D6 genotype: impact on adverse effects and nonresponse during treatment with antidepressants—a pilot study.* Clinical Pharmacology & Therapeutics, 2004. **75**(5): p. 386-393.

440. Bérard, A., et al., *Association between CYP2D6 Genotypes and the Risk of Antidepressant Discontinuation, Dosage Modification and the Occurrence of Maternal Depression during Pregnancy.* Frontiers in pharmacology, 2017. **8**: p. 402-402.

441. Nagai, M., et al., *Characterization of Transplacental Transfer of Paroxetine in Perfused Human Placenta: Development of a Pharmacokinetic Model to Evaluate Tapered Dosing.* Drug Metabolism and Disposition, 2013. **41**(12): p. 2124-2132.

442. Parry, E., R. Shields, and A.C. Turnbull, *Transit time in the small intestine in pregnancy.* J Obstet Gynaecol Br Commonw, 1970. **77**(10): p. 900-1.

443. Cappell, M.S. and A. Garcia, *Gastric and duodenal ulcers during pregnancy.* Gastroenterol Clin North Am, 1998. **27**(1): p. 169-95.

444. O'Sullivan, G.M. and R.E. Bullingham, *The assessment of gastric acidity and antacid effect in pregnant women by a non-invasive radiotelemetry technique.* Br J Obstet Gynaecol, 1984. **91**(10): p. 973-8.

445. Catterson, M.L. and S.H. Preskorn, *Pharmacokinetics of selective serotonin reuptake inhibitors: clinical relevance.* Pharmacol Toxicol, 1996. **78**(4): p. 203-8.

446. Greb, W., et al., *Absorption of paroxetine under various dietary conditions and following antacid intake.* Acta Psychiatrica Scandinavica, 1989. **80**(S350): p. 99-101.

447. Vigod, S.N., C.A. Wilson, and L.M. Howard, *Depression in pregnancy.* BMJ, 2016. **352**: p. i1547.

448. Fisher, J., et al., *Prevalence and determinants of common perinatal mental disorders in women in low- and lower-middle-income countries: a systematic review.* Bulletin of the World Health Organization, 2012. **90**(2): p. 139G-149G.

449. Byatt, N., et al., *Mental health care use in relation to depressive symptoms among pregnant women in the USA.* Arch Womens Ment Health, 2016. **19**(1): p. 187-91.

450. Geier, M.L., et al., *Detection and treatment rates for perinatal depression in a state Medicaid population.* CNS Spectr, 2015. **20**(1): p. 11-9.

451. Bérard, A., J.-P. Zhao, and O. Sheehy, *Antidepressant use during pregnancy and the risk of major congenital malformations in a cohort of depressed pregnant women: an updated analysis of the Quebec Pregnancy Cohort.* BMJ open, 2017. **7**(1): p. e013372-e013372.

452. Zakiyah, N., et al., *Antidepressant use during pregnancy and the risk of developing gestational hypertension: a retrospective cohort study.* BMC Pregnancy Childbirth, 2018. **18**(1): p. 187.

453. Nordeng, H., et al., *Pregnancy outcome after exposure to antidepressants and the role of maternal depression: results from the Norwegian Mother and Child Cohort Study.* Journal of clinical psychopharmacology, 2012. **32**(2): p. 186-194.

454. Colvin, L., et al., *Dispensing patterns and pregnancy outcomes for women dispensed selective serotonin reuptake inhibitors in pregnancy.* Birth Defects Research Part A: Clinical and Molecular Teratology, 2011. **91**(3): p. 142-152.

455. Reis, M. and B. Kallen, *Delivery outcome after maternal use of antidepressant drugs in pregnancy: an update using Swedish data.* Psychological Medicine, 2010. **40**(10): p. 1723-1733.

456. Oberlander, T.F., et al., *Major congenital malformations following prenatal exposure to serotonin reuptake inhibitors and benzodiazepines using population-based health data.* Birth Defects Research Part B: Developmental and Reproductive Toxicology, 2008. **83**(1): p. 68-76.

457. Ramos, E., et al., *Prevalence and predictors of antidepressant use in a cohort of pregnant women.* BJOG: An International Journal of Obstetrics & Gynaecology, 2007. **114**(9): p. 1055-1064.

458. Byatt, N., K.M. Deligiannidis, and M.P. Freeman, *Antidepressant use in pregnancy: a critical review focused on risks and controversies.* Acta Psychiatrica Scandinavica, 2013. **127**(2): p. 94-114.

459. Saiz-Rodríguez, M., et al., *Effect of Polymorphisms on the Pharmacokinetics, Pharmacodynamics and Safety of Sertraline in Healthy Volunteers.* Basic Clin Pharmacol Toxicol, 2018. **122**(5): p. 501-511.

460. Obach, R.S., L.M. Cox, and L.M. Tremaine, *Sertraline is metabolized by multiple cytochrome P450 enzymes, monoamine oxidases, and glucuronyl transferases in human: an in vitro study.* Drug Metab Dispos, 2005. **33**(2): p. 262-70.

461. Alfaro, C.L., et al., *CYP2D6 inhibition by fluoxetine, paroxetine, sertraline, and venlafaxine in a crossover study: intraindividual variability and plasma concentration correlations.* J Clin Pharmacol, 2000. **40**(1): p. 58-66.

462. Lam, Y.W., et al., *CYP2D6 inhibition by selective serotonin reuptake inhibitors: analysis of achievable steady-state plasma concentrations and the effect of ultrarapid metabolism at CYP2D6.* Pharmacotherapy, 2002. **22**(8): p. 1001-6.

463. Preskorn, S.H., *Pharmacokinetics of Antidepressants - Why and How They Are Relevant to Treatment.* Journal of Clinical Psychiatry, 1993. **54**(9): p. 14-34.

464. Ronfeld, R.A., L.M. Tremaine, and K.D. Wilner, *Pharmacokinetics of sertraline and its N-demethyl metabolite in elderly and young male and female volunteers.* Clinical Pharmacokinetics, 1997. **32**: p. 22-30.

465. Koh, K.H., et al., *Estradiol induces cytochrome P450 2B6 expression at high concentrations: implication in estrogen-mediated gene regulation in pregnancy.* Biochemical pharmacology, 2012. **84**(1): p. 93-103.

466. Högstedt, S., et al., *Pregnancy-induced increase in metoprolol metabolism.* Clinical Pharmacology & Therapeutics, 1985. **37**(6): p. 688-692.

467. Högstedt, S., B. Lindberg, and A. Rane, *Increased oral clearance of metoprolol in pregnancy.* European journal of clinical pharmacology, 1983. **24**(2): p. 217-220.

468. Prevost, R.R., et al., *Oral nifedipine pharmacokinetics in pregnancy-induced hypertension.* Pharmacotherapy, 1992. **12**(3): p. 174-7.

469. Kosel, B.W., et al., *Pharmacokinetics of nelfinavir and indinavir in HIV-1-infected pregnant women.* Aids, 2003. **17**(8): p. 1195-1199.

470. McGready, R., et al., *The pharmacokinetics of atovaquone and proguanil in pregnant women with acute falciparum malaria.* European journal of clinical pharmacology, 2003. **59**(7): p. 545-552.

471. Ward, S., et al., *The activation of the biguanide antimalarial proguanil co-segregates with the mephenytoin oxidation polymorphism-a panel study.* British journal of clinical pharmacology, 1991. **31**(6): p. 689-692.

472. McGready, R., et al., *Pregnancy and use of oral contraceptives reduces the biotransformation of proguanil to cycloguanil.* European journal of clinical pharmacology, 2003. **59**(7): p. 553-557.

473. Freeman, M.P., et al., *Pharmacokinetics of sertraline across pregnancy and postpartum.* J Clin Psychopharmacol, 2008. **28**(6): p. 646-53.

474. Hostetter, A., et al., *Dose of selective serotonin uptake inhibitors across pregnancy: clinical implications.* Depress Anxiety, 2000. **11**(2): p. 51-7.

475. Sit, D.K., et al., *Changes in antidepressant metabolism and dosing across pregnancy and early postpartum.* J Clin Psychiatry, 2008. **69**(4): p. 652-8.

476. Freeman, M.P., et al., *Pharmacokinetics of Sertraline Across Pregnancy and Postpartum.* 2008. **28**(6): p. 646-653.

477. Sit, D.K., et al., *Changes in antidepressant metabolism and dosing across pregnancy and early postpartum.* The Journal of clinical psychiatry, 2008. **69**(4): p. 652-658.

478. Hicks, J.K., et al., *Clinical Pharmacogenetics Implementation Consortium (CPIC) Guideline for CYP2D6 and CYP2C19 Genotypes and Dosing of Selective Serotonin Reuptake Inhibitors.* Clinical pharmacology and therapeutics, 2015. **98**(2): p. 127-134.

479. Bråten, L.S., et al., *Impact of CYP2C19 genotype on sertraline exposure in 1200 Scandinavian patients.* Neuropsychopharmacology, 2020. **45**(3): p. 570-576.

480. George, B., et al., *Application of physiologically based pharmacokinetic modeling for sertraline dosing recommendations in pregnancy.* NPJ systems biology and applications, 2020. **6**(1): p. 36-36.

481. Templeton, I.E., et al., *Quantitative Prediction of Drug-Drug Interactions Involving Inhibitory Metabolites in Drug Development: How Can Physiologically Based Pharmacokinetic Modeling Help?* CPT: pharmacometrics & systems pharmacology, 2016. **5**(10): p. 505-515.

482. Niyomnaitham, S., et al., *Bioequivalence study of 50 mg sertraline tablets in healthy Thai volunteers.* J Med Assoc Thai, 2009. **92**(9): p. 1229-33.

483. Chen, X., et al., *Development and validation of a liquid chromatographic/tandem mass spectrometric method for the determination of sertraline in human plasma*. 2006, John Wiley & Sons, Ltd: Great Britain. p. 2483.

484. Kim, K.M., et al., *Rapid and sensitive determination of sertraline in human plasma using gas chromatography-mass spectrometry.* J Chromatogr B Analyt Technol Biomed Life Sci, 2002. **769**(2): p. 333-9.

485. Saletu, B., J. Grunberger, and L. Linzmayer, *On central effects of serotonin re-uptake inhibitors: quantitative EEG and psychometric studies with sertraline and zimelidine.* J Neural Transm, 1986. **67**(3-4): p. 241-66.

486. Ronfeld, R.A., L.M. Tremaine, and K.D. Wilner, *Pharmacokinetics of sertraline and its N-demethyl metabolite in elderly and young male and female volunteers.* Clin Pharmacokinet, 1997. **32 Suppl 1**: p. 22-30.

487. Djebli, N., et al., *Physiologically based pharmacokinetic modeling for sequential metabolism: effect of CYP2C19 genetic polymorphism on clopidogrel and clopidogrel active metabolite pharmacokinetics.* Drug Metab Dispos, 2015. **43**(4): p. 510-22.

488. Gong, J., et al., *Physiologically-based pharmacokinetic modelling of a CYP2C19 substrate, BMS-823778, utilizing pharmacogenetic data.* Br J Clin Pharmacol, 2018. **84**(6): p. 1335-1345.

489. Hiemke, C., et al., *Consensus guidelines for therapeutic drug monitoring in neuropsychopharmacology: update 2017.* 2018. **51**(01/02): p. 9-62.

490. Mauri, M.C., et al., *Long-term efficacy and therapeutic drug monitoring of sertraline in major depression.* Human Psychopharmacology: Clinical and Experimental, 2003. **18**(5): p. 385-388.

491. Westin, A.A., et al., *Treatment With Antipsychotics in Pregnancy: Changes in Drug Disposition.* Clin Pharmacol Ther, 2018. **103**(3): p. 477-484.

492. Schoretsanitis, G., et al., *The impact of pregnancy on the pharmacokinetics of antidepressants: a systematic critical review and meta-analysis.* Expert Opin Drug Metab Toxicol, 2020. **16**(5): p. 431-440.

493. Abduljalil, K. and R.K.S. Badhan, *Drug dosing during pregnancy-opportunities for physiologically based pharmacokinetic models.* J Pharmacokinet Pharmacodyn, 2020. **47**(4): p. 319-340.

494. Little, B.B.J.O. and Gynecology, *Pharmacokinetics during pregnancy: evidence-based maternal dose formulation.* 1999. **93**(5): p. 858-868.

495. Lau, G.T. and B.Z. Horowitz, *Sertraline overdose.* Acad Emerg Med, 1996. **3**(2): p. 132-6.

496. Shelton and Richard, *Steps Following Attainment of Remission: Discontinuation of Antidepressant Therapy*. 2001, Prim Care Companion J Clin Psychiatry . p. 168–174.

497. Ornoy, A. and G. Koren, *SSRIs and SNRIs (SRI) in Pregnancy: Effects on the Course of Pregnancy and the Offspring: How Far Are We from Having All the Answers?* 2019. **20**(10): p. 2370.

498. Sachs, G.S., C. Guille, and S.L. McMurrich, *A clinical monitoring form for mood disorders.* Bipolar Disord, 2002. **4**(5): p. 323-7.

499. Bergink, V., et al., *Validation of the Edinburgh Depression Scale during pregnancy.* J Psychosom Res, 2011. **70**(4): p. 385-9.

500. Cox, J.L., J.M. Holden, and R. Sagovsky, *Detection of postnatal depression. Development of the 10-item Edinburgh Postnatal Depression Scale.* Br J Psychiatry, 1987. **150**: p. 782-6.

501. Güngör, S., M.S. Erdal, and Y. Özsoy, *Plasticizers in Transdermal Drug Delivery Systems* in *Recent Advances in Plasticizers*. 2012, InTech: Online. p. 91-112.

502. Patel, N. *Skin in the Game: Mechanistic Modeling of Dermal Drug Absorption.* . 2020 [cited 2021 15/12/2021]; Available from: https://www.certara.com/blog/skin-in-the-game-mechanistic-modeling-of-dermal-drug-absorption/.

503. Puttrevu, S.K., et al., *Physiologically Based Pharmacokinetic Modeling of Transdermal Selegiline and Its Metabolites for the Evaluation of Disposition Differences between Healthy and Special Populations.* Pharmaceutics, 2020. **12**(10).

504. Obach, R.S., L.M. Cox, and L.M. Tremaine, *Sertraline is metabolized by multiple cytochrome P450 enzymes, monoamine oxidases, and glucuronyl transferases in human: An in vitro study.* Drug Metabolism and Disposition, 2005. **33**(2): p. 262-270.

505. Mee Kim, K., et al., *Rapid and sensitive determination of sertraline in human plasma using gas chromatography–mass spectrometry.* Journal of Chromatography B: Analytical Technologies in the Biomedical & Life Sciences, 2002. **769**(2): p. 333.

506. Morris, M.D., *Factorial sampling plans for preliminary computational experiments.* 1991. **33**(2): p. 161-174.

Appendix A: Paroxetine

Table A1. Parameter values used for paroxetine model

Parameters	Value	Notes
Compound type	Monoprotic Base	
Molecular weight (g/mol)	329.4	
Log P	3.55	
fu	0.05	
pKa 1	9.66	
B/P	1.26	
Vss (L/kg)	12.63	Full PBPK model Parameter optimised
Papp (10^{-6} cm/s)	17	
k_a (h^{-1})	1.08	Predicted using ADAM
fa	0.946	Predicted using ADAM
Solubility (Intrinsic) (mg/mL)	0.0147	Solid dosage form (immediate release) Predicted using Simcyp
CL_r (L/h)	0.5	
$Vmax_{3A4}$	1.272	
$Vmax_{2C19}$	0.6	
$Vmax_{2D6}$	7.275	
$Vmax_{3A5}$	0.384	
$Vmax_{1A2}$	0.271	
Km_{3A4}	13.3	
Km_{2C19}	26	
Km_{2D6}	0.028	
Km_{3A5}	108	
Km_{1A2}	8.8	
Kp Scalar	1.6	
Absorption model	ADAM	
Distribution model	Full PBPK Model	

All parameters were obtained from the internal Simcyp validated database file; V_{max}: pmol/min/pmol CYP ; Km: µM.

Gestational changes in CYP 2C19 activity

Maternal CYP 2C19 activity has been determined to decrease by 62 % and 68 % during trimester 2 and 3 respectively [434, 470, 472]. These modifications were incorporated into the Simcyp Pregnancy population (Figure A1) group through the following exponential equation:

$$\text{CYP2C19 Activity} = GW_0(1+B1.GW + B2GW^2+B3GW^3 + B4GW^4)$$

where GW0 refers to the activity at GW0 (i.e.=1) and GW refers to the gestational week. B1 was set at -0.041 and B2 was set at 0.0006.

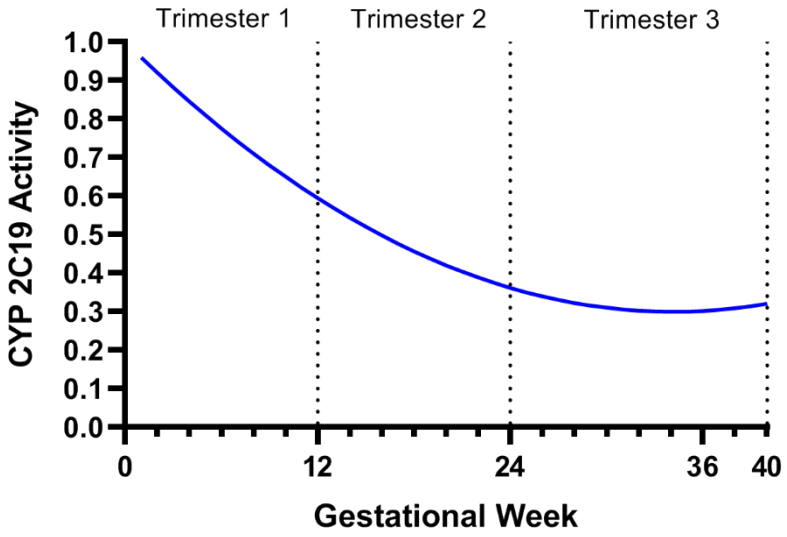

Figure A1: CYP2C19 activity during gestation

Table A2. Predicted paroxetine clearance and AUC for CYP2D6 phenotypes during gestation

		Baseline	5	10	15	20	25	30	35	38
AUC (EM)	Median	789.55	777.13	725.72	683.31	653.34	634.39	621.08	611.6	608.74
	Range	168.58-1364.4	239.44-1284.32	187.15-1226.38	152.43-1176.82	139.2-1134.43	122.62-1098.07	114.04-1066.54	112.37-1039.24	114.77-1026.61
AUC (PM)	Median	1709.27	1752.09	1610.42	1507.42	1434.88	1388.85	1368.71	1367.01	1379.39
	Range	1540.6-2454.97	1470.43-2662.66	1403.65-2535.15	1349.18-2431.11	1304.83-2350.42	1268.65-2286.27	1240.31-2239.49	1218.98-2207.52	1208.77-2195.97
AUC (UM)	Median	68.39	28.42	23.21	19.94	17.76	16.25	15.2	14.5	14.24
	Range	13.13-123.62	13.03-188.92	11.44-168.5	10.29-151.89	9.44-128.81	8.79-114.66	8.28-107.13	7.89-105.46	7.71-107.2
CL (EM)	Median	25.07	25.06	26.44	27.56	28.92	30.05	30.93	31.49	31.65
	Range	13.7-118.64	13.64-83.53	14.38-106.87	15.05-131.21	15.61-143.68	16.07-163.1	16.44-175.37	16.68-177.98	16.78-174.27
CL (PM)	Median	11.71	11.415	12.42	13.27	13.94	14.4	14.615	14.63	14.505
	Range	8.15-12.98	7.51-13.6	7.89-14.25	8.23-14.82	8.51-15.33	8.75-15.76	8.93-16.12	9.06-16.41	9.11-16.55
CL (UM)	Median	292.45	703.76	861.76	1002.92	1126.11	1231.1	1316.13	1378.92	1404.97
	Range	161.79-1522.95	105.86-1535.41	118.69-1748.88	131.67-1943.38	155.26-2119.62	174.43-2276.44	186.7-2415.78	189.65-2534.37	186.56-2594.97

AUC: Area under the curve; CL: clearance; EM: Extensive metabolisers; PM: Poor metabolisers; UM: Ultra-rapid metabolisers

Table A3. Statistical analysis of the differences between paroxetine CYP2D6 pharmacokinetics during gestation.

	Baseline *vs.* week	AUC (ng/mL.h) Mean Difference	95.00 % CI	P-value		Total CL (L/h) Mean Difference	95.00 % CI	P-value	
Extensive Metaboliser	5	34.92	-71.02 to 140.9	0.9397	ns	0.03241	-2.203 to 2.268	>0.9999	ns
	10	82.21	-23.72 to 188.2	0.2046	ns	-2.699	-4.935 to -0.4635	0.0097	**
	15	119.2	13.23 to 225.1	0.0193	*	-5.266	-7.501 to -3.030	<0.0001	****
	20	147.6	41.61 to 253.5	0.0017	**	-7.42	-9.656 to -5.184	<0.0001	****
	25	168.8	62.84 to 274.7	0.0002	***	-9.186	-11.42 to -6.951	<0.0001	****
	30	183.7	77.73 to 289.6	<0.0001	****	-10.45	-12.69 to -8.214	<0.0001	****
	35	192.6	86.69 to 298.6	<0.0001	****	-11.13	-13.37 to -8.896	<0.0001	****
	38	195.2	89.22 to 301.1	<0.0001	****	-11.24	-13.47 to -8.999	<0.0001	****
Poor Metaboliser	5	-26.57	-80.53 to 27.39	0.6572	ns	0.04	-0.4883 to 0.5683	0.9997	ns
	10	67.11	13.15 to 121.1	0.0083	**	-0.5675	-1.096 to -0.03918	0.0299	*
	15	140.7	86.73 to 194.7	<0.0001	****	-1.101	-1.630 to -0.5729	<0.0001	****
	20	197.4	143.4 to 251.3	<0.0001	****	-1.545	-2.073 to -1.017	<0.0001	****
	25	240.2	186.2 to 294.2	<0.0001	****	-1.899	-2.427 to -1.370	<0.0001	****
	30	270.4	216.4 to 324.4	<0.0001	****	-2.154	-2.682 to -1.625	<0.0001	****
	35	288.8	234.9 to 342.8	<0.0001	****	-2.301	-2.830 to -1.773	<0.0001	****
	38	294.2	240.2 to 348.2	<0.0001	****	-2.343	-2.871 to -1.814	<0.0001	****
Ultra-Rapid Metaboliser	5	-5.378	-30.90 to 20.15	0.9926	ns	-55.42	-407.1 to 296.2	0.9976	ns
	10	3.84	-21.68 to 29.36	0.9979	ns	-189.1	-540.8 to 162.5	0.5452	ns
	15	10.69	-14.84 to 36.21	0.7791	ns	-310.3	-661.9 to 41.38	0.103	ns
	20	17.76	-7.762 to 43.29	0.2796	ns	-420.1	-771.7 to -68.42	0.0134	*
	25	22.27	-3.258 to 47.79	0.0452	*	-514.3	-865.9 to -162.6	0.0018	**
	30	24.87	-0.6582 to 50.39	0.0489	*	-591.7	-943.4 to -240.1	0.0003	***
	35	25.79	0.2698 to 51.32	0.0467	*	-650	-1002 to -298.3	<0.0001	****
	38	25.58	0.05178 to 51.10	0.0493	*	-674.4	-1026 to -322.8	<0.0001	****

Statistical analysis was conducted using a Kruskal-Wallis test with a Dunn's multiple comparison post-hoc test, in comparison to baseline. AUC: Area under the curve; CL: clearance; CI: confidence interval.

Table A4. Peak and trough paroxetine plasma concentrations during each trimester for CYP2D6 phenotypes.

		Week 6				Week 20				Week 33			
		Maximum trough	Minimum trough	Percentage		C_{max}	C_{min}	Percentage		C_{max}	C_{min}	Percentage	
Dose	Phenotypes	(ng/mL)	(ng/mL)	Peak Above 60 ng/mL	Trough Below 20 ng/mL	(ng/mL)	(ng/mL)	Peak Above 60 ng/mL	Trough Below 20 ng/mL	(ng/mL)	(ng/mL)	Peak Above 60 ng/mL	Trough Below 20 ng/mL
15 mg	EM	67.9	0.08	1	71	60.11	0.06	1	79	57.34	0.06	0	81
	PM	74.63	7.49	1	40	65.81	6.43	1	52	62.62	6.5	1	56
	UM	51.92	0.06	0	80	41.76	0.05	0	84	39.61	0.05	0	86
20 mg	EM	93.25	0.11	3	42	82.82	0.09	3	53	78.98	0.09	3	55
	PM	101.25	10.03	2	24	89.4	8.62	1	31	85	8.71	1	32
	UM	81.4	0.1	2	69	67.83	0.07	1	78	64.78	0.07	1	78
30 mg	EM	146.41	0.23	16	22	130.62	0.17	12	29	124.42	0.16	10	31
	PM	156.77	15.19	24	7	138.78	13.08	18	10	131.81	13.19	12	11
	UM	145.8	0.2	16	38	125.41	0.14	11	47	120.15	0.14	10	48
40 mg	EM	202.42	0.44	42	10	181.25	0.3	30	12	172.4	0.28	27	13
	PM	215.07	20.45	52	0	190.89	17.63	42	3	181.06	17.75	39	3
	UM	216.31	0.42	28	21	189.25	0.27	23	28	181.19	0.24	20	28
50 mg	EM	260.99	1.04	59	8	234.46	0.55	54	9	222.67	0.51	51	10
	PM	275.79	25.81	68	0	245.39	22.28	63	0	232.48	22.39	61	0
	UM	291.74	1.17	43	8	258.28	0.54	36	13	246.81	0.47	32	16

C_{max}: maximum plasma concentration; C_{min}: minimum plasma concentration; EM: Extensive metabolisers; PM: Poor metabolisers; UM: Ultra-rapid metabolisers

Appendix B: Sertraline

Section 1

Table B1. Final PBPK optimised sertraline parameters

Parameters	Sertraline	Notes
Compound type	Weak Base	
Molecular weight (g/mol)	306	
Log P	5.5 [a]	
fu	0.023 [b]	
pKa 1	9.43	
B/P	1	
Vss (L/kg)	8.23	Full PBPK model with optimised Kp scalar of 1
k_a (h^{-1})	0.12	Optimised
Fa	0.98	Optimised
CLint,u_{2B6} (µL/min/pmol)	2.7	
CLint,u_{2C9} (µL/min/pmol)	5.5	
CLint,u_{2C19} (µL/min/pmol)	2.4	
CLint,u_{2E1} (µL/min/pmol)	9.5	
$K_{m,3A4}$	45	
$V_{max,3A4}$	0.6	Obtained from Obach *et al* (2005) [504]
$K_{m,2D6}$	2.6	
$V_{max,2D6}$	0.8	
fu_{mic}	0.03	
K_i 2D6	0.9	fuinc: 0.18
K_i 3A4	1.2	fuinc: 0.18
Absorption Model	First Order	
Distribution Model	Full PBPK	

Unless otherwise stated, data obtained/adapted from Templeton *et al* (2016) [481].

Section 2

Gestational changes in CYPs 2C19 and 2B6 activity

Maternal CYPs 2C19 and 2B6 activity has been determined to decrease and increase, respectively, during trimester 2 and 3 respectively [434, 470, 472], but are absent within the Simcyp Simulator. These modifications were incorporated into the Simcyp Pregnancy population (Figure B1) group through the following exponential equation:

$$\text{CYP Activity} = GW_0(1+B1.GW + B2GW^2+B3GW^3 + B4GW^4)$$

where GW0 refers to the activity at GW0 (i.e.=1) and GW refers to the gestational week.
B1 was set at -0.041(2C19) and -0.0002 (2B6) and B2 was set at 0.0006 (2C19) and 0.00071 (2B6).

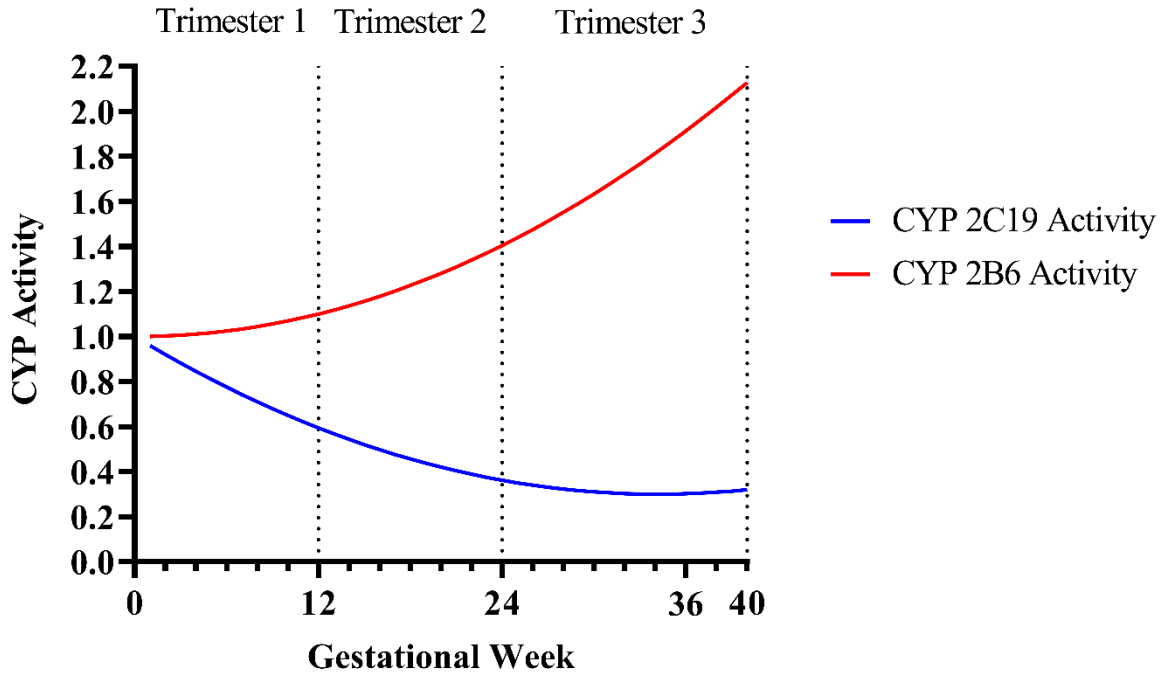

Figure B1: Changes in CYP 2C19 and 2B6 activity during gestation
Further, the enzyme abundance for CYP2C19 phenotypes was incorporated as follows for extensive metabolisers (14 pmol/mg [106 % CV]), poor metabolisers (0 pmol/mg [0 % CV]) and ultra-rapid metabolisers (18 pmol/mg [100 % CV]) [487].

Table B2: **Single and multiple dose studies pharmacokinetic**

	Study	PK Parameters	Observed	Predicted
Single	Niyomnaitham *et al* (2009) [482]	$AUC_{(0\text{-}96\ h)}$	580 (270)	
		C_{max}	20.60 (6.01)	
		tmax	5.25	
	Chen *et al* (2006) [483]	$AUC_{(0\text{-}96\ h)}$	397 (149)	
		C_{max}	10.5 (4.2)	
		tmax	8	
	Kim *et al* (2002) [505]	$AUC_{(0\text{-}72\ h)}$	267 (121)	
		C_{max}	10.3 (2.47)	
		tmax	8 (1.63)	
	Simcyp Predicted (This study)	$AUC_{(0\text{-}72\ h)}$		521.7 (211.6)
		$AUC_{(0\text{-}96\ h)}$		578.2 (236.2)
		C_{max}		11.1 (8.9)
		t_{max}		8.9 (4)
Multiple	Ronfeld *et al* (1997) [486] (Male)	$AUC_{(24h)}$ [Day 30]	2076 (549)	3712 (1758)
		C_{max} [Day 30]	118 (22)	123.2 (48.4)
		tmax [Day 30]	6.9 (1)	4.2 (3.1)
	Ronfeld *et al* (1997) [486] (Female)	$AUC_{(24h)}$ [Day 30]	3063 (1413)	4123 (2627)
		C_{max} [Day 30]	166 (65)	142.2 (65.6)
		tmax [Day 30]	6.7 (1.8)	4.4 (2.5)
	Saletu *et al* (1986) [485]	100 mg C_{max}	53.6 (17.1)	67.3 (32.2)
		200 mg C_{max}	105.2 (44.2)	134.6 (64.9)
		400 mg C_{max}	253.3 (113.2)	269.2 (129.7)

AUC: area under the curve; C_{max}: maximum plasma concentration; tmax: time to maximum plasma concentration. Data represents mean (standard deviation). AUC: ng/mL.h; C_{max}: ng/mL; tmax: h.

Table B3: CYP 2C19 phenotyped trough plasma concentration during gestation

Phenotype		Trough plasma concentration (ng/mL)			
		Baseline	**Week 10**	**Week 20**	**Week 30**
EM	Median	15.26	14.85	13.93	12.66
	Range	1.84-52.90	3.08-60.98	2.98-57.44	2.79-52.64
PM	Median	14.65	15.35	14.12	12.53
	Range	3.74-119.50	3.65-81.34	3.48-75.63	3.23-68.22
UM	Median	13.04	12.04	11.35	10.44
	Range	3.09-51.10	2.91-44.21	2.77-41.98	2.56-38.79

EM: Extensive metabolisers; PM: Poor metabolisers; UM: Ultra-rapid Metabolisers

Table B4. *In-vivo* intrinsic clearance of sertraline in EMs and UMs

Phenotype		Intrinsic *in-vivo* clearance (Cl_{int}) (L/h)								
		Baseline	**5**	**10**	**15**	**20**	**25**	**30**	**35**	**38**
EM	Median	78.44	74.22	65.85	63.38	57.96	52.54	47.12	41.7	38.45
	Range	17.55-622.10	15.59-601.64	13.84-533.86	13.32-513.77	12.18-469.84	11.04-425.90	9.90-381.97	8.76-338.04	8.08-311.68
UM	Median	105.17	97.54	90.42	83.30	76.18	69.05	61.93	54.81	50.53
	Range	24.58-77	21.75-724.61	20.16-671.70	18.57-618.79	16.99-565.87	15.40-512.96	13.81-460.05	12.22-407.13	11.27-375.39

EM: Extensive metabolisers; PM: Poor metabolisers; UM: Ultra-rapid Metabolisers

Table B5: Phenotyped based dose optimisation during gestation

Dose	Phenotype	Trimester 1 (Week 6)				Trimester 2 (Week 20)				Trimester 33 (Week 33)			
		C_{max} (ng/mL)	C_{min} (ng/mL)	% Below 10 ng/mL	% Above 75 ng/mL	C_{max} (ng/mL)	C_{min} (ng/mL)	% Below 10 ng/mL	% Above 75 ng/mL	C_{max} (ng/mL)	C_{min} (ng/mL)	% Below 10 ng/mL	% Above 75 ng/mL
25mg	EM	31.02	1.55	69	0	28.72	1.49	76	0	25.48	1.36	79	0
	PM	41.55	1.85	64	0	37.81	1.74	73	0	32.85	1.57	76	0
	UM	22.41	1.48	81	0	20.99	1.39	83	0	18.82	1.24	89	0
50mg	EM	62.03	3.10	27	0	57.44	2.98	31	0	50.96	2.72	36	0
	PM	83.11	3.69	24	1	75.63	3.48	28	1	65.70	3.14	31	0
	UM	44.82	2.95	37	0	41.98	2.77	40	0	37.64	2.49	49	0
100 mg	EM	124.07	6.20	10	5	114.87	5.96	12	2	101.93	5.45	13	1
	PM	166.22	7.39	4	8	151.26	6.95	6	5	131.40	6.28	9	2
	UM	89.65	5.90	7	1	83.97	5.54	9	1	75.28	4.98	11	1
150mg	EM	186.10	9.30	2	19	172.31	8.94	2	15	152.88	8.17	6	8
	PM	249.31	11.08	0	24	226.88	10.43	0	17	197.10	9.42	1	11
	UM	134.49	8.86	1	10	125.94	8.32	2	8	112.92	7.47	2	5
200mg	EM	248.14	12.40	0	36	229.74	11.92	0	29	203.85	10.89	0	23
	PM	332.42	14.78	0	42	302.51	13.91	0	34	262.80	12.57	0	25
	UM	179.31	11.81	0	27	167.93	11.09	0	18	150.56	9.96	1	12
250mg	EM	310.20	15.50	0	51	287.19	14.90	0	42	254.80	13.61	0	36
	PM	415.54	18.47	0	52	378.14	17.38	0	48	328.51	15.71	0	42
	UM	224.14	14.76	0	39	209.92	13.86	0	36	188.20	12.44	0	29
300mg	EM	372.25	18.60	0	64	344.61	17.87	0	60	305.76	16.34	0	48
	PM	498.66	22.17	0	69	453.77	20.86	0	61	394.19	18.85	0	49
	UM	268.94	17.71	0	47	251.89	16.63	0	40	225.83	14.93	0	38

C_{max}: maximum plasma concentration; C_{min}: minimum plasma concentration; EM: Extensive metabolisers; PM: Poor metabolisers; UM: Ultra-rapid

Section 3

Global sensitivity analysis (GSA) was conducted to investigate the effects of simultaneous parameter variations over a defined range to assess the relationships towards outcomes. The hepatic (extensive metaboliser phenotype) abundance of CYPs 2C19 and 2B6 along with albumin were assessed over a range detailed in Table B6.

Table B6: Model input parameters for GSA

Parameter	Default	Range
HSA (g/L)	49.4	25-50
2B6 (pmol/mg)	17	5-17
2C19 (pmol/mg)	14	5-14

GSA was conducted at week 6 (Trimester 1), week 20 (Trimester 2) and week 33 (Trimester 3) using a 50 mg once daily dose. The Morris [506] screening method was employed, due to the lack of (physiologically) correlation between the parameters. This method considered multiple points in the multi-dimensional parameter space and provides a more global approach to traditional one parameter at a time analysis. This approach used several different sampling trajectories which commence at random and are sampled across a grid space. Results were output global index, which was used to rank the parameter space.

The global index (*GI*) is a function of both the mean (μ) and the standard variance (σ):

$$GI = \left(\sqrt[2]{\mu^2 + \sigma^2}\right)$$

Table B7: Parameter ranking following GSA

	Ranking											
	C_{max}			**AUC**			**CL**			**V_{ss}**		
	T1	T2	T3	T1	T2	T3	T1	T2	T3	T1	T2	T3
HSA	**1**	**1**	**1**	**1**	**1**	**1**	**1**	**1**	**1**	**1**	**1**	**1**
2B6	2	2	2	2	2	2	2	2	2	2	2	2
2C19	3	3	3	3	3	3	3	3	3	2	2	2

T1: trimester 1 (week 6); T2: trimester 2 (week 20); T3: trimester 3 (week 33)

Table B8: Parameter global index following GSA

	Global index											
	C_{max}			**AUC**			**CL**			**V_{ss}**		
	T1	T2	T3	T1	T2	T3	T1	T2	T3	T1	T2	T3
HSA	0.017471	0.015515	0.013253	0.424197	0.371179	0.309781	9508.403	11808.69	15895.64	27.11609	33.84137	39.68106
2B6	0.000705	0.000804	0.000992	0.013779	0.015798	0.019607	21.10802	40.16134	105.1407	0	0	0
2C19	0.000471	0.000307	0.000185	0.009169	0.005988	0.003592	9.894014	6.961058	4.926404	0	0	0

T1: trimester 1 (week 6); T2: trimester 2 (week 20); T3: trimester 3 (week 33).